A GENETIC DISSECTION OF THE ROLE OF THE ERBB2 / NEU RECEPTOR TYROSINE KINASE IN DEVELOPMENT AND TUMORIGENESIS IN TRANSGENIC MICE.

By

ERAN R. ANDRECHEK, B.Sc.

A Thesis

Submitted to the School of Graduate Studies

in Partial Fulfillment of the Requirements

for the Degree

Doctor of Philosophy

McMaster University

ERBB2 / NEU IN DEVELOPMENT AND TUMORIGENESIS

DOCTOR OF PHILOSOPHY (2003) McMaster University

(Biology) Hamilton, Ontario

TITLE: A Genetic Dissection of the Role of the ErbB2 / Neu Receptor Tyrosine Kinase in Development and Tumorigenesis in Transgenic Mice.

AUTHOR: Eran R. Andrechek, B.Sc. (McMaster University)

SUPERVISOR: Professor W.J. Muller

NUMBER OF PAGES: xvii, 281

ABSTRACT

Amplification and overexpression of Neu (HER2, ErbB2) has been observed in a significant proportion of human breast cancers. Consistent with this, overexpression of various *neu* alleles in the mammary epithelium of transgenic mice resulted in the formation of mammary adenocarcinomas. However, these mouse models have relied upon a hormonally responsive strong viral promoter to direct transgene expression and therefore may not accurately model the human condition.

In this thesis I demonstrate that endogenously regulated expression of the activated *neuNT* allele in the mammary gland resulted in increased lateral branching and ductal escape from the fat pad. Upon amplification and overexpression of *neuNT,* these mice developed adenocarcinomas which shared several similarities with the human disease. I also created a line of mice that express *neuNT* under the control of the endogenous promoter in the germline. Surprisingly, this did not result in tumor formation, although these mice expressed *neuNT* at levels equal to the mammary specific activation. I have also examined the role of Neu in the mammary gland through a mammary specific deletion and observed delayed ductal outgrowth. In addition to examining the function of Neu in the mammary gland, I have also described mice with a conditional deletion of Neu in the skeletal muscle. These mice have profound defects in proprioception due to a lack of muscle spindles, and have a deficiency in muscle regeneration and differentiation. Taken together, these results illustrate the role of Neu in tumorigenesis and in the normal development of numerous other tissues.

ACKNOWLEDGMENTS

The years I have spent in the Muller lab have been enjoyable and there are a number of people that I wish to thank for the experience. Firstly, I would like to thank Bill for the opportunity to work in the lab. You've been a great supervisor and I will leave the lab with good memories of my time there..

This thesis would not be complete at this time if it were not for the technical support that I received from numerous people. The countless hours of animal work and genotyping that I didn't have to do were invaluable in allowing me to finish in a timely fashion and I appreciate the efforts of Monica, Carrie, Crystal, Adele and others.

During my stay in the lab I was fortunate to be taught by several excellent mentors such as Rod and Peter. The unique inhabitants of the Muller lab certainly made for interesting days – and I never knew who Ricky would be lippy to next. Thanks to Ricky, I learned that poking a committee member's belly was a bad thing to do!

I'm also thankful for the constant support of both sets of parents over the last ten years I've spent at McMaster. The cookies and other necessary school supplies have been greatly appreciated over the years. And yes, I will eventually get a real job!

Most of all I cannot begin to express how grateful I am for the constant support of and encouragement of my wife. Your positive attitude and work ethic has been an inspiration. Finally, I'd like to thank Eric for showing me what is really important in life and for staying up late at night with me while I finished the thesis.

CONTRIBUTIONS BY OTHERS

Some of the work presented in this thesis was made possible through the efforts of others and I would particularly like to acknowledge the following contributions;

William Rod Hardy for the preparation of the genomic flanks (Figure 3.2) for the targeting sequence and for the blastocyst injections of the ES cells.

Peter Siegel for the cloning and generation of the seven founding lines of MMTV-Cre transgenic mice.

Adele Girgis-Gabardo for the preparation of several myoblast cell lines and MF20 staining of them (Figure 5.9 E-F) and the confirmatory Northerns shown in Figure 3.14

Dr. Michael Laing for the *grb7 / cab1* Southern in Figure 3.15 and for the *in situs* shown in Figure 3.22 C-D.

Dr. Robert D. Cardiff for extensive histological analysis and the images provided for Figure 3.8 C-D.

Cristina Montagna for the FISH data shown in Figure 3.17 A and the preparation of the two TM cell lines from the conditionally activated NeuNT tumors.

TABLE OF CONTENTS

LIST OF FIGURES

CHAPTER 1

CHAPTER 2

No figures

CHAPTER 3

CHAPTER 4

CHAPTER 5

CHAPTER 6

LIST OF TABLES

LIST OF ABBREVIATIONS

ErbB2	Mouse epidermal growth factor receptor 2
Neu	Rat ErbB2 homologue
HER2	Human ErbB2 homologue
AFF2	Severely **Aff**ected ErbB2$^{Flox/Flox}$ MCK-Cre Myoblast Cell Line # **2**
CMV	Cytomegalovirus promoter enhancer
Cre	Cre Recombinase
DM	Double minute chromosomes
DPC	Days Post Coitum
EDL	Extensor Digitorum Longus Muscle
ES Cells	Embryonic Stem Cells
HGF	Hepatocyte growth factor
MCK	Muscle Creatine Kinase
MMTV	Mouse Mammary Tumor Virus Long Terminal Repeat
MoMuLV	Moloney Murine Leukemia Virus Promoter P
MT	Polyoma Virus Middle T Antigen
Neo	Neomycin
RSV	Rous Sarcoma Virus
TA	Tibealis Anterior Muscle
TEBS	Terminal End Buds
TGFβ	Transforming growth factor beta

CHAPTER 1

INTRODUCTION

1.1 Development of the Murine Mammary Gland

1.1.1 Development and Organization of the Mammary Gland

In the earliest embryonic stages that the rudimentary mammary gland can be discerned, it begins as two groups of ectodermal cells on either side of the embryo located between the anterior and posterior limb buds. This mammary streak, also known as the milk line, then forms 5 distinct pairs of ectodermal buds which invade into the dermal layer (Cunha, 1994) at 12 days post coitum (dpc). At this point in development, these mammary buds have differentiated sufficiently that if excised, cultured and reimplanted into a fat pad free of epithelium they will form the characteristic ductal network of a mammary gland. For the next few days of development, little change is observed in the mammary bud until embryonic day 16-17 when this mammary bud begins the process of ductal branching (Sakakura *et al.*, 1982). Additionally, at this point, the fat pad begins to develop from mesenchyme cells located in the subcutis (Sakakura *et al.*, 1982). The process of ductal extension into the fat pad occurs at this point (Hogg *et al.*, 1983) and continues at a relatively slow rate until the onset of puberty (Hennighausen and Robinson, 1998).

After approximately four weeks of postnatal development, the onset of puberty can be detected in the mouse. Prior to the initiation of puberty, the extension of the mammary gland into the fat pad was relatively slow. However, with puberty comes the formation of terminal end buds (TEB) and the rapid extension of these TEBs and the ensuing ductal network through the fat pad (Hennighausen and Robinson, 1998). The TEB is the large bulbous structure at the end of the proliferating duct composed of two cell types, the cap cells and the body cells (Figure 1.1). Data from experiments using rats has shown that the outermost layer of this bulbous structure is composed of cap cells, and it is thought that these cells give rise to the myoepithelial cells (Dulbecco *et al.*, 1982; Dulbecco *et al.*, 1983; Williams and Daniel, 1983). Within this sheath of cap cells are the layers of body cells which express a variety of genes that are mammary gland markers, including cytokeratins and E-cadherins (Dulbecco *et al.*, 1986; Daniel *et al.*, 1995). Behind this bulbous structure lies the duct itself, composed of a single layer of luminal, or cuboidal, epithelial cells encompassed by a single layer of myoepithelial cells in the primary duct. The process by which the solid TEB develops into a canalized duct is not yet well understood, but has been shown to involve selective spatial apoptosis in the TEB (Humphreys *et al.*, 1996). The structure and some of the genetic determinants of TEB formation are illustrated in Figure 1.1. During the eight weeks following the onset of puberty, the ductal network rapidly expands to fill the fat pad with the characteristic arbouraceous pattern. After approximately 12 weeks of postnatal development, when the mammary gland has filled the fat pad with primary ducts and the associated secondary and tertiary branches, the TEBs are decreased in size and are lost from the leading edge

Figure 1.1 – Structure and Selected Genetic Determinants of the TEB and Lateral Branching

The structure of a terminal end bud (TEB), lateral bud and the ductal network is shown. Hematoxylin staining an early mammary gland is also shown (inset), illustrating the TEB with a lateral bud and a duct. In addition to the structure of the TEB and duct, several genetic determinants of growth are shown. It has been shown that TGFβ will cause the regression of the TEB and prevents HGF mediated lateral branching. Moreover, in ovarectamized mice EGF and TGFα have been observed to induce the reappearance of the TEB.

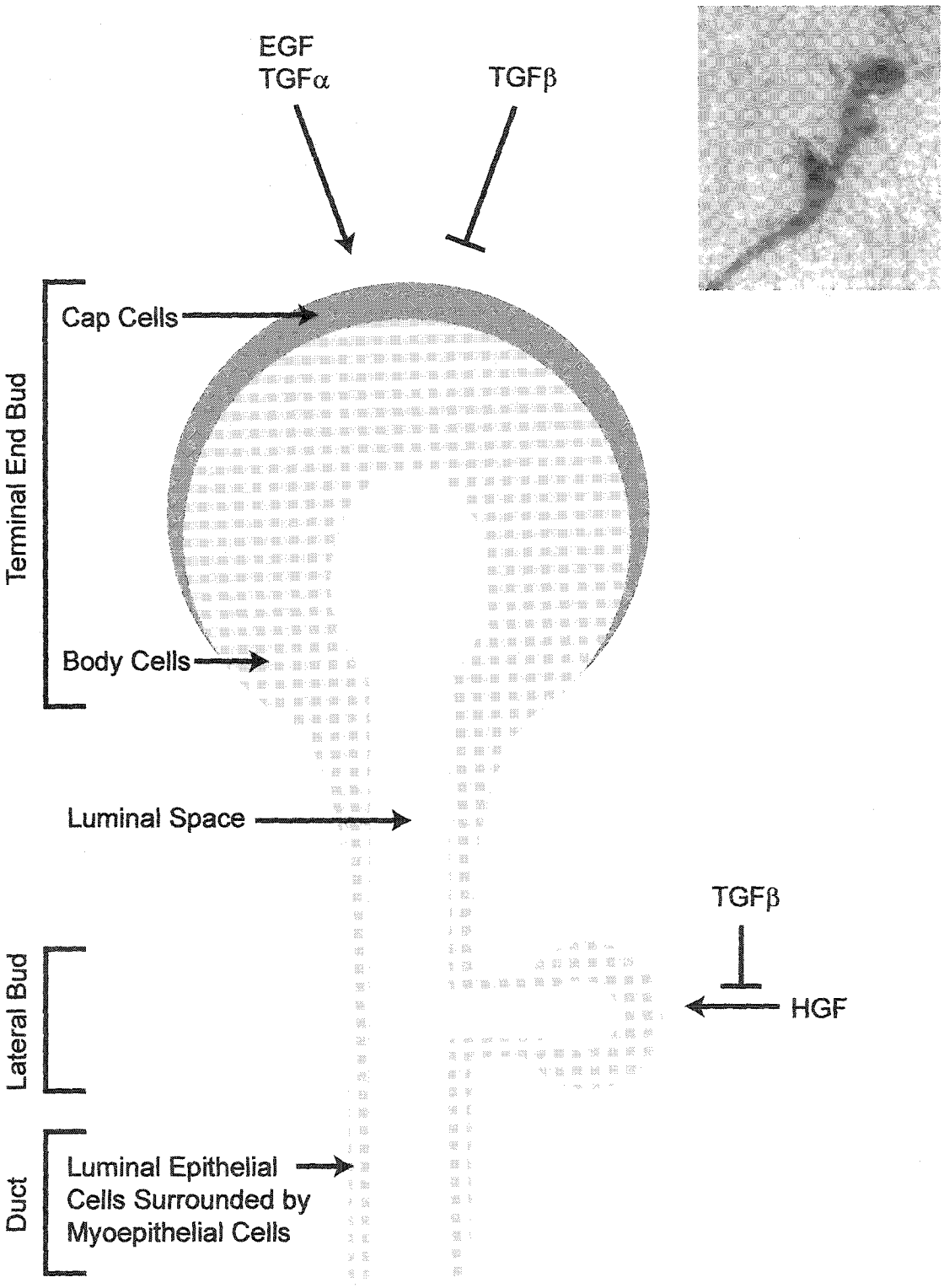
EGF
TGFα
TGFβ
Cap Cells
Terminal End Bud
Body Cells
Luminal Space
TGFβ
HGF
Lateral Bud
Duct
Luminal Epithelial
Cells Surrounded by
Myoepithelial Cells

of the ductal network and are replaced by the terminal bud. The mammary gland then remains structurally stable, with only minor changes related to the estrus cycle, until the onset of gross phenotypic alterations induced by lactation.

The early and frequent onset of lactation in females has been epidemiologically associated with a strong protective effect against breast cancer (Henderson *et al.*, 1991). However, after the changes induced by pregnancy, lactation and involution, the mammary gland appears to return to a virgin like state. During the course of pregnancy, additional branching of the mammary gland is observed. Additionally, there is substantial lobuloalveolar development and epithelial differentiation in the mammary gland that eventually culminates in the secretion of milk. Following lactation and weaning of the offspring, there is extensive apoptosis and remodelling of the mammary gland until it resembles the virgin structure again (Strange *et al.*, 1992). However, while the mammary gland phenotypically returns to a virgin-like state, the protective effect against breast cancer strongly suggests that there are molecular changes. Consistent with these observations, when virgin murine mammary glands were compared to multiparous glands through a gene expression analysis, numerous differentially expressed genes were noted. Significantly, numerous growth factors are repressed in the multiparous glands while several differentiation markers and growth inhibitory molecules such as TGFβ are elevated (D'Cruz *et al.*, 2002). While histologically similar, these results suggest that the protective effect of lactation is due to the terminal differentiation of the parous mammary gland.

1.1.2 Hormonal Influences on the Mammary Gland

In addition to the molecular control through factors that are present within the mammary gland, this organ is highly responsive to hormonal stimulation. Indeed, it is with the onset of puberty, and the corresponding elevation in steroid hormones, that the TEBs form and begin the extension of the ductal network into the fat pad. Moreover, with the onset of pregnancy, the levels of various hormones are highly elevated and induce a rapid expansion of the mammary gland through additional lateral branching and lobuloalveolar development (Fendrick *et al.*, 1998). To illustrate the critical role of steroid hormones such as estrogen and progesterone, numerous studies have shown regression of the lateral branching of the ductal network in response to surgical removal of the ovaries. The ductal network can then be restored through the addition of estrogen or progesterone (Fendrick *et al.*, 1998). Further, the importance of estrogen to mammary development during puberty was illustrated in estrogen receptor knockout mice. These mice developed the rudimentary gland commonly observed before the onset of puberty, but failed to extend the ducts after this point (Korach, 1994; Korach *et al.*, 1996). Interestingly, it was later demonstrated that the critical estrogen responsive tissue was not the mammary epithelium, but rather the stroma (Cunha *et al.*, 1997).

Studies into the role of estrogen have previously suggested a link between hormones and growth factors. Indeed, estrogen has been shown to elevate the level of both Epidermal Growth Factor (EGF) and Epidermal Growth Factor Receptor (EGFR) in the uterus (Mukku and Stancel, 1985). This estrogen mediated increase in EGF levels has also been observed in the mammary gland, and given the activity of EGF (Discussed

in Section 1.5.2), this suggests a role for estrogen in EGF mediated ductal proliferation. Consistent with these observations, elimination of estrogen through an ovarectomy results in regression of the ductal network that can be restored through the addition of EGF (Snedeker *et al.*, 1991). In addition to these EGF results, another EGFR ligand, TGFα was also shown to elicit similar effects (Snedeker *et al.*, 1991). These results suggest the importance of EGF like ligands and the EGFR family in mediating mammary development.

1.1.3 Expression of the EGFR family in the Mammary Gland

During the development of the mammary gland, various factors have been illustrated to regulate the ductal extension and lateral branching. Indeed, estrogen has been shown to elevate the levels of EGF and EGFR. The expression pattern and level of the EGFR family members (EGFR, ErbB2, ErbB3 and ErbB4) has been examined in the mammary gland in order to obtain a better understanding of how these genes contribute to normal morphogenesis. EGFR is expressed at approximately equal levels in the murine mammary gland beginning at 28 days of development until maturity. This expression level is maintained throughout pregnancy and the early stages of lactation. By the late stages of lactation, expression is slowly reduced. However, EGFR expression returns to the levels observed in development with the onset of involution. While ErbB2 and ErbB3 have similar expression patterns, their expression is weak prior to the onset of puberty and increases as the ductal network penetrates the fat pad. The remaining family member, ErbB4, has a strikingly different expression profile as it is weakly expressed

during development of the gland, is absent in lactation and is only weakly observed in involution. However, ErbB4 is highly expressed during pregnancy (Schroeder and Lee, 1998). Taken together, this expression data suggests that the various EGFR family members have discrete roles in mammary gland development and function. Through the same type of analysis, the expression pattern of various EGFR family ligands was examined in the mammary gland. Briefly, this revealed that Transforming Growth Factor α (TGFα) and betacellulin were highly expressed during mammary gland development while maximal EGF expression was noted during the late stages of pregnancy and throughout lactation (Schroeder and Lee, 1998). While this expression data reveals trends into the temporal regulation of the EGFR family members and their ligands in the mammary gland, the spatial location should also be noted. Importantly, ErbB2 has been illustrated to be localized to the mammary epithelium in both mature and lactating mice (Schroeder and Lee, 1998). The expression of ErbB2 has also been noted in the luminal margin of the TEB (Deckard-janatpour *et al.* 1997). When the temporal and spatial expression patterns of the various EGFR family members and their ligands are considered, it suggests that they have disparate roles in mammary gland development and function.

1.1.4 Role of the EGFR family in Mammary Gland Development

The timing and location of expression of the various EGFR family members have strongly implicated these genes in mammary gland development. Interestingly, the waved-2 line of mice, identified due to their characteristic coat texture, contain a

mutation in EGFR which greatly reduces the activity of the kinase domain (Luetteke *et al.*, 1994). The mammary glands in these waved-2 mice had a reduced ability to lactate and a significant proportion of progeny die postnatally (Fowler *et al.*, 1995). Further examination of these mice has also revealed that there is a defect in the progression of the ducts into the fat pad. Moreover, these waved-2 mammary glands also exhibited a reduction in lateral branching that was observed to be an inherent property of the waved-2 or EGFR knockout epithelium (Sebastian *et al.*, 1998). This data implicates EGFR as an essential gene in the development and function of the mammary gland. Since the expression patterns of the remaining EGFR family members are distinct from EGFR, these observations strongly suggest that there are separate and essential roles in the mammary gland for the various receptors. The examination of a loss of function mutation in ErbB2 in the mammary gland has been previously been limited to an examination of mice overexpressing a dominant negative *erbB2* allele. These transgenic mice expressed a truncated *erbB2* allele lacking the kinase domain and carboxy terminus. Interestingly, these mice had no observed perturbations in mammary gland development but had minor defects in lactation, but these modest alterations did not prevent these mice from being lactationally competent (Jones and Stern, 1999). Similar studies examining the function of ErbB4 revealed that this receptor may be primarily involved at the latter stages of lactation (Jones *et al.*, 1999), consistent with the ErbB4 expression pattern (Schroeder and Lee, 1998). While these results are intriguing, the creation of a dominant negative allele will not only inhibit signalling through homodimerization with the dominant negative receptor, but will also have an impact on heterodimerization.

Additionally, when the kinase dead *erbB2* allele was examined for ability to ablate phosphorylation of ErbB2, it only mildly reduced the extent of tyrosine phosphorylation *in vitro* (Jones and Stern, 1999). When the effect of overexpression of various activated ErbB2 alleles on mammary gland development is examined, it is clear that there is an increase in the lateral branching (Siegel *et al.*, 1999). Taken together, these observations have strongly suggested that there is a role for ErbB2 in mammary gland development, but this role has not yet been completely elucidated.

1.1.5 Other Genetic Determinants of Mammary Gland Development

While the development of the mammary gland and the branching of the ductal network is a physically well defined process shown to involve the EGFR family, numerous questions about the molecular regulation of mammary gland development remain to be addressed. For instance, how is the secondary and tertiary branching controlled and prior to their disappearance, how do the TEBs spatially sense that they have reached the terminus of the fat pad? One factor that may play an integral function in both of these processes is Transforming Growth Factor β (TGFβ). Indeed, implanting a slow release pellet containing TGFβ into the fat pad of a developing mammary gland resulted in the disappearance of the TEBs as they approached the pellet (Silberstein and Daniel, 1987). Interestingly, this had no effect on the lobuloalveolar expansion associated with pregnancy (Daniel *et al.*, 1989). It has been postulated that this data strongly suggests, but has not directly shown, that TGFβ may one of the defining molecules that demarcates the terminus of growth into the fat pad (Daniel *et al.*, 1989).

Consistent with these results, transgenic mice expressing TGFβ in the mammary gland had reduced ductal penetration into the fat pad but were fully capable of lactating (Pierce *et al.*, 1993). Moreover, it was noted in this strain of mice that there was a virtual absence of lateral branching after thirteen weeks of development (Pierce *et al.*, 1993). Taken together with the observation that hepatocyte growth factor (HGF) stimulates lateral branching *in vitro* (Kamalati *et al.*, 1999), and is negatively regulated by TGFβ, this provides compelling evidence linking TGFβ and lateral branching (Silberstein, 2001)(Figure 1.1). In addition to regulating HGF levels, TGFβ has been shown to strongly repress the Muc4 complex (See section 1.5.2) and thus may reduce the ability of the EGFR family members to interact in specific locations within the mammary gland. Given the strict temporal and spatial control of the EGFR family, the regulation of heterodimerization through TGFβ mediated control of Muc4 levels suggests that TGFβ may also regulate the EGFR family.

1.2 The Incidence and Genetic Basis of Breast Cancer

Normal mammary gland development is dependent on the precise regulation and expression of numerous genes and the disruption of this regulation can result in the induction of breast cancer. Over the course of the past year there were approximately 67000 new cases of cancer and approximately 31000 recorded deaths due to cancer in Canadian women. Breast cancer was the most commonly diagnosed cancer in the female portion of the population, accounting for over 30% of the newly diagnosed cancers and over 17% of the cancer related deaths. Over the lifetime of an average Canadian female,

there is a 1 in 9 chance of developing breast cancer and a 1 in 25 chance of mortality caused by the primary tumor and associated metastasis (NCIC, 2002). Given the prevalence of this disease, the genetic factors that mediate the progression of breast cancer have presented an appropriate target for research.

The progression of breast cancer is associated with the accumulation of genetic changes within the developing tumor. The growth advantages conferred by these genetic changes are associated with mutations in two broad classes of genes; genes mediating proliferative signals and tumor suppressors. In the 7-20% of total breast cancer cases that are hereditary (Reviewed in Claus *et al.*, 1996), the most frequently observed mutations are found in the BRCA family of tumor suppressors (Miki *et al.*, 1994; Wooster *et al.*, 1995). Indeed, germline mutations in BRCA1 have been found in greater than 50% of hereditary breast cancer and a further 35% of these hereditary breast cancers show mutations in BRCA2 (Rahman and Stratton, 1998). Consistent with these clinical observations, mice with a conditional ablation of *brca1* in the mammary gland developed tumors after a long latency (Xu *et al.*, 1999). In the tumors that developed in the *brca1* null mice, the *p53* locus is often mutated in addition to other regions of genetic instability. While p53 is the most commonly altered gene in sporadic and hereditary breast cancer (Elledge and Allred, 1994; Elledge and Allred, 1998), the ablation of this gene in mice rarely results in the formation of mammary tumors due to the rapid occurance of lymphomas (Donehower *et al.*, 1992). When a portion of the p53 null mammary gland was implanted into the cleared fat pad of a wild type recipient, mammary adenocarcinomas were observed (Jerry *et al.*, 2000). In both the mouse

models and clinical data, the loss or mutation of either BRCA family members or p53 has been shown to result in further genomic instability, allowing the accumulation of additional mutations. However, a significant percentage of familial breast cancers do not contain mutations in p53 or BRCA but harbour loss of heterozygosity (LOH) in other chromosomal regions, suggesting the presence of numerous other tumor suppressors (Bieche and Lidereau, 1995; Garcia *et al.*, 1999). For example, while it only appears to be associated with the familial breast cancers observed in Cowden disease, PTEN loss has been observed in human breast cancer (Garcia *et al.*, 1999). Taken together, these mutations in genes that regulate and maintain genomic integrity are seen to be integral in the progression of breast cancer.

In addition to the loss of function mutations observed in the various tumor suppressors, gain of function mutations in various proto-oncogenes that regulate cell growth and survival are often observed in sporadic human breast cancer. One of the most frequently amplified proto-oncogenes in breast cancer is *c-myc*. Myc is a transcription factor that has an integral function in the regulation of numerous cellular activities, including proliferation and apoptosis. Amplification of *c-myc* has been observed in 15-30% of human breast cancers (Nesbit *et al.*, 1999; Liao and Dickson, 2000) and in Myc expressing tumors with rapid reoccurrence, *c-myc* amplification was noted in 56% of cases (Pertschuk *et al.*, 1993). In addition to *c-myc*, another gene that is frequently amplified in human breast cancer is *cyclin D1*. Amplification of *cyclin D1* has been found in 15-20% of all human breast cancers (Bieche and Lidereau, 1995). The amplification of *cyclin D1* has been shown to impact on cell cycle progression, entry into

S phase and DNA replication. However, the *cyclin D1* amplicon is large and encompasses numerous other genes that may impact tumor development (Bekri *et al.*, 1997). Importantly, mouse models overexpressing either Myc or Cyclin D1 in the mammary gland developed tumors, albeit with a long latency suggesting that other mutations were required for tumorigenesis (Stewart *et al.*, 1984; Leder *et al.*, 1986; Wang *et al.*, 1994).

1.3 HER2 and Breast Cancer, Incidence and Treatment

The progression from a mammary epithelial cell to a malignant phenotype involves multiple genetic events, including the activation of dominant activating oncogenes and inactivation of specific tumour suppressor genes. In addition to the previously discussed genes, amplification and overexpression of the HER2 (Neu is the rat homologue and ErbB2 is the mouse homologue) proto-oncogene was observed in 20–30% human breast cancer (Slamon *et al.*, 1987; Venter *et al.*, 1987; van de Vijver *et al.*, 1988; Slamon *et al.*, 1989; Zeillinger *et al.*, 1989). The amplification and overexpression of this receptor tyrosine kinase has been shown to correlate with a poor prognosis (Hynes and Stern, 1994) and in breast cancers that have amplified and overexpressed HER2, it has been demonstrated that there is an increased risk of relapse and death after treatment (Gullick, 1991; Andrulis *et al.*, 1998). While HER2 overexpression has also been observed in numerous other cancers, the role of this receptor tyrosine kinase has been best described in breast cancer.

Given the poor prognosis associated with elevated HER2 expression in malignancies of the breast, the development of specific therapies to target HER2 mediated tumors has been a key goal in clinical research. A large body of work has culminated in the development of a humanized monoclonal antibody against the extracellular domain of HER2 for clinical use (Carter *et al.*, 1992). This monoclonal antibody, Herceptin (trastuzumab), has been used to treat tumors that overexpress HER2 with substantial effectiveness (Greenberg *et al.*, 1996). Indeed, when combined with chemotherapy, this antibody has been shown to increase antitumor efficacy in terms of time to tumor progression, response rate and overall survival. Additionally, the combination of chemotherapy and Herceptin resulted in a 20% reduction in the risk of death when compared to chemotherapy alone (Slamon *et al.*, 2001). While these results are encouraging, it should be noted that Herceptin is only effective in 25% patients with HER2 positive metastatic breast cancers (Pegram *et al.*, 1998; Simon *et al.*, 2001; Vogel *et al.*, 2002). Although Herceptin has been successful in treating a portion of HER2 expressing breast cancer, the remaining 75% (Pegram *et al.*, 1998; Simon *et al.*, 2001; Vogel *et al.*, 2002) of patients that are not responsive to this treatment provide compelling reasons to pursue alternative therapies. Toward this end, numerous other experimental approaches to treat HER2 mediated breast cancers are being developed (Agus *et al.*, 2002). The poor prognosis associated with overexpression of HER2 and the lack of clinical response to standard treatments in these tumors stresses the requirement to better understand HER2 and the role it plays in mediating tumorigenesis.

1.4 The EGFR family and Breast Cancer Incidence

HER2 is a member of the epidermal growth factor receptor family of receptor tyrosine kinases which is composed of EGFR (ErbB1, HER) (Ullrich *et al.*, 1984), ErbB2 (HER2, Neu) as well as ErbB3 (HER3) (Kraus *et al.*, 1989) and ErbB4 (HER4) (Plowman *et al.*, 1993). While HER2 has been well characterized in breast cancer, the other EGFR family members have also been shown to be involved in tumorigenesis. EGFR overexpression has been noted in carcinomas of the cervix, ovaries and breast (Bauknecht *et al.*, 1989), head and neck (Ford and Grandis, 2003) as well as in glioblastomas (Reis *et al.*, 2000). As with HER2, there are clinical trials underway using monoclonal antibodies to target EGFR overexpressing tumors (Arteaga, 2002; Shawver *et al.*, 2002; Jungbluth *et al.*, 2003). Further, as has been observed in tumors with elevated HER2 levels, EGFR overexpression in carcinomas correlates with a poor clinical prognosis (Harris *et al.*, 1992). In addition to EGFR and HER2, ErbB3 was identified as a member of the EGFR family and during the characterization of this receptor tyrosine kinase, it was shown to be overexpressed in several breast cancer cell lines (Kraus *et al.*, 1989). Subsequently, ErbB3 was shown to be elevated in 22% of human breast cancers without amplification of the endogenous *erbB3* allele (Kraus *et al.*, 1989; Lemoine *et al.*, 1992). ErbB3 expression has also been noted in ovarian and bladder cancers (Rajkumar *et al.*, 1996). The more recent addition of ErbB4 to the EGFR family also illustrated that this family member is overexpressed in various breast cancer cell lines (Plowman *et al.*, 1993) and it has been shown that splice variants of ErbB4 are associated with childhood medulloblastoma (Gilbertson *et al.*, 2001). Expression of ErbB4 has been detected in a

large percentage of ovarian cancer cell lines, but is co-expressed with HER2 and was not thought to be the initiating oncogenic event (Gilmour *et al.*, 2001). Although the various members of the EGFR family are expressed in various cancers, the most compelling data indicating a role in tumorigenesis is the amplification and overexpression of HER2 in breast cancer.

1.5 The Neu / ErbB2 Receptor Tyrosine Kinase

1.5.1 Structure and Function of Neu / ErbB2 and the EGFR Family

To better understand the role of the EGFR family members, and particularly HER2, in mediating breast cancer, the structure and function of these receptor tyrosine kinases has been examined in detail. The *neu* proto-oncogene, the rat homologue of HER2, was originally described after DNA isolated from nitrosoethylurea induced rat neuroblastomas was transfected into fibroblasts, causing the induction of focus formation (Shih *et al.*, 1981). Subsequently, DNA prepared from these transformed foci was used again in a focus assay to determine that this gene encoded for a phosphoprotein of 185 kDa (Padhy *et al.*, 1982). This 185 kDa protein was then detected through cross-reaction with a polyclonal antibody against EGFR, suggesting homology to this receptor (Schechter *et al.*, 1984). Using *v-erbB*, a retroviral counterpart of *c-EGFR*, as a screening probe, the cDNA encoding ***Human EGF Receptor 2*** (*HER2*) was isolated and was found to correspond to the chromosomal location of p185 (Coussens *et al.*, 1985; Schechter *et al.*, 1985). The rat homolog was cloned (Bargmann *et al.*, 1986) and after comparison of the transforming cDNA (*neuNT*) to the wild type cDNA (*neu*) in both focus assays and

sequence comparison, it was noted that there was a single point mutation at base pair position 2012, causing the replacement of a valine residue with a glutamic acid (Bargmann *et al.*, 1986). This mutation was found to occur in the transmembrane domain and it was suggested that this mutation could cause the activation of the receptor without ligand activation (Bargmann *et al.*, 1986). After the identification and characterization of EGFR and Neu, homology screening resulted in the identification of two additional members of the EGFR family, ErbB3 and ErbB4, as discussed above.

When the entire EGFR family is compared at the amino acid level, it should be noted that they share all of the protein motifs originally identified in the EGFR. Structurally, these receptors contain two cystein rich motifs in the extracellular region of the protein that were observed to be conserved at 36-48% in comparison to the EGFR. Additionally, there is a single pass transmembrane domain. In the intracellular region of the protein there is a well conserved kinase domain and a C-terminus region containing numerous tyrosine residues, conserved at 24-33% with respect to the EGFR. The kinase domain is approximately 80% identical in Neu and ErbB4 when compared to EGFR, while ErbB3 is only 59% similar (Earp *et al.*, 1995) (See the schematic in Figure 1.2). Three residues that are conserved in the kinase domain of numerous protein kinases, including the EGFR family, have been lost in ErbB3. Moreover, the kinase activity of ErbB3 is greatly reduced in comparison to the EGF receptor (Guy *et al.*, 1994). This impaired kinase activity is not due to an inability of ErbB3 to bind ATP, but is due to impaired phosphotransfer from ATP to the tyrosine residues in the carboxy terminus (Knighton *et al.*, 1993; Guy *et al.*, 1994). In addition to having homology within the

Figure 1.2 – Signalling Mediated by the EGFR family and their Ligands

The ligands bound by the EGFR family are shown divided into the three groups that bind EGFR, ErbB3 and ErbB4 or EGFR and ErbB4. Additionally, Muc4, composed of ASGP1 and ASGP2 with the two EGF like domains (black boxes) is shown facilitating the interaction between ErbB2 and ErbB3. The structure of the various EGFR family members is shown and the star adjacent to ErbB3 denotes the inactivity of the kinase domain. While the adaptor molecules are not shown interacting with the ErbB2 / ErbB3 heterodimer, this dimer is capable of activating signalling cascades such as the PI3'K and Ras. The activation of Ras results in the activation of the MapK pathway culminating in the activation of Cyclin D1 to mediate entry into S phase.

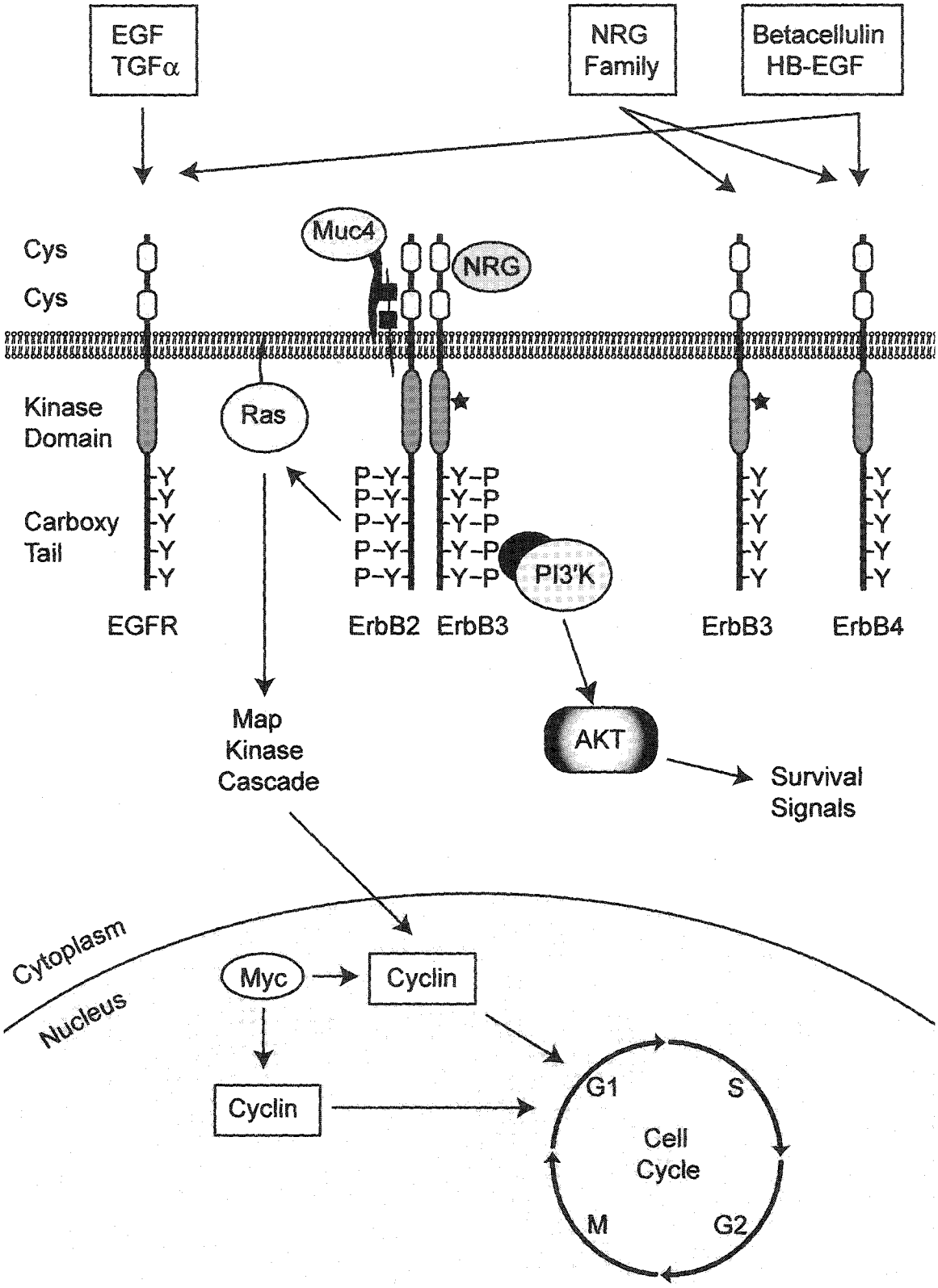
EGF
TGFα
NRG
Family
Betacellulin
HB-EGF
Cys
Cys
Muc4
NRG
Kinase
Domain
Ras
Carboxy
Tail
Y
P-Y
Y-P
PI3'K
EGFR
ErbB2
ErbB3
ErbB3
ErbB4
Map
Kinase
Cascade
AKT
Survival
Signals
Cytoplasm
Nucleus
Myc
Cyclin
Cyclin
G1
S
Cell
Cycle
M
G2

same species, these proteins are also well conserved between various model organisms. For example, a comparison of sequence homology between *erbB2* and *neu* cDNAs revealed fewer than 10% of divergent base pairs (S. Brown and W.J. Muller, unpublished observations).

As discussed above, the EGFR family contains a kinase domain that can phosphorylate the tyrosine residues contained in the carboxy terminus of the protein. This kinase domain is typically activated after ligand mediated dimerization. This was initially characterized for the EGF receptor, but was subsequently extended as a method of activation to the entire family (Dougall *et al.*, 1994; Hynes and Stern, 1994; Heldin, 1995). While ligand induced homodimerization can cause the induction of kinase activity for the EGFR, no ligand has been described for Neu. However, this orphan receptor tyrosine kinase can function through heterodimerization with other family members that have bound a ligand. (This is discussed more completely in section 1.5.3.)

Ligand receptor interactions that mediate dimerization are one clearly defined mechanism to activate kinase activity and tyrosine phosphorylation in the EGFR family, however alternative mechanisms have also been characterized for the activation of *neu*. The valine to glutamic acid point mutation observed in the *neuNT* cDNA is also capable of inducing the kinase activity of this receptor (Bargmann and Weinberg, 1988; Weiner *et al.*, 1989). One of the theories extended for the constitutive activation of this receptor was that the mutation fostered NeuNT oligomerization (Weiner *et al.*, 1989). Interestingly, further studies into tumorigenesis induced by overexpression of Neu resulted in the identification of several additional mutations. Numerous mutations were

observed in the extracellular domain juxtaposed to the transmembrane domain in Neu induced tumors (Siegel *et al.*, 1994). Upon further examination, the deletions were found to affect conserved cystein residues in the extracellular domain and were shown to induce dimerization, likely through the formation of disulphide bonds between the receptors (Siegel and Muller, 1996). Although these types of mutations have not been observed in human tumors, a human splice variant that bears remarkable homology to the deletion mutants has been identified. However, upon examination of expression levels, the proportion of this splice variant in comparison to the wild type mRNA was observed to be low. Indeed, this splice variant was only observed at 5% of the wild type mRNA level (Siegel *et al.*, 1999). These types of mutations illustrate a second mechanism to activate the kinase domain of Neu.

In addition to ligand mediated activation and mutational activation as two methods to induce dimerization and activity of the Neu kinase domain, another alternative has been offered for Neu. Amplification and overexpression of wild type *neu* mRNA and the resulting protein has been identified in a large percentage of human breast cancers. Overexpression of the wild type *neu* cDNA has been illustrated to cause focus formation in NIH 3T3 fibroblasts (Di Fiore *et al.*, 1987), but expression of the same cDNA at reduced levels is not associated with transformation (Bargmann *et al.*, 1986; Samanta *et al.*, 1994). It has also been illustrated that the extent of phosphorylation of Neu corresponds to the extent of expression, suggesting that high levels of the receptor may promote homodimerization (Stern *et al.*, 1988). Taken together, it can be seen that

activation of the Neu kinase domain can occur through ligand mediated heterodimerization, mutation or overexpression of the wild type allele.

1.5.2 EGFR Family Ligands

The EGFR family has been shown to bind numerous ligands in various tissues, however a distinct specificity of ligands for various receptors exists and is briefly outlined here. The EGF receptor has been shown to bind several ligands including EGF, TGFα and amphiregulin (Normanno *et al.*, 1994), as well as heparin binding EGF, epiregulin and betacellulin (Riese *et al.*, 1998), resulting in the activation of the kinase domain. In addition to binding to the EGF receptor, heparin binding EGF, betacellulin and epiregulin have been illustrated to bind to ErbB4 but have been shown to cause differential phosphorylation of these two receptors in a ligand dependent manner (Riese *et al.*, 1998). There is an additional class of ligands that have been shown to bind only to ErbB3 and ErbB4 which is composed of the neuregulins (NRG or NDF) which have alternative gene products including heregulins, glial growth factor and acetylcholine receptor inducing activity (ARIA). Many of the ligands in this class are alternative splice forms from the NRG-1 and NRG-2 loci (Fischbach and Rosen, 1997) and the activity of many of these NRGs is dependent on a single domain, the EGF-Like domain, for their activity (Fischbach and Rosen, 1997) (Summarized in Figure 1.2).

Although many studies have attempted to define a ligand for Neu, it still remains an orphan receptor. One potential ligand for Neu has been the ASPG2. Interestingly, ASGP2 has two EGF-Like domains with high homology to the EGF-like domain found

in the NRGs (Sheng *et al.*, 1990; Sheng *et al.*, 1992) and when ErbB2 and ASGP2 are co-infected into an insect cell line lacking all known EGFR family members, ErbB2 phosphorylation is observed (Carraway *et al.*, 1999). However, ASGP2 is a membrane bound protein that interacts with ASGP1 in the extracellular domain to form Muc4, a sialomucin complex that is postulated to facilitate heterodimerization and phosphorylation of Neu by enhancing the interaction with the other EGFR family members (Sheng *et al.*, 1992) and is therefore not thought to be a ligand (Figure 1.2). Interestingly, ASGP2 has been shown to be involved in various tumors and is potently repressed by TGFβ in the mammary gland (Carraway *et al.*, 2000). While not a ligand for Neu, the interaction of ASGP2 and entire Muc4 complex with the EGFR family to facilitate dimerization is an interesting facet of EGFR family regulation.

1.5.3 Signalling Pathways Activated by the EGFR family

Given the wide variety of ligands that are capable of interacting with the EGFR family, it is not surprising that there are numerous divergent signal transduction cascades that can be activated by these growth factor receptors. An examination of the carboxy terminus of Neu reveals a number of tyrosine residues that are phosphorylated after dimerization and activation of the kinase domain and these phosphorylated residues may then interact with various adaptor molecules (Hazan *et al.*, 1990; Akiyama *et al.*, 1991). The phosphotyrosine and surrounding amino acids provide and determine potential binding domains in the carboxy terminus of Neu for molecules containing Src Homology 2 (SH2) regions (Pawson, 1995) or phosphotyrosine binding (PTB) domains (Kavanaugh

et al., 1995). Briefly, a number of molecules can associate directly with the phosphorylated Neu including; Grb7 (Stein *et al.*, 1994), c-src and c-yes (Muthuswamy and Muller, 1994; Muthuswamy and Muller, 1995), CHK (Zrihan-Licht *et al.*, 1997), Grb2 (Stein *et al.*, 1994), Shc and Ras-GAP (Reviewed in (Dankort and Muller, 1996). The interaction of these various docking proteins with the C-terminus of the EGFR family members results in the activation of several distinct cascades, including the signalling pathways downstream of Ras and Src (Reviewed in (Dankort and Muller, 1996)(Figure 1.2).

In addition to the various pathways activated by Neu homodimers, there are several additional proteins that bind to the other EGFR family members. Indeed, heterodimerization of the various EGFR family members can result in the specific activation of unique pathways that can mediate a variety of responses. For example, heterodimerization with Neu can result in the interaction of PLCγ1 (Peles *et al.*, 1991), PTP1D (Vogel *et al.*, 1993), and the p85 subunit of phosphadityl inositol 3' kinase (PI3'K) (Prigent and Gullick, 1994) with the various EGFR receptors. Interestingly, multiple binding domains for PI3'K (YXXM) are only found in ErbB3 (Prigent and Gullick, 1994). Coupled with the reduction in the kinase activity of ErbB3, this suggests ErbB3 heterodimers stimulate the PI3'K cell survival pathway (Tansey *et al.*, 1996). ErbB2/ ErbB3 mediated activation of PI3'K (Kita *et al.*, 1994; Soltoff *et al.*, 1994) has been implicated in stimulation of a number of important cell survival elements including Akt serine kinase (Burgering and Coffer, 1995; Franke *et al.*, 1995). One result of activation of Akt is the corresponding phosphorylation of Bad and the activation of Bcl2

(Alessi and Cohen, 1998; Blume-Jensen and Hunter, 2001). Taken together, the selective activation of AKT and cellular survival mechanisms illustrates that specificity in signal transduction is possible through differential homo and heterodimerization.

Consistent with the concept of differential signalling mediated through homo and heterodimerization is the idea that specific EGFR family ligands induce differential signals. Indeed, since ligands such as EGF and TGFα bind exclusively to EGFR, they will not activate PI3'K signalling unless EGFR heterodimerizes with ErbB3. This concept of differential signalling (Sweeney and Carraway, 2000) can then be extended by examining which EGFR family members are expressed in the cell or tissue of interest to determine what pathways may be activated.

1.6 Mouse Models of Mammary Tumorigenesis

1.6.1 Effects of Mammary Specific Overexpression of Oncogenes

The molecular basis underlying the change from a normal mammary epithelial cell to a tumorigenic state is a basic tenet that has been examined through numerous mouse models. Several of these basic models are briefly discussed to illustrate what is known of the progression of this disease.

Amplification and overexpression of c-myc has been observed in human breast cancer (see Section 1.2), and placing this proto-oncogene under the control of the Mouse Mammary Tumor Virus (MMTV) Long Terminal Repeat Promoter Enhancer resulted in high levels of mammary specific expression in the epithelium. Consequently, these transgenic mice developed adenocarcinomas (Stewart *et al.*, 1984). Interestingly, when

myc expression was induced under the control of a tetracycline inducible system, tumor formation was noted that was reversible in many instances simply by removing expression of the *c-myc* transgene (D'Cruz *et al.*, 2001). The tumors that did not regress following repression of the transgene expression were found to contain mutations in K-ras (D'Cruz *et al.*, 2001). This mouse model clearly illustrates the multistep pathway involved in tumorigenesis, suggesting that activation of the Ras pathway is integral to c-myc mediated tumor formation. Since Ras has been shown to be an essential component of Myc mediated tumorigenesis, mice engineered to express *ras* under the control of the MMTV promoter were developed. These MMTV-Ras transgenics developed mammary gland carcinomas with a latency of just over 5 months. However, when the MMTV-Ras mice were interbred with the MMTV-Myc mice, a synergistic effect was seen in the reduction of tumor latency and in the increase of tumor penetrence in these transgenic strains (Sinn *et al.*, 1987). Although tumors arose more rapidly with the overexpression of these two potent oncogenes, it was suggested that the tumors required multiple additional activating mutations since the tumors were focal in nature (Sinn *et al.*, 1987).

One of the molecular targets of Myc is Cyclin D1 and Myc mediated activation of Cyclin D1 has been shown to induce entry into the S phase of the cell cycle. As previously discussed, *cyclin D1* amplification is observed in human breast cancer (See Section 1.2). Overexpression of *cyclin D1* under the control of the MMTV promoter resulted in significant lobuloalveolar development shortly after the termination of puberty. Moreover, after a long latency these mice developed focal mammary tumors

(Wang *et al.*, 1994). Taken together, these model systems have illustrated the roles of Myc, Ras and Cyclin D1 in the progression of mammary tumorigenesis.

One molecule that has been identified to activate the Ras pathway, culminating in Myc and Cyclin D1 activation, is the Polyomavirus Middle T antigen (MT). Expression of MT under the control of the MMTV promoter resulted in multifocal mammary tumors after a very short latency (Guy *et al.*, 1992). In comparison to the MMTV-Ras and MMTV-Myc models, there is an extremely short tumor latency, suggesting that the other pathways activated by MT, such as the Src pathway, are also playing an important role in tumorigenesis. Perhaps the most interesting facet of this tumor model is the pulmonary metastasis associated with tumor development which is dependent on the activity of the PI3'K pathway (Webster *et al.*, 1998). Like the MT antigen, HER2 has been shown to be capable of activating Ras, Src and PI3'K through homo or heterodimerization and unlike MT, HER2 is amplified and overexpressed in human breast cancer.

1.6.2 Mouse Mammary Models Expressing EGFR family members and Ligands

Amplification and overexpression of HER2 has been noted in a large proportion of human breast cancers. Consistent with the human data, when the activated rat homologue was placed under the control of the MMTV promoter it resulted in rapid tumorigenesis (Muller *et al.*, 1988; Bouchard *et al.*, 1989; Guy *et al.*, 1996). Importantly, these experiments defined NeuNT as playing a causal function in the etiology of breast cancer. While the MMTV-NeuNT mice developed multifocal mammary adenocarcinomas in 50% of female mice by 89 days, these mice were expressing an

activated cDNA which had no comparable mutations in the human allele (Muller *et al.*, 1988). Thus, to examine the oncogenic potential of the wild type allele in the mammary epithelium, transgenic mice were created that expressed with wild type *neu* cDNA under the transcriptional control of the MMTV promoter. These animals developed focal mammary tumors in 50% of female mice by 205 days, with frequent metastases in the lungs (Guy *et al.*, 1992). It was later observed that the tumors in these mice contained activating mutations in the extracellular domain of *neu*, juxtaposed to the transmembrane domain, suggesting that the wild type cDNA required somatic mutations for oncogenic transformation (Siegel *et al.*, 1994). Further, when transgenic mice were created that had two of these type of mutations in *neu* under the transcriptional control of the MMTV promoter, tumor latency was observed to be intermediate between the activated and wild type Neu transgenics (Siegel *et al.*, 1999). Taken together, these results strongly suggest that both overexpression and activation of Neu play integral yet separate roles in mediating tumor formation. Moreover, ErbB3 overexpression has been noted in tumors from several lines Neu transgenic mice (Siegel and Muller, 1996), suggesting that ErbB2 / ErbB3 heterodimers are required for tumorigenesis. Consistent with the activation of both mitogenic and anti-apoptotic pathways by an ErbB2 / ErbB3 heterodimer, recent *in vitro* results have suggested that the ductal lumen can only be filled in a model of ductal carcinoma in situ (DCIS) with the expression of both a proliferative signal and an anti-apoptotic signal (Debnath *et al.*, 2002). These *in vivo* and *in vitro* results suggest that ErbB2 / ErbB3 heterodimers play a pivotal role in mediating tumorigenesis.

While the mouse models expressing the various Neu alleles under the control of the MMTV promoter have demonstrated the causal role that this gene plays in tumor formation, the remainder of the EGFR family should also be examined. Indeed, since EGFR expression has been noted in carcinomas of the breast (Bauknecht *et al.*, 1989; Klijn *et al.*, 1992) it was examined in a mouse model to determine whether EGFR had a causative role in tumor induction. Expression of EGFR under the control of the MMTV promoter resulted in enlarged ducts and numerous hyperplastic alveolar nodules with tumor development only after numerous pregnancies (Brandt *et al.*, 2000). This data suggests that overexpression of EGFR in the mammary epithelium can predispose the gland to tumor formation. During the identification of ErbB3 and ErbB4, their expression was noted to be elevated in several breast cancer cell lines (Kraus *et al.*, 1989; Plowman *et al.*, 1993). Moreover, ErbB3 was shown to be elevated in over 20% of human breast cancers (Lemoine *et al.*, 1992). Although mice overexpressing ErbB3 or ErbB4 in the mammary gland have not yet been described, recent work has suggested that ErbB4 may act as a tumor suppressor since a mammary specific knockout of ErbB4 accelerated Neu mediated tumor formation (E.R. Andrechek, D.F. Stern and W.J. Muller, unpublished results). Consistent with this, a comparison of constitutively activated ErbB2 and ErbB4 revealed that unlike ErbB2, activated ErbB4 did not cause the induction of cell proliferation, suggesting again that ErbB4 may act to suppress tumor formation (Penington *et al.*, 2002). These results serve to underscore the differential signalling and cellular responses possible in normal and tumor biology through homo and heterodimerization of the various EGFR family members.

Given the importance of differential signalling in tumor biology and the variability of heterodimerization mediated through the various EGFR family ligands, the overexpression of ligands for the EGFR family has also been examined in mouse model systems. Two examples are presented here, TGFα which binds to the EGFR receptor and NRG which binds to ErbB3 or ErbB4 and can cause heterodimerization with ErbB2. Murine models overexpressing TGFα in the mammary gland were characterized as having alveolar and terminal duct hyperplasia that progressed to adenocarcinomas after a long latency (Jhappan *et al.*, 1990; Matsui *et al.*, 1990; Sandgren *et al.*, 1990; Halter *et al.*, 1992; Sandgren *et al.*, 1995; Muller *et al.*, 1996). In contrast to the small proportion of TGFα transgenics susceptible to tumor formation, the expression of NRG under the transcriptional control of MMTV resulted in a complete penetrence of tumor formation in female mice, albeit with a long latency (Krane and Leder, 1996; Muller *et al.*, 1996). Interestingly, phosphorylation of the kinase deficient ErbB3 receptor, but none of the other EGFR family members, was noted in cell lines derived from a tumor from these transgenic mice (Krane and Leder, 1996). Collectively these observations have illustrated the varied potential for tumor development through the ligand mediated activation of the EGFR family of receptor tyrosine kinases.

1.6.3 Combinatorial Crosses to Elucidate the Importance of Neu Mediated Signalling Pathways

The various transgenic strains expressing Neu alleles under the control of the MMTV promoter have described how activation of Neu appears to be a critical step in

the induction of mammary tumors. Additional evidence implicating Neu and the importance of various pathways that it funnels through has been derived through combinatorial crosses with other lines of mice. For example, interbreeding the MMTV-TGFα mice with the MMTV-Neu line resulted in the synergistic reduction of tumor latency, indicating that Neu and TGFα can cooperate to induce mammary tumorigenesis (Muller *et al.*, 1996). The advent of gene targeting to ablate specific genes has allowed the importance of specific signalling molecules to tumor formation to be determined. Since Neu mediated tumors are thought to mediate their mitogenic effects through the Ras / MapK pathway (See Figure 1.2), the importance of genes such as Cyclin D1 could now be assessed through interbreeding Cyclin D1 deficient mice to the MMTV-Neu mice. Indeed, when this experiment was completed for MMTV transgenic mice expressing Neu, Ras, Myc or Wnt in a Cyclin D1 deficient background, tumors failed to develop in the Neu and Ras transgenic mice (Yu *et al.*, 2001). Although these observations suggest that Neu and Ras signaling funnel through Cyclin D1, it is important to note that these effects may also be due to the mammary phenotype of the Cyclin D1 knockout mice. However, if there is an absolute dependence on Cyclin D1 for tumorigenesis mediated by Neu, these observations immediately suggest intervention possibilities for the human breast cancer.

1.6.4 Relevance and Suitability of the Various Mouse Models

Mouse models have provided a tremendous opportunity to examine the various molecules involved in the progression of breast cancer. Importantly, a survey of various

models has revealed that there are numerous pathological similarities to the human disease (Cardiff *et al.*, 2000). In addition to modelling the progression of the human disease, much has been learned of the role of these genes in the biology of mammary gland development and function. An examination of the similarities and differences of the mammary gland in both mouse and human has revealed only slight differences in both the lobules that form and in the tissues surrounding the lobuloalveolar subunits. In humans, the lobules are surrounded by loose stroma which is then surrounded by a dense layer of connective tissue. However, in the rodent mammary gland the lobules are surrounded by diminutive amounts of connective tissue and are embedded in a large fat pad (Russo *et al.*, 1990). In addition, the human mammary gland also contains a greater number of more differentiated lobules than the rodent (Russo *et al.*, 1990). Other than these differences, the architecture of the normal mouse and human mammary glands is remarkably similar. In addition to the similarities in normal development, there are distinct parallels between breast cancer in the mouse and in humans.

Tumor progression in humans is a well characterized process with graded stages of tumor development dependent on the histological examination of the tumor, the involvement of the surrounding tissue, presence in the lymph nodes and potential sites of metastasis. On the whole, this detailed characterization has not been completed in most mouse models and the similarities cannot be established (Cardiff *et al.*, 2000). However, the tumors that develop in several lines of transgenic mice do mimic the histological abnormalities observed in human tumors with alterations in the expression of the same gene. For example, overexpression of HER2 is often noted in ductal carcinoma in situ

(DCIS) in humans, and was also observed in mouse models overexpressing Neu (Cardiff and Wellings, 1999). The similarities in the normal biology and tumor development indicate the utility of the mouse to model the human mammary gland.

During the comparison of various transgenic mouse models and the associated human cancers, it is interesting to note that the causal genetic event results in a distinct pathology in the tumor. Indeed, based on the phenotype of the tumors that formed in the mouse models, it is possible to predict the genotypic event causing the tumor (Cardiff *et al.*, 1991). For instance, while Neu and Ras mediated tumors are associated with poorly differentiated cells containing abundant cytoplasm, Wnt mediated tumors are more differentiated and form structures reminiscent of branched ducts (Rosner *et al.*, 2002). These phenotypic differences were based on the initiating oncogenic event and suggest that there should be molecular differences associated with these tumors. Consistent with this concept, tumors caused by overexpression of Neu and Ras were seen to express several neoplastic marker genes that were not observed in Myc or Wnt mediated tumors (Morrison and Leder, 1994). These results have been extended through the advent of gene expression profiling and the comparison of tumors derived from several lines of transgenic mice have revealed that there are distinct divergent markers of the various tumors (Desai *et al.*, 2002), suggesting therapeutic applications based on the initiating events. Moreover, when various human breast cancers were compared, the gene expression results observed in the mouse models were replicated in the human disease (Perou *et al.*, 2000). This data has suggested that the various mouse model systems elicit

similar molecular responses to the human condition dependent on the initiating oncogenic event which is then also reflected in the pathology of the tumor.

Although the transgenic mouse models expressing various genes under the control of the MMTV promoter have striking similarities to the human condition and have elucidated the importance of various signal transduction pathways, these mice may not be ideal models of tumorigenesis. Indeed, given the hormonal cues that are integral to mammary gland development and tumor growth, it is disquieting to observe that the MMTV promoter is also hormonally responsive. While the MMTV promoter is active in several tissues including the mammary gland, the highest levels of MMTV directed transgene expression occurs in the mammary gland during pregnancy (Choi *et al.*, 1987; Henrard and Ross, 1988). This tissue and hormonal specific regulation of the MMTV promoter is due to several well characterized domains within the promoter. One of these domains, the Hormone Response Element (HRE) interacts with a hormone bound receptor (Mitchell and Tjian, 1989) that causes a 10-50 fold induction of MMTV directed transcription (Parks *et al.*, 1974). However, this tissue specific expression is not only due to the hormonal control of the promoter but it is also dependent on promoter methylation. For example, MMTV directed transgene expression is not commonly observed in tissues such as the liver where the MMTV promoter is found to be highly methylated. Whereas in the mammary gland, where MMTV directed expression is noted, the MMTV promoter has been found to be unmethylated (Mangues *et al.*, 1995). Given the creation of a number of knockout and transgenic mouse models in different genetic backgrounds, it is important to recognize that the MMTV methylation and silencing in the mammary gland

is more likely to occur in strains such as C57 and balb/c as opposed to the FVB strain (Breznik *et al.*, 1984; Chaillet *et al.*, 1995; Weichman and Chaillet, 1997). Thus, MMTV driven transgene expression may not accurately reflect the human condition and clearly illustrates the requirement for more relevant mouse models.

1.7 Expression and Role of the EGFR family in other tissues

1.7.1 Embryonic Development

The various transgenic mouse models have illustrated a causal role for ErbB2 in mediating mammary tumorigenesis but analysis of the function of ErbB2 in mammary gland biology has been hampered due the phenotype observed in the ErbB2 null mice. Indeed, the germline ablation of ErbB2 has resulted in the identification of a number of phenotypes in tissues other than the mammary gland that are instructive in understanding the importance of ErbB2. Moreover, a detailed examination of the role of the EGFR family may lead to better treatments for breast cancer due to the knowledge of the role these genes play in other tissues. For example, the germline ablation of ErbB2 resulted in cardiac abnormalities (Lee *et al.*, 1995) in mice. These data are in accordance with the observation that Herceptin treatment for HER2 mediated breast cancer resulted in cardiac dysfunction in 28% of human patients (Slamon *et al.*, 2001; Sparano, 2001).

The germline ablation of ErbB2 resulted in embryonic lethality at 10.5 days post coitum and was associated with defects in cardiac development. Specifically, these embryos did not form cardiac trabeculae, the tissue associated with the maintenance of blood flow during the development of the heart (Lee *et al.*, 1995). While the lack of

cardiac trabeculation was thought to be the primary cause of embryonic lethality in these mice, additional defects in neural development were noted. The embryonic lethality associated with inactivation of erbB2 has previously been rescued by myocardial expression of an *erbB2* transgene (Morris *et al.*, 1999; Woldeyesus *et al.*, 1999; Lin *et al.*, 2000). However, these mice die at birth due to loss of motor neurons and defects in Schwann cell development. To avoid this perinatal lethality, specific deletions may be created to address the role of ErbB2 in various adult tissues through the use of the Cre / LOXP1 recombinase system (Sternberg *et al.*, 1981; Gu *et al.*, 1994). This approach has previously been used to generate peripheral nerve specific deletion of ErbB2 that resulted in the extensive demylenation of the nerves (Garratt *et al.*, 2000).

Gene targeting experiments have revealed that the other EGFR family members also play critical roles in regulating development. For example, germline ablation of ErbB4 resulted in embryonic lethality that resembled ErbB2 mediated lethality at day 10.5 of embryogenesis due defects in cardiac and neural development (Gassmann *et al.*, 1995). Although inactivation of ErbB3 function had a less severe impact on cardiac development, embryonic lethality is also observed due to defects in neural and Schwann cell differentiation (Erickson *et al.*, 1997; Riethmacher *et al.*, 1997; Britsch *et al.*, 1998). Interestingly, elimination of EGFR receptor function results in a strain dependent perinatal lethality (Threadgill *et al.*, 1995; Hansen *et al.*, 1997; Sibilia *et al.*, 1998). Thus the entire EGFR family appears to be critical for normal development of the mammalian embryo, which can preclude the study of these genes in adult tissues.

1.7.2 Muscle Development

The germline ablation of ErbB2 resulted in embryonic lethality, preventing the examination of the role of this gene in the development and maintenance of other adult tissues. When the expression pattern of ErbB2 was surveyed in the adult mouse it was noted that ErbB2 was expressed in skeletal muscle and was concentrated at the neuromuscular junction (NMJ) along with ErbB3 and ErbB4 (Altiok *et al.*, 1995; Moscoso *et al.*, 1995; Zhu *et al.*, 1995). EGFR family members have been implicated as important functional components of the NMJ (Jo *et al.*, 1995). In addition to the EGFR family members, neuregulins (NRG) serve as ligands for ErbB3 and ErbB4 and are released from the motor neuron end plate where they are thought to activate these receptor tyrosine kinases (Moscoso *et al.*, 1995). Heterodimerization and tyrosine phosphorylation of ErbB2 / ErbB3 has been shown to regulate the expression of various subunits of the acetylcholine receptor and is thought to be an integral part of the switch from the juvenile to adult acetylcholine receptor (Si *et al.*, 1996; Tansey *et al.*, 1996; Won *et al.*, 1999). During the development of the NMJ, the γ subunit in the juvenile acetylcholine receptor (composed of $\alpha 2\beta\gamma\delta$) is replaced by a ε subunit during the first week of postnatal development. It has been shown that this switch in acetylcholine receptor subunits is likely due to the stimulation of ErbB2 / ErbB3 heterodimers by ARIA (Missias *et al.*, 1996). Furthermore, the ARIA mediated increase in ε subunit expression has been shown to require Shc interaction with an EGFR family member (Won *et al.*, 1999). The importance of the maturation of the acetylcholine receptor and the subunit switch has been illustrated through the generation of mice lacking the gene encoding the

ε subunit. These mice suffer from premature death 2-3 months after birth due to progressive muscle weakness and impaired neuromuscular transmission (Witzemann *et al.*, 1996; Missias *et al.*, 1997). These results strongly suggest that ErbB2 / ErbB3 heterodimers play a critical role in the development of the neuromuscular junction.

1.8 Experimental Rationale

Amplification and overexpression of HER2 has been observed in a significant proportion of human breast cancer (Slamon *et al.*, 1987; Slamon *et al.*, 1989). Overexpression of the activated rat homologue, NeuNT, under the control of the MMTV promoter revealed a causal role in breast cancer for this receptor tyrosine kinase, as did several subsequent mouse models with various *neu* alleles (Muller *et al.*, 1988; Guy *et al.*, 1992; Siegel *et al.*, 1999). However, due to the hormonal control and potency of the viral MMTV promoter, these mouse models may not accurately reflect the human condition. Accordingly, I placed an activated *neu* allele under the control of the endogenous promoter so that the expression and hormonal response in the ensuing mammary glands and tumors would better mimic the human condition. Due to the embryonic lethality associated with the ablation of *neu*, this was done in a mammary specific manner (Andrechek *et al.*, 2000). Chapter 3 describes the generation and characterization of this tissue specific activation of NeuNT. The tumors that developed in this conditional model system were then compared to MMTV-Neu induced tumors to determine how each model reflected the human condition. However, the tissue specific activation of Neu resulted in tumors with an exceedingly long latency. Therefore, in an

attempt to reduce the latency I also describe the generation and characterization of mice expressing NeuNT under the control of the endogenous promoter in the germline of mice.

While previous experiments and the results presented in Chapter 3 have defined the effect of overexpression of an activated *neuNT* allele in mammary gland biology, the development of a mammary gland deficient in Neu expression has not previously been described. These studies have previously been limited due to the embryonic lethality associated with the germline ablation of Neu (Lee *et al.*, 1995). Consequently, I have engineered mice with a mammary specific deletion for Neu and have examined the impact on mammary gland development, function and tumorigenesis. These results are presented in Chapter 4. However, Neu expression is not only noted in the mammary epithelium in wild type mice. Given the expression and postulated role of ErbB2 in skeletal muscle and in neuromuscular junction development, I have also generated mice that lack Neu specifically in skeletal muscle (Andrechek *et al.*, 2002). These mice have not only illustrated a novel role for Neu in the skeletal muscle, but have also begun to establish the involvement of Neu in a reciprocal signalling loop between the muscle and its afferent. These results have clearly identified the importance of examining the function of genes in an *in vivo* model system to understand development and tumor biology.

CHAPTER 2

MATERIALS AND METHODS

2.1 Plasmid Constructs

The construction of the vectors used to create the MMTV-Cre, FloxNeo NeuNT and Flox Neu mice was previously described in detail in a previous thesis (Andrechek, 1997). Accordingly, these three constructs are discussed only briefly.

To create the plasmid used to derive the MMTV-Cre transgenics, the 1.5 kb *Cre* cDNA was ligated into the p206 vector containing the MMTV promoter enhancer and the SV40 poly adenylation signal. To prepare the MMTV-Cre injection fragment for microinjection, the plasmid was linearized using a Sal1 / Spe1 digest. The injection fragment was isolated after electrophoresis on a 1% agarose gel and was prepared as described previously (Sinn *et al.*, 1987).

To derive the FloxNeo NeuNT construct, the 1.8 kb neomycin cassette (Neo) containing the PGK promoter, the *neomycin* cDNA and an HSV poly adenylation sequence was flanked by loxP sites. The loxP oligo contains the loxP sequence, a Sac1 site and is flanked by a T and G to recreate the EcoR1 and HindIII restriction sites when this oligo is ligated next to EcoR1 or HindIII sites that have been filled in using DNA Polymerase I (Klenow). Once the loxP flanked Neo was derived, it was ligated into the NeuNT targeting vector as a HindIII fragment and the correct orientation was determined

through a BamHI digest. The NeuNT targeting vector contained 5' arm of homology and a 3' arm of homology that were used to direct homologous recombination to the genomic ErbB2 locus. The targeting strategy replaced exon one of the genomic *erbB2* allele with the sequences contained between the arms of homology. The FloxNeo NeuNT targeting vector contained the loxP flanked Neo, followed by the *neuNT* cDNA and a HSV poly adenylation sequence between the arms of homology. This strategy placed the loxP flanked Neo *neuNT* cDNA under the control of the endogenous promoter. However, due to the poly adenylation sequence in the Neo cassette, the *neuNT* cDNA was not designed to be expressed until the Neo cassette was removed through the expression of Cre Recombinase. This plasmid was restricted by Not1 to linearize the construct prior to electroporation of embryonic stem cells.

The construction of the Flox Neu targeting vector used the same regions of homology to direct recombination as did the FloxNeo NeuNT vector. However, the loxP sites flanked the wild type *neu* cDNA in this construct. The final vector harbored a loxP flanked *neu* cDNA, followed by a HSV poly adenylation sequence and this was followed by the Neo cassette described above without the addition of the loxP sites. The targeted strategy was designed to replace exon one with the *neu* cDNA under the control of the endogenous promoter until Cre mediated recombination occurred at which time a null allele would be created due to the poly adenylation sequence that would remain downstream of the endogenous ErbB2 promoter. This plasmid was restricted by Not1 to linearize the targeting construct prior to embryonic stem cell electroporation.

To derive the pJ4ΩFloxneo NeuNT Forward and Reverse constructs, the 5.8 kb EcoR1 fragment containing the loxP flanked Neo cassette and *neuNT* cDNA was ligated into the EcoR1 site of pJ4Ω. After determining the orientation of the loxP Neo *neuNT* insert, the plasmids containing the fragment in the correct orientation (Forward) and in the opposite orientation (Reverse) were kept.

To create the construct containing the fragment of *cre* cDNA for RNase protections, pGEM7 and the *cre* cDNA were restricted with BamH1 and Cla1 and were ligated together. pGEM7 plasmids containing the 450 bp insert were sequenced to determine that the portion of *cre* cDNA was free from mutations. The plasmids containing the PGK and Neu riboprotection probes were obtained from Peter Siegel.

To create probes for Northern analysis of amplified genes, RT-PCR was conducted on mouse RNA using the promoters specified in Table 2.1 for *MDGI, glycam1* and *serglycin.* Using 5' primers with an added EcoR1 site and 3' primers with an added BamH1 site, these three genes were cloned into the Bluescript vector (pBS). Plasmids were screened by digests and by sequence analysis and positive clones were used in large scale DNA preparations.

2.2 Embryonic Stem Cell Targeting

Embryonic stem cell (ES Cell) culture was performed on gelatinized plates, prepared by covering plates with 0.1% autoclaved gelatin (Fisher) for 5 minutes followed by aspiration. The ES Cells (R1 cells obtained from Janet Rossant) and fibroblasts were previously prepared by Rod Hardy. The media used to culture the cells was Dulbecco's

Table 2.1 List of Oligonucleotides Used

A list of the oligonucleotides used is shown. For each sequence, the name of the gene or sequence is shown. Unless otherwise specified, the sequence of the genes is murine in origin. The use of each set of primer pairs for the various genes is shown under the assay column. The primer sequences are shown in 5' to 3' orientation with the 5' primer listed first. As specified in the text, the underlined sequences correspond to the restriction sites added for cloning purposes.

Table 2.1 List of Oligonucleotides Used

Description	Assay	Primer Sequence
WDNM1	LightCycler	5' TCT TTG TTC TGG TAG CTT TGA TTT 3' 5' GTT TGC AGG CAT GAC CAC AG 3'
Epsilon Casein	LightCycler	5' CTT TTG GCC GTT GCT CTT G 3' 5' TTG CTG TAT CGT TTC ATT TTG TTC 3'
CEA10	LightCycler	5' TGG TAC AAG GGA AAC AGT GG 3' 5' CAA GGA GGG TAA AAG TGA GG 3'
GAPDH	LightCycler	5' TCA TGA CCA CAG TGG ATG CC 3' 5' GGA GTT GCT GTT GAA GTC GC 3'
Neu – Universal	LightCycler	5' CCC AGA TCT CCA CTG GCT CC 3' 5' TTC AGG GTT CTC CAC AGC ACC 3'
Neu – Rat Specific	LightCycler	5' AAC CAC GTC AAG ATT ACA GAT 3' 5' AAA TCA GGG ATC TCC CGG 3'
Serglycin	Northern	5' GAA TTC CTG TTT TGA TGG AAG GAC CC 3' 5' GGA TCC CGA GTT AAT GAG GAA AGG GG 3'
MDGI	Northern	5' GAA TTC ACC ATC ATC GAG AAG AAC GG 3' 5' GGA TCC TTA TTG ACC TTG GAG CAC CC 3'
Glycam1	Northern	5' GAA TTC ACC TCT CTT GCT CTC CTG CC 3' 5' GGA TCC TCA GAT GAG CAG AAT GTG GC 3'
LoxP1 Site	Cloning	5' TAG CTC ATA ACT TCG TAT AGC ATA CAT TAT ACG AAG TTA TG 3'

All nucleotides were generated by the MOBIX central facility. Underlined sequences correspond to restriction sites added for cloning purposes.

Modification of Eagle's Medium (dMEM) (Invitrogen) supplemented with Fetal Bovine Serum (Hyclone), MEM non-essential amino acids, Penicillin / Streptomycin, Glutamax, Sodium Pyruvate, Leukemia Inhibitory Factor (Invitrogen) and β-mercaptoethanol (Sigma). The linearized constructs were electroporated into the ES Cells using electroporation buffer (20 mM HEPES, 137 mM NaCl, 5 mM KCl, 0.7 mM Na_2HPO_4 (dibasic) 6 mM dextrose (D-glucose) and 0.1 mM B-mercaptoethanol). One day after the transfection, Genetecin (G418) was added at 0.2 mg per ml from a 2 mg/ml stock and media with G418 was changed daily. Once colonies had developed, 288 colonies were picked and grown before examining them for the recombination event. DNA was prepared from ES cells by the addition and overnight incubation in ES lysis buffer (10 mM Tris HCL pH8, 100mM NaCl, 10 mM EDTA, 0.5% SDS) supplemented with Protinase K (10 μl of 10 mg/ml stock in 500 μl). An equal volume of isopropanol was added and the plates were vigorously shaken for several hours before the DNA was extracted and resuspended in water. ES Cells that were positive for the targeted recombination event were expanded, rescreened for homologous recombination through Southern analysis using the external probe and were grown to confluency in a 6 cm plate prior to injection. Additional Southern blots were completed to ensure that the recombinant allele was correct in these ES cells selected for injection. A blastocyst injection of the various ES cell lines was performed by William Hardy using standard methods in the Central Animal Facility. Utility of the chimerics was assessed on the basis of coat color of the resulting pups and through Southern analysis.

2.3 Southern Analysis

DNA was extracted for Southern analysis (Southern, 1975) from tails, various tissues, tumors or ES Cells and was resuspended in 50 µl of water. 10 µl of DNA was digested overnight at 37°C with 70 units of high concentration enzyme. The digested DNA was then electrophoresed on a 0.8% agarose gel. After the transfer process to Hybond-N Nitrocellulose (Amersham Life Science), the membrane was fixed by UV crosslinking and was hybridized with ^{32}P dCTP (Dupont) labeled probes generated through random priming (Feinberg and Vogelstein, 1983). When necessary, Southern blots were quantitated by phosphoimager analysis. For extent of amplification, a control tissue without amplification was included and the relative intensity of the wild type and knock-in allele were multiplied to be set to equal levels. The relative intensities of the experimental samples were then multiplied by the same factors and the level of amplification was determined.

2.4 RNA Analysis

2.4.1 RNA Preparation

RNA was isolated from tissues and cells using the CsCl sedimentation gradient modification as previously outlined (Chirgwin *et al.*, 1979). Briefly, tissue was placed in 3 ml of Guanidinium thiocyanate (GIT) homogenization solution (4M GIT, 25 mM sodium citrate and 100mM β-mercaptoethanol), was homogenized and layered over 5.7 M CsCl. RNA was pelleted by centrifugation at 32 000 rpm at 18°C for at least 18 hours. The pellet was resuspended in sterile water with 300mM sodium acetate and was

precipitated with 2 volumes of 95% EtOH. RNA concentration was determined by absorption at 260 nm.

RNA was also isolated for Affymetrix GeneChip analysis using the RNeasy Midi Kit (Qiagen) following the manufacturer's directions. RNA was resuspended and concentration was determined as above. Affymetrix GeneChips were conducted on a pay per service basis by the OHRI gene expression facility and the data was analyzed using Microsoft Excel 2000.

2.4.2 RNase Protection Analysis

RNase protection assays were performed as previously described (Melton *et al.*, 1984). Briefly, the riboprobes were constructed in Bluescript vectors and were designed to be restricted with blunt cutters or 5' overhangs. Linearized probes were purified after gel electrophoresis using Glassmilk (Geneclean) and after quantification, 1 μg was used to synthesize the labeled probe. Synthesis occurred in a cocktail containing 1 μg of template, 15 mM DTT, 40 U RNAguard (Pharmacia), the appropriate transcription factor and associated buffer, 100 μCi ^{32}P UTP, 1 mM of rATP. rCTP, rGTP and 0.1 mM of rUTP. The reaction proceeded for 45 minutes at 37 degrees, was spiked with an additional 30 U of the appropriate transcription factor and allowed to proceed for an additional 30 minutes. Termination of the reaction was accomplished with 1 μl of 0.5M $MgCl_2$ and 20 U of RNase free DNase I (Beohringer) at 37 degrees. The labeled probe was purified by a phenol chloroform extraction and was precipitated in the presence of a yeast tRNA carrier by ethanol / sodium acetate precipitation at -80°C. After synthesis of

the riboprobe, 30 μg of total RNA, 1μl of experimental probe and 1 μl of control probe were incubated in 40 mM piperazine-N, N'-bis (2-ethanesulfonic acid) (PIPES) buffer and in 80% deionized formamide at 85°C for 5 minutes and then 50°C overnight. The experimental samples were digested with 300 μl of 300 mM NaCl, 10 mM Tris and 5mM EDTA with 40 μg/ml RNase A and 2 μg/ml RNase T1 at 37 degrees for 30 minutes. The negative controls were derived from 1 μl of sample which was digested without the presence of the RNases. Digestion termination was accomplished through the addition of 10% SDS and 10μg of Protinase K. Following phenol chloroform extraction again using yeast tRNA as a carrier, the samples were ethanol precipitated, and dried. The pellets were resuspended in 10μl of RNase Sample Loading Buffer and were denatured at 90 degrees before being electrophoresed on a 6% urea polyacrylamide gel. After electrophoresis in 1X TBE (0.1M Tris, 0.08 M boric acid, 2mM EDTA), the gel was dried and exposed to film.

2.4.3 Northern Analysis

For Northern analysis, 0.8% agarose gels were made using 10X MOPS (50mM sodium acetate, 10 mM EDTA, 200mM MOPS) in a solution containing 0.666% formaldehyde. Samples were loaded after 6.75 μl containing 20 μg total RNA was combined with 3μl 10X MOPS 15 μl deionized formamide and 5.25 μl 37% formaldehyde. These samples were placed at 55 degrees for 15 minutes, cooled, combined with 3.3 μl loading dye (1mM EDTA, 1μg/μl xylene cyanol FF, 1 μg/μl bromophenol blue and 50% glycerol) and were run in 1X MOPS buffer. After rinsing the

gel twice in ddH_2O, the gel was incubated twice in 20X SSC (3 M NaCl, 0.34 M sodium citrate) for ten minutes. RNA was transferred from the gel to HybondN membrane by capillary action as previously described in the Southern analysis. RNA was crosslinked to the membrane by crosslinking and was placed in prehybridization buffer (1% BSA FV (Sigma), 500mM sodium phosphate buffer pH 7.2 (67g $Na_2HPO_4 \bullet 7H_20$ and 2 ml of 85% H_3PO_4 in 1L), 1mM EDTA and 7% SDS) for three hours. While the membrane was in prehybridization solution, probes were generated using the RediPrime Kit (Amersham) following the manufacturer's instructions. The ^{32}P dCTP labeled probes were incubated with the membrane in the prehybridization buffer overnight and non-specific hybridization was removed the following day by one 15 minute wash at 65 degrees in low stringency wash (0.5% BSA FV, 1mM EDTA, 40mM sodium phosphate buffer and 5% SDS). Following the low stringency wash, two 15 minute high stringency washes (1mM EDTA, 40mM sodium phosphate buffer and 1% SDS) at 65 degrees were completed. Following these washes, the Northern blots were exposed to film.

2.4.4 Quantitative RT-PCR

For quantitative RT-PCR, the reverse transcription, denaturation, PCR and quantification were carried out in a single capillary using the LightCycler RNA Amplification Kit SYBR Green 1 (Roche). The manufacturer's protocols were followed to determine optimal $MgCl_2$ concentration for each primer pair. The suggested protocol was also followed in the RT-PCR reactions using 200 ng of total RNA. The primer pairs used in the LightCycler analysis are shown in Table 2.1. The PCR reaction was stopped

while all samples were in the log-linear phase of amplification and when necessary, samples were diluted so that all reactions would be in this phase of amplification at or near the same cycle. The PCR reaction was then terminated and the product was subject to a melting curve analysis. To determine that the product defined by the melting temperature was the actual amplified product, the samples were electrophoresed on a 1.5% agarose gel during optimization of the primers. The samples were then standardized against a quantitative GAPDH RT-PCR reaction.

2.5 Protein Analysis

2.5.1 Protein Extract Preparation from Cell Culture

Media was aspirated from tissue culture plates and the cells were washed twice with 5 mL of ice cold PBS. For 10 cm plates, 600 µl of TNE lysis buffer (50mM Tris, 150mM NaCl, 2mM EDTA, 10mM NaF and 0.1% Nonidet-P-40) was added after being activated with sodium orthovanadate (1 mM Na_3VO_4), 10 µg/ml aprotinin, 10 µg/ml leupeptin and 10 µg/ml PMSF. The tissue culture plates remained on ice for 30 minutes with occasional swirling to ensure adequate coverage of the plate with lysis buffer. The protein extract was collected with a sterile cell scraper and the cellular debris was removed by centrifugation at 4°C for 20 minutes. The protein concentration was examined using a Bradford assay using the Protein Assay Reagent (BioRad) and absorbance was measured at 595 nm. A standard curve for quantification was generated each time a Bradford assay was performed.

2.5.2 Protein Extraction from Tissue and Tumor Samples

Tissue samples were flash frozen in liquid nitrogen and were ground using a chilled mortar and pestle. 2 ml of activated TNE lysis buffer was added to the samples after the liquid nitrogen had been removed and were occasionally agitated while the sample incubated in the lysis buffer for 30 minutes. Cellular debris was cleared by centrifugation at 4°C and the protein concentration was determined using the Bradford assay as described above.

2.5.3 Antibodies

Antibodies used included rabbit polyclonal antibodies to Grb2 and Grb7 (Santa Cruz), mouse monoclonal antibodies to Neu (Oncogene Science AB3), a phosphotryosine specific antibody (PY20 Upstate Biotechnology), anti-ErbB3 (C-17 Santa Cruz), and anti-ErbB4 (C-18 Santa Cruz). Primary antibodies used for immunoblotting were diluted 1:1000 in TBST Milk (20 mM Tris-HCl pH 8 and 150mM NaCl with 3% skim milk and 0.1% Tween-20). Secondary antibodies included anti-mouse, anti-rabbit and anti-goat IgG which were conjugated to horseradish peroxidase. These secondary antibodies were diluted 1:2500 in TBST Milk. MF20 (Developmental Studies Hybridoma Bank) was used in immunohistochemistry to determine terminal differentiation of myotubes. AKT and MAPK Kits (Cell Signaling) were used to detect phosphorylation and levels of AKT and MAPK. After detecting the phosphorylated forms of MAPK or AKT, the immunoblots were stripped and re-blotted for the non-phosphorylated form using the manufacturer's directions.

2.5.4 Immunoblotting

Protein lysates (50 to 500 μg of total protein lysates) were combined with SDS-PAGE loading buffer (125 mM Tris (pH 6.8), 20% glycerol, 4% SDS, 2mM DTT and 0.1% bromophenol blue) and the samples were then denatured at 100°C for 10 minutes. Protein lysates were resolved on SDS-polyacrylamide gels and were electrophoretically transferred onto polyvinylidine difluoride (PVDF) membranes (Immobilon-P) by wet transfer. After transfer to the PVDF membrane, the membrane was blocked for 1 hour in 3% milk in 1X TBS or 3% BSA in 1X TBS. Membranes were then incubated with the primary antibody overnight at 4°C. After 3 five minute washes in 1X TBST, the immunoblots were incubated with the secondary antibody at room temperature for 45 minutes. The membrane was washed two times for 20 minutes in 1X TBST and once in TBS for 20 minutes before application of the enhanced chemiluminescence system (ECL, Amersham). The immunoblots were then exposed to film for 10 seconds and 2 minutes to determine the optimal exposure time.

2.5.5 Immunoprecipitations

Immunoprecipitations were performed by incubating the primary antibody with 600 μg of protein in 600 μl of TNE lysis buffer. 20 μl of Protein G Sepharose was added to each immunoprecipitation and the mixture was incubated at 4°C overnight with constant agitation. Before the samples were electrophoresed on the gel as described

above, the samples were centrifuged and washed with TNE three times. After the final aspiration of TNE, the pellet was resuspended in 2X SDS PAGE sample loading buffer.

2.5.6 Immunohistochemistry

Immunohistochemistry was performed on thin sections of formalin fixed, paraffin embedded samples mounted on Aptex (3-aminopropyltriethoxysilane) treated slides. After standard deparafinization treatment with xylenes and several washes in absolute alcohol, the endogenous peroxidase activity in the formalin fixed tissue was suppressed by a methanol peroxidase treatment (0.3% H_2O_2 in methanol). The sections were then hydrated through a graded alcohol series and were rinsed in TBS. The sections were blocked with 10% normal goat serum in TBS for 20 minutes in a humid chamber at 37 degrees. The primary antibody was diluted 1:300 in 5% normal goat serum diluted in TBS and was incubated with the sections overnight at 4°C. Negative controls lacking the primary antibody were included for all samples. The following day, the excess antibody was removed though two brief TBS washes and a biotinylated secondary antibody was incubated with the sections for one hour at 37°C. The excess was again removed by TBS washes and the Vectastain Elite ABC kit containing the streptavidin-peroxidase complex was added. Excess reagent was again removed by TBS washes and DAB (Vector Labs) was added. Five minutes after the addition of the DAB substrate, the color reaction was stopped by a H_2O rinse and the sections were counterstained with Hematoxyin, dehydrated and mounted.

2.6 Cell Culture

2.6.1 Culture Conditions

Rat 1 cell lines were maintained in Dulbecco's Modified Eagle Medium (DMEM, Invitrogen), unless otherwise noted. DMEM was supplemented with 10% Fetal Bovine Serum (FBS, Invitrogen), 100IU/mL and 100μg/mL of penicillin and streptomycin (Invitrogen) respectively and 1.25 μg/mL Fungizone (Invitrogen). Cell lines were maintained at 37°C in 5% CO_2 with media changes occurring every three days.

Primary myoblast cultures were generated as previously described (Rando and Blau, 1994) and were cultured in Proliferation Media composed of HAMS F10 (Invitrogen), 20% FBS, bFGF (2.5 ng/ml) with Penicillin / Streptomycin and Fungizone as described above. To induce differentiation, the media was switched to 5% Horse Serum in HAMS F10 with the same antibiotic supplements. The proliferation media was changed daily, while the differentiation media was changed every second day.

Primary tumor cell lines were cultured in Mammary Epithelial Cell Growth Medium (MEGM) constituted of DMEM with 10% FBS and the Clonetics SingleQuat supplements. The final concentrations of the Clonetics supplements were; 10 ng/mL hEGF (human recombinant Epidermal Growth Factor), 5 μg/mL Insulin, 0.5 μg/mL Hydrocortisone, 50 μg/mL Gentamycin and 13 mg/ml BPE (bovine pituitary extract). Media was changed every third day.

Cells were passaged at 90% confluency except for primary myoblast cultures which were passaged at 70% confluency. Cells were passaged using 2 mL of 1X trypsin / EDTA in 1X PBS on a 100mM plate after being rinsed with 1X PBS. Trypsin was

inactivated by the addition of the appropriate media and the cells were then reseeded onto dishes at various densities.

To remove double minute chromosomes from the primary tumor cell lines, cells were passaged sixteen times in the presence of various amounts of hydroxyurea as previously described (Snapka and Varshavsky, 1983; Canute *et al.*, 1996; Canute *et al.*, 1998). Cell lines were maintained in 0, 50 100 or 150 μM hydroxyurea and were monitored for aberrant cell death or cytopathalogical effects.

2.6.2 Adenoviral Infection

Primary myoblasts were infected with recombinant adenoviral vectors from the laboratory of Frank Graham expressing either Cre Recombinase or LacZ. Infection of cells in a monolayer was accomplished by removing the media, washing with 1X PBS and then adding high titer virus at a multiplicity of infection of 10-20 plaque forming units per cell. The recombinant adenovirus was incubated with the cells in 1mL of PBS +/+ for a 100mM plate. PBS +/+ was composed of 1X PBS supplemented with 100X $CaCl_2$ (1g in 100mL H_2O) and 100X $MgCl_2$ (1g in 100mL H_20). After 30 minutes at 37 degrees with occasional agitation, media was added to the infected cells.

2.6.5 Annexin / Propidium Iodide staining

To determine whether cells in culture were undergoing apoptosis or necrosis, the cells were assayed using an Annexin / Propidium Iodide kit (Annexin-V-Fluor, Roche). The manufacturer's directions were followed for the differentiating myoblast cell lines.

2.6.6 Terminal Differentiation of Myotubes

To determine whether myoblasts that had been differentiated to myotubes were completely differentiated, immunohistochemistry for a terminal marker was conducted. Using MF20, an antibody that interacts with meromysin, immunohistochemistry was performed as previously described (Bader *et al.*, 1982).

2.6.7 Matrigel Invasion Assays

Cell lines expressing the Grb7 antisense construct were tested for invasiveness in modified Boyden chambers coated with Matrigel. The manufacturer's directions were followed and 1000 cells were seeded into the wells in a 24 well plate. The invasive index was calculated according to the manufaturer's directions. Briefly, the number of cells that migrated through the membrane containing Matrigel were divided by the number of cells that migrated through the uncoated membrane. The percent invasion of the parental cell line was set to 1 and invasive index of the experimental cells was calculated by determining the ratio of the two percentage invasion values.

2.7 Animal Studies

2.7.1 Mammary Gland Wholemounts

To examine mammary gland effects, the #4 gland was excised from the nipple to the end of the fat pad and a portion of the surrounding fascia was included. The #4 mammary gland was taken since the lymph node serves as an important reference point

for outgrowth of the epithelium. The mammary gland was spread out on a glass slide and the fascia was pulled at the periphery to extend the gland. The glands were then allowed to air dry overnight. The slides were then immersed in acetone overnight and then were stained in Harris' Modified Hematoxylin Mercury Free (Sigma) overnight. The stained glands were destained by repeated immersion in a solution of 70% EtOH and 1% HCl for several hours depending on the extent of the staining. Once destaining was complete, the slides were incubated in absolute ethanol for one hour and then in xylenes overnight prior to mounting with a non-yellowing media (Permount, Sigma).

2.7.2 Histology

For all samples, unless otherwise specified, fixation was in 10% formalin at 4 degrees overnight. Samples were then taken to the Histology Service in the McMaster University Medical Center and were processed, paraffin embedded, sectioned and stained as requested. For immunohistochemistry, sections were placed onto APTEX treated slides rather than glass to prevent loss of sample.

2.7.3 Urea Silver Nitrate Stain

To visualize muscle spindles, a urea silver nitrate stain was performed as previously described (Butler and Payk, 1986). However, since there are several modifications, the protocol is described in detail. The preferential staining of the neurons was accomplished by euthanizing the mice via CO_2 then stripping the skin from the hindlimb. The extensor digitorum longus (EDL) muscle was removed and pinned in an

extended position to a small piece of Styrofoam. The muscle was then immersed in Bouin's fixative (Sigma) overnight at room temperature. After a series of ethanol washes, the tissue was embedded in paraffin for longitudinal sections. Thick sections (14-16 microns) were cut and the sections were allowed to dry overnight. The following day the sections were deparafinized in xylenes overnight followed by a fresh xylene treatment for 1 hour. After a graded ethanol wash to hydrate the samples with steps at 30 minute durations, the slides were placed into fresh prewarmed Urea Silver Nitrate Solution (0.088 M Silver Nitrate, 3.3 M Urea U-15 grade, 3 drops MCPA solution (0.04 M mercuric cyanide, 0.044 M picric acid) in 200 mL H_2O). The sections were incubated at 60 degrees for 3-4 hours and then were dipped through 4 changes of room temperature distilled water. The stain was then reduced for 2 minutes at room temperature with gentle agitation in Reducer Solution (0.8 M Sodium Sulfite Anhydrous, 0.27 M hydroquinone and 6.6 M urea U-15 grade). The slides were then dipped through 4 changes of distilled water and then were briefly rinsed in 50% and 80% EtOH. After examination under a microscope, the slides were either placed in xylenes for 5 minutes and then mounted using Permount (Sigma) or a modified staining procedure was repeated. This modified stain intensified the neuron specific staining and encompassed a repeated immersion in the Urea Silver Nitrate Solution at 60 degrees for 15 minutes. This was followed by 4 brief distilled water washes and the sections were reduced for three minutes as described above. After dipping through 4 water washes and dehydrating in a 50% and 80% EtOH wash again the slides were examined under a microscope. This procedure was repeated as necessary and for 14 micron thick sections, it was usually necessary to have three

repeats. The mounted sections were examined under a microscope where the background muscle stain was a golden color and the neural specific stain was black.

2.7.4 Embryo Analysis

2.7.4.1 Embryo Harvest

To examine the development of embryos at various stages of development, timed matings between stud males and females in estrus were initiated. Females in estrus were determined by eye. The following morning, females were examined for the presence of a copulation plug. Females with a plug were identified as being at 0.5 days post coitum (dpc). At 9.5 to 14.5 dpc the embryos were extracted for examination. After excision of the entire uterus from the female donor, the uterus was cut into sections containing a single embryo and these pieces were placed into ice cold PBS. The extraembryonic tissue surrounding the embryos was dissected free until the visceral yoke sac was exposed under a dissecting microscope. The visceral yoke sac was retained for genotyping and the embryo was fixed either for histology or *in situ* analysis or the embryos were flash frozen for protein or RNA extraction. For routine histology, the embryos were fixed in 10% formalin. However, for *in situ* analysis, the embryos were fixed in fresh 4% paraformaldehyde-0.2% glutaraldehyde (Fisher Scientific), were then dehydrated through a graded series of methanol-PBT (1x PBS, 0.1% Tween 20) washes and were stored in 100% methanol at -20°C. Prior to fixation or freezing, the embryos were examined for a beating heart and general signs of viability. Additionally, the stage of development was confirmed by visual analysis of various hallmarks of embryogenesis.

2.7.4.2 Embryo *in situs* Analysis

To determine whether embryos had normal neurological development an *in situ* analysis for Phox2a was completed as previously published (Wilkinson and Nieto, 1993; Chan *et al.*, 2002). Briefly, the Phox2a riboprobe plasmid, was digested and transcribed with T3 RNA polymerase to generate an antisense riboprobe. A sense riboprobe was generated from the sample plasmid using a different linearization site and T7 RNA polymerase. The *in vitro* transcription reactions occurred in distilled water (diethyl pyrocarbonate [DEPC] treated), with 10x transcription buffer (Boehringer Mannheim), DIG RNA labelling mix (Boehringer Mannheim), 1 μg of template DNA, 30 U of RNAGuard (Pharmacia), and 30 U of RNA polymerase (Boehringer Mannheim or Gibco-BRL). Reactions were allowed to proceed for two hours at 37°C and were terminated by the addition of 20 U of DNase I (Boehringer Mannheim).

2.7.4.3 Embryo Histology

To examine the histological changes in various embryos, the embryos were fixed as previously described. The samples were then processed by the Histology Department in the McMaster University Hospital and I embedded the embryos for sectioning. Embryos were embedded so that sections would be taken though the longitudinal plane. I then cut serial sections through the entire embryo at 5 microns. 5 sections were placed on each slide and every fourth slide was stained in hematoxylin and eosin by standard methods while the remaining slides were retained for further analysis.

2.7.5 Gait Analysis

To create a record of the normal and abnormal gait of wild type and mutant mice, the hind limbs of mice were dipped into India Ink (Sigma) and the mice were allowed move down a 15 cm wide corridor lined with blotting paper (3M). The stained blotting paper was scanned and adjusted for brightness and contrast in Adobe Photoshop.

2.7.6 Induced Regeneration of Skeletal Muscle

Skeletal muscle regeneration was induced through a mechanical crush injury as previously described (Megeney *et al.*, 1996). Briefly, after mice were anesthetized using Avertin, the TA muscle was exposed and a crush injury was applied using sterile forceps for several seconds. Mice were sutured and allowed to recover for two weeks. The crushed muscle and the contralateral controls were then examined by serial sections stained with hematoxylin and eosin.

CHAPTER 3

EXAMINATION OF MAMMARY GLAND DEVELOPMENT AND TUMORIGENESIS WITH EXPRESSION OF AN ONCOGENIC NEU ALLELE UNDER THE REGULATION OF THE ENDOGENOUS PROMOTER

3.1 Introduction

One of the most frequently observed cancers in females is that of the breast. HER2 is amplified and consequently overexpressed in 20-30% of all human breast cancers and is associated with a poor clinical outcome (Slamon *et al.*, 1987; Slamon *et al.*, 1989; Andrulis *et al.*, 1998). While the amplification and overexpression of HER2 suggests a role in the progression of the disease, expression of the activated *neuNT* allele under the control of the Mouse Mammary Tumor Virus Promoter Enhancer resulted in the rapid induction of multifocal mammary tumors and illustrated the potency of the *neu* oncogene (Muller *et al.*, 1988; Bouchard *et al.*, 1989). In contrast to the rapid tumor progression observed with the expression of an activated *neu* allele, expression of the wild type *neu* allele in the mammary gland resulted in focal mammary tumorigenesis after an extended latency (Guy *et al.*, 1992). Upon examination of the juxta-transmembrane region of the extracellular domain of the wild type *neu* cDNA, numerous activating mutations were identified. These mutations reproducibly involved cystein residues thought to be integral to disulphide mediated receptor dimerization. While these

type of mutations have not been observed in HER2 induced human tumors, a splice variant that is capable of inducing disulphide mediated homodimerization has been identified (Siegel *et al.*, 1999).

These mouse models of Neu mediated tumorigenesis have provided important insights into initiation and progression of the disease but these models are also problematic due to the MMTV promoter. The MMTV promoter enhancer is hormonally responsive and is induced during pregnancy and lactation (Henrard and Ross, 1988). However, the hormonal nature of breast cancers suggests that studies using a hormonally dependent viral promoter may not be entirely appropriate to mimic the human disease.

To generate a mouse model of breast cancer that was hormonally relevant, I placed the activated *neuNT* cDNA under the control of the endogenous promoter in a mammary specific manner. This resulted in altered development of the mammary architecture and focal tumor formation after a long latency. Interestingly, these conditionally activated tumors closely mirrored the human condition as they had both amplified and overexpressed the recombinant *neu* allele. These tumors were then compared to the MMTV-Neu induced tumors both phenotypically and through an analysis of gene expression. These studies further illustrated the similarity of the endogenously regulated *neu* tumor model to the human condition.

In an attempt to accelerate the onset of detectable tumors in the endogenously regulated model, I expressed the activated *neu* allele under the control of the endogenous promoter in all tissues. This germline activation of *neu* expression resulted in embryonic lethality in the homozygous state indicating that expression of constitutively activated

Neu was not able to rescue the embryonic lethality associated with the germline ablation of ErbB2. However, when these heterozygous mice were compared to the conditionally activated tumor model, several differences were noted both phenotypically and through an examination of gene expression. Taken together, these observations further define the role of Neu in mediating mammary tumorigenesis.

3.2 Results

3.2.1 Generation of Mice Expressing Activated Neu under the control of the endogenous promoter in the mammary gland

The MMTV regulated Neu models of mammary tumorigenesis have revealed important insights into the requirements of various signal transduction cascades in Neu induced tumors and have demonstrated a causal role for Neu in mediating tumor formation. However, the hormonal regulation of this strong viral promoter makes these mouse models of questionable relevance to the human condition. To create a more appropriate mouse model of Neu induced mammary tumorigenesis, I have used a gene targeting strategy to express the activated *neu* allele, *neuNT*, under the control of the endogenous mouse promoter. However, given the role of ErbB2 in mediating embryonic development (Lee *et al.* 1995), a loxP flanked neomycin cassette was inserted between the promoter and the *neuNT* cDNA since expression of the activated *neuNT* allele may cause developmental defects. In order to determine whether the loxP flanked neomycin cassette was capable of interfering with expression of *neuNT* until it was excised through

Cre mediated recombination, the construct was tested *in vitro*. The loxP flanked neomycin cassette followed by the *neuNT* cDNA was ligated into the pJ4Ω vector so that upon removal of neomycin, *neuNT* expression was controlled by the MoMuLV promoter (Figure 3.1, Panel A). Electroporation of this plasmid into Rat1 fibroblasts with and without a subsequent electroporation of PGK-Cre plasmid was followed by changing the media conditions to allow formation of foci. The loxP flanked neomycin cassette was shown to effectively block formation of NeuNT mediated focus formation. However, with the addition of PGK-Cre and the proposed excision of the loxP flanked neomycin cassette, foci were noted indicating that the neomycin cassette was indeed removable (Figure 3.1, Panel B). To ensure that Cre recombinase was mediating the excision of the neomycin cassette, DNA was prepared from the focus assay and was subjected to a Southern analysis. Based upon the strategy shown in Figure 3.1 Panel A, it was clear that the addition of Cre recombinase was mediating the excision of the loxP flanked sequence (Figure 3.1, Panel C). Given these results, the targeting strategy to replace exon one of the endogenous ErbB2 allele with the conditionally activated *neuNT* allele was pursued.

To place the activated *neu* allele under the transcriptional control of the endogenous promoter, a targeting strategy was designed to replace exon one of the endogenous gene with the *neuNT* cDNA. However, given the potential adverse consequences of expressing an activated allele during development, the loxP flanked neomycin cassette was placed between the endogenous promoter and the *neuNT* cDNA (Figure 3.2, Panel A). Electroporation of this targeting vector into ES Cells containing the genomic allele should have resulted in homologous recombination resulting in the

Figure 3.1 – Selective NeuNT expression with a loxP flanked *neo* allele.

Since the expression of the activated *neu* allele under the endogenous promoter may result in embryonic lethality, a loxP flanked neomycin cassette was placed 5' to the *neuNT* cDNA. To determine whether the neomycin allele could be excised and inhibit expression of NeuNT by a strong promoter, the EcoR1 fragment containing the loxP flanked neomycin and the NeuNT cDNA was ligated into pJ4Ω (A). While only the forward orientation is shown (A), the reverse orientation was used as a control. Expression of Cre Recombinase should excise the neomycin fragment, placing the neuNT cDNA under the control of the Molony Murine Leukemia Viral Promoter Long Terminal Repeat (MoMULV-LTR) promoter enhancer. The forward construct (A) and the reverse were electroporated into Rat1 cells and selection for neomycin was applied. The resulting colonies were pooled and were either electroporated with a plasmid containing Cre Recombinase under the control of the PGK promoter or were electroporation with an empty vector. The results of the focus assay are shown for both the forward and reverse constructs, with and without the presence of Cre Recombinase (B). Clearly, there are a large number of foci with both the forward NeuNT construct and Cre Recombinase. To determine whether excision of the loxP flanked neomycin cassette had occurred, the DNA from the pooled colonies containing the forward construct was harvested, digested with EcoR1 and probed with a portion of the neuNT cDNA. The predicted size shift (A) from 5.8 kb to 4.0 kb is apparent with the addition of PGK-Cre (C). Additionally, the probe detected a genomic band at approximately 25 kb.

A

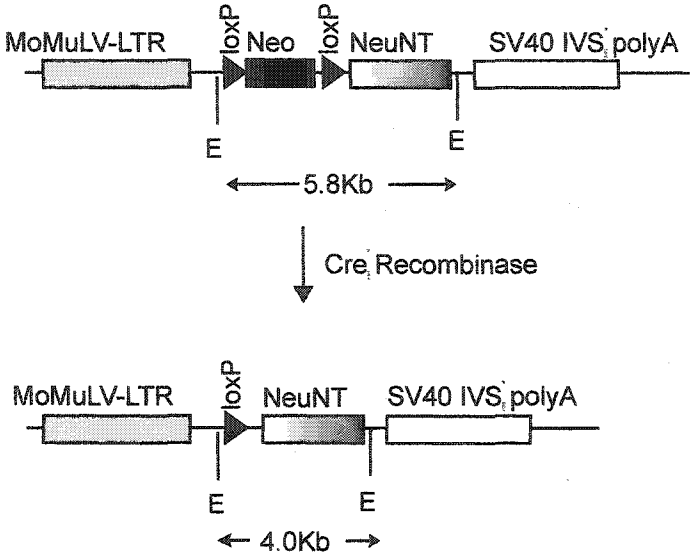
MoMuLV-LTR
loxP
Neo
loxP
NeuNT
SV40 IVS polyA
E
E
5.8Kb
Cre Recombinase
MoMuLV-LTR
loxP
NeuNT
SV40 IVS polyA
E
E
4.0Kb

B

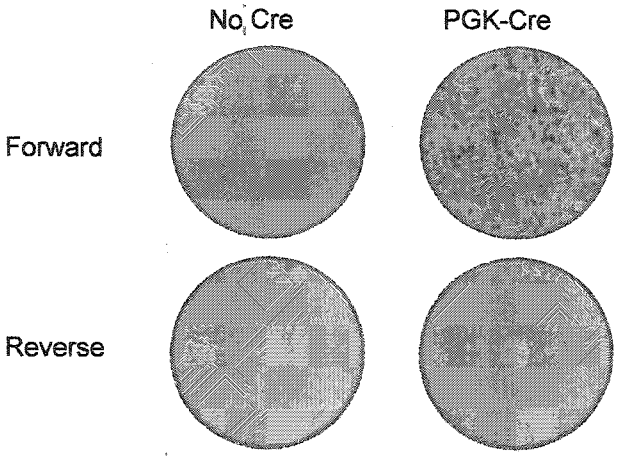
No Cre
PGK-Cre
Forward
Reverse

C

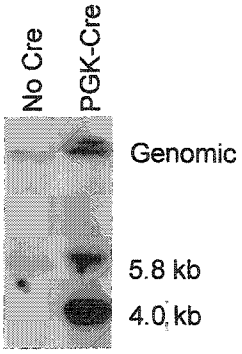
No Cre
PGK-Cre
Genomic
5.8 kb
4.0 kb

Figure 3.2 – Embryonic Stem Cell Targeting of a Tissue Specific Activatable *neuNT* allele

A schematic representation of the targeting construct, strategy and the genomic erbB2 allele is shown (A). The 2.5 kb 5' arm of homology (Sph1 to Nar1) and the 8 kb 3' arm of homology (Kpn1 to Sal1) were used to direct the homologous recombination to the wild type allele. The targeting strategy replaces the first exon of the genomic erbB2 allele with a loxP (triangles) flanked neomycin cassette (neo) followed by the neuNT cDNA and the SV40 polyA (NeuNT). The probe external to the directed recombination event is also illustrated. The recombinant allele (B) has the loxP flanked neomycin allele between the endogenous erbB2 promoter and the NeuNT cDNA and is essentially a null allele for erbB2 until the removal of the loxP flanked sequence. The size of band detected in a Southern analysis with the external probe after a HindIII digest is illustrated for both the genomic (7.5 kb) and for the recombinant allele (4.6 kb). After electroporation of the embryonic stem cells, selection and screening of the cell lines, 6 cell lines containing the recombinant allele were identified. Upon blastocyst injection and breeding of the chimeric mice, the recombinant allele was passed to the offspring. A representative Southern blot of tail DNA from mice that contain either two wild type alleles or one wild type allele and one recombinant allele is shown (C)

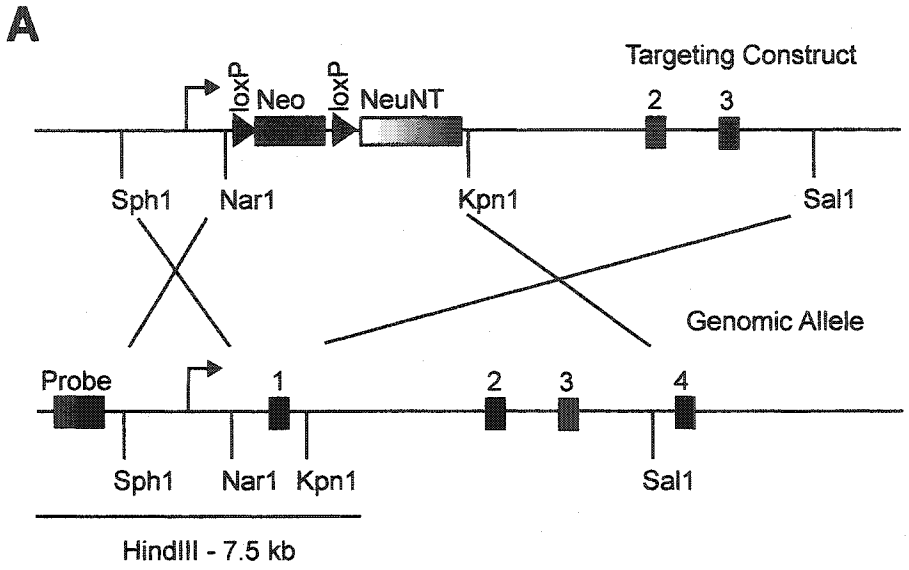
A
Targeting Construct
loxP
Neo
loxP
NeuNT
2
3
Sph1
Nar1
Kpn1
Sal1
Genomic Allele
Probe
1
2
3
4
Sph1
Nar1
Kpn1
Sal1
HindIII - 7.5 kb

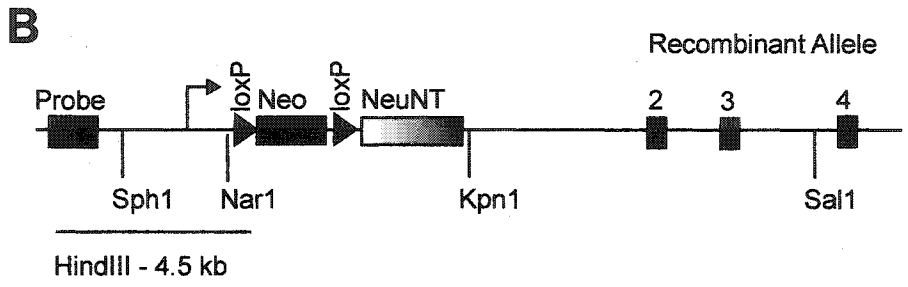
B
Recombinant Allele
Probe
loxP
Neo
loxP
NeuNT
2
3
4
Sph1
Nar1
Kpn1
Sal1
HindIII - 4.5 kb

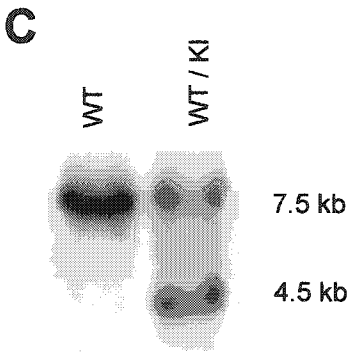
C
WT
WT / KI
7.5 kb
4.5 kb

recombinant allele (Figure 3.2, Panel B). It is important to note that this recombinant allele is essentially a null allele for *erbB2* until the removal of the loxP flanked sequence. Screening the cell lines by Southern analysis using a probe external to the targeted recombination resulted in the identification of 6 positive clones out of 288 possible cell lines. After the subsequent expansion of these ES cell lines, blastocyst injections and breeding of the chimeric mice, mice containing one wild type allele and one recombinant allele were generated as identified by Southern analysis (Figure 3.2, Panel C). Interbreeding these mice generated only wild type mice and the parental strain indicating that the recombinant allele was functioning as a null allele in the homozygous state. Importantly, other results from our laboratory have shown that replacement of the first exon with a wild type cDNA completely rescued the embryonic lethality associated with the germline ablation of ErbB2.

Activation of *neuNT* expression in a mammary specific manner required expression of Cre recombinase targeted to the mammary gland. To accomplish this, the *Cre* cDNA was placed under the transcriptional control of the MMTV promoter enhancer (Figure 3.3, Panel A). After the creation of seven founder lines of transgenic mice through microinjection of the linearized construct, the lines were propagated and six passed the transgene to their progeny. To screen these lines for expression of the transgene, an RNase protection was conducted using the outlined riboprobe (Figure 3.3, Panel A). An examination of Cre expression in the testes, virgin and lactating mammary glands from the six lines of founders resulted in the identification of three lines that expressed the transgene at appreciable levels. While the Cre-2 and Cre-3 lines expressed

Figure 3.3 – Screening of MMTV-Cre transgenic lines for expression.

A schematic diagram of the construct is shown (A). The *cre recombinase* cDNA has been placed under the control of the Mouse Mammary Virus Long Terminal Repeat (MMTV-LTR) promoter enhancer. The riboprobe used in RNase protections detects a 480 bp sequence in the HSV polyadenylation (HSV polyA) region. After creation of seven lines of transgenic mice through microinjection, the six lines that passed the transgene were screened for expression (B). The RNase protection on the lactating mammary gland (L. Mam), virgin mammary gland (V. Mam) and testes shows expression in the Cre-2, Cre-3 and Cre-7 lines. The *pgk* riboprobe was included as an internal loading control.

A

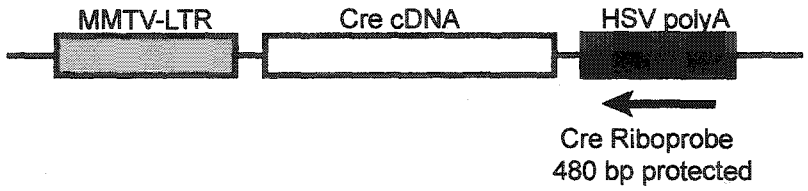
MMTV-LTR
Cre cDNA
HSV polyA
Cre Riboprobe
480 bp protected

B

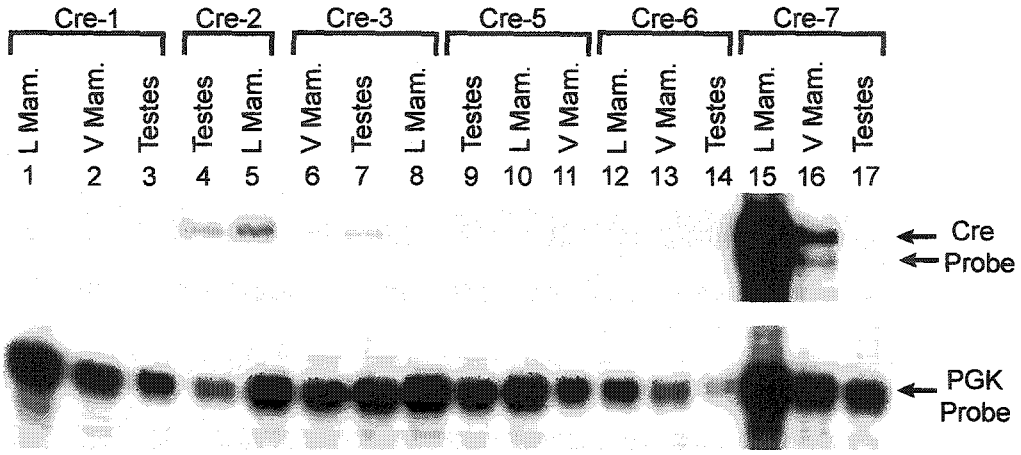
Cre-1
Cre-2
Cre-3
Cre-5
Cre-6
Cre-7
L Mam.
V Mam.
Testes
Testes
L Mam.
V Mam.
Testes
L Mam.
Testes
L Mam.
V Mam.
L Mam.
V Mam.
Testes
L Mam.
V Mam.
Testes
1
2
3
4
5
6
7
8
9
10
11
12
13
14
15
16
17
Cre Probe
PGK Probe

the transgene at relatively low levels, the Cre-7 line showed high levels of transgene expression (Figure 3.3, Panel B). Given that the MMTV promoter enhancer frequently directs expression to a variety of other tissues other than the mammary gland and realizing that expression and excision in other tissues could result in embryonic lethality, the tissue specificity of expression of the three transgenic lines was determined. RNase protections on various major organs in the Cre-2 and Cre-3 lines revealed expression in other tissues that would render the lines potentially unsuitable, such as the brain and ovaries (Figure 3.4, Panels A and B). However, RNase protection on the Cre-7 line revealed that expression was highest in the mammary gland and male accessory sex organs. Indeed, expression in tissues such as the heart and brain were extremely low or non-existent (Figure 3.4, Panel C). The tight control of high levels of Cre expression in the Cre-7 line rendered this line an ideal choice to generate a mammary specific activation of the *neuNT* oncogene.

Mice containing the inducible activated *neuNT* allele were interbred with the MMTV-Cre-7 transgenics resulting in bigenic mice at the expected Mendelian ratio. To determine whether the Cre transgene was mediating excision of the loxP flanked neomycin cassette (Figure 3.5, Panel A), DNA was collected from various tissues and was subjected to a Southern analysis. Excision of the loxP flanked neomycin cassette by Cre recombinase was observed in the mammary gland, salivary gland and spleen (Figure 3.5, Panel B). When compared with the RNase protection characterizing the Cre-7 line, salivary gland expression is seen however the levels in the spleen are almost undetectable, indicating that only low levels of the transgene are required for excision.

Figure 3.4 – Expression pattern characterization for MMTV-Cre transgenic mice.

A variety of tissues from the three MMTV-Cre lines expressing the transgene were examined through an RNase protection. The Cre-2 line revealed that there were high levels of expression in the both the brain and the ovaries, while the level of expression of Cre in the mammary gland was relatively low in comparison (A). The PGK riboprobe was included as a control for loading. In the Cre-3 line of transgenic mice, *cre recombinase* was expressed at high levels in the male sex organs, including the epidimius and the seminal vesicles (B). Again, the level of expression in the mammary gland was relatively low. Finally, the Cre-7 line was screened and revealed expression in the epidimus and seminal vesicles, but showed a high level of expression in the mammary gland. The low level of expression in tissues such as the heart and brain should also be noted. Salv. Gl. – Salivary Gland, Mam. Gl. – Mammary Gland, Epid. – Epidimus, Sem. Ves – Seminal Vesicles.

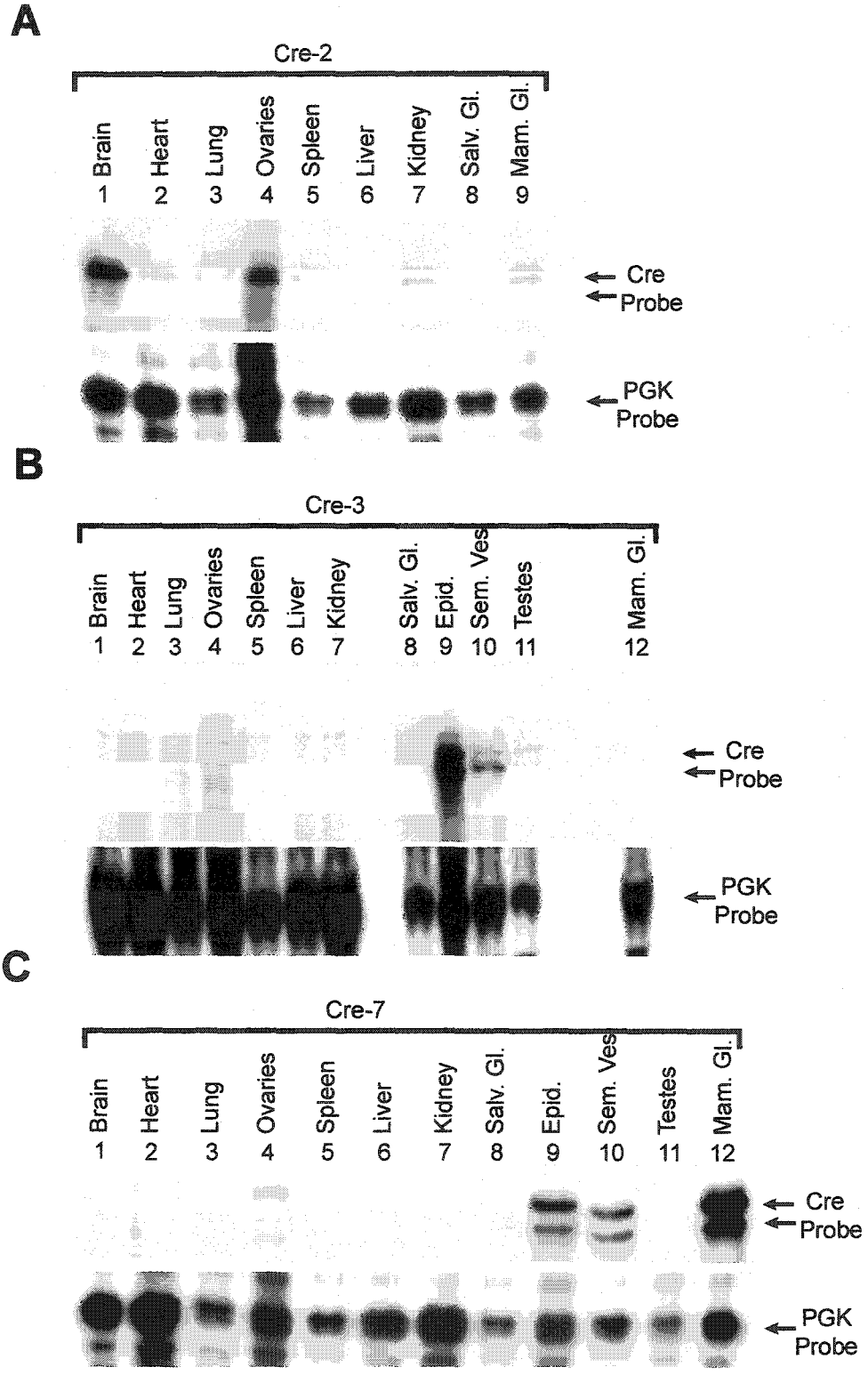
A
Cre-2
Brain 1
Heart 2
Lung 3
Ovaries 4
Spleen 5
Liver 6
Kidney 7
Salv. Gl. 8
Mam. Gl. 9
Cre Probe
PGK Probe
B
Cre-3
Brain 1
Heart 2
Lung 3
Ovaries 4
Spleen 5
Liver 6
Kidney 7
Salv. Gl. 8
Epid. 9
Sem. Ves 10
Testes 11
Mam. Gl. 12
Cre Probe
PGK Probe
C
Cre-7
Brain 1
Heart 2
Lung 3
Ovaries 4
Spleen 5
Liver 6
Kidney 7
Salv. Gl. 8
Epid. 9
Sem. Ves 10
Testes 11
Mam. Gl. 12
Cre Probe
PGK Probe

Figure 3.5 – Tissue Specific Excision mediated by MMTV-Cre.

A schematic diagram of the recombinant allele before and after Cre Recombinase mediated excision of the neomycin cassette (A). Also illustrated are the sizes of bands detected in a Southern analysis using a portion of the *neuNT* cDNA as a probe after an EcoR1 digest. Prior to the excision event, the endogenous promoter will not express the *neuNT* oncogene due to the presence of the intervening *neomycin* allele. Upon excision of the neomycin cassette, the endogenous promoter will regulate the expression of *neuNT*. A Southern analysis reveals that excision is limited to the salivary gland, spleen and mammary gland with the introduction of the 4 kb band (B). In these three tissues, *neuNT* is now under the control of the endogenous promoter.

A

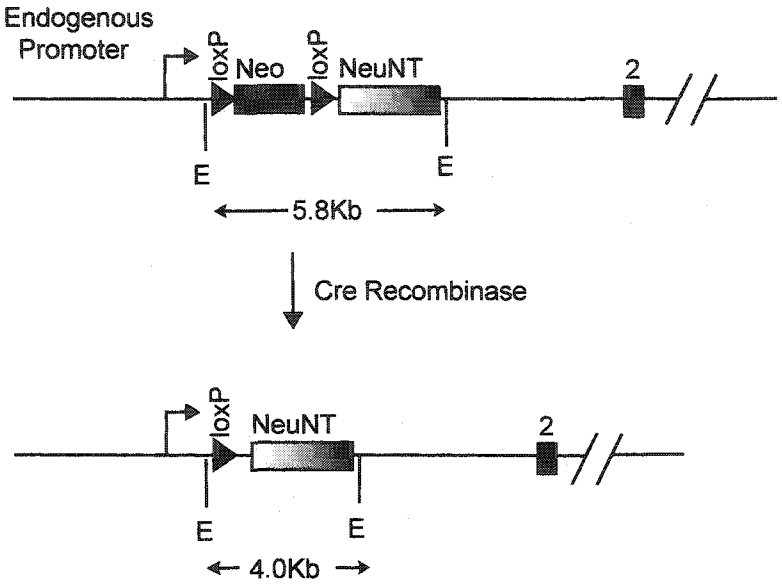
Endogenous
Promoter
loxP
Neo
loxP
NeuNT
2
E
E
5.8Kb
Cre Recombinase
loxP
NeuNT
2
E
E
4.0Kb

B

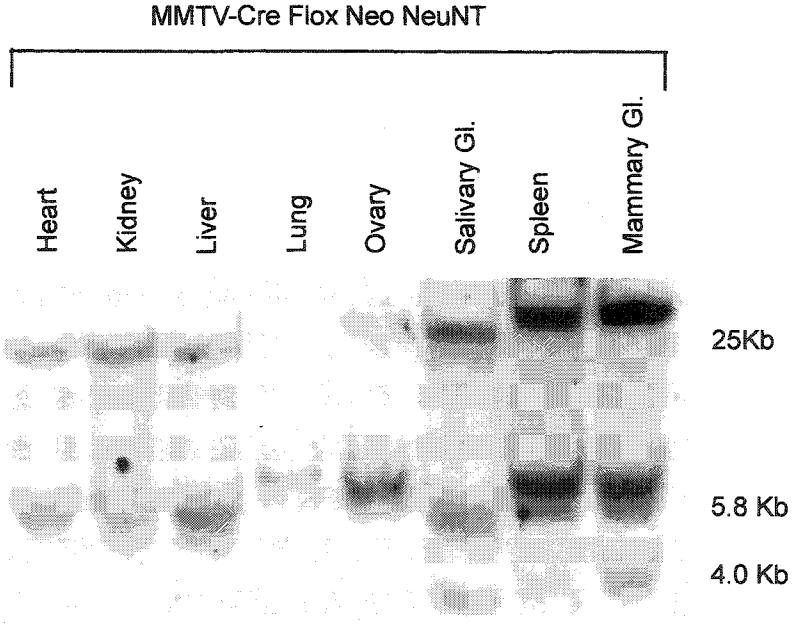
MMTV-Cre Flox Neo NeuNT
Heart
Kidney
Liver
Lung
Ovary
Salivary Gl.
Spleen
Mammary Gl.
25Kb
5.8 Kb
4.0 Kb

Quantitative phosphoimager analysis of this and other Southern blots revealed that excision was approximately 30-40% complete. Importantly, these results demonstrate that the activated *neuNT* cDNA is now under the control of the endogenous promoter in the mouse mammary gland.

3.2.2 Mammary Gland Development and Tumorigenesis in the Conditionally Activated Model

Mammary specific expression of *neuNT* under the control of the endogenous promoter was achieved through excision of the loxP flanked neomycin cassette between the endogenous promoter and the cDNA in the recombinant allele. The removal of this sequence in the mammary gland and the ensuing *neuNT* expression should have predisposed this tissue to the formation of tumors. To examine the conditionally activated mammary gland for phenotypic effects, they were examined both through wholemount and histology. Low power magnification of the wild type control mammary gland (Figure 3.6, Panel A) illustrates the normal confines of the mammary growth into the fat pad. In contrast, when the conditionally activated mammary gland is examined, it is clear that the epithelium is no longer maintained entirely within the normal confines of the fat pad (Figure 3.6, Panel B, Arrows). This effect is repeatedly observed in the conditionally activated mice and these epithelial outgrowths often appear to be contained within the small deposits of fat surrounding the blood vessels that enter and exit the mammary gland. In addition to this escape from the fat pad, the conditionally activated mammary gland also appears to have increased branching. Higher magnification of a

Figure 3.6 – Expression of NeuNT in the Mammary Gland Results in Aberrant Growth.

A representative virgin wild type mammary gland (A, C, E) and conditionally activated NeuNT mammary gland (B, D, F) are shown. At 9 months of age in the wild type control wholemount at low magnification, the gland can clearly be seen to be constrained within the confines of the fat pad (A). In contrast, the mammary gland conditionally expressing NeuNT in the mammary epithelium is seen to escape the normal limits of epithelial penetration of the fat pad (B, arrows). Additionally, there is a mild hyperplasia present and increased branching within the fat pad. In contrast to the smooth ducts with occasional branching in the wild type (C), the conditionally activated gland exhibits increased branching and the formation of numerous lobuolalveolar buds (D). Matched histology illustrates the increased epithelial content of the activated mammary gland in relation to the control (E vs. F).

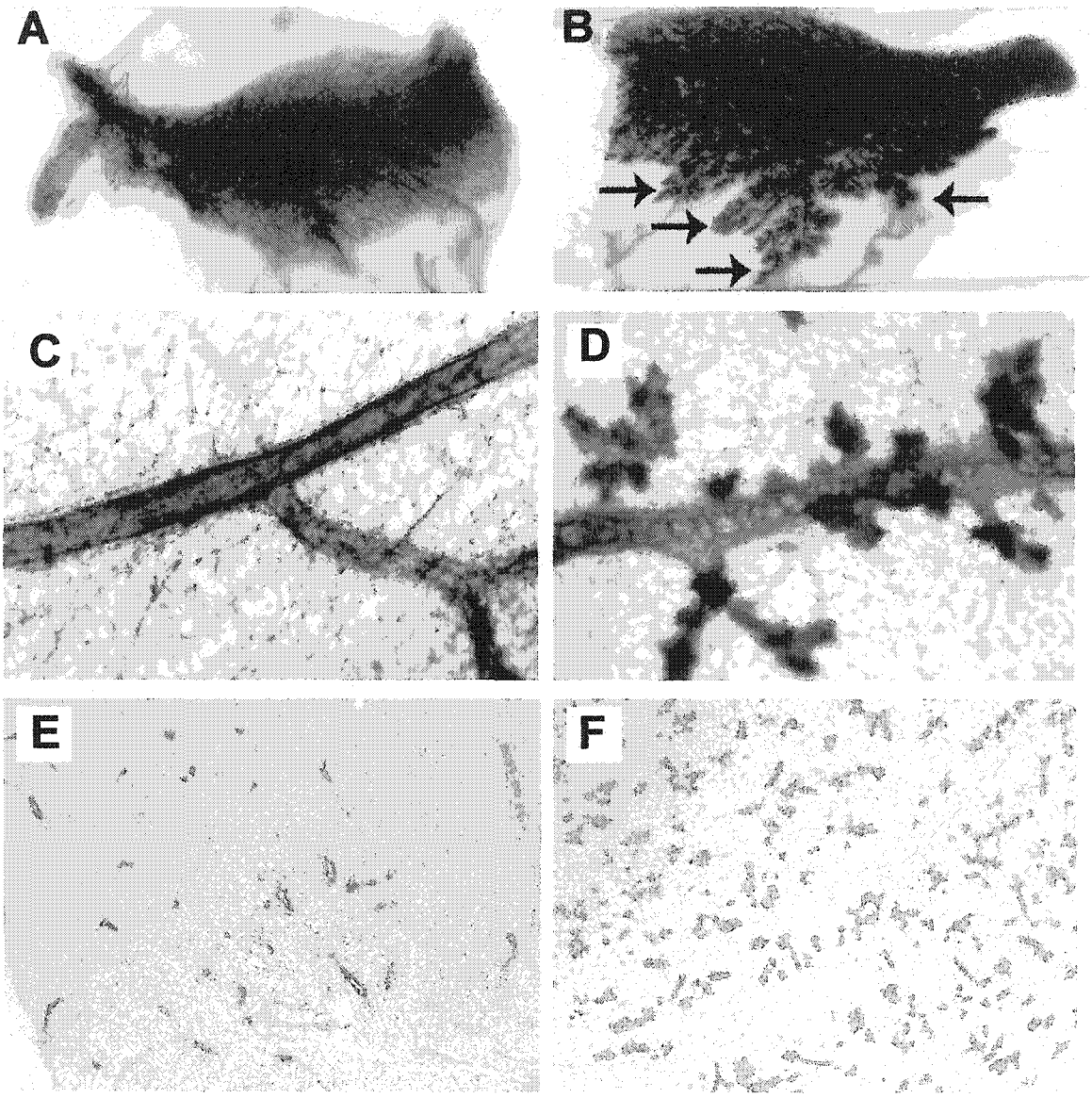
A
B
C
D
E
F

wild type mammary gland illustrates the smooth surface of the duct with few side branches (Figure 3.6, Panel C). In contrast, the mammary gland expressing neuNT contains numerous lobuloalveolar side buds and is more heavily branched (Figure 3.6, Panel D). The increase in branching is more clearly seen when the mammary glands of the wild type control and the conditionally activated mice are compared in cross section (Figure 3.6, Panel E vs. F). Taken together, these results indicate that expression of an activated *neuNT* allele under the control of the endogenous promoter results in alterations in mammary gland structure.

The conditional expression of a potent oncogene under the control of the endogenous promoter resulted in a mammary gland with an increased level of branching and formation of lobuloalveolar side branches. Consistent with the increased proliferation in the mammary gland, focal mammary tumors developed in these mice after a long latency (Figure 3.7). At 15.9 months of age palpable tumors were noted in 50% of female mice (n=41). While greater than 80% of mice examined developed a mammary tumor, the remaining mice died of natural causes without detection of a tumor. Given the long latency, it is possible that these mice may have developed tumors if they had lived past the two year time point. When the adjacent mammary glands from mice containing a tumor were examined through wholemount analysis, no neoplastic lesions were observed. While there were numerous preneoplastic lesions, these mice consistently developed a focal tumor. Further, when metastasis to the lung was examined through numerous histological sections, only one of the 41 mice examined showed

Figure 3.7 – Kaplan-Meier analysis of Tumor Latency.

Tumor palpation in the conditionally activated mice was regularly conducted and the age at when a tumor was first palpated was noted. Invariably, there was a focal adenocarcinoma detected and the latency of detection is illustrated here. The Kaplan-Meier plot has the percentage of tumor free mice on the Y axis and the age in months on the X axis. A palpable tumor was noted in 50 % of female mice by 15.9 months of age (n=41). In the population examined, 18 % of mice failed to develop a tumor, however many of these mice died before the two year timepoint.

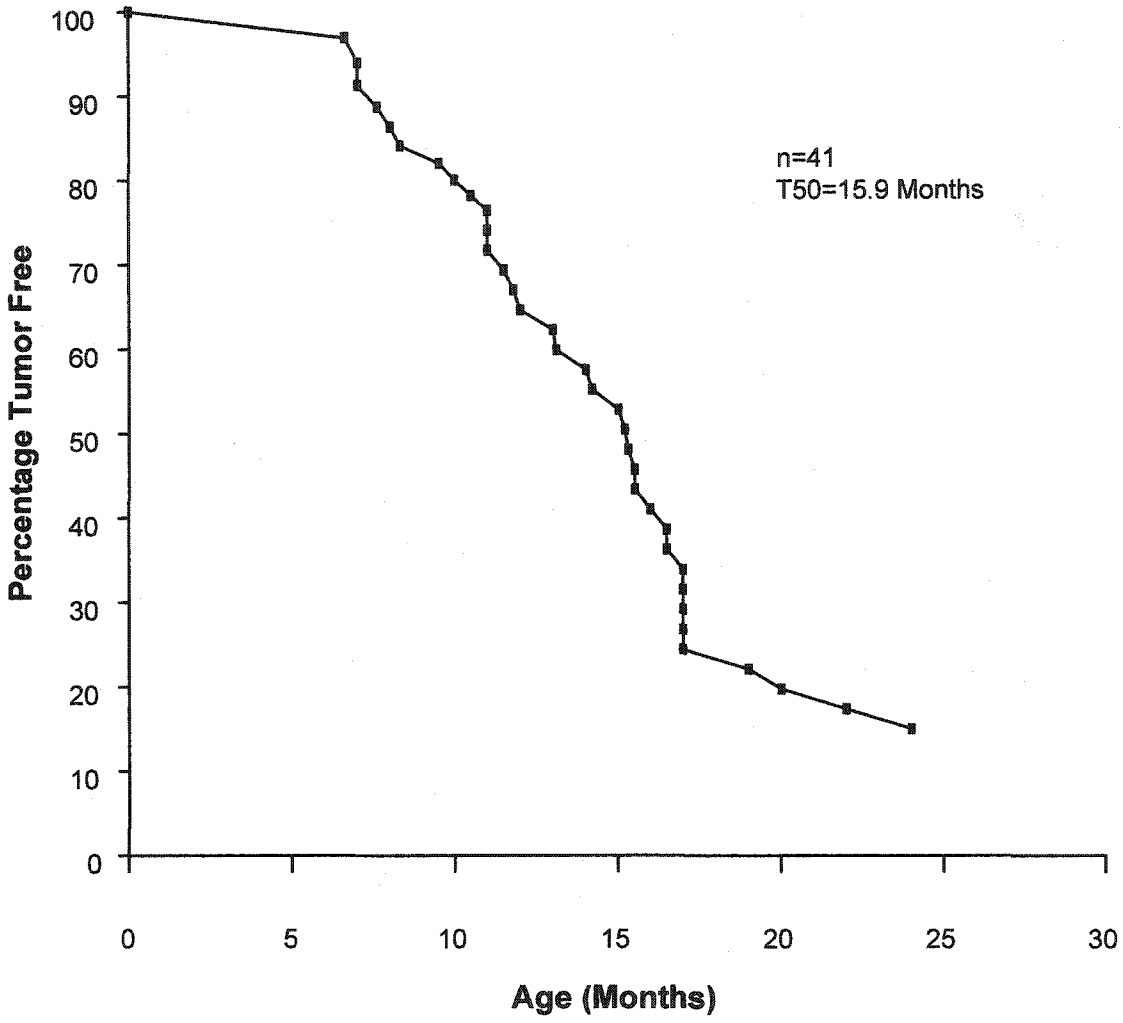
100
90
80
70
60
50
40
30
20
10
0
Percentage Tumor Free
n=41
T50=15.9 Months
0
5
10
15
20
25
30
Age (Months)

evidence of a pulmonary metastasis. Interestingly, the parity of the mouse did not appear to have a discernable effect on the latency of tumor formation in these mice.

The lobuloalveolar structures that have developed on the side of the duct in the conditionally activated model (Figure 3.6, Panel D) were examined further through both histology and immunohistochemistry. A cross section through this structure (Figure 3.8, Panel A) reveals that these lobuloalveolar units have formed acinar structures that are not solid dysplasias. Interestingly, although there are clear effects on mammary gland formation and tumorigenesis in this mouse model system, immunohistochemistry revealed low levels of NeuNT expression in these abnormal structures (Figure 3.8, Panel A). As discussed above, after a long latency focal comedo-adenocarcinomas develop in these mammary glands of these mice. At endpoint, the tumors frequently contain necrotic regions but maintain defined boundaries between the adenocarcinoma and the adjacent mammary gland (Figure 3.8, Panel B). Interestingly, an immunohistochemical analysis of these tumors revealed that in comparison to the lobuloalveolar side buds there is a high level of NeuNT overexpression (Figure 3.8, Panel C). The localization of NeuNT in the conditionally activated mice was compared to a MMTV-NDL tumor (Siegel *et al.*, 1999) (Figure 3.8, Panel D). This comparison revealed that while the MMTV driven tumors have primarily membrane specific Neu expression, NeuNT expressed under the control of the endogenous promoter resulted in tumors with NeuNT primarily located in the cytoplasm. These results suggest that the conditionally activated model has both a high level expression and rapid internalization of NeuNT.

Figure 3.8 – A Histological examination of Tumor Formation and Expression of NeuNT in the Conditionally Activated Mammary Gland.

Sections across the lobuolalveolar buds seen in the wholemounts in Figure 3.6 were cut and subject to an immunohistolochemical analysis for NeuNT (A). Although the histology of the lobuolalveolar bud is abnormal, expression of NeuNT is only weakly observed in the acinar structures at this time. Additionally, it should be noted that while these lobuolalveolar buds are abnormal they are not dysplastic. After an extended latency period, tumors developed in the conditionally activated mammary glands and were examined through a histological analysis (B). This low magnification view reveals that the comedo-adenocarcinoma contains necrotic regions and that the tumor is relatively well encapsulated. The adjacent mammary gland exhibits enlarged ducts but contains no adenocarcinomas. Immunohistochemical analysis on these tumors (C) and an MMTV-NDL control (D) illustrate high levels of Neu expression. The contrast in the localization of the signal indicated by the arrows should also be noted. The conditionally activated tumors frequently show cytoplasmic Neu expression while the MMTV-NDL tumors reveal membrane localization of the signal.

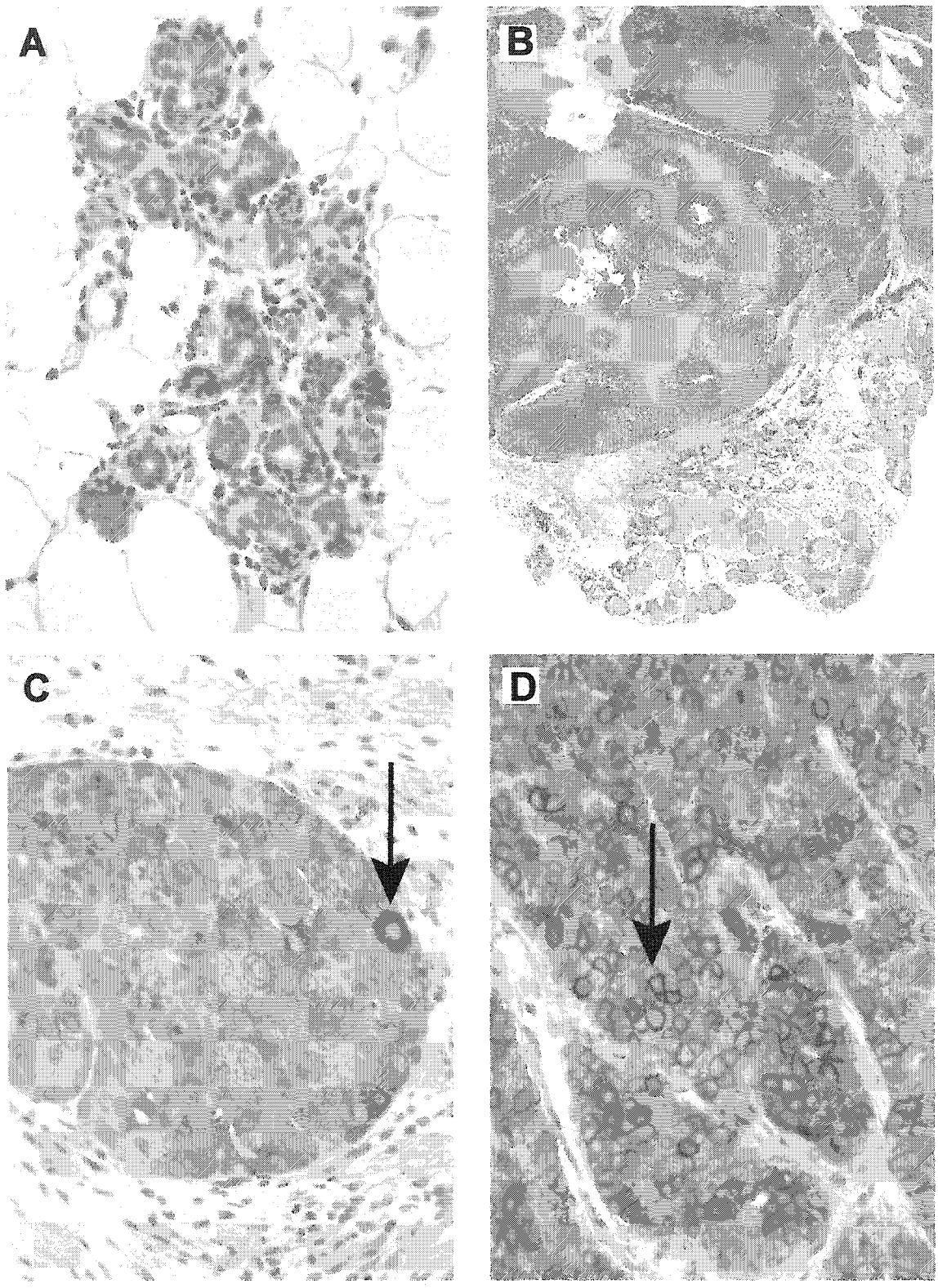
A
B
C
D

3.2.3 Neu overexpression and amplification in the Conditionally Activated Mice

The conditional activation of NeuNT expression in the mammary gland of mice resulted in the induction of focal tumors with long latency that expressed high levels of NeuNT in the tumor, but not in preneoplastic lesions as measured by immunohistochemistry. To confirm these findings, NeuNT expression was examined in virgin and multiparous mammary glands which were compared to tumor samples and the matched adjacent mammary glands. Immunoblotting for Neu in these samples revealed NeuNT expression strictly in the tumor samples (Figure 3.9, Panel A). To determine whether NeuNT was active in these tumors, samples were immunoprecipitated with an antibody against Neu and then were immunoblotted to examine tyrosine phosphorylation. Consistent with the overexpression of Neu in the tumors, phosphorylation of Neu was only detected in the tumor samples (Figure 3.9, Panel B). Given that previous mouse models expressing elevated levels of Neu have also expressed elevated levels of other EGFR family members such as ErbB3 (Siegel and Muller, 1996), levels of other EGFR family members were examined. While EGFR and ErbB4 were unaffected (results not shown), ErbB3 levels were significantly elevated specifically in the tumor samples (Figure 3.9, Panel C).

To determine whether the observed elevation in levels of NeuNT correlated with an elevation in the level of *neuNT* mRNA, RNA was isolated from various tumors and controls and was subjected to an RNase protection experiment. While the samples were all quantitated and equal amounts were used, the PGK internal loading control indicated that there were discrepancies in the levels of RNA examined. However, this RNase

Figure 3.9 – Overexpression of activated Neu in Tumors.

Given the high levels of expression observed in the immunohistochemical analysis of the conditionally activated tumors (Figure Seven), the tumor were examined for Neu expression by Western analysis (A). Virgin and multiparious mammary glands as well as tumor and adjacent mammary gland controls were examined for Neu expression. Neu overexpression is readily noted only in the tumor samples. Grb2 was included as an internal loading control. After immunoprecipitating for Neu, a blot was probed with an antibody for phosphorylated tyrosine (P-Tyr), demonstrating that the overexpressed Neu was also catalytically active (B). Another family member, ErbB3, was also found to be overexpressed specifically in the tumor samples. Interestingly, the mammary glands adjacent to the tumors were seen to have ErbB3 levels similar to the multiparious control. Grb2 was again included as an internal loading control.

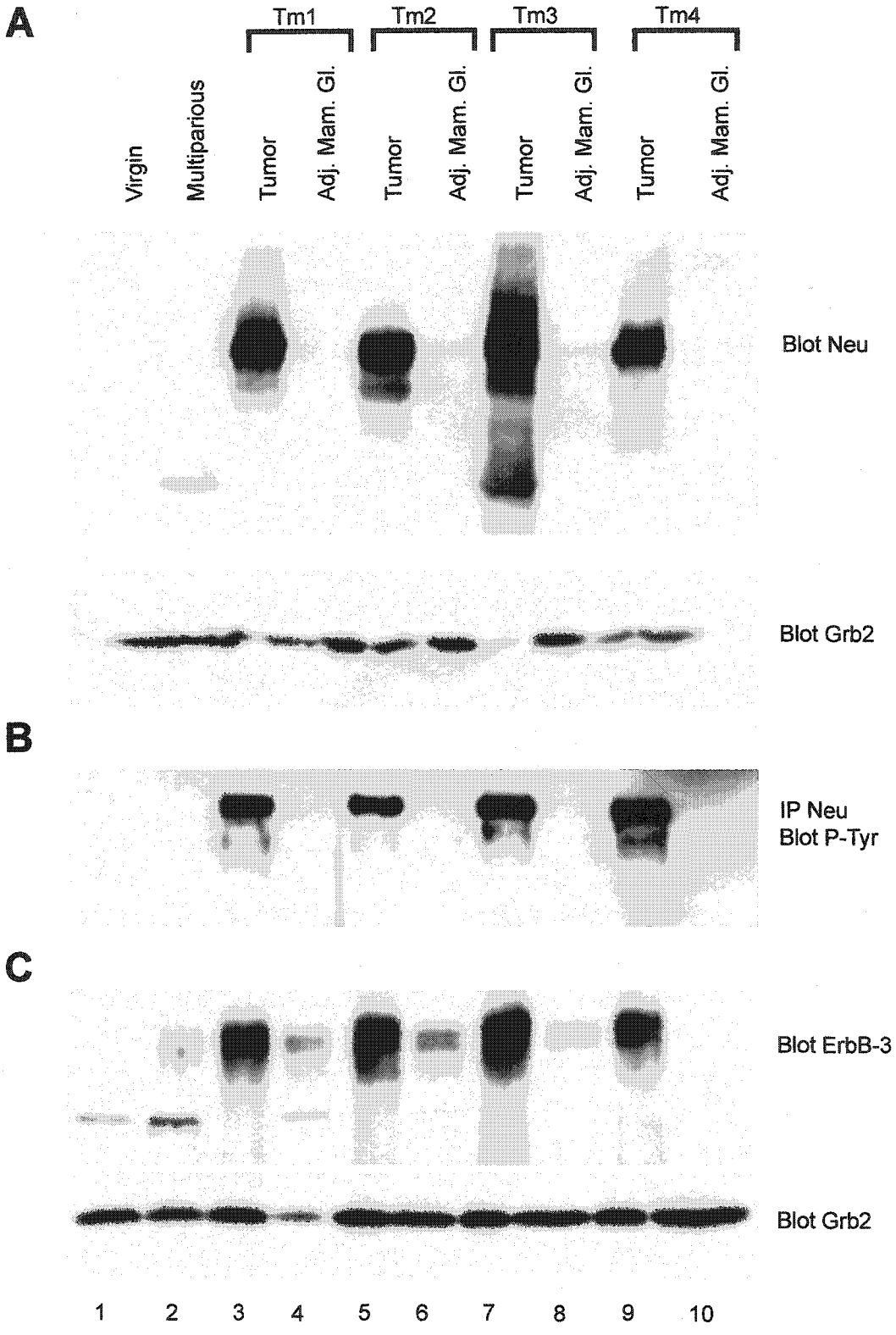
A
Tm1
Tm2
Tm3
Tm4
Virgin
Multiparious
Tumor
Adj. Mam. Gl.
Tumor
Adj. Mam. Gl.
Tumor
Adj. Mam. Gl.
Tumor
Adj. Mam. Gl.
Blot Neu
Blot Grb2
B
IP Neu
Blot P-Tyr
C
Blot ErbB-3
Blot Grb2
1 2 3 4 5 6 7 8 9 10

protection does show that NeuNT is expressed at significant levels in the tumors (Figure 3.10). Indeed, since the expression in the NDL control has previously been shown to be entirely composed of the NDL transcript, the reaction was likely not complete and proportion of the wild type *neu* allele is likely artificially high. Quantitative RT-PCR using mouse and rat homologue specific primers showed that the *neu* expression in these tumors is almost entirely composed of expression from the recombinant allele (data not shown). Taken together, these results illustrate that the recombinant allele is overexpressed both at the level of the transcript and protein.

In HER2 mediated breast cancer, the endogenous human allele is overexpressed and this overexpression is commonly observed in conjunction with amplification of the HER2 locus. Intending to determine whether amplification was involved in the conditionally activated NeuNT mouse model of mammary tumorigenesis, DNA was extracted from tumors and an adjacent mammary gland. Since the adjacent mammary gland does not overexpress NeuNT, it should serve as a control for no amplification in a Southern analysis. Using the Southern probe used to detect both the wild type and recombinant alleles (See Figure 3.2), the tumors were examined for amplification. This Southern analysis clearly illustrated that the recombinant *neuNT* allele at 4.5 kb was amplified relative to the endogenous allele at 7.5 kb (Figure 3.11, Panel A). There are distinct differences in the extent of relative amplification between the samples, for example contrast samples TM4 and TM6. Additionally, in several of the samples, a new band has been introduced above the wild type allele and is likely a result of the amplification process. Quantitative phosphoimager analysis was completed on this

Figure 3.10 – Overexpression of *neuNT* in mammary tumors.

Using a probe that spans the transmembrane domain of *neuNT*, an RNase protection reveals that the MMTV-Cre FlenoNeuNT tumors overexpress the activated form of *neu*. The mammary gland from a virgin conditionally activated mouse was included as a control, as was the tumor sample from the MMTV-NDL 1-4 line of transgenic mice. The full length probe is labelled (Full Length), the wild type protected fragment is labelled as Neu, and the mutant allele are shown as NDL 1-4 and NeuNT, corresponding to their activating mutation. PGK was used as an internal loading control. Previous experiments have shown that the NDL tumors express primarily the NDL allele and not the wild type allele, suggesting that the digestion was incomplete.

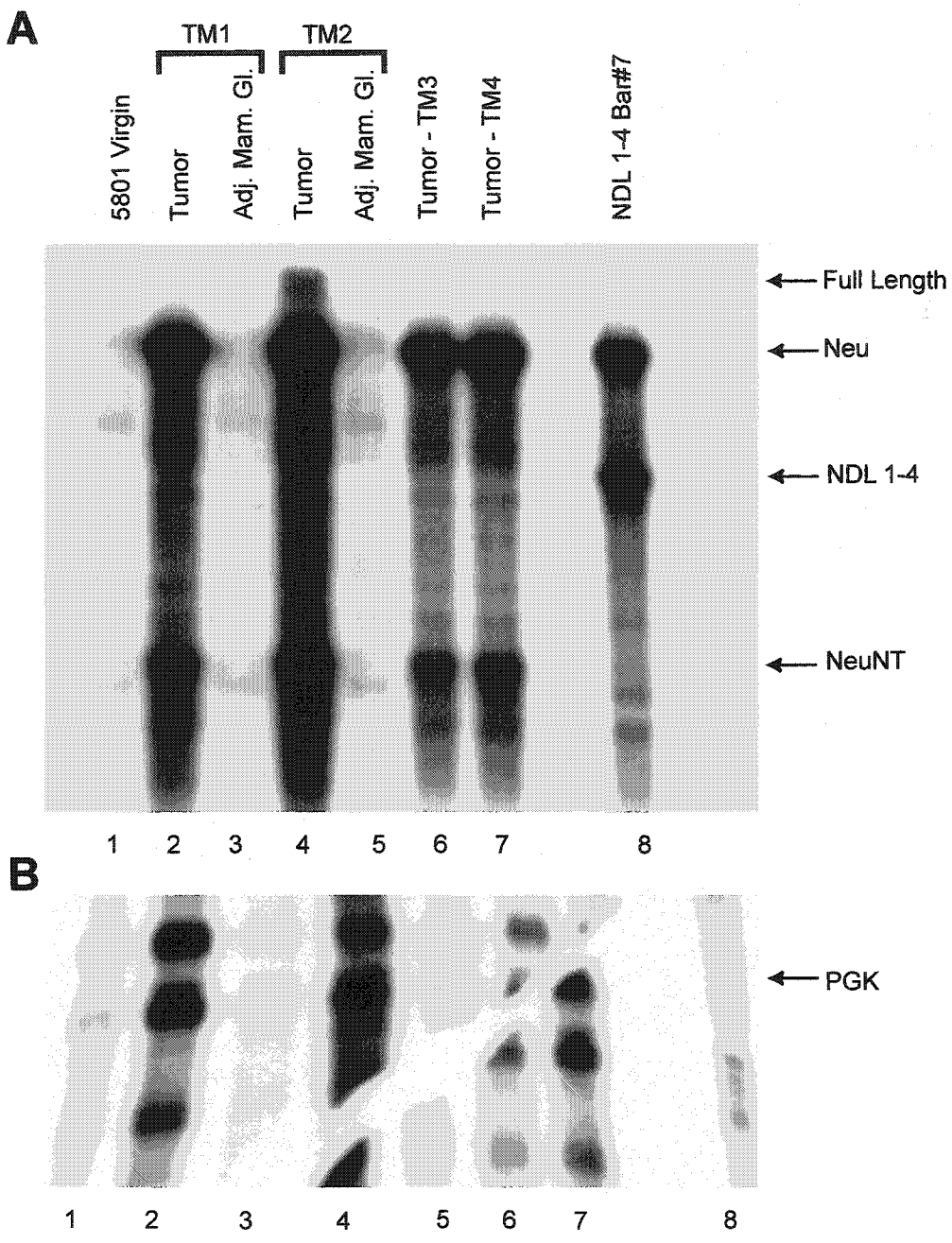
A
TM1
TM2
5801 Virgin
Tumor
Adj. Mam. Gl.
Tumor
Adj. Mam. Gl.
Tumor - TM3
Tumor - TM4
NDL 1-4 Bar#7
Full Length
Neu
NDL 1-4
NeuNT
1 2 3 4 5 6 7 8
B
PGK
1 2 3 4 5 6 7 8

Figure 3.11 – Amplification of *neuNT* in mammary tumors.

Given that human tumors overexpressing HER2 often amplify the proto-oncogene, the tumors in the conditionally activated mice were examined for amplification. Using the same Southern protocol outlined in Figure Two, the wild type and conditionally activated alleles were compared for gene amplification (A). Using DNA from an adjacent gland as a control, it is clearly seen that the activated allele is preferentially amplified. Further, there is a wide range of extent of the amplification, as seen when comparing samples TM4 and TM6. This Southern analysis was subjected to a Phosphoimager analysis to quantify the increase in *neuNT* copy number relative to the wild type allele (B). The differences in detection levels of the different sized fragments was negated through the standardization of the adjacent control, which was then set to a value of 1 activated allele for 1 wild type allele. The results of the quantification for each of the tumor samples are shown. The copy number ranged from 2 to 22 with an average of 8.8 copies of the activated allele for each copy of the wild type allele.

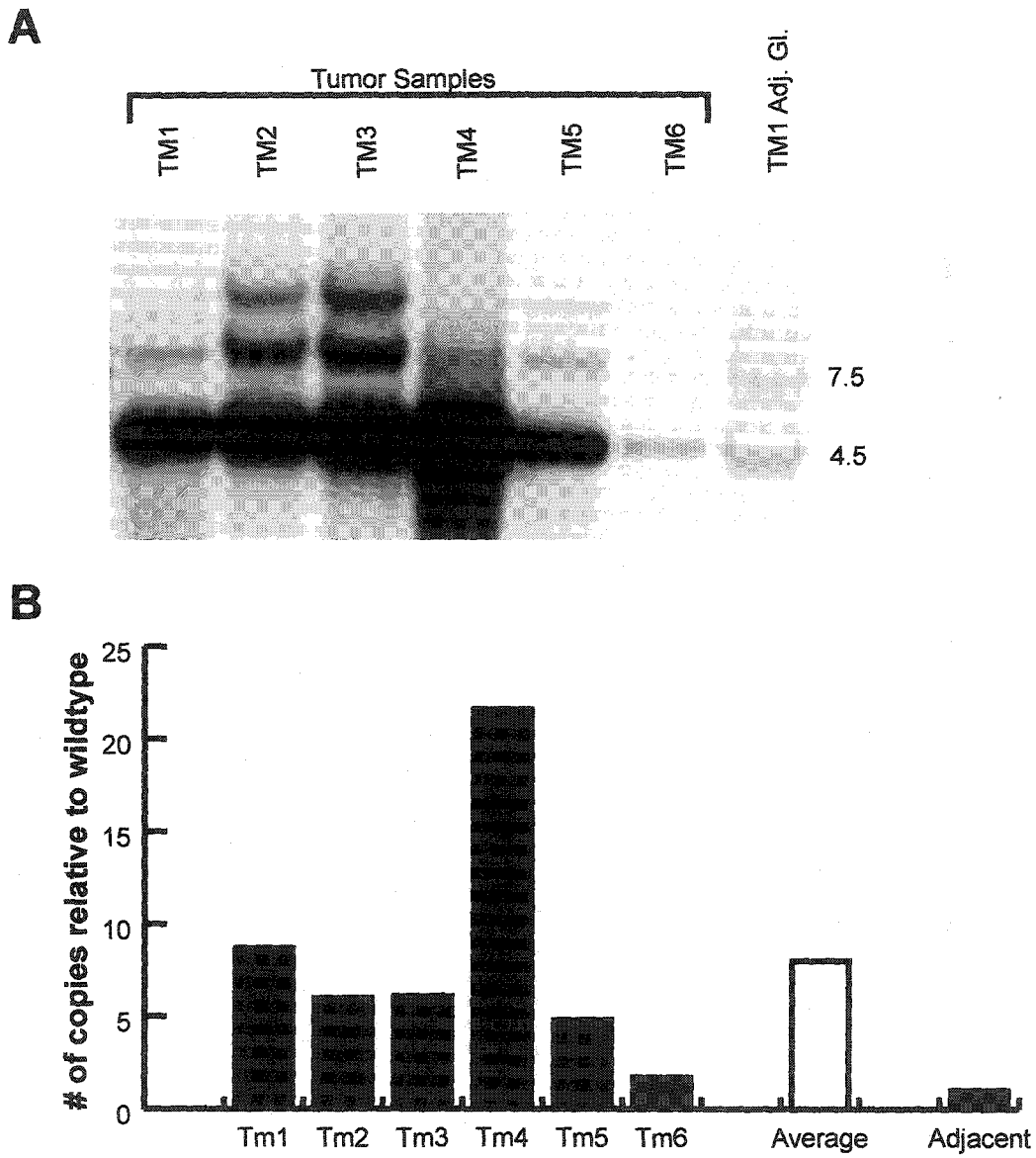
A
Tumor Samples
TM1
TM2
TM3
TM4
TM5
TM6
TM1 Adj. GI.
7.5
4.5
B
# of copies relative to wildtype
25
20
15
10
5
0
Tm1
Tm2
Tm3
Tm4
Tm5
Tm6
Average
Adjacent

Southern analysis and the extent of amplification of the conditionally activated *neuNT* allele is shown relative to the adjacent mammary gland control (Figure 3.11, Panel B). For these samples, the copy number ranged between 2 and 22 with an average of 8.8 copies of the *neuNT* allele for every copy of the endogenous allele. This data illustrates that expression of NeuNT under the control of the endogenous promoter results in tumorigenesis but requires amplification and overexpression of the conditionally activated allele.

3.2.4 Phenotypic and Gene Expression Comparison of Neu Mediated Tumors

In the conditionally activated Neu induced tumors, amplification and overexpression are observed, mirroring the human condition. These events are not observed in conventional MMTV based Neu models of tumorigenesis, likely due in part to the strength of the viral promoter. However, the signal transduction pathways activated in these two models should be similar and should lead to histologically similar tumors. Indeed, the initiating event is often associated with the histological classification of the tumor (Rosner *et al.*, 2002). Thus, a direct comparison of these two Neu induced tumor systems should reveal important insights into mechanisms of tumor induction in the endogenously regulated model system. The conditionally activated tumors were compared to NDL 1-2 tumors, which expressed an activated Neu allele under the control of the MMTV promoter (Siegel *et al.*, 1999). Initially, the mammary glands of these two models were examined prior to tumor formation. In contrast to the wild type mammary gland (Figure 3.12, Panel A), the conditionally activated and the NDL 1-2 mammary

Figure 3.12 – Differences between endogenously regulated and MMTV directed Neu mediated mammary development and tumorigenesis.

To examine the differences in mammary development and tumorigenesis in mice carrying the endogenously regulated and the MMTV regulated activated *neu* expression, a wholemount analysis was undertaken. Wild type (A, D), conditionally activated (B, E) and MMTV-NDL1-2 (C, F) mammary glands are shown. Clearly the smooth ducts and end buds seen in the wild type control have been replaced with abnormal lobuloalveolar development in both the conditional NeuNT and NDL strains. While the conditionally activated NeuNT mammary epithelium shows an ability to escape the confines of the fat pad (arrows), the NDL mammary gland is contained within the normal boundaries (B vs. C). At higher magnification, the excessive side branching terminating in lobuloalveolar units seen in the conditionally activated gland is not observed in the NDL strain (E vs. F). The histological section of the wild type control (G) is compared to the tumors from the conditional activation (H) and the NDL1-2 (I). When histological sections of tumors from the two strains are compared, the tumors are noted to be similar in appearance (H vs. I).

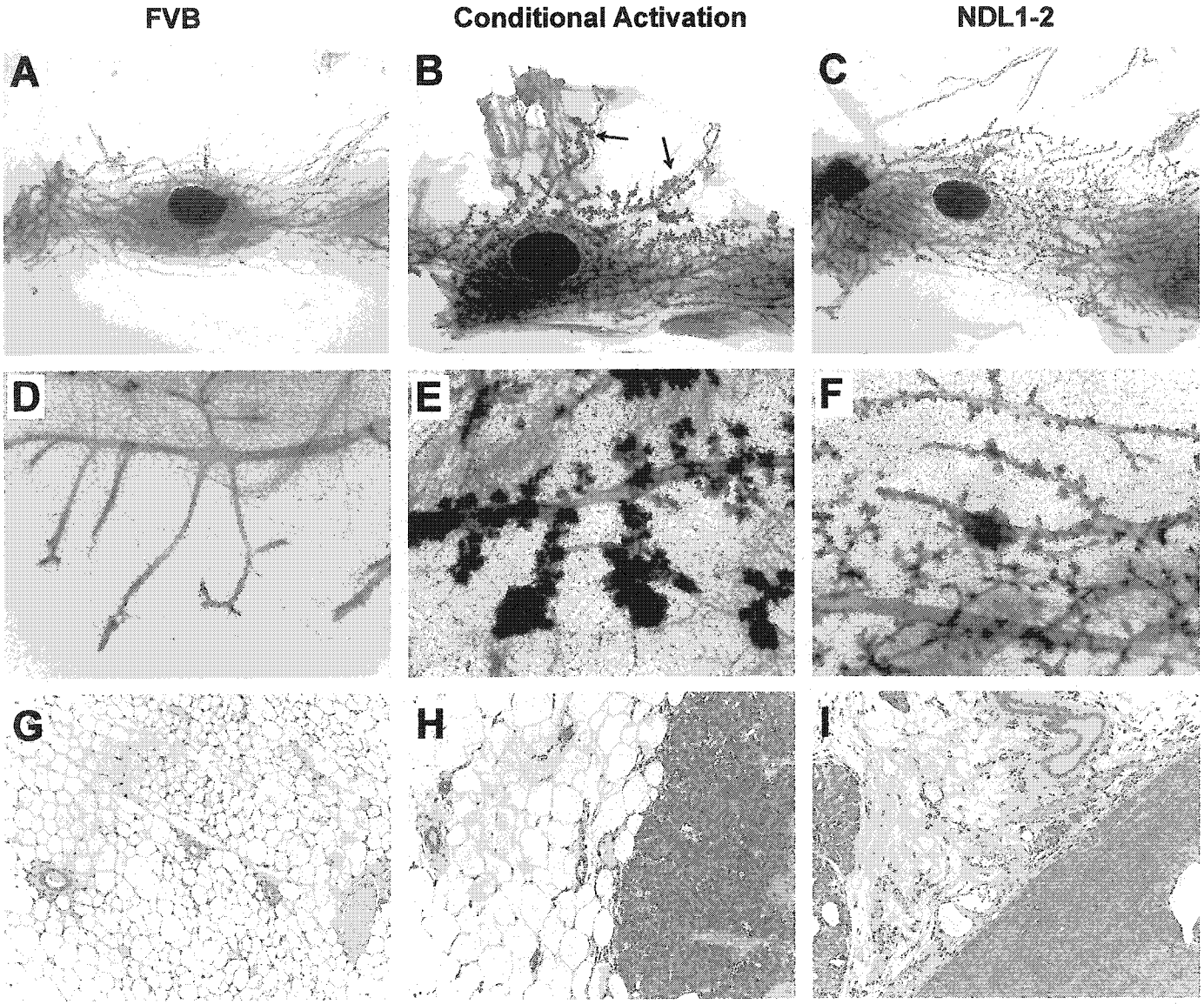
FVB
Conditional Activation
NDL1-2
A
B
C
D
E
F
G
H
I

glands both exhibit an increased amount of ductal branching (Figure 3.12, Panels B and C). As previously discussed, the conditional expression of NeuNT in the mammary gland allows the escape of the mammary epithelium from the fat pad and these aberrant ducts appear to follow blood vessels out of the normal confines of the fat pad (Figure 3.12, Panel B and Figure 3.6 Panel B). However, the expression of activated Neu in the NDL 1-2 model does not promote the mammary epithelium to escape the normal boundaries (Figure 3.12, Panel C). At higher magnification, the smooth ducts observed in the wild type control are compared to aberrant branching observed in the two models expressing activated *neu* alleles (Compare Figure 3.12 Panels D-F). In the mice expressing the activated allele under the endogenous promoter, the lobuloalveolar endbuds are frequently hyperplastic, but in the MMTV based system, these hyperplastic regions quickly develop into adenocarcinomas. Further, the presence of lobuloalveolar side buds is clearly seen in both mammary glands expressing an activated *neu* allele. While the wild type controls do not develop tumors (Figure 3.12, Panel G), the two strains expressing activated Neu in the mammary gland develop comedo-adenocarcinomas that are histologically quite similar (Compare Figure 3.12, Panels H and I). Further, examination of the histology of both tumors reveals a distinct margin separating the adjacent tissue from the tumor.

The latency of tumor formation in the MMTV regulated and endogenously regulated Neu induced tumors is strikingly different. Indeed, when the latency of Neu induced tumor formation is compared on a Kaplan Meier plot (Figure 3.13, Panel A), the difference is immediately apparent. While the NDL 1-2 mice develop tumors in 50% of

Figure 3.13 – Differences in endogenously and MMTV regulated Neu mediated tumorigenesis and metastasis.

While the Neu mediated tumors are histologically similar, the latency is far different (A). Tumors were palpated in 50% of the NDL1-2 female mice by 4.5 months of age (open squares). However, tumors are not palpated in 50% of conditionally activated NeuNT mice until 15.9 months of age (closed circles). Further examination of these mice revealed that 60% of the NDL tumors resulted in metastasis to the lungs (B). In stark contrast, lung metastases have been detected in only 2.5% of the conditionally activated mice bearing tumors. Clearly, while there are similarities in tumor formation and histology, there are numerous differences between these two strains.

A

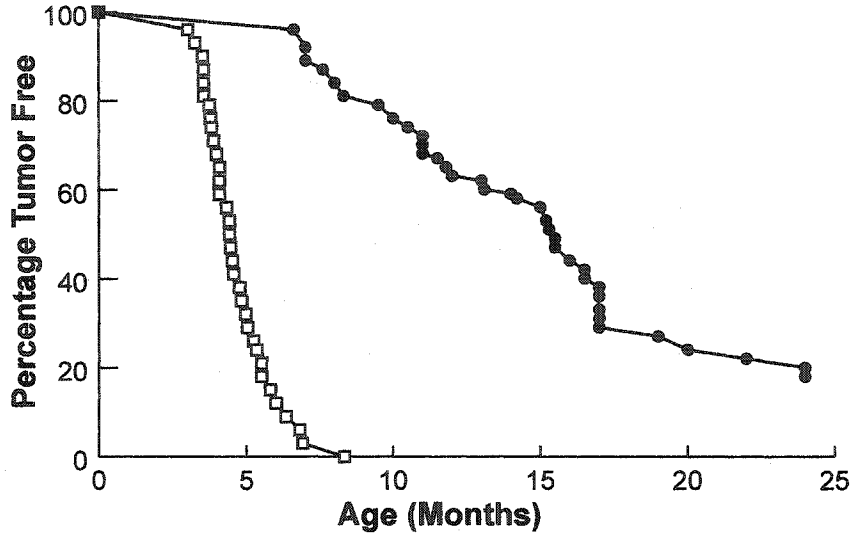
Percentage Tumor Free
100
80
60
40
20
0
0
5
10
15
20
25
Age (Months)

B

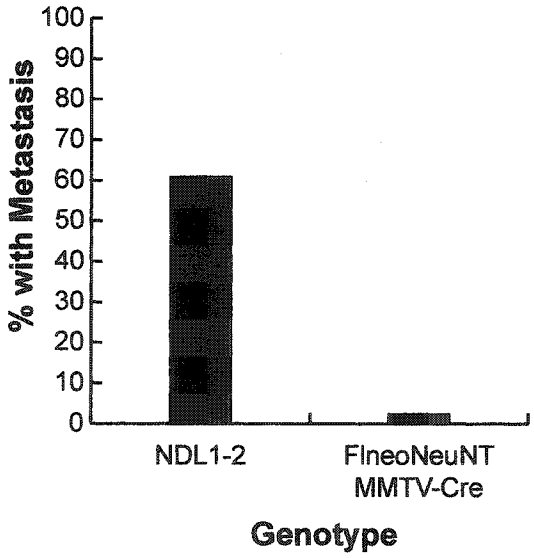
% with Metastasis
100
90
80
70
60
50
40
30
20
10
0
NDL1-2
FlneoNeuNT
MMTV-Cre
Genotype

female mice by 4.5 months, it takes 15.9 months for the conditionally activated Neu mice to develop focal mammary adenocarcinomas. However, in addition to the differences in latency, there are striking differences in the frequency of pulmonary metastasis in these two models. While 60% of NDL 1-2 tumors were shown to metastasize to the lungs, less than 3% of the conditionally activated tumors metastasized. Indeed, this 2.5% metastatic rate represents a single pulmonary metastasis among the 41 tumors that were examined. Although there are clear differences in mammary gland development, tumor latency and metastatic frequency, the tumors in the two lines were histologically similar and were characteristic of Neu induced carcinomas.

To further explore the molecular basis for the differential metastatic potential of these two different Neu induced tumor types, the gene expression profile was compared for tumors derived from transgenic mice expressing activated *neuNT* under the transcriptional control of the endogenous promoter with those expressing activated NDL from the mouse mammary tumor virus promoter. RNA from 10 tumors from each line was pooled and was compared through an Affymetrix GeneChip analysis. The major results from this analysis is summarized in Table 3.1. The fold elevation is expressed as a positive value when the transcript level from the endogenously regulated *neuNT* tumor was higher than the transcript level from the MMTV regulated tumor. In general, most of the genes detected were expressed at higher levels in the endogenous promoter model than there were in the MMTV based system. The various genes with > 5 fold difference between the two tumor samples were then classified into categories based upon their function. One category of genes that arose from these analyses are mammary gland

Table 3.1 – Detected mRNA differences between endogenously regulated and MMTV controlled activated Neu tumors.

To further examine differences between Neu mediated tumors under the control of the endogenous promoter or the MMTV promoter, RNA from 10 tumor samples from each strain were pooled and examined by Affymetrix chip analysis. The results of the chip are shown under several distinct family headings. Genes that can be loosely defined as being involved in mammary gland differentiation, glycoproteins or are transcription factors were separated and listed in order of their fold elevation of endogenous over MMTV induced tumors. Additionally, the Pubmed Nucleotide accession number is listed as is the chromosomal location, when known. For selected genes, further confirmation was completed, as listed, to verify the chip data. Additionally, a final heading entitled Amplicon was added for genes with a chromosomal location identical to *erbB2*. *Grb7* and *cab1* were both elevated in the conditional model and are juxtaposed to *erbB2* in the mouse genome.

Table 3.1 Gene Expression Results

Gene	Accession Number	Fold Elevation	Confirm	Chromosonal Location
Differentiation Markers				
Glycam1	m93428	144.4	Northern	15 - 63.0 cM
WAP	j00649	128.6		11 - 0.5 cM
keritan-epidermial	m13806	99.1		Undefined
PSP	X01697	43.6	Northern	2 - 88.0 cM
von Ebner Salivary	U46068	32.8		2 - 76.3 cM
epsilon-casein	v00740	26.8		Undefined
keritan-epidermial	k02108	23.7		Undefined
cytokeritan	m28698	23.6		Undefined
MDGI	u02883	22.3	Northern	4 - 61.0 cM
alpha-amylase	v00719	20.9		Undefined
Proliferin	k02245	12.7	Northern	13 - 6.0 cM
Gamma-casein	d10215	8.4		5 - 45 cM
alpha-casein	m36780	5.4		5 - 44.9 cM
beta-casein	x04490	5.4		5 - 45.0 cM
Glycoproteins				
AEG-1	m92849	153.21		17 - 21.0 cM
Serglycin	x16133	10.6	Northern	Undefined
MUC1	m65132	5		3 - 44.8 cM
Clusterin	i08235	2.5		14 - 28.0 cM
MUC10	U37531	-53.6		Undefined
Transcription Factors				
HMG-1(y)	j04179	14.3	Northern	17 - 13.2 cM
MSG1	msa.2467.0	9.4		Undefined
Krox-20	x06746	8.5	Northern	10 - 35.0 cM
PEA3	x63190	6.6		11 - 60.0 cM
ELF3	af016294	5.7		Undefined
Albumin D-box	u29762	-11.5		7 - 23.0 cM
Amplicon				
Grb7	aa216863	38	Western	11 - 57.0 cM
CAB1	Msa.2277.0	26.3	Lightcycler	11 - 57.0 cM

differentiation markers, including genes such as *whey acidic protein* (*wap*) (128 fold elevation)(Hennighausen and Sippel, 1982), several members of the casein family (5 to 26 fold elevation) and members of the keratin family (23 to 99 fold elevation). The presence of a putative tumor suppressor, Mammary Derived Growth Inhibitor (MDGI)(Grosse *et al.*, 1992), was also noted to be elevated 22 fold in the conditionally activated Neu model. Taken together, the genes in this class (Table 3.1) indicate that while the tumors may have been histologically similar they are quite distinct on the molecular level. Further, these results highlight the difference in differentiation between two tumors with different metastatic potential.

The identification of a number of glycoproteins overexpressed in the endogenously regulated model is also intriguing given that MUC4 may serve in the regulation of Neu signaling through the facilitation of heterodimerization with ErbB3 (Jepson *et al.*, 2002). An examination of the over and under expressed glycoproteins reveals several interesting findings. *Acidic epididymal glycoprotein 1* (*AEG-1, CRISP-1*) is overexpressed 153 fold and is normally expressed in the male genital tract and the salivary gland. However, the same analysis of the *AEG-1* promoter revealed a consensus binding domain for PEA3 (Schwidetzky *et al.*, 1997), which was also overexpressed in the endogenously regulated Neu mediated tumors. Interestingly, *muc1* is also overexpressed in these tumors and has been observed to be overexpressed in many human tumors. Further, it has been illustrated that EGFR and MUC1 interact at the cell membrane, resulting in the recruitment of c-Src (Li *et al.*, 2001). Clearly these various

glycoproteins serve to recruit and activate specific pathways that will alter the properties of the carcinoma.

Significantly, another category of genes that were noted to be differentially expressed between the two tumor models were transcription factors. Given the potential role of specific transcription factors in regulating transcription from the endogenous promoter, it is conceivable that several of these may play a direct role in regulating expression of the activated *neu* allele. Indeed, members of the Ets family including *PEA3* and *Elf3* were elevated in the endogenous promoter driven model compared to MMTV Neu mediated tumors. Interestingly, both sets of transcription factors have previously been implicated in the regulation of *erbB2* promoter function (Baert *et al.*, 1997; Benz *et al.*, 1997; Chiang *et al.*, 2000; Xing *et al.*, 2000; Shepherd *et al.*, 2001). Another interesting transcription factor that is upregulated in the endogenous promoter model is the Zinc finger transcription factor Krox20 (Egr2) (Chavrier *et al.*, 1988). Although no direct evidence linking ErbB2 expression with Krox-20 exists, there is evidence suggesting that this class of transcription factors is part of the same genetic pathway. In this regard it is interesting to note that Krox20 and ErbB2 exhibit overlapping patterns of expression during embryonic development (Garratt *et al.*, 2000). However the precise role of these transcription factors in regulating ErbB2 expression remains to be evaluated.

The final group of genes identified through the gene expression analysis were genes that were found to be chromosomally juxtaposed to the endogenous allele (Table 3.1). Classified as being a portion of the amplified region, or amplicon, this class of genes was exclusively overexpressed in the endogenously regulated model and included

both *grb7* (38 fold overexpression)(Keegan and Cooper, 1996) and *cab1*(26 fold overexpression). Interestingly, both of these genes have previously been identified as being overexpressed in human breast cancers overexpressing HER2, suggesting a remarkable similarity between the human condition and the conditionally activated mouse model (Kauraniemi *et al.*, 2001; Varis *et al.*, 2002). To further validate that the level of overexpression observed in the Affymetrix GeneChip result was accurate, the expression of various genes in the individual tumor samples was examined through Northern blotting, Western blotting or quantitative RT-PCR (Summarized in Table 3.1). Additionally, the chromosomal location of the various genes is illustrated in Table 3.1

An example of the Northern analysis confirming of the gene expression data is shown in Figure 3.14. Northern analysis was completed for *glycam1*(144 fold overexpression)(Lasky *et al.*, 1992), *serglycin* (10 fold overexpression)(Kjellen *et al.*, 1989) and *MDGI* (22 fold overexpression)(Grosse *et al.*, 1992). Although the average fold up-regulation of these markers was in close agreement with the Microarray analysis, the Northerns revealed that individual tumors were highly variable in the expression of these differentiation markers. For example whereas three of the five conditionally activated tumors expressed high levels of *glycam1* and *MDGI* relative to primary tumors derived from the MMTV-NDL (Figure 3.14, compare lanes 2-4 to 6-10 in Panel A and C,) two of the tumors derived from the endogenous promoter driven model expressed relatively low amounts of these differentiation markers (Figure 3.14, lanes 1,5 in Panel A and C). These analyses suggest that state of differentiation of these ErbB2 induced tumors may vary. However, while the expression patterns of various tumors for *MDGI*

Figure 3.14 – Northern confirmation of mRNA chip data.

In order to ensure the accuracy of the chip data, Northerns were performed for several samples. Three examples are shown here for *glycam1* (A), *serglycin* (B), and *MDGI* (C). *Glycam1* was elevated 144 fold in the chip data from 10 pooled tumors, and is clearly seen to be expressed in several of the conditionally activated tumor samples at extremely high levels (TM28). However, expression levels in other conditionally activated tumors are indistinguishable from the NDL tumor expression level (TM9 vs. 6744). However, the trend is for elevated *glycam1* expression in the conditionally activated tumors. In the same fashion, *serglycin* was elevated 10 fold as assayed by chip analysis and is seen to be elevated in the Northern analysis. The expression pattern for MDGI appears remarkably similar to the glycam1 expression pattern, and again reveals that while the chip data identified the genes as being overexpressed the tumors are a heterogenous population. The ethidium stain from the MDGI Northern is shown as a loading control.

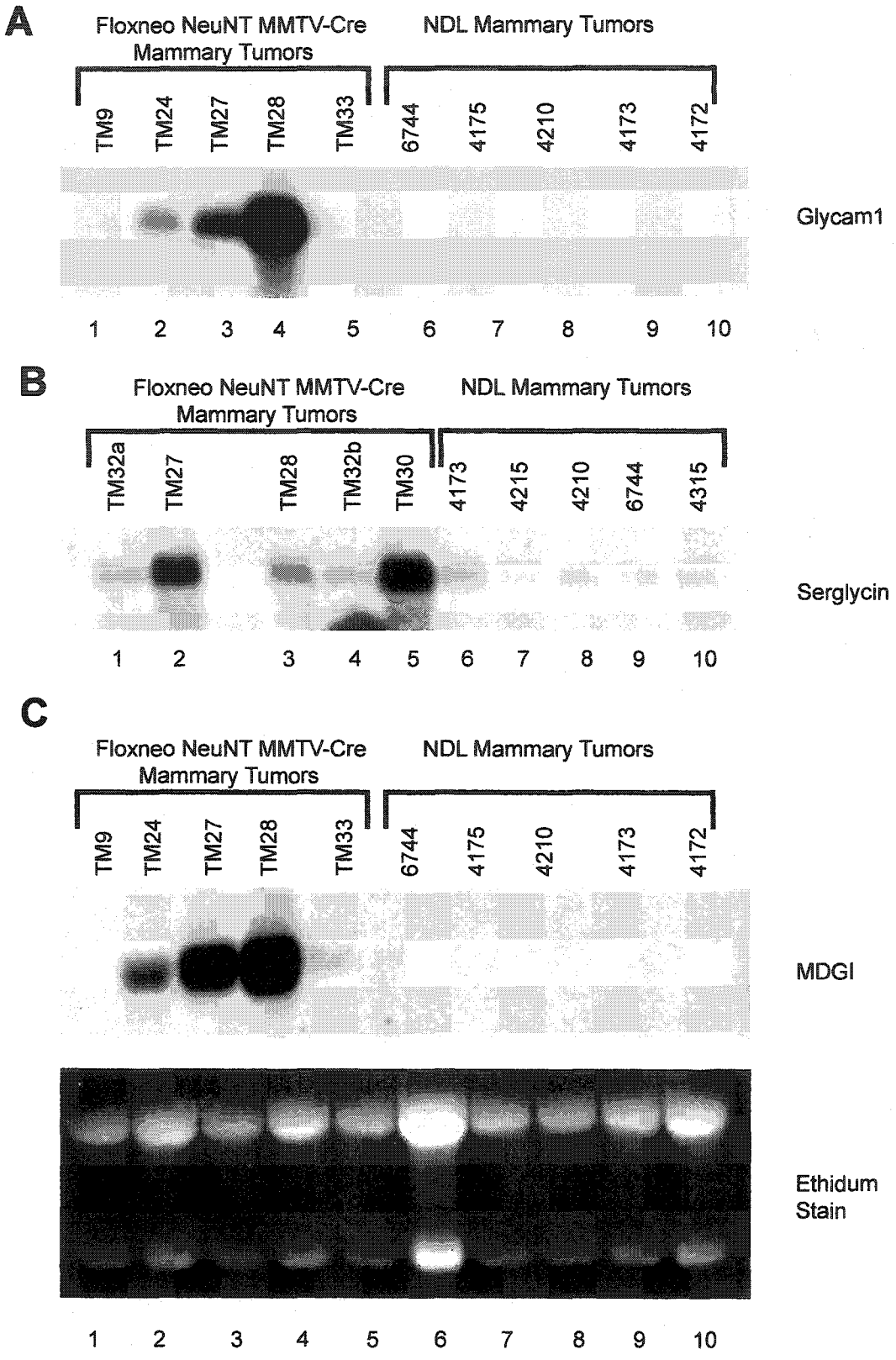
A
Floxneo NeuNT MMTV-Cre Mammary Tumors
NDL Mammary Tumors
TM9
TM24
TM27
TM28
TM33
6744
4175
4210
4173
4172
Glycam1
1 2 3 4 5 6 7 8 9 10
B
Floxneo NeuNT MMTV-Cre Mammary Tumors
NDL Mammary Tumors
TM32a
TM27
TM28
TM32b
TM30
4173
4215
4210
6744
4315
Serglycin
1 2 3 4 5 6 7 8 9 10
C
Floxneo NeuNT MMTV-Cre Mammary Tumors
NDL Mammary Tumors
TM9
TM24
TM27
TM28
TM33
6744
4175
4210
4173
4172
MDGI
Ethidum Stain
1 2 3 4 5 6 7 8 9 10

and *Glycam1* were identical, these genes are on separate chromosomes (Table 3.1) indicating that they are regulated through common pathways rather than through an amplification event like the genes in the amplicon classification. Further, the expression pattern observed for samples in one gene cannot predict the expression pattern for another gene. For example, while TM27 had lower levels of *glycam1* and *MDGI* than sample TM28 (Figure 3.14, lanes 3 vs. 4 in Panels A and C), when the level of *serglycin* was examined, TM27 had higher levels of expression than TM28 (Figure 3.14, Panel B lanes 2 vs. 3). Taken together, these results show that the individual tumor samples from the conditionally activated line are expressing higher levels of various differentiation markers, consistent with the Affymetrix GeneChip data.

To establish whether the observed elevated expression of *cab1* and *grb7* correlated with gene amplification, both amplification and expression of these genes was examined in greater detail. To assess whether the extent of *grb7* and *cab1* overexpression was due to gene amplification, a Southern blot analyses was conducted on various conditionally activated tumor samples. Using a probe that will detect both the wild type allele (7.5 kb) and the knock-in activated *neu* allele (4.5kb), the degree of amplification of *neuNT* in these samples was observed to correlate with the extent of gene amplification for both *grb7* and *cab1* (Figure 3.15, Panel A). These analyses suggest that unlike the MMTV-NDL model, the expression of Grb7 and Cab1 is closely linked to extent of *neu* amplification. To confirm that Grb7 was overexpressed in addition to being amplified, immunoblot analyses were performed on primary tumors from both transgenic models with Grb7 specific antisera. As shown in Figure 3.15 Panel B, tumors derived

Figure 3.15 – Coamplification and overexpression of genes contained within the ErbB2 amplicon.

Genes that were thought to be chromosomally juxtaposed to ErbB2 were further examined after being identified as overexpressed in the gene chip experiment. As previously observed, in a Southern analysis amplification of the knock-in *neuNT* allele (4.5 kb) was observed in the majority of tumor samples while the wild type allele (7.5 kb) has not been noted to be amplified. When the same samples were examined for amplification of *grb7* and *cabl*, an identical pattern of amplification was noted, indicating that these genes have been co-amplified with the activated *neu* allele. To further examine Grb7 expression, immunoblotting for Grb7 from tumor lysates from both the conditionally activated and the NDL lines revealed that it was highly overexpressed in the conditionally activated tumors. This is consistent with the 38 fold overexpression noted in the gene chip data.

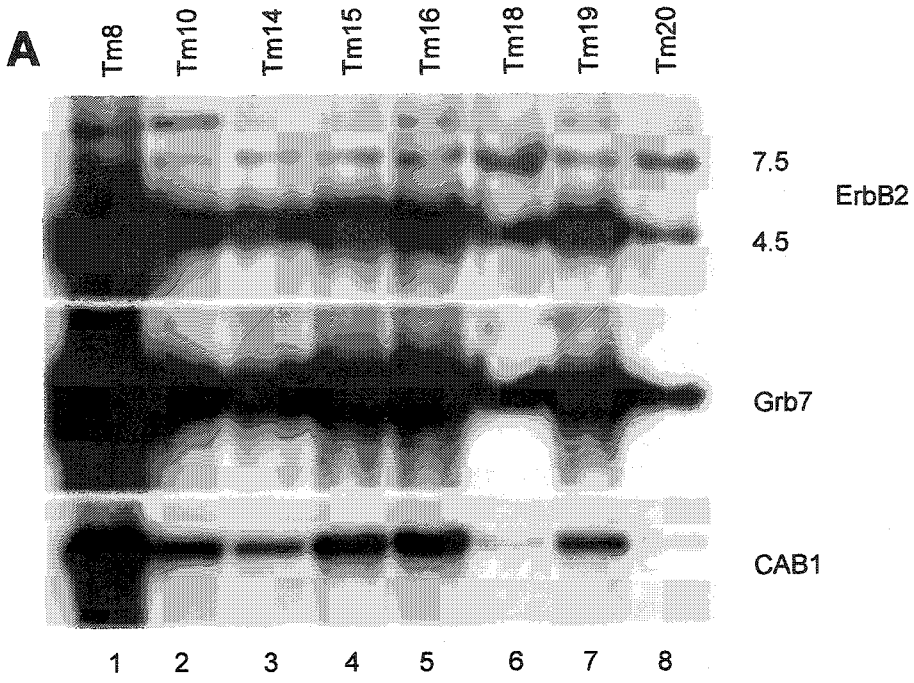
A
Tm8
Tm10
Tm14
Tm15
Tm16
Tm18
Tm19
Tm20
7.5
ErbB2
4.5
Grb7
CAB1
1
2
3
4
5
6
7
8

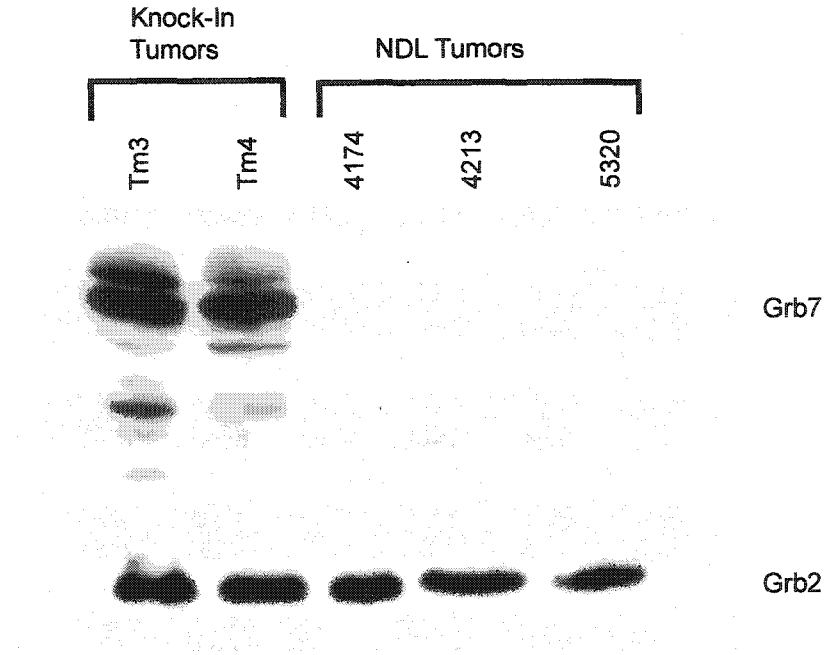
B
Knock-In Tumors
NDL Tumors
Tm3
Tm4
4174
4213
5320
Grb7
Grb2

from the endogenously regulated model expressed elevated levels of Grb7 protein (Figure 3.15 Panel B). In contrast, tumors derived from the MMTV-NDL model did not express detectable levels of Grb7 (Figure 3.15 Panel B). Taken together, these observations indicate that like human breast cancers with overexpression and amplification of HER2, co-amplification of *neu*, *grb7* and *cab1* is correlated with elevated expression of the individual components of this amplicon in the conditionally activated NeuNT mouse model of mammary tumorigenesis.

3.2.5 The effect of Grb7 ablation on Invasiveness

Human breast cancers overexpressing HER2 and the mouse model described above have both been shown to express Grb7 at high levels. While overexpression of Grb7 has been shown to enhance cellular migration in both Chinese Hamster Ovary (CHO) and Esophageal Cancer cell lines, the role of Grb7 in mammary epithelial tumors has not been demonstrated (Tanaka *et al.*, 1998; Han and Guan, 1999). Primary cell lines from tumors expressing NeuNT under the endogenous promoter were generated (Cell Lines TM15 and TM22) and were shown to overexpress both Neu and Grb7 by immunoblot analysis (data not shown). To determine the role of Grb7 in the invasiveness of these cell lines, a construct was prepared that placed a portion of the *grb7* cDNA in reverse orientation under the control of the cytomegalovirus (CMV) promoter. This construct should result in the expression of antisense *grb7*, resulting in the downregulation of the *grb7* overexpressed from the endogenous locus (Figure 3.16, Panel A). Transfection of this construct into the TM15 primary cell line was followed by

Figure 3.16 – The Role of Grb7 in Invasion

To determine the role of the overexpressed Grb7 in the TM15 cell line, a construct was created to express an antisense RNA message containing bp 749 to 1887 of the Grb7 cDNA in reverse orientation. This antisense cDNA was placed under the control of the CMV promoter. When transfected into cells, zeocin selection was applied and colonies were screened for Grb7 expression. A comparison of the primary tumors reveals expression of the 51 and 59 kDa isoforms of Grb7 (Panel B, Lanes 1-2). Additionally, the parental TM15 cell line expresses both splice forms (Lane 3). Four cell lines are shown after zeocin selection including two where there was no effect of the level of Grb7 (Lanes 4-5) and two lines where the level of the 51 kDa splice form was visibly reduced while the 59 kDa splice variant was visibly increased (Lanes 6-7). To determine what effect the expression of the antisense construct was having on the tumor cell lines, a Matrigel invasion assay was conducted. The invasive index of the antisense TM15 cell line compared to the parental TM15 cell line revealed that the cell lines with reduced expression of the 51 kDa Grb7 splice variant had increased the propensity for invasion by up to 3.5 fold.

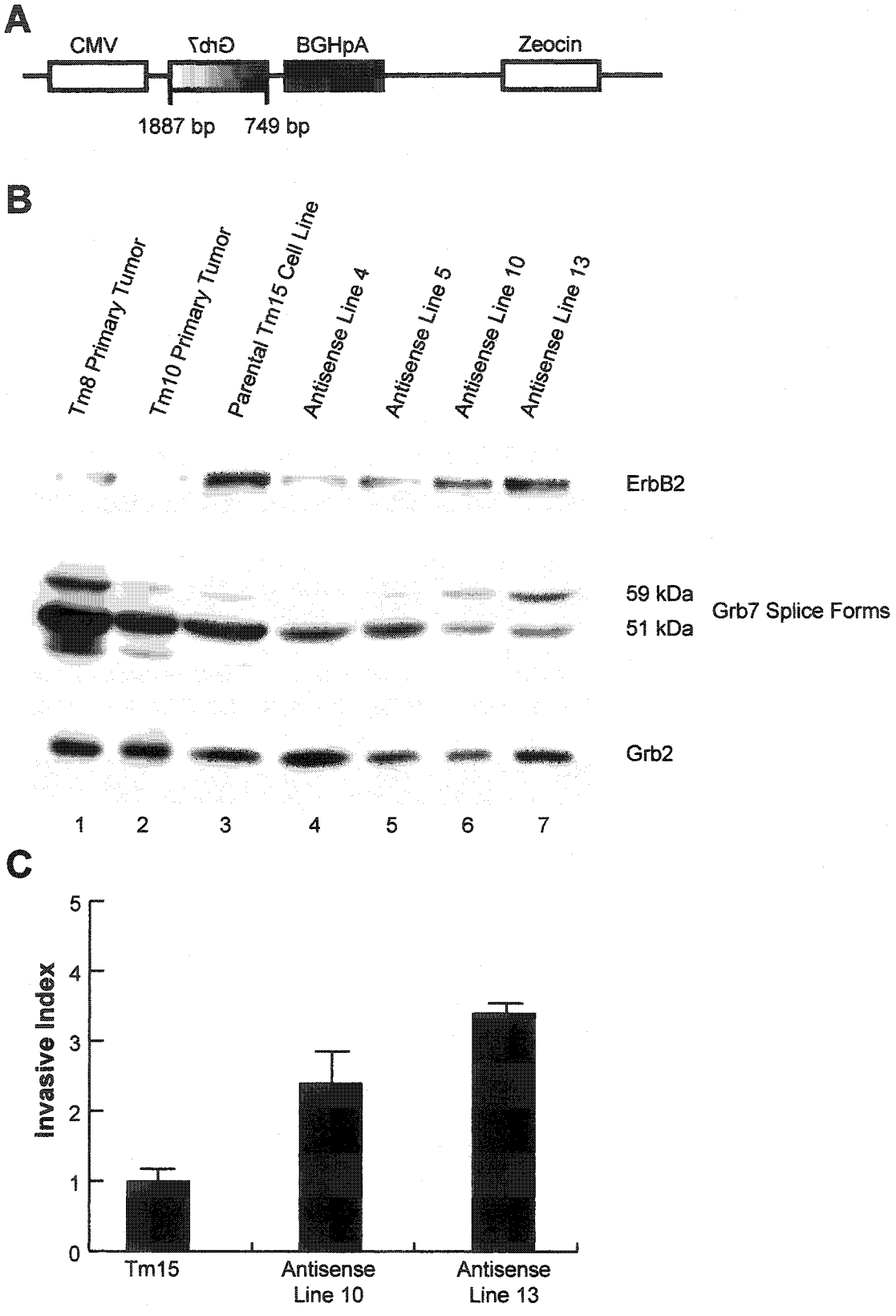
A
CMV
ΓdrƆ
BGHpA
Zeocin
1887 bp
749 bp
B
Tm8 Primary Tumor
Tm10 Primary Tumor
Parental Tm15 Cell Line
Antisense Line 4
Antisense Line 5
Antisense Line 10
Antisense Line 13
ErbB2
59 kDa
51 kDa
Grb7 Splice Forms
Grb2
1
2
3
4
5
6
7
C
Invasive Index
0
1
2
3
4
5
Tm15
Antisense Line 10
Antisense Line 13

selection for zeocin resistance and individual colonies were picked and expanded for characterization. The level of Neu expression from these various cell lines and from primary tumor lysate controls is shown In addition, the level of Grb7 for the controls and the various cell lines is also shown (Figure 3.16, Panel B). While the primary tumor lysates and the parental TM15 cell line show high levels of the 51 kDa isoform of Grb7, they also exhibit weak immunoreactivity for the 59 kDa splice variant (Figure 3.16, Panel B Lanes 1-3). While numerous Grb7 antisense cell lines were characterized that showed no effect on the levels of Grb7 in comparison to the parental cell line control (Figure 3.16, Panel B, Lanes 4-5), there were several cell lines that showed a reduction in the levels of the 51 kDa isoform of Grb7 (Figure 3.16, Panel B, Lanes 6-7). Interestingly, in these cell lines there was a corresponding elevation in the 59 kDa Grb7 splice variant, such that the ratio of 51 kDa to 59 kDa splice forms was shifted towards a predominance of the 59 kDa isoform (Figure 3.16, Panel B, Lanes 6-7). To determine what effect the expression of the antisense Grb7 construct had on the invasive properties of the tumor cell line, a Matrigel invasion assay was completed on the parental cell line and the four antisense cell lines shown in Figure 3.16, Panel B. The invasive index of the parental cell line, that is the percentage of cells migrating through the Matrigel relative to the number of cells migrating without a Matrigel insert, was determined and was set to 1 (Figure 3.16, Panel C). The antisense cell lines that had no change in the levels of Grb7 were not significantly different from the parental controls (data not shown). However, the cell lines that had reduced the levels of the 51 kDa isoform with a corresponding increase in the levels of the 59 kDa isoform had an increased level of invasiveness.

Indeed, the invasive index was increased up to 3.5 fold over the parental control. Interestingly, the parental cell line was derived from the endogenously regulated NeuNT tumor model which was previously shown to rarely metastasize to the lungs.

3.2.6 Role of Double Minute Chromosomes in Neu Mediated Tumors

During the characterization of the endogenously regulated NeuNT tumor model described above, numerous similarities to the human condition were noted. Given the amplification observed in both the human disease and in the mouse model, spectral karyotyping (SKY) and comparative genome hybridization (CGH) was completed on various tumor samples to establish a baseline for future molecular analysis of these tumors (Montagna *et al.*, 2002). Since these results directly pertain to the characterization of the mouse model described above, the results are briefly summarized. Consistent with the amplification of *neuNT*, *grb7* and *cab1* detected by Southern analysis, amplification in chromosome 11 was noted. Further, a deletion of a portion of chromosome four was described for 70% of the tumor samples tested (n=10). When this deletion is compared with the Affymetrix data (Table 3.1), there were no genes detected at high levels in the MMTV driven model that were lost in the endogenously regulated model on chromosome 4. However, this does not preclude the possibility that the MMTV regulated tumors also contain a deletion in chromosome four. In addition to the characterization of the chromosomal aberrations, no losses or gains in copy number were reported for *p53*, *myc* or *brca1* (Montagna *et al.*, 2002). Finally, fluorescent in situ hybridization (FISH) for Neu revealed that there were numerous double minute (DM)

chromosomes present in cell lines derived from this model of Neu induced tumorigenesis (Montagna *et al.*, 2002) (FISH result is also reproduced in Figure 3.17, Panel A). To determine whether the high levels of NeuNT expression in the cell lines derived from the endogenously regulated NeuNT tumors was derived from the amplification present on chromosome 11 or whether expression originated from the DMs, the DMs were selectively eliminated through repeated passages in media containing hydroxyurea. Without the addition of hydroxyurea to the cell lines, the NDL 1-2 control, the TM15 and the TM22 cell lines all showed high levels of Neu expression (Figure 3.17, Panel B, Lanes 1, 3 and 5). Interestingly, with the addition of 150 μM hydroxyurea to the media for 16 passages to remove the DMs, Neu expression was lost in the TM22 cell line (Figure 3.17, Panel B, Lane 6). These results suggest that Neu expression in the TM15 cell line is from chromosome 11 while the TM22 cell line derived a large portion of Neu expression from the DMs. When expression of ErbB3 was examined in the various cell lines prior to hydroxyurea treatment, ErbB3 was only detected at high levels in the TM15 cell line (Figure 3.17, Panel C, Compare Lanes 1, 3 and 5). Interestingly, with the hydroxyurea induced loss of Neu expression in the TM22 cell line there was a corresponding increase in the levels of ErbB3 (Figure 3.17, Panel C, Lane 6). These results suggest that the other EGFR family members are able to compensate for the loss of Neu. Finally, when cells from the TM22 cell line, cultured with and without hydroxyurea, were injected subcutaneously into the flanks of mice, there was no difference in the rate of tumor formation (data not shown). Taken together, this data suggests that there are numerous tumorigenic events that have transformed the mammary

Figure 3.17 – Expression of ErbB2 from Double Minute Chromosomes

Expression of ErbB2 was assayed in the NDL, TM15 and TM22 cell lines by immunoblotting, revealing high levels of ErbB2 expression. The TM15 and TM22 cell lines were noted to have double minute chromosomes that contained *erbB2* as detected through a FISH analysis (Panel A, Chromosomes in red, *erbB2* probe in yellow). To determine whether expression of ErbB2 in these samples was primarily from the double minute chromosomes present in TM15 and TM22 (Panel A), or if expression was from the genomic amplification of ErbB2, the cells were treated with hydroxyurea for 16 passages. After culturing the cells through 16 passages in the presence of hydryoxyurea, these cell lines were re-examined for the overexpression of ErbB2. After 16 passages without hydryoxyurea, the three cell lines still express high levels of ErbB2 (Panel B, Lanes 1, 3 and 5). However, when treated with hydryoxyurea only the TM22 cell line exhibited an ablation of ErbB2 expression, indicating that ErbB2 expression in this cell line was derived from the double minute chromosomes (Panel B, Lane 5 vs. 6). Grb2 is shown as an internal loading control. ErbB3 overexpression was also noted in the TM15 cell line prior to hydroxyurea treatment (Panel C, Lane 3). However, with the ablation of ErbB2 expression in the TM22 cell line, ErbB3 was observed to be upregulated (Panel C, Lanes 5 vs. 6).

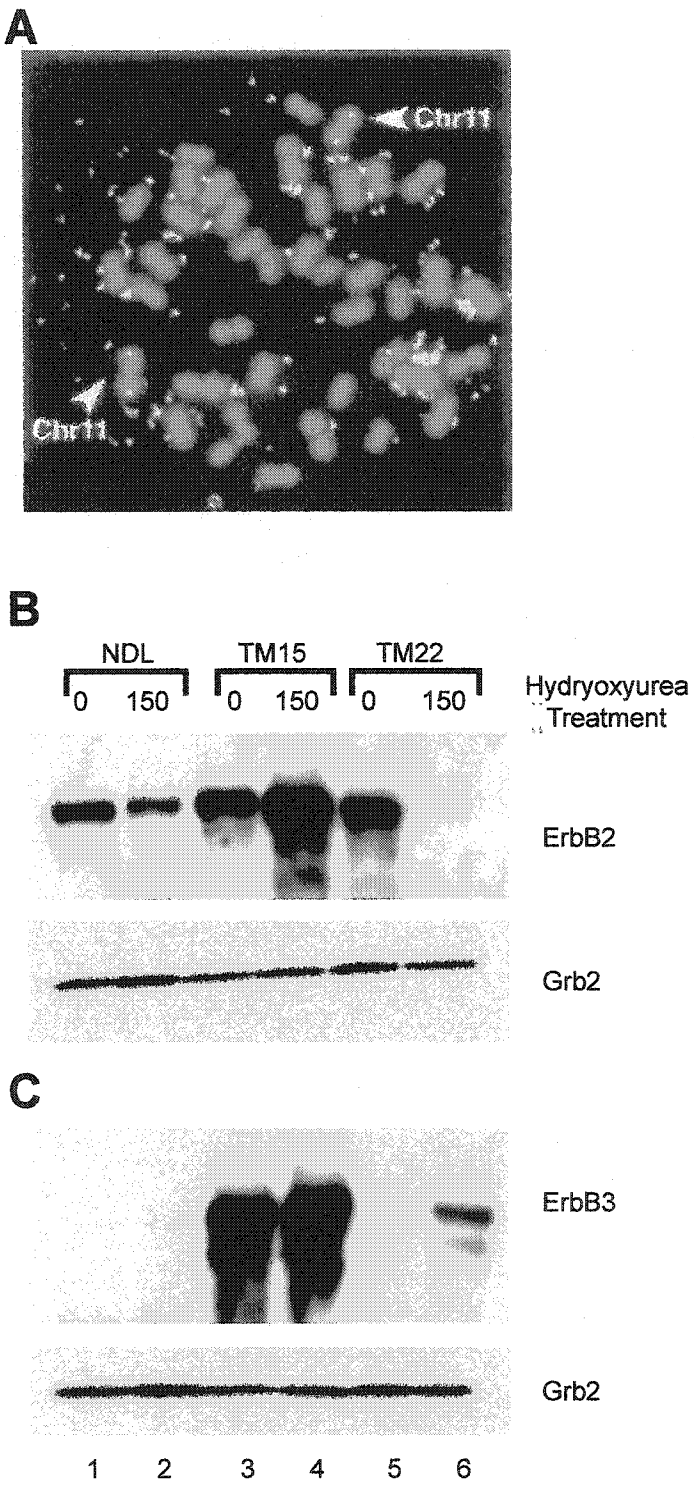
A
Chr11
Chr11
B
NDL
TM15
TM22
0
150
0
150
0
150
Hydryoxyurea Treatment
ErbB2
Grb2
C
ErbB3
Grb2
1
2
3
4
5
6

epithelium in the conditionally activated tumor model and removal of one initiating factor does not alter the tumorigenicity of the cell lines.

3.2.7 Germline Expression of Activated Neu causes Embryonic Lethality

The conditional activation and expression of *neuNT* under the control of the endogenous promoter resulted in focal tumors with remarkable similarity to the human disease. However, given the long latency of this tumor model it is not an ideal choice for many studies. It has previously been shown that the wild type allele can serve as a dominant negative allele when present with the activated allele, which may contribute in part to the long latency of the tumor model (Nikitin *et al.*, 1996). Since the recombinant allele contains a loxP flanked neomycin cassette between the endogenous promoter and the *neuNT* cDNA prior to Cre mediated excision, this recombinant allele functions as a null allele and cannot be maintained in a homozygous state. In order to attempt to decrease the tumor latency in this model, I attempted to engineer mice that would contain and express two copies of the *neuNT* cDNA under the control of the endogenous promoter. To derive mice with two copies of *neuNT* under the control of the endogenous promoter, single cell embryos with one copy of the recombinant allele (Figure 3.18, Panel A) were microinjected with a non-linearized plasmid containing Cre Recombinase under the control of the chicken β-actin promoter. The β-actin promoter is expressed at the two cell phase in the mouse embryo and should direct excision in the germline to place *neuNT* under the control of the endogenous promoter in all tissues it is normally expressed in (Figure 3.18, Panel B)(Araki *et al.*, 1995). The microinjected embryos were then

Figure 3.18 – Derivation of NeuNT Germline Mice

Given the long latency of tumor formation in the mice expressing NeuNT under the control of the endogenous promoter, we attempted to create a strain of mice that would harbour two activated Neu alleles to accelerate tumorigenesis. Since the FloxneuNeuNT allele (A) is a null allele until removal of the loxP flanked neo cassette, we proposed to excise this sequence in the germline. Non-linearlized plasmid DNA containing Cre recombinase under the control of the chicken β-actin promoter was microinjected into one cell embryos from a cross between two mice heterozygous for the FloxneoNeuNT allele. This should result in the germline activation and expression of the NeuNT cDNA under the control of the endogenous promoter (B). The resulting heterozygous mice were assayed for Cre recombinase mediated deletion of the loxP flanked Neo cassette by Southern analysis using an EcoR1 digest and a portion of the *neuNT* cDNA as a probe. The excision in the tails of subsequent progeny is shown (C).

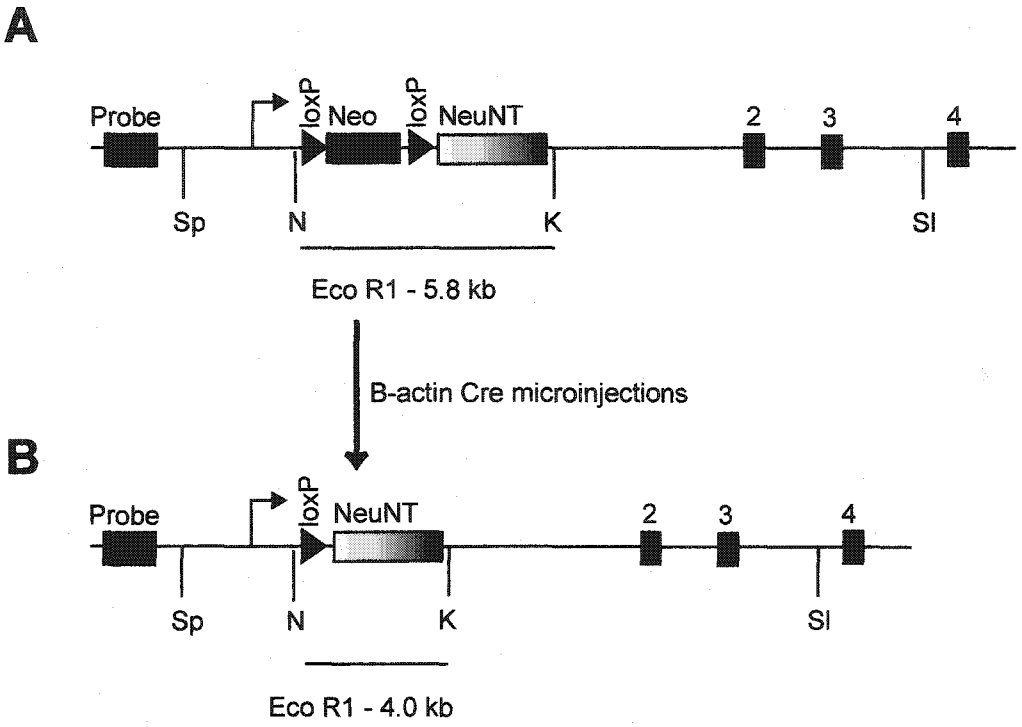
A
Probe
loxP
Neo
loxP
NeuNT
2
3
4
Sp
N
K
Sl
Eco R1 - 5.8 kb
B-actin Cre microinjections
B
Probe
loxP
NeuNT
2
3
4
Sp
N
K
Sl
Eco R1 - 4.0 kb

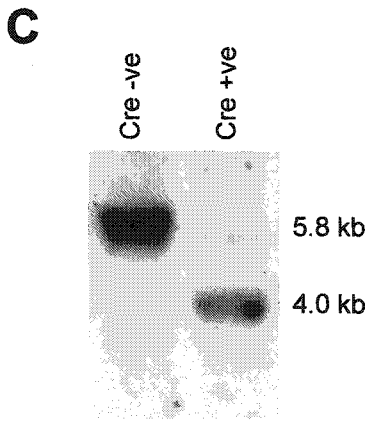
C
Cre -ve
Cre +ve
5.8 kb
4.0 kb

reimplanted into foster mothers and were allowed to develop to term. The resulting progeny were genotyped and those containing one wild type allele and one recombinant allele were examined for excision of the loxP flanked neomycin gene in DNA extracted from the tail. In several of the Cre-injected progeny there was complete excision of the loxP flanked sequence as detected in a Southern analysis (Figure 3.18, Panel C). These mice were capable of passing the germline activated *neuNT* allele to their progeny, which were also tested to ensure that the excised allele was inherited. Analysis of these heterozygous germline NeuNT mice did not reveal any striking abnormalities during development of the mice and these mice were also capable of rearing their pups. However, a reduction in fertility was noted in these mice but was not characterized as the mice were still capable of reproducing.

To examine tumor formation in mice that harboured two *neuNT* alleles under the control of the endogenous promoter, the heterozygous germline NeuNT mice ($ErbB2^{WT/NT}$) were interbred to generate homozygous offspring. However, mice containing only the *neuNT* allele ($ErbB2^{NT/NT}$) were not observed when the progeny were genotyped. The expected Mendelian ratio for the interbreeding is shown in black for the observed number of progeny (Figure 3.19, Panel A). The observed genotypes from the viable progeny are shown in grey and clearly illustrate a lack of $ErbB2^{NT/NT}$ mice (Figure 3.19, Panel A). A close examination of newborn progeny from $ErbB2^{WT/NT}$ interbreedings confirmed that none of the pups were suffering from postnatal lethality. Additionally, unlike the wild type cDNA knock-in mice (Chan *et al.*, 2002), mice harbouring one neuNT allele and one knockout allele were not viable (results not shown).

Figure 3.19 – Embryonic Lethality in mice harbouring two *neuNT* alleles.

Mice that contained a single *neuNT* allele under the control of the endogenous promoter in the germline were interbred to generate mice that would be homozygous for the recombinant *neuNT* allele. The expected Mendellian ratio of wild type ($ErbB2^{WT/WT}$), heterozygous ($ErbB2^{WT/NT}$) and homozygous ($ErbB2^{NT/NT}$) mice is shown in black (A). The observed number of mice after genotyping is shown in grey (A). Clearly the mice harbouring only the *neuNT* allele under the control of the endogenous promoter are not viable. To determine the timepoint of embryonic lethality, timed matings were set up and embryos were harvested from 10.5 days post coitum (dpc) to 13.5 dpc. The expected number of embryos homozygous for the *neuNT* allele is shown by the black bars (B). The number of viable embryos at the various timepoints is represented by the grey bars (B). The number of embryos that are dead, dying or that were in the process of being resorbed at these various stages of development are represented by the white bars (B). Clearly the homozygous *neuNT* embryos are viable at 10.5 dpc but start to suffer from embryonic lethality at 11.5 dpc and no viable embryos have been observed at or later than 13.5 days post coitum.

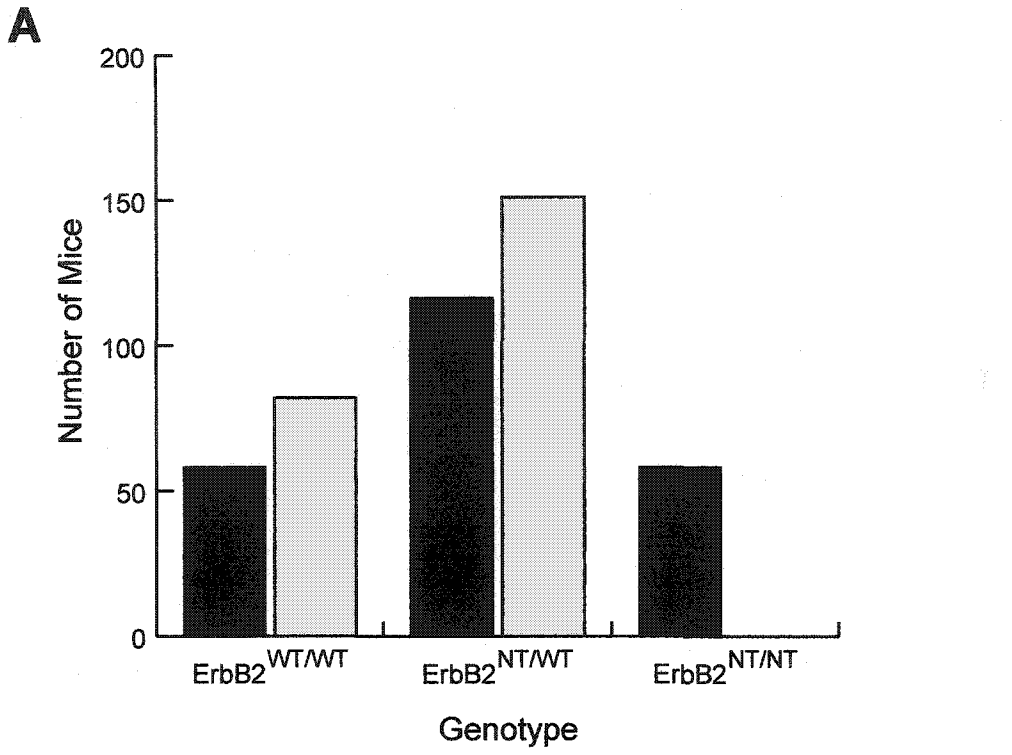
A
200
150
100
50
0
Number of Mice
ErbB2WT/WT
ErbB2NT/WT
ErbB2NT/NT
Genotype

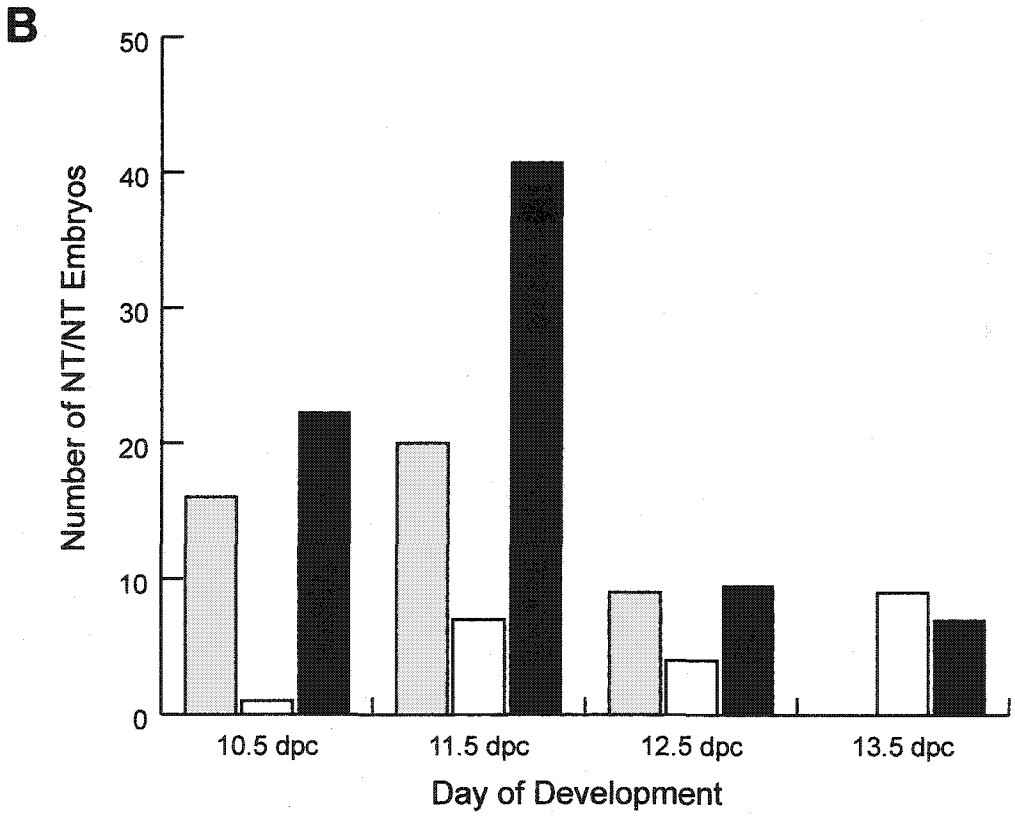
B
50
40
30
20
10
0
Number of NT/NT Embryos
10.5 dpc
11.5 dpc
12.5 dpc
13.5 dpc
Day of Development

To determine when the ErbB2$^{NT/NT}$ mice were succumbing to embryonic lethality, timed matings were established and embryos were harvested between 10.5 and 13.5 dpc. Based on an expected 1:2:1 ratio of ErbB2$^{WT/WT}$: ErbB2$^{WT/NT}$: ErbB2$^{NT/NT}$ embryos, the expected number of only ErbB2$^{NT/NT}$ embryos from the timed matings are shown via the black bars in Figure 3.19, Panel B. During the dissection of the embryos, they were examined for a beating heart and general signs of viability. Both viable embryos and embryos that had suffered from embryonic lethality were retained for analysis. The visceral yoke sac was retained for genotyping and after the number of ErbB2$^{NT/NT}$ embryos were determined, the point of embryonic lethality was determined (Figure 3.19, Panel B). The majority of ErbB2$^{NT/NT}$ embryos are viable at 10.5 dpc but begin to suffer from embryonic lethality at 11.5 and 12.5 dpc. No viable ErbB2$^{NT/NT}$ embryos were observed later than 12.5 dpc. These results suggest that expression of the activated *neuNT* allele is able to extend the embryonic lethality observed at 10.5 dpc in the knockout to 12.5 dpc but is incapable of completely rescuing this embryonic lethality.

The expression of NeuNT under the control of the endogenous promoter was expected to be at approximately 10% of the level of the wild type allele based on other knock-in mouse models using an identical targeting strategy (Chan *et al.*, 2002). However, when ErbB2$^{NT/NT}$ embryos were examined at 10.5 dpc, before embryonic lethality is observed, I was not able to detect significant levels of Neu (Figure 3.20, Panel A). While the level of Neu in the ErbB2$^{WT/NT}$ embryos appeared to be approximately 50% of the wild type levels, it is clear that the ErbB2$^{NT/NT}$ embryos are not expressing detectable levels of Neu. This analysis was repeatedly confirmed and was extended to

Figure 3.20 – NeuNT expression levels in embryogenesis

The level of Neu expression in the wild type, heterozygous and mice that were homozygous for the germline NeuNT allele was assayed at 10.5 dpc by Western analysis (A). While Neu is readily detected in the wild type controls, the level of Neu in the heterozygous mice appears to be greatly reduced. Further, Neu was not detected in the homozygous mice by Western analysis. The viability of these mice was determined by the presence of a heartbeat and their general appearance at 10.5 dpc. This analysis was repeated at 11.5 dpc with identical results (data not shown). To determine whether the levels of mRNA contributed to the reduction of Neu expression in the embryos, quantitative RT-PCR was conducted on RNA collected from the embryos at 10.5 dpc using primers that would anneal to both the rat and mouse alleles. Results from four separate embryos for each genotype were averaged together and the wildtype control was set to the 100 % level (B). Clearly, the embryos harbouring two NeuNT alleles had a greatly reduced level of *neuNT* mRNA. However, when the wild type and heterozygous levels were compared, an expected level for the homozygous embryos could be generated. When the expected and observed levels are compared, the observed level appears to be far lower than expected (B). Error bars represent standard deviation.

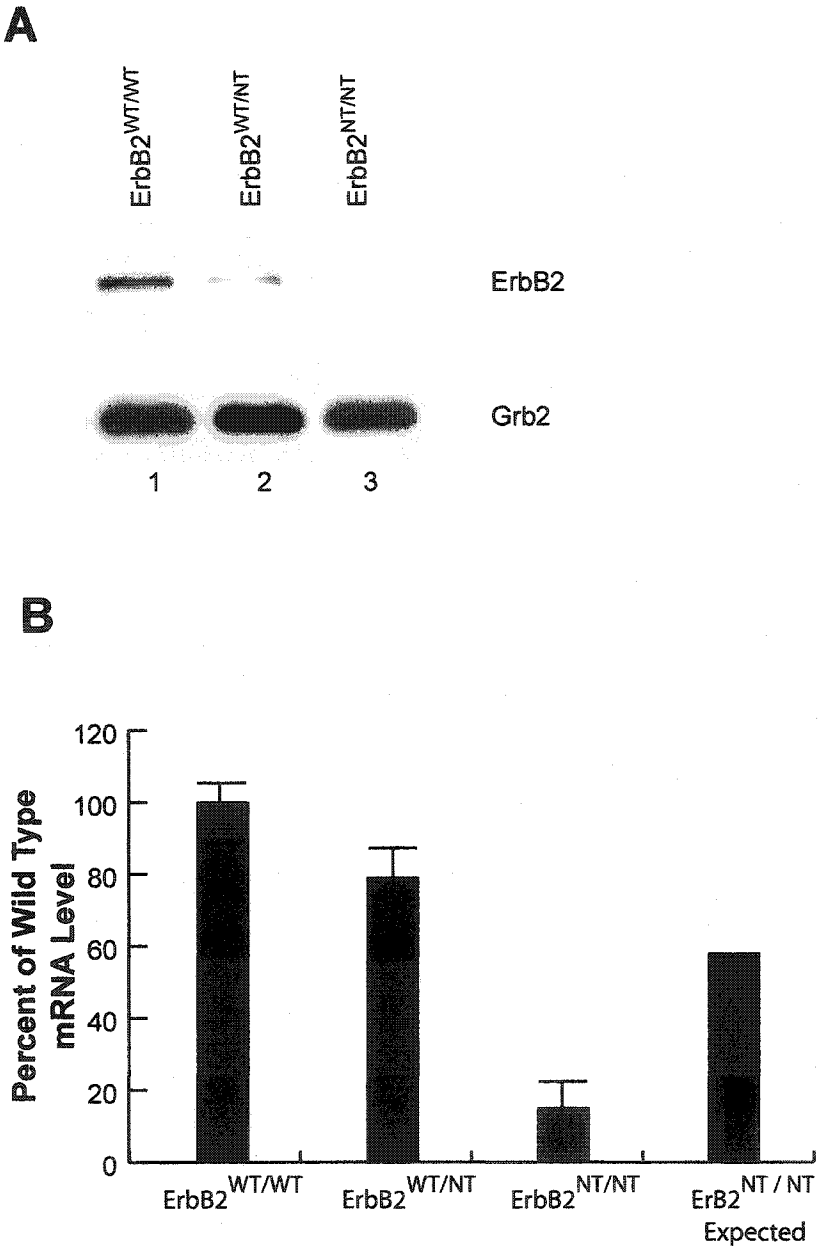
A
ErbB2WT/WT
ErbB2WT/NT
ErbB2NT/NT
ErbB2
Grb2
1
2
3
B
Percent of Wild Type mRNA Level
120
100
80
60
40
20
0
ErbB2WT/WT
ErbB2WT/NT
ErbB2NT/NT
ErB2NT / NT Expected

the 11.5 dpc timepoint where identical results were obtained. Since mRNA levels were unchanged while protein levels were reduced in other strains of mice using the identical targeted recombination strategy (Chan *et al.*, 2002), the levels of *neuNT* mRNA were analysed in the ErbB2$^{NT/NT}$ embryos. At 10.5 dpc, embryos were harvested for RNA extraction followed by quantitative RT-PCR for *neu* using primers that anneal to both the mouse and rat *neu* homologues. After standardization to *GAPDH*, the level of *neu* expressed in ErbB2$^{WT/WT}$ embryos was set to 100%. The ErbB2$^{WT/NT}$ embryos were then observed to express *neu* at slightly lower levels (78%) than the wild type control (Figure 3.20, Panel B). Additionally, the ErbB2$^{NT/NT}$ embryos were shown to have greatly reduced levels of *neu* expression relative to the wild type control (15%). Interestingly, if the wild type allele in the heterozygous embryos contributes 50% of the expression level observed in the wild type control, then the recombinant *neuNT* allele would contribute the remaining 28% of the reduced expression (78% of wild type levels) observed in the heterozygous controls. Extending this conjecture to predict the level of *neuNT* expression in the ErbB2$^{NT/NT}$ embryos, one might expect to see the homozygous knock-in embryos expressing neu at 59% of the wild type levels, not the observed 15%. Indeed based on previous work, a difference in the levels of mRNA expression was not predicted. These results raise the possibility that expression of activated *neuNT* may trigger a feedback loop which regulates the activity of the endogenous promoter.

With the germline ablation of Neu, the embryos suffered from defects in cardiac trabeculation that led to embryonic lethality at 10.5 dpc (Lee *et al.*, 1995). To investigate the cause of the embryonic lethality observed in the ErbB2$^{NT/NT}$ embryos, timed matings

were established and embryos were harvested at 12.5 dpc. The visceral yoke sac was retained for genotyping and the embryos were fixed for routine histology. Serial sections of ErbB2$^{WT/WT}$, ErbB2$^{WT/NT}$ and ErbB2$^{NT/NT}$ embryos were examined for defects in morphology of various organs. The ErbB2$^{WT/WT}$ and ErbB2$^{WT/NT}$ embryos were indistinguishable. However, the ErbB2$^{NT/NT}$ embryos could be distinguished based on defects observed in cardiac development. While the ErbB2$^{WT/WT}$ and ErbB2$^{WT/NT}$ embryos had normal cardiac trabeculation (Figure 3.21, Panel A, Arrow), the ErbB2$^{NT/NT}$ embryos had a reduction in the amount of trabeculation (Figure 3.21, Panel B, Arrow). Unlike the germline ablation which lacked trabeculae entirely, the ErbB2$^{NT/NT}$ embryos do have small trabeculae, which has likely allowed these embryos to survive for two days longer than their null counterparts. Additionally, in several of the ErbB2$^{NT/NT}$ embryos that were examined there were variable levels of pitting and abnormal development of the hindbrain (data not shown) suggesting neural defects in these embryos.

To examine the ErbB2$^{NT/NT}$ embryos more thoroughly for alterations in the peripheral nervous system, the expression of the *phox2a* transcription factor was examined through an *in situ* analysis. *Phox2a* transcripts in the whole embryos at 10.5 and 11.5 dpc were examined in the *in situ* analysis using an antisense *phox2a* riboprobe to reveal how the development of the sympathetic chain ganglia was progressing. In both the ErbB2$^{WT/WT}$ and ErbB2$^{WT/NT}$ embryos, the presence of *phox2a* expression in the developing sympathetic chain ganglia was clearly present (Figure 3.22, Panels A and C). However, the presence of *phox2a* expression could not be detected in the ErbB2$^{NT/NT}$

Figure 3.21 – Defects in Cardiac Development in ErbB2$^{NT/NT}$ embryos.

At 12.5 dpc, viable embryos were examined through longitudinal section to determine the cause of the embryonic lethality in the ErbB2$^{NT/NT}$ embryos. Wild type and heterozygous controls were indistinguishable (results not shown). However, at 12.5 dpc the ErbB2$^{WT/NT}$ and ErbB2$^{NT/NT}$ embryos could be distinguished on the basis of the development of the heart. While the ErbB2$^{WT/NT}$ embryos had extensive cardiac trabeculation (A, arrow), the ErbB2$^{NT/NT}$ embryos did not (B, arrow). While the cardiac trabeculation was affected in the ErbB2$^{NT/NT}$ embryos, it should be noted that it was not entirely absent as it existed around the periphery of the developing heart.

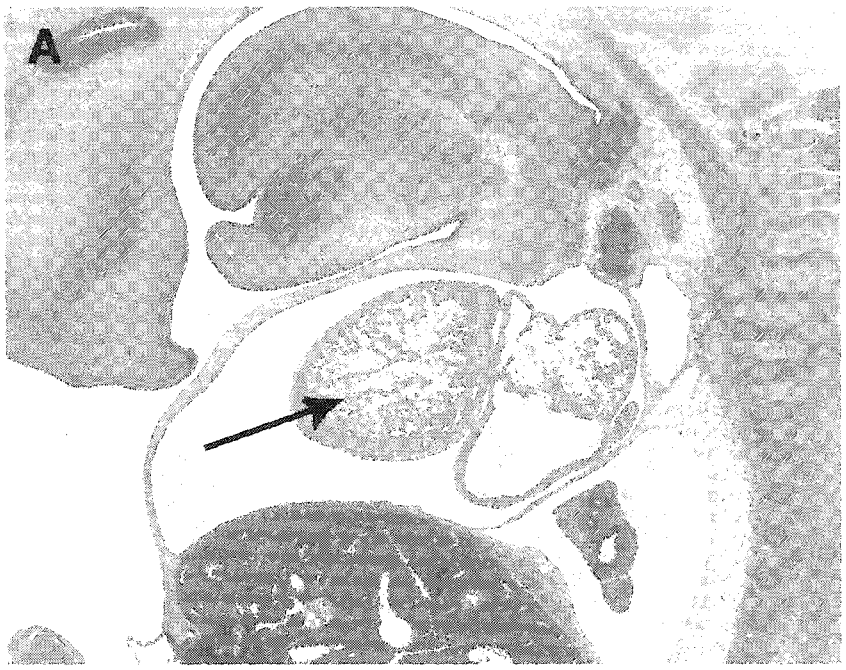
A

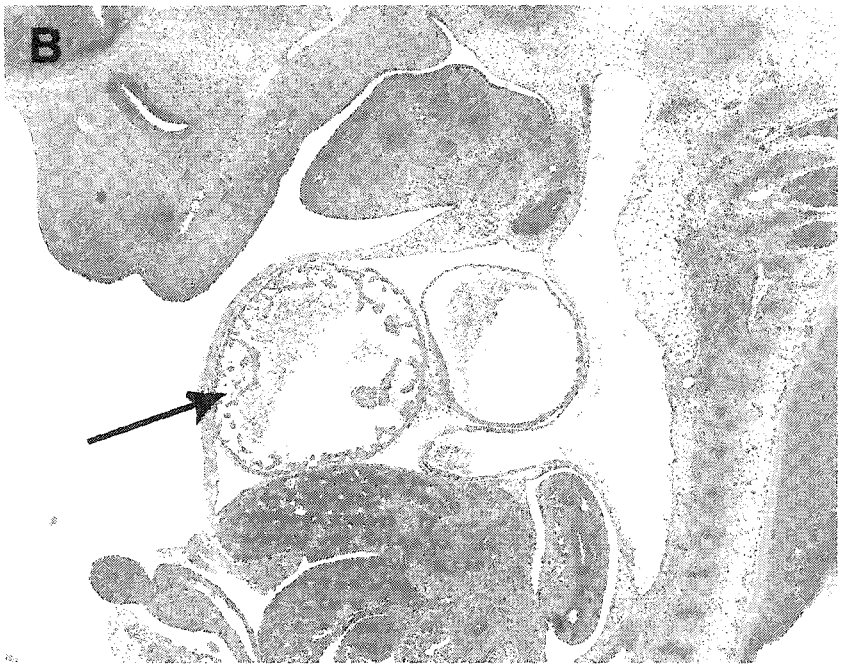
B

Figure 3.22 – Neurological Defects in ErbB2$^{NT/NT}$ embryos.

Embryos were examined though an in situ analysis for neurological development. The presence of the sympathetic chain ganglia in the various embryos was detected by an in situ hybridization analysis using an antisense *phox2a* riboprobe. In the heterozygous controls at both 10.5 dpc (A) and 11.5 dpc (C) the presence of the developing sympathetic chain is readily detected (open arrowheads). The heterozygous and wild type embryos were essentially indistinguishable (results not shown). In contrast, the ErbB2$^{NT/NT}$ embryos at 10.5 dpc (B) and 11.5 dpc (D) did not exhibit any evidence of a developing sympathetic chain ganglia.

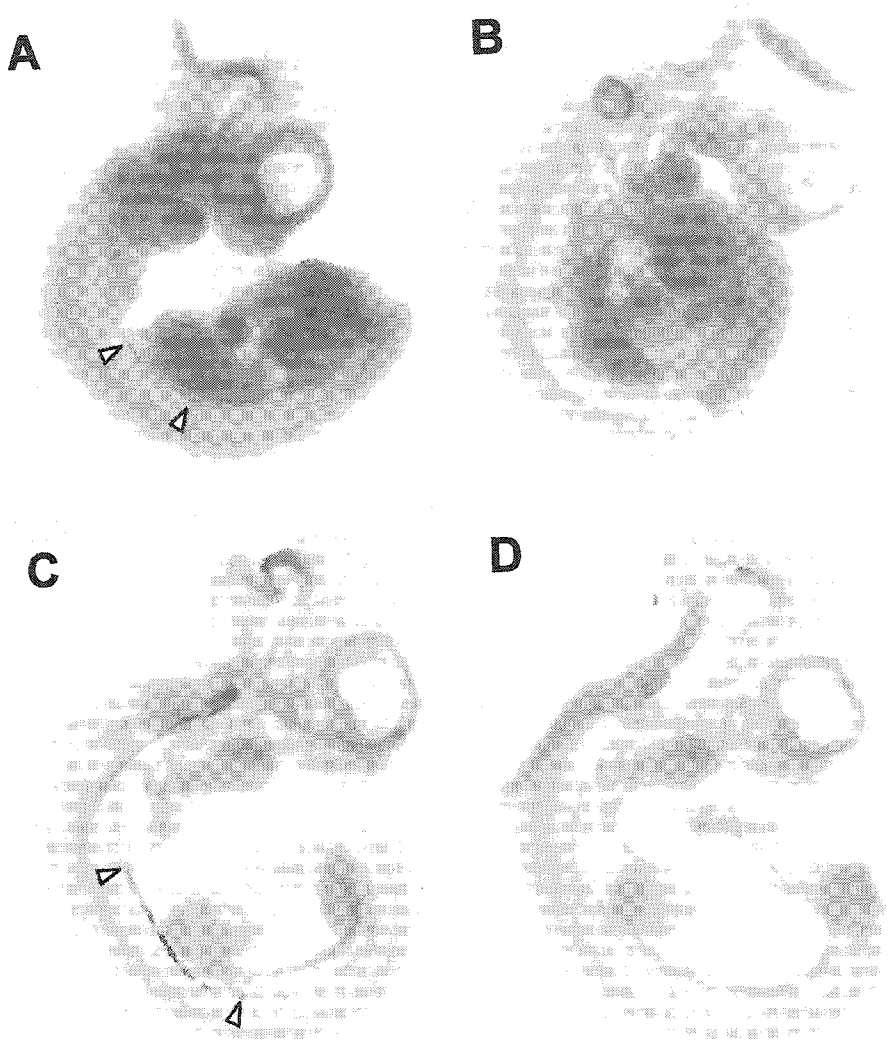
A
B
C
D

embryos. These results suggest that the expression of an activated *neuNT* allele under the control of the endogenous promoter results in both cardiac and neurological defects.

3.2.8 Comparison of Conditional and Germline expression of Activated Neu on Mammary Gland Development and Tumorigenesis

The original hypothesis that a mouse with two copies of *neuNT* under the control of the endogenous promoter should result in a reduction in tumor latency compared to the conditional activation model could not be tested due to the embryonic lethality associated with the ErbB2$^{NT/NT}$ embryos. However, one might also predict that the germline ErbB2$^{WT/NT}$ mice should develop mammary adenocarcinomas at the same rate as the mammary specific conditional activation model. Further, these germline ErbB2$^{WT/NT}$ mice may also develop tumors in other tissues where *erbB2* is normally expressed in the mouse. Thus, in order to examine the germline heterozygotes for these effects, a number of mice were generated and were monitored for tumor development. Additionally, the development of the mammary gland in the germline ErbB2$^{WT/NT}$ mice was contrasted to the mammary gland in wild type mice and the condition activation of NeuNT (Figure 3.23). Surprisingly, when the germline mice expressing the activated *neuNT* oncogene under the control of the endogenous promoter were compared to the wild type controls, no differences were seen in either wholemounts or histology of the mammary gland (Figure 3.23, Compare Panels A and B vs. C and D). In contrast, mice that expressed the *neuNT* oncogene under the control of the endogenous promoter, after MMTV-Cre mediated excision, exhibited alterations in branching and had hyperplastic lobuloalveolar

Figure 3.23 – Mammary Comparison of Germline and Conditional Activation of NeuNT

Mice expressing a wild type allele (A, B), or the oncogenic *neuNT* allele under the control of the endogenous promoter (C-F) were assayed for mammary gland phenotypes at 18 months of age. Expression of *neuNT* under the endogenous promoter occurred in all tissues that the endogenous promoter is active in (Germline Activation, C-D) or was limited to the mammary epithelium through the use of the MMTV-Cre strain (Conditional Activation, E-F). While there is a striking difference in wholemounts (C vs. E), it should be noted that the same FloxneoNeuNT targeted allele was used in both the germline and conditional activation. The difference between these two strains was the method of excision, β-actin Cre for the germline and MMTV-Cre for the conditional activation. Thus, it is surprising that the germline and conditional expression of *neuNT* have strikingly different phenotypes in the mammary gland. While the germline expression of *neuNT* does not cause an appreciable change from the wild type control in either wholemount or histological analysis (A-B vs. C-D), the conditional activation causes an obvious difference. The conditional activation causes hyperplasia throughout the mammary gland (E-F) and it is not surprising that these mice are susceptible to tumor formation as previously described. Clearly the temporal and spatial difference in *neuNT* expression is capable of causing profound differences in mammary gland development.

FVB

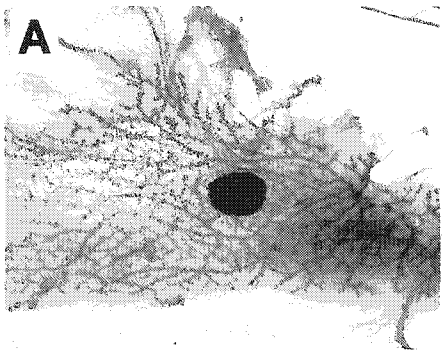

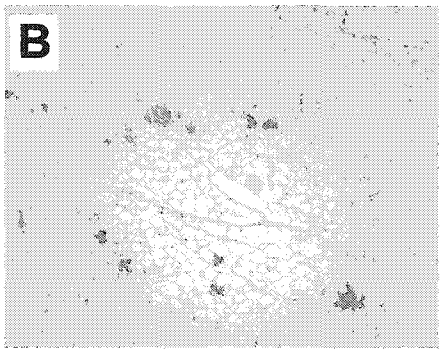

Germline Activation

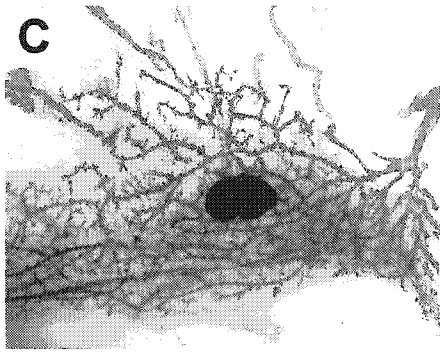

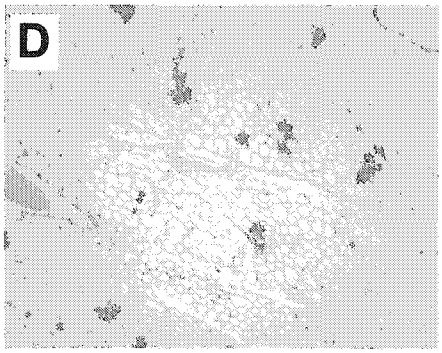

Conditional Activation

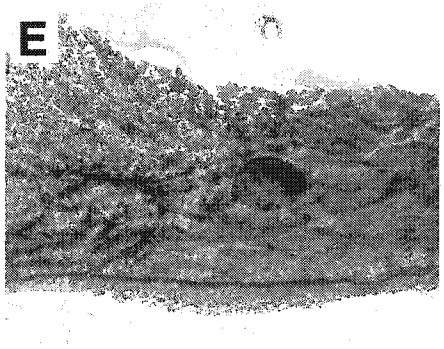

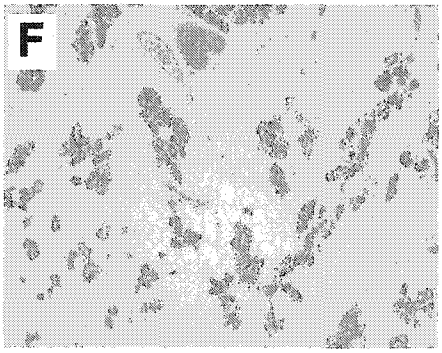

endbuds as previously described and shown again in Figure 3.23, Panels E and F. It is important to note that the same recombinant allele expressing activated *neuNT* under the control of the endogenous promoter was present in both the germline and conditional mouse models, the only difference was in the method of excision of the loxP flanked sequence required for expression of the oncogene. These results indicate that while both models should express the *neuNT* oncogene, the differences in either the temporal or spatial expression pattern are capable of causing striking changes in the susceptibility of the mammary gland to hyperplasia and tumorigenesis.

Upon observing the profound differences in mammary gland structure between the conditional and germline activation of *neu* expression, the possibility existed that the differences in time or location of activation could result in different levels of expression. To confirm that *neuNT* was expressed at equal levels in the mammary gland of the conditional and germline activation mouse models, RNA was extracted from wild type control mammary glands, the two experimental systems and from *neuNT* induced tumors from the conditional activation mouse model. Three samples for each genotype were tested in triplicate and were standardized to *GAPDH.* Importantly, since the expression data from the embryo suggested that the recombinant *neuNT* allele would be expressed at far lower levels than the wild type allele (Figure 3.20, Panel B), a set of rat homologue specific primers was constructed. These primers were shown to be more than 20 fold more specific for the rat homologue over the mouse homologue in the embryos (data not shown). When these primers were used in quantitative RT-PCR, the level of *neuNT* expression in the germline activation mammary gland was set to 1 (Figure 3.24, Panel A).

Figure 3.24 – Conditional and Germline NeuNT Expression and Tumorigenesis

Given the striking differences in mammary gland phenotypes between the conditional and germline activation of *neuNT*, the expression level of *neuNT* was determined through quantitative RT-PCR (A). Using primers that were 20 fold more specific for the rat allele over the mouse allele (data not shown), the level of *neuNT* in wild type, conditional and germline NeuNT mammary glands and a conditionally activated NeuNT tumor were assayed. The level of expression in the germline mammary gland was set to be equal to 1 and the other samples were measured accordingly. The wild type control expresses only the mouse allele and illustrates the specificity of the primers as it shows low levels of expression. Importantly, the conditional and germline activation of NeuNT both express *neuNT* at approximately equal levels in the mammary gland. The elevated expression of *neuNT* in the conditionally activated tumors is clearly seen in the tumor control. Despite the equal level of *neuNT* expression, the mammary differences previously observed were also reflected in the rate of tumorigenesis in these two strains (B). The previously described tumor latency curve for the conditional activation is shown again (squares) and is contrasted to the germline activation (triangles). Mice harbouring the germline activation remain tumor free for their entire lifespan (n=25 at 2 years).

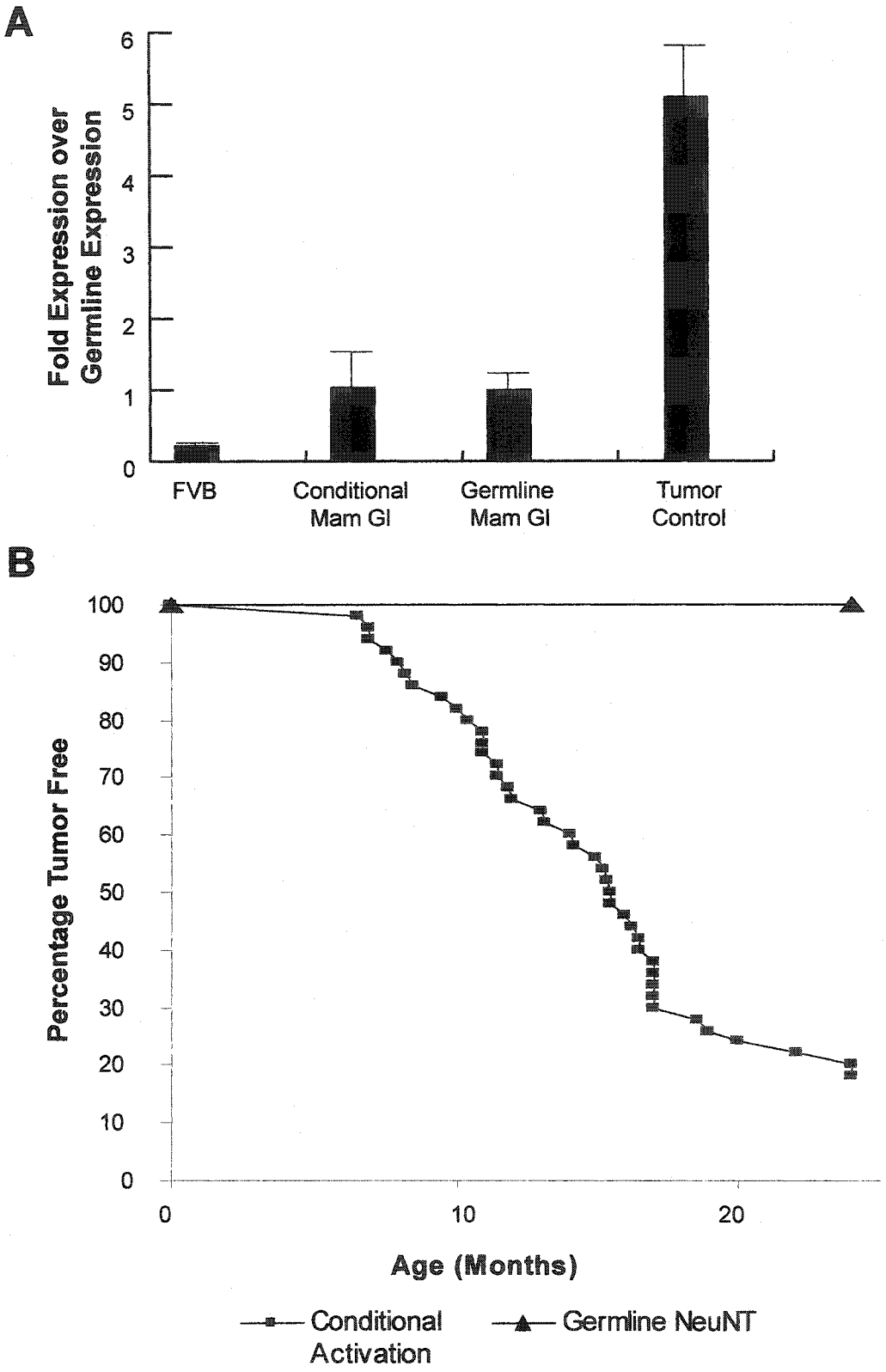
A
Fold Expression over Germline Expression
0
1
2
3
4
5
6
FVB
Conditional Mam GI
Germline Mam GI
Tumor Control
B
Percentage Tumor Free
100
90
80
70
60
50
40
30
20
10
0
0
10
20
Age (Months)
Conditional Activation
Germline NeuNT

Demonstrating the specificity of the primers, a low background level of mouse expression was detected in the wild type controls. Importantly, the level of *neuNT* expression in the conditional and germline models was not seen to be statistically different. Further, the known elevation of *neuNT* expression in the tumor model was also demonstrated to be elevated by 5 fold through this analysis (Figure 3.24, Panel A). These results illustrate that despite the dramatic difference in phenotype, the conditional and germline Neu mammary glands express equal levels of *neuNT* mRNA.

Although the germline and conditional activation of *neuNT* expression resulted in equal expression of the potent oncogene, there were striking differences in the mammary gland. Consistent with these effects, when mammary glands were examined for the presence of tumors in the two strains a remarkable difference was observed (Figure 3.24, Panel B). As previously described, the conditional expression of *neuNT* resulted in mammary tumorigenesis in 50% of female mice by 15.9 months of age (Figure 3.24, Panel B, Squares). In contrast, when 25 germline activated *neuNT* mice were regularly examined until 2 years of age, they remained tumor free (Figure 3.24, Panel B, Triangles). Indeed, not only were these mice free from mammary tumors, but from tumors of any origin for their entire lifespan. During routine examination, there were no defects, other than a slight reduction in fertility, noted in these mice. Interestingly, these results suggest that expression of a potent oncogene under the control of the endogenous promoter with normal temporal and spatial regulatory cues is not sufficient to induce tumorigenesis.

3.2.9 Gene Expression Profiling of the Differences between Mammary Glands Expressing Activated Neu Conditionally and in the Germline

Mammary glands from the germline and conditionally activated *neuNT* models were shown to express equal levels of *neuNT* transcripts. Additionally, these two strains of mice had striking differences in their susceptibility to mammary tumorigenesis. To further explore the molecular basis for the differential carcinogenic potential of these two different *neuNT* expressing mammary glands, their gene expression profile was compared. RNA from 10 mammary glands from each line was pooled into two sets of 5 glands and was compared through a set of Affymetrix gene chip analyses. The results of these analyses are summarized in Table 3.2 and Table 3.3. In Table 3.2, a portion of the genes that are expressed at a higher level in the conditional model in both repeats of the gene chip experiment are shown with the average fold increase. The genes have been broadly separated into various categories. Interestingly, in the first category, markers of mammary gland differentiation and lactation are observed including genes such as *epsilon casein* (21 fold increase), *wap* (11 fold increase) and *alpha-lactalbumin* (4 fold increase). Included in this list of differentiation markers is *glycam1* (9 fold increase) which was previously seen to be overexpressed in tumors arising in the conditional activation of *neu* (See Table 3.1 and Figure 3.14). The number of differentiation markers and the similarity of these results to the differentiation markers expressed in the conditional activation tumors (Table 3.1) suggests that these mammary glands have already become predisposed to tumorigenesis.

Table 3.2 – Comparison of Germline and Conditionally Activated Mammary Glands – Elevated Genes

Mammary glands from both the conditional and germline NeuNT mice were compared through an Affymetrix chip analysis. A portion of the results of this analysis is shown here. Genes that were expressed at higher levels in the conditionally activated glands are shown in this table. Since the conditional activation of NeuNT in the mammary gland renders the mice succeptable to tumors, it is not surprising that there are many potential neoplastic markers that were elevated. The table shows the fold difference in expression levels, the gene name, and a brief description of the function or role in tumorigenesis. The PubMed accession number for each gene is also listed.

Table 3.2 Comparison of Germline and Conditionally Activated Mammary Glands - Elevated Genes

Fold Change	Gene Name	Ontology	Accession #
Mammary Gland Differentiation Markers			
21.1	Epsilon Casein	Subject to hormonal stimulation	V00740
11.7	Fatty Acid Binding Protein	Differentiated Mam. Gl. marker	X14961
11.3	WAP		V00856
8.9	Glycam1	Elevated in FIneo NeuNT tumor model	M93428
8.6	Glycoprotein		Z22552
8.3	Connexin-30	Differentiation Marker	Z70023
4.8	Connexin-26	Expressed in Pregnancy	M81445
4.3	alpha-lactalbumin	Subject to hormonal stimulation	M87863
3.2	Butyrophilin	Milk Protein	U67065
Potential Neoplastic Markers			
8.3	MRP8	Elevated in breast cancer (Bera, 2001)	M83218
8.0	Cea10 related tag	Some Cea members are deregulated in tumors	AV381191
5.3	Cea10	Some Cea members are deregulated in tumors	L38422
4.9	Glycerol kinase	Raf induces expression in MCF10a	U48403
5.1	WDNM1	Elevated in ErbB2 and Ras tumors (Morrison, 1994)	X93037
4.4	lactotransferrin	Elevated in ErbB2 and Ras tumors (Morrison, 1994)	J03298
4.3	CAII	Inhibitors have anti-tumor properties	M25944
3.7	Ceruloplasmin	Copper transporter, some Breast cancer evidence	U49430
9.2	MRP14	See MRP8	M83219
3.0	Kappa-casein	Elevated in ErbB2 and Ras tumors (Morrison, 1994)	M10114
2.8	CRBPI	Elevated in ErbB2 and Ras tumors (Morrison, 1994)	X60367
7.0	CAB1	Co-amplified with ErbB2	X82457
3.0	MAT-8	Elevated in ErbB2 and Ras tumors (Morrison, 1994)	X93038
Other Genes			
4.9	beta-1-globin		V00722
3.7	Arginase II		AF032466

Table 3.3 – Comparison of Germline and Conditionally Activated Mammary Glands – Decreased Genes

Mammary glands from both the conditional and germline NeuNT mice were compared through an Affymetrix chip analysis. A portion of the results of this analysis are shown here. Genes that were expressed at higher levels in the germline mammary gland are shown in this table. Since the germline NeuNT mice are not succeptable to tumors, it is not surprising that there are several tumor supressors that are expressed at higher levels in these mammary glands. The table shows the fold difference in expression levels, the gene name, and a brief description of the function or role in tumorigenesis. The PubMed accession number for each gene is also listed.

Table 3.3 Comparison of Germline and Conditionally Activated Mammary Glands - Decreased Genes

Fold Change	Gene Name	Ontology	Accession #
Tumor Supressors			
-3.9	EBI-1	G-protein coupled receptor - anti-tumor immunity	L31580
-3.4	Neuronatin	Identified as a tumor supressor	X83569
-3.1	Similar to 53BP1	Similar to p53 binding protein	AI593074
RA Pathway Genes			
-4.9	retinal oxidase	Absent in MCF7cells	AB017482
-4.1	ALDR	Induced by retinoic acid	Z48670
Other Genes			
-8.9	Reelin	Upregulated in esophogeal cancer	U24703
-6.7	Adrenergic receptor		X72862
-4.6	Similar to PKC		AV336804
-4.4	S3-12	Adipocyte secreted or cell surface protein	AF064748
-4.3	MUP V	Urinary protein	M16360
-4.1	Mesenchyme homeobox 2		Z16406
-4.0	Slfn1	Growth regulatory genes	AF099972
-3.6	matrilin-2		U69262

Consistent with the fact that the conditional activation of *neuNT* results in mammary glands that are predisposed to forming focal mammary tumors, the next category of genes listed in Table 3.2 can be described as Potential Neoplastic Markers. With the expression of various oncogenes in the mammary epithelium, characteristic tumors develop histologically (Rosner *et al.*, 2002). In addition to specific changes in histology, these various oncogenes cause the induction of specific signaling pathways that in turn promote tumorigenesis. Neu and Ras mediated tumors have previously been shown to express a number of characteristic molecular markers (Morrison and Leder, 1994). Surprisingly, in the hyperplastic mammary gland of the conditionally activated *neu* mice, a number of these neoplastic markers were identified as being overexpressed. Indeed, *WDNM1* (5.1 fold increase), *lactotransferrin* (4.4 fold increase), *kappa-casein* (3.0 fold increase) and *CRBP1* (2.8 fold increase) were identified in both sets of gene expression data. Additionally, *mat-8* (3.0 fold increase) was noted in one of the sets of gene expression data. The elevated expression of these various neoplastic markers found in Neu and Ras mediated tumors strongly suggests that the mammary glands are predisposed to tumor induction through Neu mediated signaling. In addition to the Neu neoplastic markers, MRP8, MRP14 and ceruloplasmin were all identified as being overexpressed in the conditional activation of *neu*. Interestingly, these genes have all previously been shown to be involved in human breast cancer (Bera *et al.*, 2001).

While numerous neoplastic and differentiation markers are expressed at elevated levels in the mammary glands in the conditional activation model, there are a number of genes that were expressed at higher levels in the mammary glands of the germline

activation of *neuNT*. Given that the germline mammary glands are expressing a potent oncogene but are resilient to tumorigenesis, it is not surprising that a number of tumor suppressors, or molecules that interact with tumor suppressors were identified (Table 3.3). In addition to tumor suppressors, several genes that are involved in the retinoic acid pathway were activated. Given the ability of retinoic acid to prevent numerous cancers (Chytil and Ong, 1976; Altucci and Gronemeyer, 2001), the activation of this pathway is quite intriguing. Indeed, the retinoic acid pathway has been shown to downregulate Neu protein and mRNA expression in cell lines isolated from tumors overexpressing Neu, resulting in the arrest of cell growth (Grunt *et al.*, 1998). Thus, these gene expression results are entirely consistent with the tumor susceptibility observed in the two strains.

To confirm the accuracy of the gene expression data, quantitative RT-PCR was performed for various samples from the conditional and germline activation models in addition to NeuNT induced tumor, wild type virgin and lactating controls. After an RT-PCR reaction for *epsilon casein* was completed, the samples were collected and electrophoresed as shown (Figure 3.25, Panel A). The quantization for these samples is also shown (Figure 3.25, Panel B). In addition, quantitative RT-PCR was completed for *WDNM1* and *cea10*, illustrating that the trends revealed by the gene chip were indeed accurate (Figure 3.25, Panels B and C). Interestingly, while these genes were elevated in the conditional model mammary gland and tumors over both the wild type virgin control and over the germline activation of NeuNT, the lactating mammary gland expressed far higher levels of these genes. Further, as observed in the confirmation of the previous gene expression data (Figure 3.14), the samples had widely divergent ranges of

Figure 3.25 – Confirmation of Affymetrix Data

To confirm the accuracy of the chip data shown in Tables 3.2 and 3.3, quantitative RT-PCR was preformed on various samples. In addition to the conditional and germline activated NeuNT mammary gland samples that were used in the chip analysis, wild type mammary gland controls from both virgin and lactating mice were included. In addition to the wild type controls, several conditionally activated NeuNT tumor controls were added. After quantitative RT-PCR for *epsilon casein*, the samples were collected and electrophoresed on a gel (A). The quantification of the RT-PCR for the same samples is shown below (B). The average of the germline NeuNT mammary samples was set to 1 and the other samples were compared to this. While the chip data indicated an elevation of 21 fold for *epsilon* casein in the conditionally activated NeuNT samples, quantitative RT-PCR showed an increase of 14 fold. Further, *WDNM1* was 5.1 fold on the chip and 4.7 fold higher by RT-PCR (C). Finally, *cea10* was elevated 5.3 fold in conditionally activated samples on the chip and only 2.9 fold by RT-PCR (D). While the averages roughly correspond to the chip data, the individual samples reflect the heterogeneity of the various mammary glands.

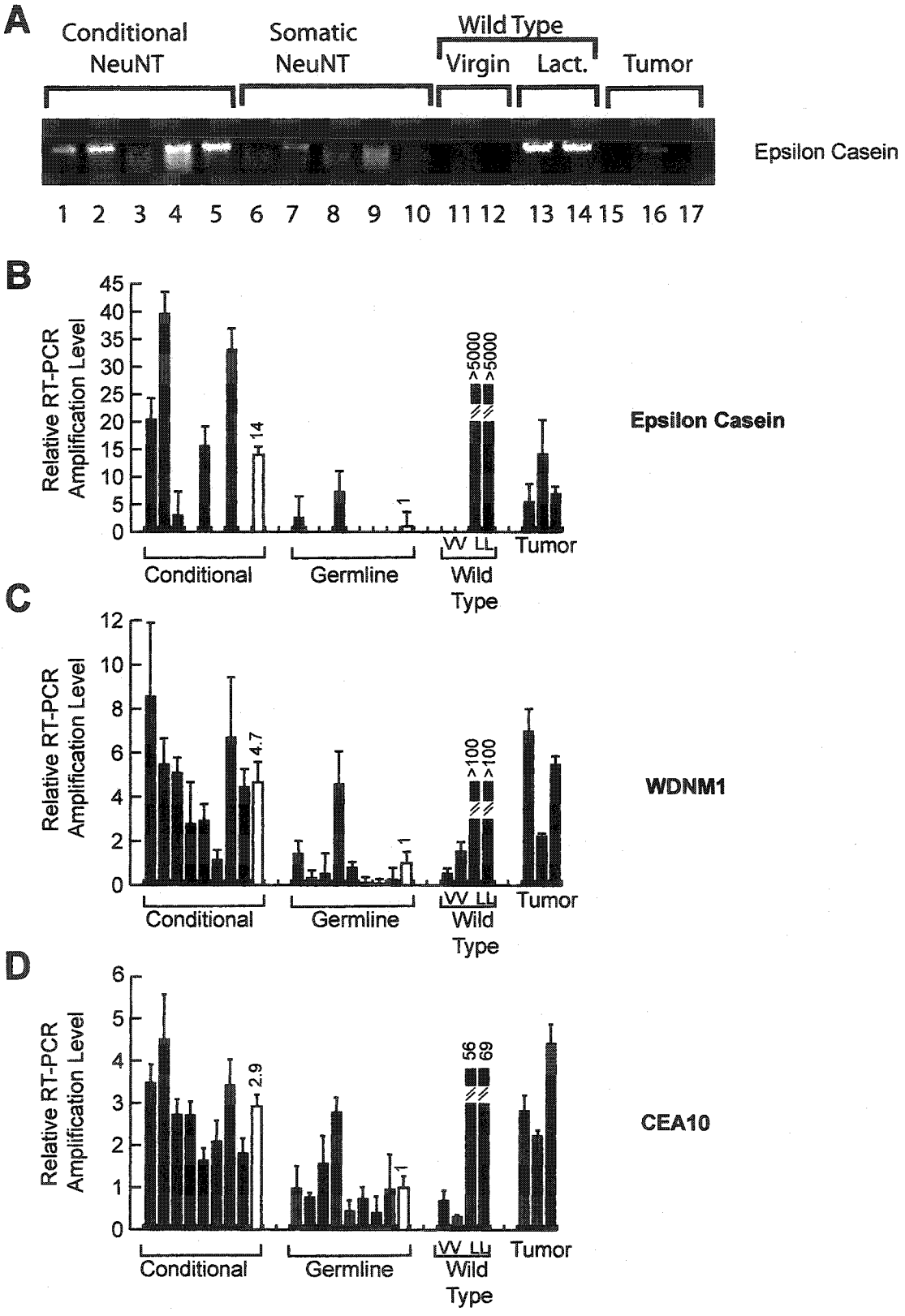
A
Conditional NeuNT
Somatic NeuNT
Wild Type
Virgin
Lact.
Tumor
Epsilon Casein
1 2 3 4 5 6 7 8 9 10 11 12 13 14 15 16 17
B
Relative RT-PCR Amplification Level
45
40
35
30
25
20
15
10
5
0
14
1
>5000
>5000
Conditional
Germline
W
L
Wild Type
Tumor
Epsilon Casein
C
Relative RT-PCR Amplification Level
12
10
8
6
4
2
0
4.7
1
>100
>100
Conditional
Germline
W
L
Wild Type
Tumor
WDNM1
D
Relative RT-PCR Amplification Level
6
5
4
3
2
1
0
2.9
1
56
69
Conditional
Germline
W
L
Wild Type
Tumor
CEA10

expression (Figure 3.25, Panels B-D). Taken together, this data supports the gene expression results reported in Tables 3.2 and 3.3.

3.3 Discussion

3.3.1 Mammary Tumorigenesis in Conditionally Activated NeuNT Mice

Previous mouse models of Neu induced mammary tumorigenesis have relied upon MMTV to direct high level expression of the various transgenes. To generate a mouse model of breast cancer that was hormonally relevant, the *neuNT* cDNA was placed under the transcriptional control of the endogenous promoter in a mammary specific manner (Figure 3.5). Prior to generation of the mice, the utility of the loxP flanked *neomycin* sequence to interfere with *neuNT* expression was demonstrated *in vitro*. Since it is conceivable that placing the PGK-neomycin cassette in the same orientation as the gene that is being ablated may result in inappropriate expression of the target gene due to the strength of the PGK promoter, this was directly tested prior to generation of the targeting vector. However, when no foci were observed without Cre mediated excision in Figure 3.1, this suggested that the loxP flanked sequence is effectively interfering with the expression of the *neu* oncogene without inappropriate PGK mediated expression.

Upon creation of the conditionally activated mice by interbreeding the loxP flanked neomycin NeuNT mice with the MMTV-Cre mice, excision of the loxP flanked sequence was observed in the mammary gland, salivary gland and the spleen (Figure 3.5). Interestingly, the level of Cre expression in the salivary gland was detectable while expression in the spleen was not observed (Figure 3.4). However, the expression of Cre

in these tissues was only examined in the adult and it is possible that MMTV could be expressed at higher levels at an earlier time point. Importantly, these results demonstrated that the *neuNT* oncogene was now under the control of the endogenous promoter in the mammary gland in these mice.

Endogenous regulation of *neuNT* in the mammary gland resulted in enhanced branching of the ductal network, proliferation of lobuloalveolar side buds and mammary epithelium that had an increased propensity to escape the normal confines of the fat pad (Figure 3.6). While the formation of the preneoplastic lesions and the enhanced branched observed in these mice was easily predicted based on previous studies using the MMTV promoter (Siegel *et al.*, 1999), the outgrowth of the epithelium was unexpected. The normal boundaries of epithelial penetration into the fat pad is regulated by a number of factors, one of these being TGFβ. As the epithelium moves towards the edge of the fat pad, the gradient of TGFβ increases and the developing duct turns away from the TGFβ concentration increase (Daniel *et al.*, 1989). Further proof of this principle was seen when pellets that slowly released TGFβ were implanted into the mammary fat pad (Silberstein and Daniel, 1987). A clear zone of exclusion existed around the TGFβ releasing pellet that the ductal network would not penetrate. If the endogenously regulated expression of *neuNT* had reduced the sensitivity of these mammary epithelial cells to TGFβ, then the ductal network would have increased branched and may follow the small deposits of fat surrounding the blood vessels that enter and exit the mammary gland. To definitively test whether the epithelium expressing neuNT is TGFβ insensitive, the original TGFβ pellet experiments could be repeated using wild type and NeuNT

mammary glands. If the conditional activation of *neuNT* does result in TGFβ insensitive ducts, the zone of epithelial exclusion around the pellets should be measurably reduced in size.

Consistent with the theory that the mammary gland expressing NeuNT may be insensitive to the effects of TGFβ, escape of the mammary epithelium was observed in an additional mouse model. Overexpression of ASGP2 in the mammary gland under the control of the MMTV promoter resulted in a similar mammary escape phenotype (E.R Andrechek and W.J. Muller, unpublished data). Since ASGP2 is repressed by TGFβ (Carraway *et al.*, 2000), and since it may function in the facilitation of Neu hetero and homodimerization, it is concievable that the effects observed in these two mammary model systems are linked through their response to TGFβ. It is possible that the elevated expression of ASGP2 in the transgenics has ablated the ability to respond to TGFβ. Further, if the activated NeuNT protein is incapable of interacting with the ASGP2 complex, then NeuNT would not respond to the TGFβ / ASGP2 control of mammary gland growth and development. Clearly, future studies will be directed towards the examination of the interplay between Neu, ASGP2 and TGFβ.

While the potential block in the interaction of NeuNT with ASGP2 presents a viable hypothesis for the inability of NeuNT to respond to TGFβ mammary regulation, given the large number of factors that control various aspects of mammary development, it would be a better approach to compare this gland to another that did not escape from the fat pad and ask what the differences were at the molecular level. In addition to monitoring differences in tumor formation, this experimental question has been addressed

in Table 3.2 and 3.3. The examination of gene expression revealed changes in several growth inhibitors, such as the reduction of *slfn1* expression as seen in Table 3.3, however none of these genes has previously been implicated in the regulation of the development of the mammary gland. These results suggest that while there may be a reduced sensitivity to growth inhibitory signals present at the periphery of the fat pad resulting in escape from the normal confines, no obvious defects in gene expression are noted.

In addition to causing alterations in mammary gland development, the expression of the activated *neuNT* allele under the control of the endogenous promoter in the mammary gland resulted in mice that were susceptible to mammary tumors after a long latency (Figure 3.7). These tumors exhibited high levels of *neuNT* expression and had morphology characteristic of Neu induced tumors (Figure 3.8). Interestingly, before the development of the comedo-adenocarcinomas, *neuNT* expression in the preneoplastic lesions was found to be low through immunohistochemistry (Figure 3.8). While low levels of *neuNT* expression were capable of causing altered mammary gland development, it was not sufficient to drive tumorigenesis. One of the mutations commonly observed in the human condition is amplification of HER2 in addition to overexpression. Strikingly, amplification of the recombinant *neuNT* allele and the consequent overexpression was one of the requirements for tumorigenesis in this mouse model (Figure 3.11). The strong selection for amplification of *neuNT* during the transition from preneoplastic lesion to comedo-adenocarcinoma may reflect the requirement of a threshold level for Neu for oncogenic conversion. Consistent with a multistep model of tumorigenesis, overexpression of ErbB3 was also noted (Figure 3.9),

and has been observed in previous models of Neu mediated tumors (Siegel and Muller, 1996) and in the human disease (Quinn *et al.*, 1994; Bodey *et al.*, 1997) suggesting that it is the major heterodimerization partner for Neu. While tumorigenesis in this model is undoubtedly a multistep process involving numerous other genes, when the average number of chromosomal aberrations was examined in this model (Montagna *et al.*, 2002), it was seen to be surprisingly low in comparison to other carcinomas, consisting primarily of amplification of a portion of chromosome eleven and a deletion in chromosome four. Taken together, these results suggest that amplification and overexpression of NeuNT coupled with the loss of a portion of chromosome four are the key events required to mediate tumorigenesis in this model system. Clearly, the identification of the gene or genes deleted on chromosome four will be a target for future investigation.

When the conditionally activated Neu model of tumorigenesis was contrasted with the MMTV-NDL 1-2 mouse model, several important similarities and differences were noted. Indeed, one of the most striking similarities in the mammary glands in these two models was the observation of preneoplastic lesions (Figure 3.12). While the NDL1-2 preneoplastic lesions developed into multifocal comedo-adenocarcinomas, there was only focal tumor development in the endogenously regulated *neuNT* model. Further, examination of *WDNM1*, a marker of Neu induced tumorigenesis (Morrison and Leder, 1994), revealed equal levels of expression between the conditionally activated mammary gland and the tumors that arose, although there was a significant induction over *WDNM1* expression in control glands (Figure 3.25). These results suggest that the preneoplastic

lesions in both models reflect the expansion of a cellular population targeted by NeuNT expression.

While the tumors that develop in the endogenously regulated and the MMTV regulated activated Neu models are histologically similar, they have profound differences in their latency and their ability to metastasize (Figure 3.13). When the tumors were compared and contrasted through a gene expression analysis, there was a clear elevation of differentiation markers in the tumors that were poorly metastatic (Table 3.1). Thus, while the histological examination of these two tumor models confirmed that they were both Neu induced tumors, the molecular analysis was required to illustrate the difference in the metastatic potential. The confirmation of the gene expression data through Northern blot analysis revealed that while the trends identified in the array were valid (Figure 3.14), the individual tumors were remarkably different. Taken together, these results highlight the importance of molecular characterization of tumors to develop individualized rational therapies in the human condition.

The experimental approach of comparing these two Neu mediated tumors has also identified transcription factors that are essential in mediating tumorigenesis (Table 3.1). While both tumor sets overexpress activated Neu and have histologically similar tumors, the tumors differentially express transcription factors dependent on the promoter driving expression of the *neu* allele. In the model where the endogenous promoter drives *neuNT* expression, several interesting transcription factors are upregulated. For example, the PEA3 transcription factor has previously been illustrated to play a role in Neu mediated tumorigenesis and is upregulated in this model. PEA3 has been shown to bind to the Neu

promoter and regulates expression of endogenously transcribed *neu* (Xing *et al.*, 2000). Further, it has been shown that PEA3 also serves to regulate Neu mediated tumorigenesis as a dominant negative PEA3 transgene increased the tumor latency of MMTV-Neu mice (Shepherd *et al.*, 2001).

In addition to PEA3, another notable transcription factor involved in Neu mediated tumorigenesis under the endogenous promoter is Krox-20 (8.5 fold elevation) (Table 3.1). Krox20 (EGR2) has previously been linked to Neu induced tumorigenesis (Sweeney *et al.*, 2001) and studies of other EGFR family members suggests a role in signaling mediated by Neu. Specifically, both the muscle specific deletion of *neu* and the knockout of *EGR3* both resulted in a lack of muscle spindles (see Chapter 5) (Tourtellotte and Milbrandt, 1998; Andrechek *et al.*, 2002). Further, the general neurological defects seen with *neu* knockouts are remarkably similar to the defects in the Krox20 knockouts (Schneider-Maunoury *et al.*, 1993; Garratt *et al.*, 2000; Voiculescu *et al.*, 2001). Clearly, a detailed examination of this signaling pathway is warranted in the future.

The identification of a number of glycoproteins through the gene expression comparison of the two tumors is also intriguing given that MUC4 may serve in the regulation of Neu signaling through the facilitation of heterodimerization with ErbB3 (Jepson *et al.*, 2002). An examination of the over and under expressed glycoproteins reveals several interesting findings. *Acidic epididymal glycoprotein 1* (*AEG-1, CRISP-1*) is overexpressed 153 fold (Table 3.1) and is normally expressed in the male genital tract and the salivary gland. However, the same analysis of the *AEG-1* promoter revealed a consensus binding domain for PEA3 (Schwidetzky *et al.*, 1997), which was also

overexpressed in the endogenously regulated Neu mediated tumors. Interestingly, *muc1* is also overexpressed in these tumors (Table 3.1) and has been observed to be overexpressed in many human tumors. Further, it has been illustrated that EGFR and MUC1 interact at the cell membrane, resulting in the recruitment of c-Src (Li *et al.*, 2001). Clearly these various glycoproteins serve to recruit and activate specific pathways that will alter the properties of the carcinoma.

The final group of genes identified in the gene chip analysis were genes identified as being in close proximity to the location of the endogenous *neu* allele. The co-amplification of *grb7* and *cab1* with *HER2* has been well documented in the human condition (Kauraniemi *et al.*, 2001; Varis *et al.*, 2002) and the identification of these genes in the mouse model illustrates the similarity of the amplification process. Additionally, these genes were illustrated to be not only amplified, but are also overexpressed, leading to questions about their role in the progression of Neu mediated breast cancer (Figure 3.15). To examine the role of Grb7 in metastasis, a construct was engineered to express an antisense *grb7* mRNA and was transfected into a cell line derived from a conditionally activated Neu tumor. This resulted in the decrease in the 51 kDa Grb7 splice variant and an increase in the level of the 59 kDa isoform. Since the 59 kDa isoform has previously been identified as the splice form that is activated (Tanaka *et al.*, 1998), it is not surprising that this resulted in the increase in invasiveness of this cell line (Figure 3.16). However, future experiments using an alternate method, such as siRNA, may address how the ablation of Grb7 affects the invasiveness of the cell lines both *in vitro* and *in vivo*.

In contrast to the MMTV based model systems which have yielded information about the signaling pathways that are activated during Neu mediated tumorigenesis, the conditional model has illustrated several similarities to the human condition. A more detailed analysis of the chromosomal alterations in this model of Neu mediated tumor formation revealed that there were double minute chromosomes present in the cell lines generated from the primary tumors (Figure 3.17 Panel A). Elimination of these DMs through hydroxyurea treatment resulted in the loss of Neu expression in one cell line, suggesting that Neu expression was primarily mediated through the amplified *neuNT* allele contained within the DM. However, with the elimination of Neu expression, ErbB3 was observed to be overexpressed, suggesting that the EGFR family could compensate for the loss of a family member (Figure 3.17). When considered in combination with the relatively low number of chromosomal alterations (Montagna *et al.*, 2002) in this tumor model, these results have implications for the design of rational human therapies. Indeed, these results suggest that treatment of a single oncogenic event may not be sufficient treatment given the multistep nature of tumor formation.

3.3.2 Embryonic Lethality In Germline ErbB2$^{NT/NT}$ Mice

While the previously discussed work has illustrated the similarities of the conditional activation of Neu in the development of mouse mammary tumors to HER2 mediated breast cancers, the major limitation in this model is the extended latency. While not determined, this may have been due to the ability of the wild type allele to counteract the effect of the recombinant allele (Nikitin *et al.*, 1996). In an attempt to

reduce the latency of tumor formation, mice expressing *neuNT* under the control of the endogenous promoter in the germline of mice were created to avoid the generation of a null allele (Figure 3.18). These germline ErbB2$^{WT/NT}$ mice were derived by expressing Cre recombinase under the control of a chicken β-actin promoter in the conditional *neuNT* embryos. However, when germline ErbB2$^{WT/NT}$ mice were interbred, germline ErbB2$^{NT/NT}$ mice were not observed in the viable progeny. Indeed, embryonic lethality at 12.5 dpc was noted due to defects in cardiac trabeculation and development of the nervous system (Figures 3.19, 21 and 22). Interestingly, expression of the activated *neuNT* allele was able to allow the germline ErbB2$^{NT/NT}$ embryos to proceed past the point of embryonic lethality observed in the ErbB2 null mice, but was not sufficient to rescue embryonic lethality. Importantly, when the wild type cDNA was used in the place of the *neuNT* cDNA, the resulting mice were viable (Chan *et al.*, 2002). These results suggest that normal signalling from Neu is required for development of the mouse. Indeed, given that the *neuNT* allele is constitutively activated and is thought to function primarily through homodimerization, the embryonic lethality suggests that Neu may be required to activate alternative signalling pathways. For example, Neu / ErbB3 heterodimers may be required to activate crucial cell survival pathways during embryogenesis. In addition to the embryonic lethality observed in the germline ErbB2$^{NT/NT}$ embryos, there was a dramatic loss of NeuNT expression (Figure 3.20). The inability to detect Neu protein was inconsistent with previous publications using mice created with an identical targeting strategy. Indeed, the inability to detect Neu is also inconsistent with the survival of the embryos for two full days longer than embryos that

are lacking ErbB2. Taken together, these results strongly suggest that while Neu is expressed, it is rapidly turned over after activating the cellular signalling pathways required for development to 12.5 dpc and is therefore not easily detected in immunoblot analysis.

To further examine the reduced expression in the germline ErbB2$^{NT/NT}$ embryos, the levels of *neuNT* transcript were examined (Figure 3.20). Using primers that detect both mouse and rat *neu* homologues, the levels of *neu* transcript in wild type, heterozygous and homozygous embryos was assessed. Interestingly, the level of *neu* mRNA in germline ErbB2$^{NT/NT}$ embryos was only 15% of that observed in the wild type controls. Further, when the expected level of *neu* mRNA was calculated from the heterozygous control, relative to the wild type control, the level of observed *neu* expression was observed to be far lower than expected (Figure 3.20). Previous results using the same targeting strategy for alternate *neu* alleles resulted in unchanged levels of *neu* mRNA (Chan *et al.*, 2002). Coupled with the reduction in protein levels, these observations led to the hypothesis that the lack of splicing was contributing to the reduction in Neu expression (Chan *et al.*, 2002). However, the reduction of *neu* mRNA in this model suggests that expression of activated *neu* has triggered a feedback loop that regulates the promoter activity of *neu,* in addition to any defects in splicing. Future experiments should allow this premise to be tested. For example, mice expressing an activated *neu* allele in the mammary gland under the control of the MMTV promoter should have greatly reduced mRNA levels of the mouse *neu* homologue in comparison to a wild type control. Since the MMTV promoter is not responsive to the normal

regulation of the Neu promoter, any activation of a feedback loop would only impinge on the levels of the endogenous transcript while MMTV would ensure Neu levels were artificially high. Indeed, the identification and characterization of this putative Neu expression feedback loop could have beneficial consequences in the development of therapies to treat HER2 induced carcinomas.

3.3.3 Conditional and Germline Expression of NeuNT, Impact on Mammary Gland Development and Tumorigenesis

Since embryonic lethality has precluded the examination of the possibility of altered tumorigenetic latency in germline ErbB2$^{NT/NT}$ mice, the germline ErbB2$^{WT/NT}$ mice were compared to their conditionally activated counterparts. Given that both of these mouse models were expressing a single *neuNT* allele under the control of the endogenous promoter in the mammary gland, it was surprising to observe that the germline ErbB2$^{WT/NT}$ mice did not develop tumors in the mammary gland (Figure 3.24). Further, Neu expression has been noted in the epidermis of the mouse and when transgenic mice were created expressing activated *neu* in the epidermis, squamous cell carcinomas were detected in >90 of mice by 6 months of age (Kiguchi *et al.*, 2000). Since the germline ErbB2$^{WT/NT}$ mice were expressing an activated allele where the endogenous promoter is normally expressed, the mice were also examined for skin tumors, but none were noted. While the conditional and germline activation mouse models have different susceptibilities to tumor induction, they were constructed using the same construct (Figure 3.2) but excision of the loxP flanked sequence was mediated by

Cre expression under different promoters. To determine that the differences in the ability to form tumors was not due to differences in expression of *neuNT*, quantitative RT-PCR was conducted which illustrated that the conditional and germline models expressed equal levels of *neuNT* transcripts. The creation of two mouse models expressing an identical oncogene under the control of an identical promoter at identical levels with different phenotypes was a surprising result. However, these differences may be attributed to a number of factors. In contrast to the conditional model, the germline ErbB2$^{WT/NT}$ mice should express the *neuNT* allele in both the epithelial and stromal components of the mammary gland. This change in epithelial / stromal interaction may be sufficient to prevent tumorigenesis. This possibility could be tested in the future by implanting the *neuNT* expressing epithelium from a germline donor into the cleared fat pad of a wild type mouse, and vice versa. However, the lack of tumor formation in any tissue in the germline ErbB2$^{WT/NT}$ mice strongly suggests that this is not a viable hypothesis.

Another hypothesis explaining the lack of tumor formation in the germline ErbB2$^{WT/NT}$ mice is that the transcription of the *neuNT* allele is selectively downregulated. Indeed, the downregulation of the *neuNT* allele was observed in the germline ErbB2$^{NT/NT}$ embryos (Figure 3.20). However, expression levels in the mammary gland of the conditional and germline activated NeuNT mice were observed to be equal by quantitative RT-PCR (Figure 3.24). Clearly these results illustrate that a selective downregulation of *neuNT* expression is not responsible for the lack of tumorigenesis observed in the germline ErbB2$^{WT/NT}$ mice.

An alternative hypothesis to explain the absence of tumors in the germline endogenously regulated expression of the potent *neuNT* oncogene is that the expression of an activated allele in place of the wild type allele from the earliest stages of embryonic development has resulted in compensation during development of susceptible tissues by various feedback loops and signal transduction pathways. Indeed, these results are reminiscent of experiments using the Rous Sarcoma Virus (RSV) in avian experiments and Moloney murine sarcoma virus in pre-implantation murine embryos (Jaenisch, 1980; Dolberg and Bissell, 1984). Infection of newly hatched chicks with RSV results in the formation of a sarcoma at the site of injection and is associated with the expression of active v-src. However, when the infection was completed *in ovo*, there was no corresponding sarcoma development (Dolberg and Bissell, 1984; Howlett *et al.*, 1988). Interestingly, in the chickens that were infected *in ovo*, v-src was still detected to be both expressed and active despite the lack of sarcoma formation (Howlett *et al.*, 1988). Given that the germline expression of *neuNT* occurs in the embryonic state and that the conditional activation would result in excision and activation of *neuNT* in the postnatal mouse due to increased MMTV expression during puberty (Henrard and Ross, 1988), there are striking similarities in these results. However, when chickens infected with RSV *in ovo* are wounded as adults they develop sarcomas at the wound site, suggesting that tumor induction in these chickens is actually inappropriate wound repair (Dolberg *et al.*, 1985). Since the germline ErbB2$^{WT/NT}$ mice have been subjected to wounding intentionally (tail cutting and ear tagging) and unintentionally (fight wounds) in tissues that express Neu (Kiguchi *et al.*, 2000), the theory of wounding in relation to tumor

formation does not appear to apply in these mice. However, the premise that there is a developmental regulation of additional factors or signalling pathways, analogous to the RSV experiments, remains. In order to determine whether the aberrant regulation of these factors or pathways has impeded the ability of the germline ErbB2$^{WT/NT}$ mice to form Neu mediated tumors, future experiments may address this through interbreeding MMTV-NDL transgenics with the germline ErbB2$^{WT/NT}$ mice.

To more completely define the differences in the susceptibility to tumorigenesis of the mice with a conditional activation of *neuNT* as compared to the germline ErbB2$^{WT/NT}$ mice, a comparison of gene expression in these mammary glands was conducted (Table 3.2 and 3.3). Consistent with the increased branching and preneoplastic lesions, numerous markers that are associated with differentiation and lactation are elevated in the conditional model. Interestingly, numerous genes that have previously been associated with Neu and Ras mediated tumorigenesis were also noted in the mammary gland of the conditional model. While these mammary glands only have preneoplastic lesions, the expression of these neoplastic marker genes suggests that there has been an expansion of a Neu responsive target cell population in the conditional model. Further, the elevation of tumor suppressors and genes involved in the retinoic acid pathway in the germline model reinforce the idea that this mammary gland is reduced in tumor forming ability. Although these observations confirm that the conditional activation of *neuNT* result in a mammary gland that is predisposed to tumorigenesis, the data did not establish a premise as to why the germline expression of *neuNT* resulted in mice that are not susceptible to tumor formation. Clearly the elevation

of tumor suppressors and the retinoic acid pathway in the germline mammary gland is interesting, yet it is doubtful that these changes are capable of inhibiting the potent oncogenic activity associated with the activated *neuNT* oncogene. Moreover, rather than a single event, this data suggests that there may be numerous genetic changes that act synergistically to reduce Neu mediated tumorigenesis. For future work, the potential changes in signalling downstream of Neu could be examined through the generation and stimulation of mammary epithelial cell lines from both mouse models. Indeed, the ability of mice to adapt to the expression of a powerful oncogene will clearly be the focus of future work in the hope that human therapies may be designed on the basis of the inhibition of the molecular effects of activated Neu.

CHAPTER 4

MAMMARY GLAND DEVELOPMENT AND TUMORIGENESIS IN THE ABSENCE OF ERBB2

4.1 Introduction

The role of ErbB2 in mediating the progression of breast cancer in women is well established and ErbB2 has been an attractive target for new therapies. Conversely, relatively little is known of the role of ErbB2 in normal mammary gland development. Previous examination of mammary gland development in mouse models lacking ErbB2 has been hampered due to the embryonic lethality observed at day 10.5 of embryogenesis (Lee *et al.*, 1995). Myocardial specific expression of an ErbB2 transgene in the ErbB2 null background has rescued the embryonic lethality associated with the knockout of ErbB2. Unfortunately, mammary gland development could not be examined in these mice since they died at birth due to a loss of motor neurons and defects in Schwann cell development (Morris *et al.*, 1999; Woldeyesus *et al.*, 1999; Lin *et al.*, 2000).

Expression of ErbB2, and the remainder of the EGFR family, has been examined in the mouse mammary gland. ErbB2 expression has been observed in the endbud of a normal mammary gland. Interestingly, ErbB2 expression has also been noted in the stroma in a developing gland but is absent at later timepoints (Schroeder and Lee, 1998). When expression of the entire EGFR family is compared, several trends quickly become

apparent. EGFR is expressed at the same level throughout development, pregnancy, early lactation and involution and while ErbB2 and ErbB3 are similar, expression increases during the transition from early to late development and is absent in the latter stages of lactation. Conversely, ErbB4 is expressed weakly in the virgin and lactating glands, moderately in the regressing gland and highly in the pregnant mammary gland (Schroeder and Lee, 1998). These observations point towards individual roles for the EGFR family members in development of the mammary gland. Consistent with these observations is the induction of additional branching and lobuloalveolar side bud formation in the mammary glands of mice expressing an activated *neu* allele (Siegel *et al.*, 1999)(Also see Chapter 3). However, the precise function of ErbB2 in mediating ductal development is not clear.

One approach that has been used in an attempt to define the function of ErbB2 in the mammary gland is by expression of a dominant negative *erbB2* allele (Jones and Stern, 1999). While transgenic mice expressing this construct did have subtle mammary defects in late pregnancy and lactation, the expression of the dominant negative construct only mildly reduced the extent of ErbB2 phosphorylation when tested *in vitro*. Further, a dominant negative *erbB2* allele will affect not only ErbB2 function, but all other members of the EGFR family as well. In addition, since the mammary gland is hormonally responsive, the expression of a dominant negative under the control of a hormonally responsive promoter is problematic. To avoid these limitations and to circumvent the embryonic lethality observed the knockout, a mammary specific knockout of ErbB2 was created. The excision of *erbB2* in the mammary gland resulted in delayed

ductal outgrowth that persisted into the twelfth week of development. However, no deviation from normal pregnant, lactating or regressing wild type mammary glands was noted in the conditional knockouts.

In addition to modulating mammary development, ErbB2 is also involved in tumorigenesis. Interestingly, MMTV-MT mediated tumors have been shown to overexpress ErbB2, illustrating the multistep nature of MT mediated tumor formation (Personal communication, J. Pollard). To examine the role of ErbB2 in tumor formation, mice harboring the mammary specific deletion of ErbB2 were interbred with the MMTV-MT mice. An initial examination of ErbB2$^{Flox/WT}$ MMTV-Cre MMTV-MT mice revealed that the hyperplastic mammary gland did not express high levels of ErbB2. Importantly, the tumors that developed in these mice did. Generation and examination of ErbB2$^{Flox/Flox}$ MMTV-Cre MMTV-MT mice revealed that the latency of MT mediated tumorigenesis was increased by over two weeks. However, the tumors that developed in these mice expressed ErbB2 and metastasized to the lung. Taken together, this data illustrates a role for ErbB2 both in mammary gland development and in tumorigenesis.

4.2 Results

4.2.1 Mammary Gland Development in the Absence of ErbB2

The generation of a mammary specific ablation of ErbB2 through the Cre / loxP recombination system employed the MMTV-Cre transgenic mice (See Chapter 3). In addition, a targeting construct to replace exon one of the endogenous *erbB2* allele with a

loxP flanked *neu* cDNA and a *neomycin* selectable marker was prepared (Figure 4.1, Panel A). The targeted allele was designed such that the endogenous promoter would control the expression of the cDNA replacing exon one. However, with the addition of Cre recombinase the cDNA should be excised, resulting in the ablation of ErbB2. The targeting construct, targeted recombination, genomic allele and recombinant allele are all illustrated (Figure 4.1, Panel A and B). Electroporation of the targeting vector resulted in several independent ES cell lines that carried the recombinant allele which were used in blastocyst injections. After germline transmission of this recombinant allele (Figure 4.1, Panel C), the $ErbB2^{Flox/WT}$ mice were interbred. The expected Mendelian ratio of $ErbB2^{WT/WT}$: $ErbB2^{Flox/WT}$: $ErbB2^{Flox/Flox}$ mice was observed, indicating that the cDNA recombinant allele was expressed at levels sufficient to rescue the embryonic lethality observed in the ErbB2 null mice. To determine the level of ErbB2 in these mice, an immunoprecipitation followed by an immunoblot for ErbB2 was conducted on both $ErbB2^{WT/WT}$ and $ErbB2^{Flox/Flox}$ mice. Strikingly, the mice containing the recombinant allele only express approximately 10% of the level of ErbB2 detected in the wild type controls (Figure 4.1, Panel D). This is consistent with other data from our laboratory for other constructs using an identical targeting procedure. However, although the level of ErbB2 was reduced in the $ErbB2^{Flox/Flox}$ mice, they were still able to interbreed and lactated normally. Indeed, even after numerous cycles of lactation and involution the $ErbB2^{Flox/Flox}$ mice reared normal sized litters with no appreciable runting of the pups.

In order to generate a mammary specific ablation of ErbB2, Cre recombinase was introduced to generate a null allele (Figure 4.2, Panel A). This was accomplished by

Figure 4.1 – Embryonic Stem Cell Targeting Strategy for a Tissue Specific Null ErbB2

A schematic representation of the targeting construct, strategy and the genomic erbB2 allele is shown (A). The 2.5 kb 5' arm of homology (Sph1 to Nar1) and the 8 kb 3' arm of homology (Kpn1 to Sal1) were used to direct the homologous recombination to the wild type allele. This targeting strategy replaces the first exon of the genomic erbB2 allele with a loxP (triangles) flanked *neu* cDNA followed by the SV40 polyA (Neu). This is followed by a neomycin cassette (neo) for selection. The probe external to the directed recombination event is shown. The recombinant allele (B) has the loxP flanked *neu* cDNA under the control of the endogenous promoter and should act as a wild type allele until excision of the loxP sequence, creating a a null allele. The size of band detected in a Southern analysis with the external probe is illustrated for both the genomic (7.5 kb) and for the recombinant allele (4.6 kb). After electroporation of the embryonic stem cells, 7 cell lines containing the recombinant allele were identified. Upon blastocyst injection and breeding, the recombinant allele was passed. A Southern blot of tail DNA from mice that contain either two wild type alleles or one wild type allele and one recombinant allele is shown (C). When mice with one copy of the knock-in allele were interbred, homozygotes were detected at normal Mendellian ratios and were observed to develop normally. However, when levels of Neu were surveyed by immunoprecipitation and Western analysis it was seen the homozygous $ErbB2^{Flox/Flox}$ mice expressed approximately 10% of the level of Neu when compared to the wild type (D).

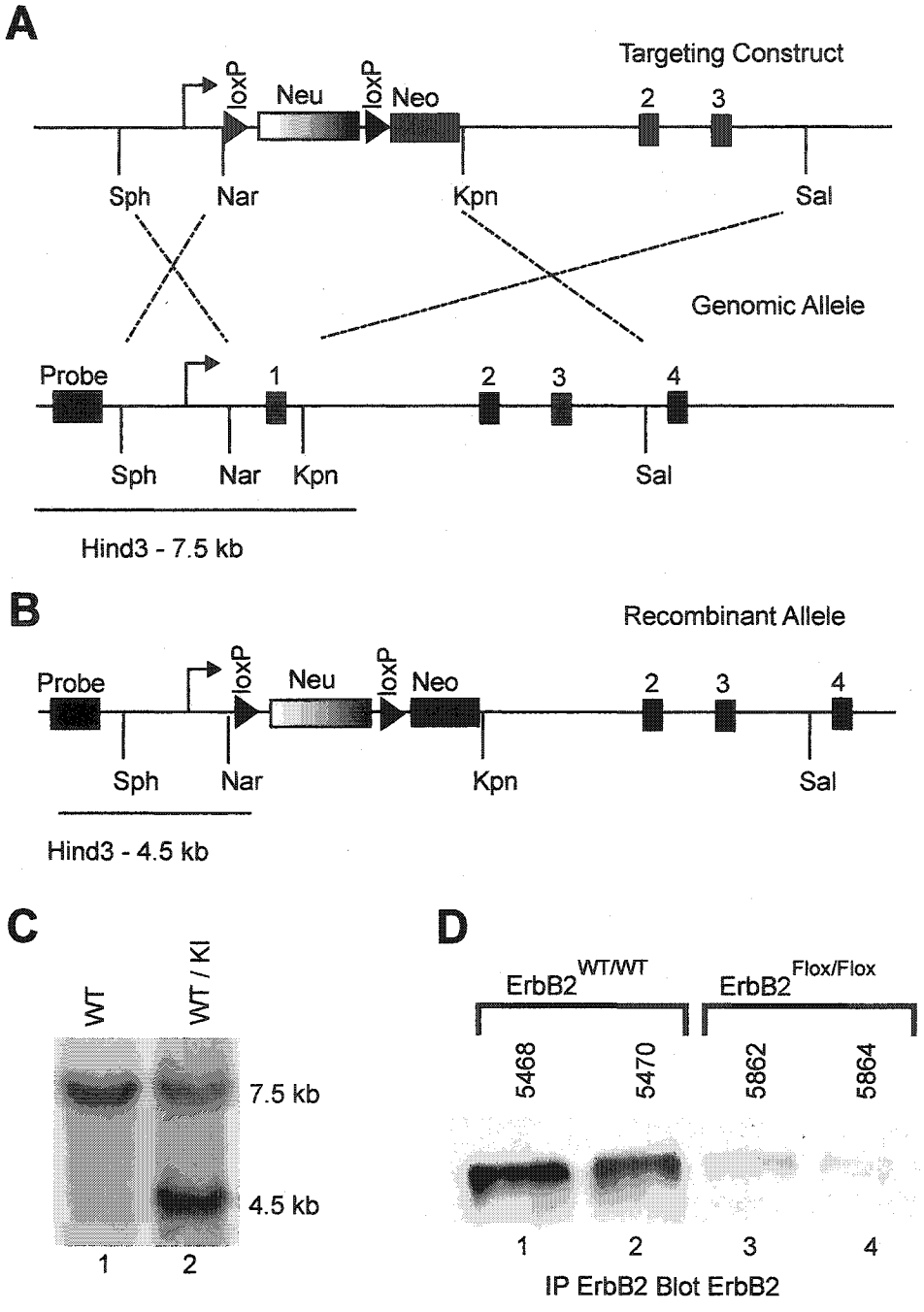
A
Targeting Construct
loxP
Neu
loxP
Neo
2
3
Sph
Nar
Kpn
Sal
Genomic Allele
Probe
1
2
3
4
Sph
Nar
Kpn
Sal
Hind3 - 7.5 kb
B
Recombinant Allele
Probe
loxP
Neu
loxP
Neo
2
3
4
Sph
Nar
Kpn
Sal
Hind3 - 4.5 kb
C
WT
WT / KI
7.5 kb
4.5 kb
1
2
D
ErbB2 WT/WT
ErbB2 Flox/Flox
5468
5470
5862
5864
1
2
3
4
IP ErbB2 Blot ErbB2

Figure 4.2 – Excision in the ErbB2$^{Flox/Flox}$ Mammary Gland

A schematic diagram of the recombinant allele before and after Cre Recombinase mediated excision of the *neu* cDNA (A). Also illustrated are the sizes of bands detected in a Southern analysis using a portion of the *neo* cDNA as a probe after a HindIII digest. Prior to the excision event, the endogenous promoter will express the neu cDNA normally in all tissues the endogenous promoter is active in. However, upon excision of the neu cDNA, a null allele is created due to the lack of the first exon and the remaining *neo* sequence between the promoter and the remainder of the genomic allele. A Southern analysis (B) revealed that excision occured in a control sample as expected after an injection of β-actin Cre (Sample from R. Chan). However, in all mammary glands surveyed from the ErbB2$^{Flox/Flox}$ MMTV-Cre mice, excision does not occur. Given previous data suggesting that the MMTV promoter / enhancer is silenced by methylation in various backgrounds, the ErbB2$^{Flox/Flox}$ MMTV-Cre mice were intergressed into a FVB background by 12 backcrosses. Upon examination of the mammary glands by Southern analysis after the strain was derived onto an FVB background, excision was noted (C). The probe used in the Southern contained a portion of the polyA sequence and detected a floxed allele at 10 kb, an excised product at 6 kb and the polyA from the MMTV-Cre construct just below 6 kb. As seen in lanes 5-8, excision is occurring in these mammary glands.

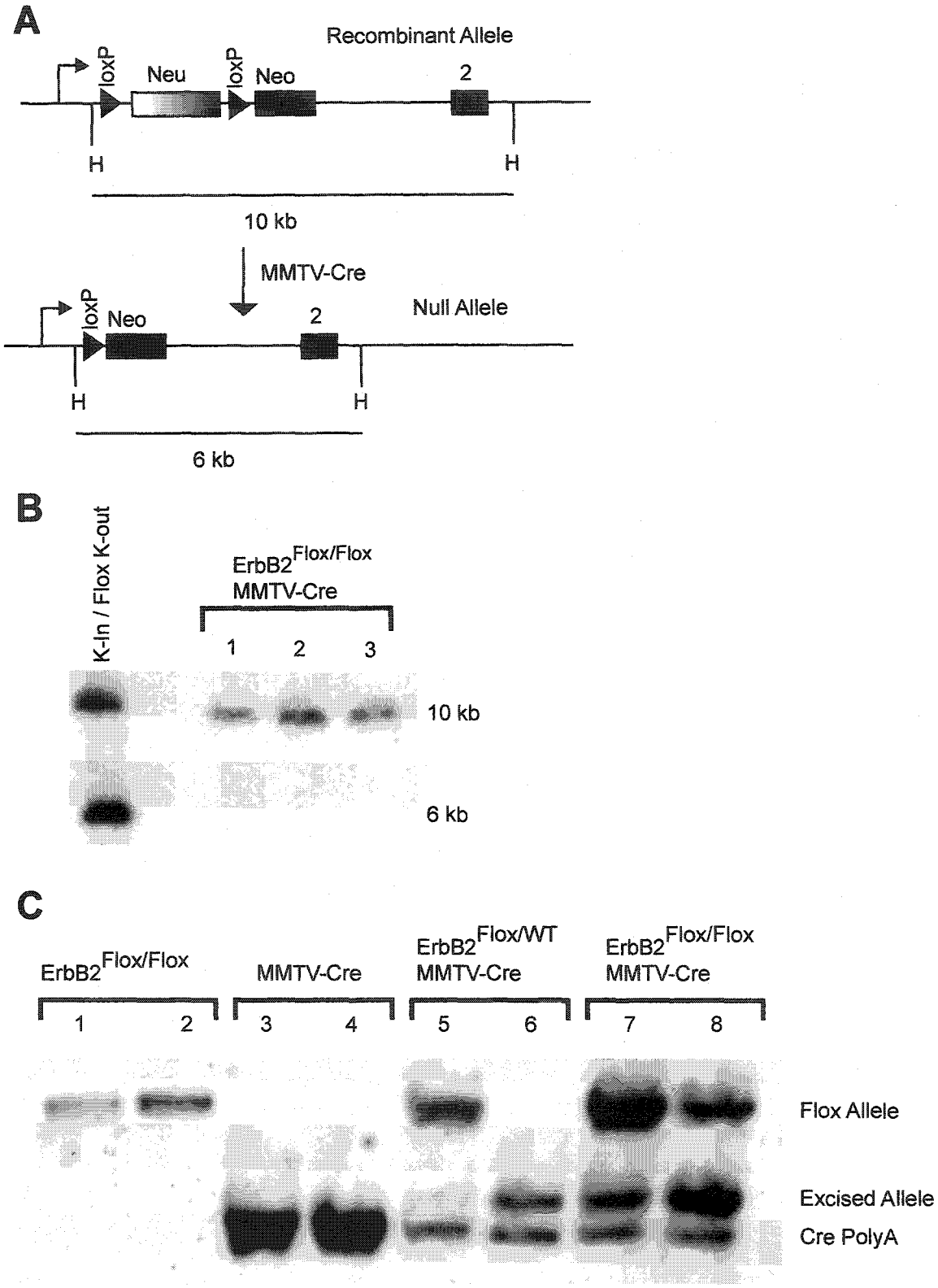
A
Recombinant Allele
loxP
Neu
loxP
Neo
2
H
H
10 kb
MMTV-Cre
loxP
Neo
2
Null Allele
H
H
6 kb
B
K-In / Flox K-out
ErbB2Flox/Flox
MMTV-Cre
1
2
3
10 kb
6 kb
C
ErbB2Flox/Flox
MMTV-Cre
ErbB2Flox/WT
MMTV-Cre
ErbB2Flox/Flox
MMTV-Cre
1
2
3
4
5
6
7
8
Flox Allele
Excised Allele
Cre PolyA

interbreeding the ErbB2$^{Flox/Flox}$ mice with the MMTV-Cre transgenics. The resulting ErbB2$^{Flox/WT}$ MMTV-Cre mice were obtained and were interbred to obtain both control and ErbB2$^{Flox/Flox}$ MMTV-Cre mice. From these crosses all genotypes were obtained at the expected ratios. To control for excision of the loxP flanked allele, ErbB2$^{Flox/WT}$ mice were interbred and the single cell embryos were injected with the previously described β-actin Cre construct (See Chapter Three). Progeny from this experiment carrying one excised floxed allele and one wild type allele were interbred with a line of mice with two wild type Neu cDNA knock-in alleles (lacking the loxP sites). The resulting mice carrying one wild type cDNA knock-in allele and one excised loxP flanked allele were used as a control for the excision event (Sample from R. Chan). In a Southern analysis on the control tissue, the knock-in allele is seen at 10 kb and the excised allele is seen at 6 kb using a portion of the *neomycin* cDNA as a probe (Figure 4.2, Panel B). Surprisingly, in a survey of several ErbB2$^{Flox/Flox}$ MMTV-Cre mammary glands, no excision was detected in any of the samples (Figure 4.2, Panel B). Further, an RNase protection revealed that MMTV-Cre transgenics were no longer expressing the transgene (data not shown). To ensure that there was no selection against ErbB2 null mammary epithelium, these results were then duplicated for ErbB2$^{Flox/WT}$ MMTV-Cre mammary glands which once again showed an absence of excision. Since the MMTV promoter / enhancer is often methylated in strains other than FVB (Chaillet *et al.*, 1995; Zhou *et al.*, 2001), the ErbB2$^{Flox/Flox}$ mice were interbred with FVB mice. After 12 generations of backcrosses, the progeny and the MMTV-Cre mice were interbred to derive the ErbB2$^{Flox/Flox}$ MMTV-Cre mice on a pure FVB background. Using a portion of the neomycin cDNA and the

polyA that is common to the polyA used in the MMTV vector as a probe in a Southern analysis, the various controls and conditional null ErbB2 mammary glands were examined. Strikingly, excision was observed both in the ErbB2$^{Flox/WT}$ MMTV-Cre and ErbB2$^{Flox/Flox}$ MMTV-Cre mice (Figure 4.2, Panel C, lanes 5-8). As previously observed (see Chapter 3), MMTV-Cre mediated excision in the mammary gland was not complete, except in lane 6. The complete excision observed in the heterozygous control is likely an artifact of where the sample was taken in the mammary gland since all subsequent analysis with other samples have failed to show complete excision. Importantly, the development of the mammary gland in the absence of ErbB2 could now be examined.

To examine the role of ErbB2 in mammary gland development, the conditional ErbB2 null mice were examined at various stages of development by mammary wholemount analysis. At three weeks of development there was a striking difference between the littermate control and the ErbB2$^{Flox/Flox}$ MMTV-Cre mammary glands (Figure 4.3, Panels A vs. B). While the control mammary gland has grown away from the nipple, with numerous ducts and has already established several side branches, the conditional null has just begun to grow away from the nipple and has far fewer ducts and side branches. In addition, the littermate control has numerous terminal endbuds (TEBs) at the ends of the ducts while the conditional null has not developed any at the same time point. By four weeks of development, the ductal network in the wild type control mammary gland has reached the lymph node and the TEBs are still clearly visible as the epithelium pushes through the fat pad (Figure 4.3, Panel C). Conversely, the ducts in the conditional null mice have moved half the distance from the nipple to the lymph node

Figure 4.3 – Mammary Gland Development in the absence of ErbB2

To determine the effects of erbB2 on mammary gland development, mammary glands were examined at a variety of timepoints by wholemount analysis in mice lacking erbB2 specifically in the mammary gland. At three weeks of development (A-B), the wild type mammary gland has grown out from the nipple and numerous terminal end buds (White Arrowheads) have formed and are extending into the surrounding fat pad (A). Conversely, $ErbB2^{Flox/Flox}$ MMTV-Cre mammary gland appears developmentally delayed. Large terminal end buds have not yet formed and the branching is clearly less extensive (B). By four weeks of age (C-D), the wild type mammary gland has reached the lymph node (LN) and still exhibits numerous terminal end buds (C). The delay in the condition null mammary gland is clear as the mammary epithelium has only exended approximately half the distance from the nipple to the lymph node (D). By twelve weeks of age (E-F), the wild type mammary epithelium has completely filled the mammary gland and the terminal end buds have regressed (E). Strikingly, the $ErbB2^{Flox/Flox}$ MMTV-Cre mammary epithelium is just reaching the boundaries of the fat pad and there are still several terminal end buds visible. Further, there is a clear reduction in the extent of branching at this time point. Several weeks later these two mammary glands are essentially indistinguishable (data not shown).

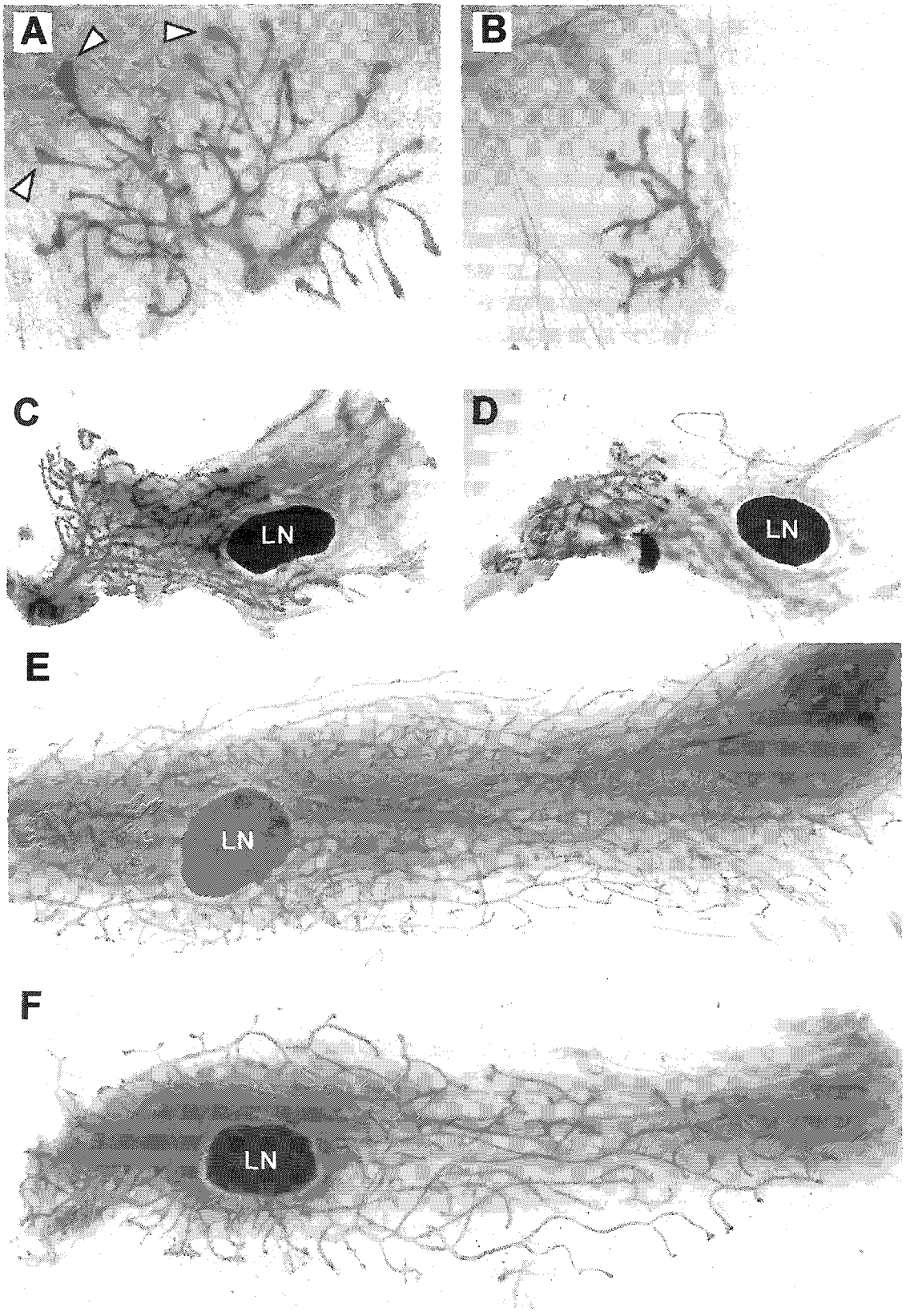
A
B
C
LN
D
LN
E
LN
F
LN

and clearly lag behind the wild type control. However, in contrast to the three week time point, by four weeks the conditional ErbB2 null mammary gland has developed TEBs (Figure 4.3 Panel D). At twelve weeks of age, the wild type control female mouse has completed puberty, the mammary gland has completely filled the fat pad and the TEBs have regressed as seen in the control (Figure 4.3, Panel E). In contrast, the ErbB2$^{Flox/Flox}$ MMTV-Cre mammary gland is still developmentally delayed as there are fewer ducts towards the terminus of the fat pad and the amount of lateral branching is also markedly reduced (Figure 4.3, Panel F). However, when the region between the lymph node and the nipple is compared to the wild type control, no differences are readily apparent, suggesting that the conditional null is simply delayed in development. Consistent with this, experimental and control wholemounts at 20 weeks are indistinguishable (data not shown).

The female ErbB2$^{Flox/Flox}$ MMTV-Cre mice were observed to suckle their offspring normally through numerous cycles of lactation and involution with no abnormal runting of the pups. Thus, when the wholemounts and histological sections of mammary glands from the ErbB2$^{Flox/Flox}$ MMTV-Cre mice throughout pregnancy, lactation and involution were compared to the controls, it was not surprising that no striking differences were noted. Indeed, any differences noted in the various sections were well within the range of normal variation. As an example, sections from mice at day 10 of lactation that had been removed from their offspring 5 hours earlier are shown for ErbB2$^{Flox/WT}$ MMTV-Cre and ErbB2$^{Flox/Flox}$ MMTV-Cre mice (Figure 4.4, Panels A-D). The low magnification images (Figure 4.4, Panels A and B) illustrate that the majority of

Figure 4.4 – Lactation in the absence of ErbB2

To determine the effects of ErbB2 on mammary gland function, mammary glands were examined at a variety of timepoints during lactation and involution by histological analysis in mice lacking erbB2 specifically in the mammary gland. At the midpoint of lactation 5 hours after removing the progeny, the wild type mammary gland illustrates the characteristic lactational histology with a fat pad almost completely filled with lobuloalveolar units and the ductal network (A). The conditional deletion of ErbB2 results in the same pattern (B). At higher magnification it is clear that both the wild type (C) and the conditional null (D) have produced lipid rich milk and should feed their young without difficulty. The inability to detect phenotypic differences was also consistent at all stages of pregnancy and involution that were assayed (data not shown).

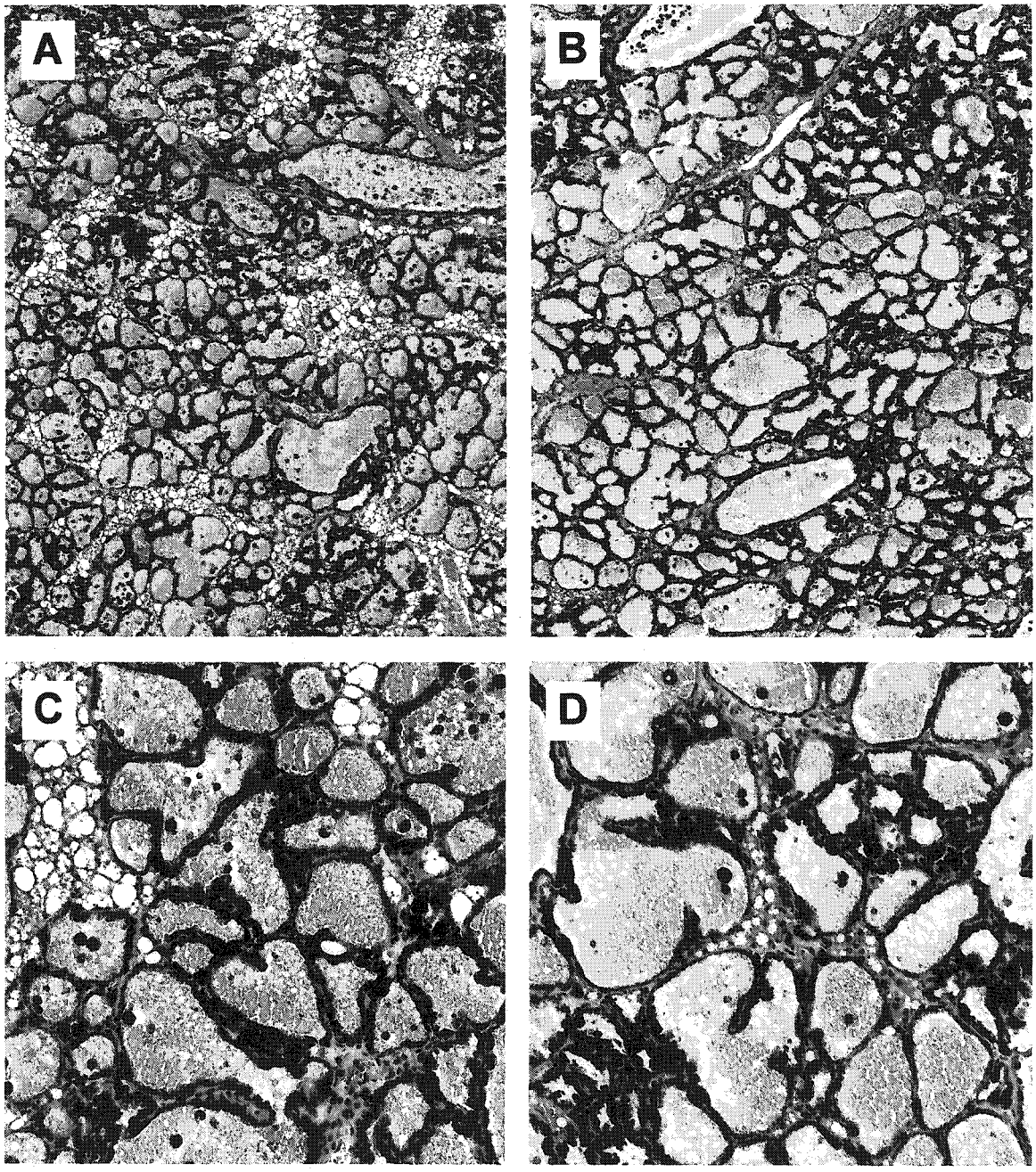
A
B
C
D

the mammary fat pad is filled with enlarged lobuloalveolar units. Higher magnification (Figure 4.4, Panels C-D) reveal that these mice have indeed produced lipid rich milk. Taken together, these results suggest that ErbB2 is not essential for lactation or involution, but is integral for normal ductal outgrowth during development.

4.2.2 The Role of ErbB2 in MMTV-MT Mediated Tumorigenesis

To determine the role of ErbB2 in the multistep tumor progression in the MMTV-MT mediated tumors, the ErbB2$^{Flox/Flox}$ MMTV-Cre line was interbred with the MMTV-MT mice. The resulting ErbB2$^{Flox/WT}$ MMTV-Cre MMTV-MT mice were allowed to develop tumors. Tumors bearing one wild type copy of ErbB2 and one null allele were then examined for overexpression of ErbB2. In addition, when available, a hyperplastic mammary gland from the same mouse was also examined for ErbB2 overexpression. In the resulting Western analysis, the control for ErbB2 overexpression obtained from a conditionally activated ErbB2 tumor (See Chapter 3) illustrated high levels of ErbB2 expression (Figure 4.5, Panel A). From the three ErbB2$^{Flox/WT}$ MMTV-Cre MMTV-MT mice that were examined, the primary tumor (sample 1) and most of the secondary tumors (samples 2 and 3) overexpressed ErbB2. Interestingly, the smallest tumors or hyperplastic tissue (sample 4) had reduced levels of ErbB2 (Figure 4.5, Panel A, 1113-4, 0979-3 and 0979-4). To determine whether the overexpression of ErbB2 in these samples was due to amplification of the *erbB2* locus, Grb7 was examined (See Chapter 3). While the control tumor illustrated high levels of Grb7 expression, none of the MMTV-MT mediated tumors overexpressed Grb7. This immunoblot strongly suggested

Figure 4.5 – Overexpression of ErbB2 in MMTV-MT Tumors

To determine whether MMTV-MT tumors overexpressed ErbB2, a series of MMTV-MT ErbB2$^{WT/Flox}$ MMTV-Cre mice were generated and tumors harvested. Four tumor samples were collected from each mouse at endpoint. The tumor samples are labelled 1-4 with sample 1 being the primary tumor while samples 2-3 were smaller tumors and sample 4 contained a hyperplastic mammary gland when possible. Protein from these various samples was harvested and levels of ErbB2 were assayed (A). A control from a conditionally activated NeuNT tumor was included as a positive control for ErbB2 overexpression. Clearly, the primary MT driven tumors overexpress ErbB2 while some samples from hyperplastic tissue or small tumors do not. However, unlike the conditionally activated NeuNT tumor, the MT mediated tumors do not overexpress Grb7 indicating that the *erbB2* allele is likely not amplified (B). Grb2 is shown as a loading control. To determine that the *erbB2* allele was not amplified, a Southern analysis examining the wild type and loxP flanked neu cDNA was conducted and clearly indicated that neither allele was amplified relative to the other allele (data not shown). Given the differences in ErbB2 levels in several of the tumor samples (1113 #2 vs. 1113 #4 and 0979 #1 vs. 0979 #4), the histological sections from these tumor samples were examined (1113#4 – C, 0979#4 – D, 1113#2 – E and 0979#1 – F). Strikingly, samples with low levels of ErbB2 (C, D) originated from hyperplastic mammary glands and the higher levels of ErbB2 were observed in the carcinomas (E, F). This data indicates that ErbB2 is overexpressed during the transition from hyperplasia to carcinoma.

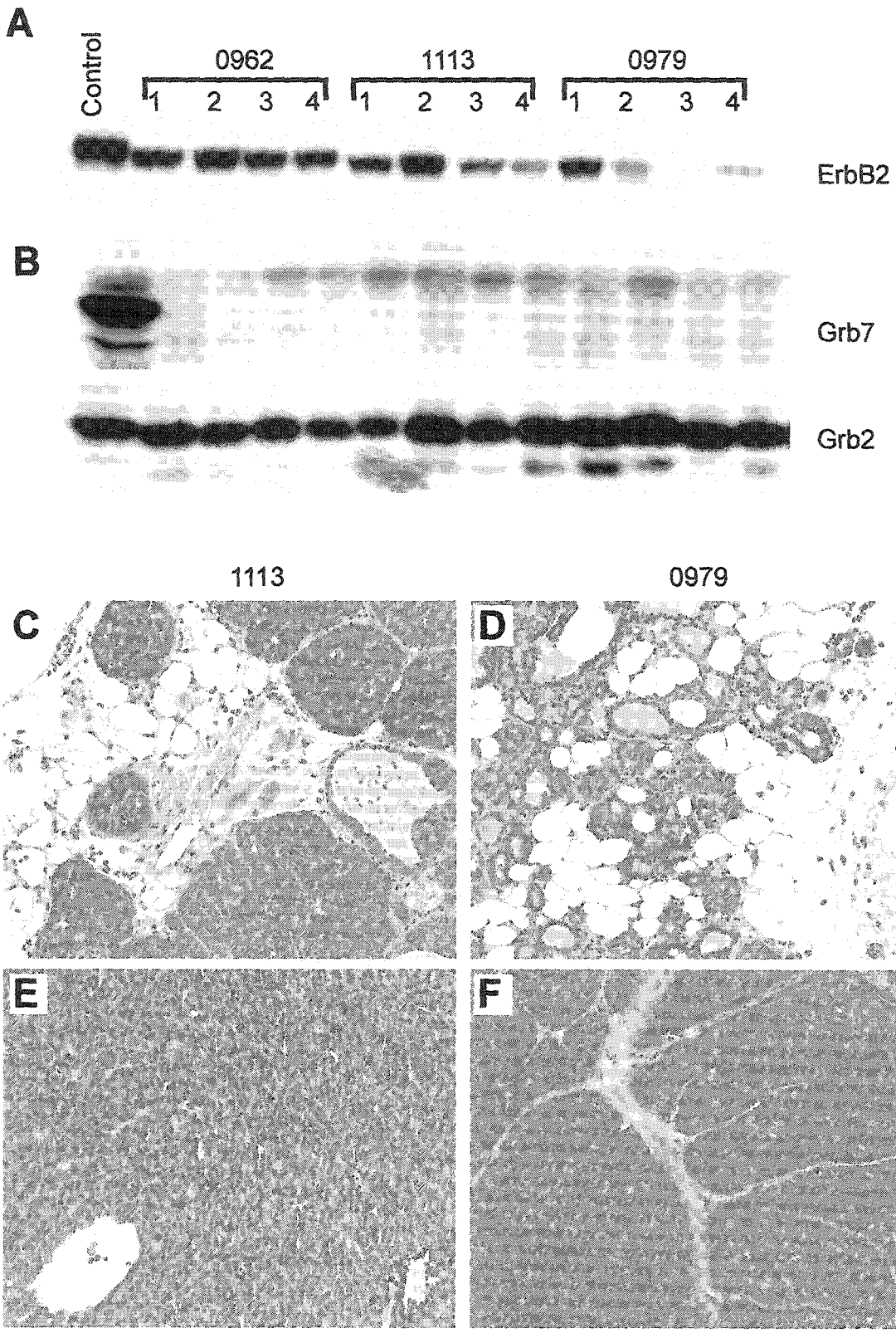
A
Control
0962
1113
0979
1 2 3 4 1 2 3 4 1 2 3 4
ErbB2
B
Grb7
Grb2
1113
0979
C
D
E
F

that *erbB2* was not amplified. To confirm that there was no amplification of the wild type or null allele, DNA was prepared from the tumors that were examined in the Western analysis that both did and did not show overexpression of ErbB2. This DNA was used in a Southern analysis as outlined in Chapter Three to examine amplification of *erbB2*. Consistent with the Grb7 expression results, there was no appreciable amplification of *erbB2* (data not shown). In order to investigate the difference between samples that had high or low levels of ErbB2 expression, the matched histology from the tissue sample was examined through hematoxylin and eosin staining. Samples with low levels of ErbB2 expression appear to have originated in early tumors or hyperplastic mammary tissue (Figure 4.5, Panels C and D). Conversely, high levels of ErbB2 expression correlated with tumor tissue (Figure 4.5, Panels E and F). Taken together, these data suggest that the overexpression of ErbB2 is associated with the shift from a hyperplasia to a tumor.

To test how the absence of ErbB2 would impact the transition from hyperplasia to tumor in MMTV-MT driven tumorigenesis, $ErbB2^{Flox/Flox}$ MMTV-Cre MMTV-MT mice were generated and were compared to $ErbB2^{Flox/WT}$ MMTV-Cre MMTV-MT mice. Tumor formation in these strains was assessed weekly by palpation and the results are illustrated in Figure 4.6. Strikingly, the ablation of ErbB2 in MT mediated tumors has increased the tumor latency by 16 days on average. Consistent with the MMTV-MT data (Guy *et al.*, 1992), mice containing at least one functional *erbB2* allele were seen to develop tumors with an average latency of 56 days in 50% of females. The targeted ablation of ErbB2 in the mammary gland of these MMTV-MT mice resulted in

Figure 4.6 – Lack of ErbB2 delays MMTV-MT mediated Tumorigenesis

By interbreeding the ErbB2$^{Flox/Flox}$ MMTV-Cre mice with the MMTV-MT transgenics we were able to examine MMTV-MT mediated tumorigenesis in mammary glands with and without ErbB2. The differences in tumor latency are shown (A). ErbB2$^{WT/Flox}$ MMTV-Cre MMTV-MT mice, which have one wild type erbB2 allele, develop tumors at the same rate as MMTV-MT mice (closed squares). In contrast, ErbB2$^{Flox/Flox}$ MMTV-Cre MMTV-MT mice develop tumors more slowly (open squares). Indeed, the entire curve on the Kaplan-Meier plot illustrates the delay in tumorigenesis, from time of detection of the first tumors to the time of detection of the tumors with the longest latency. Clearly, the absence of ErbB2 in the mammary gland delays MT mediated tumorigenesis.

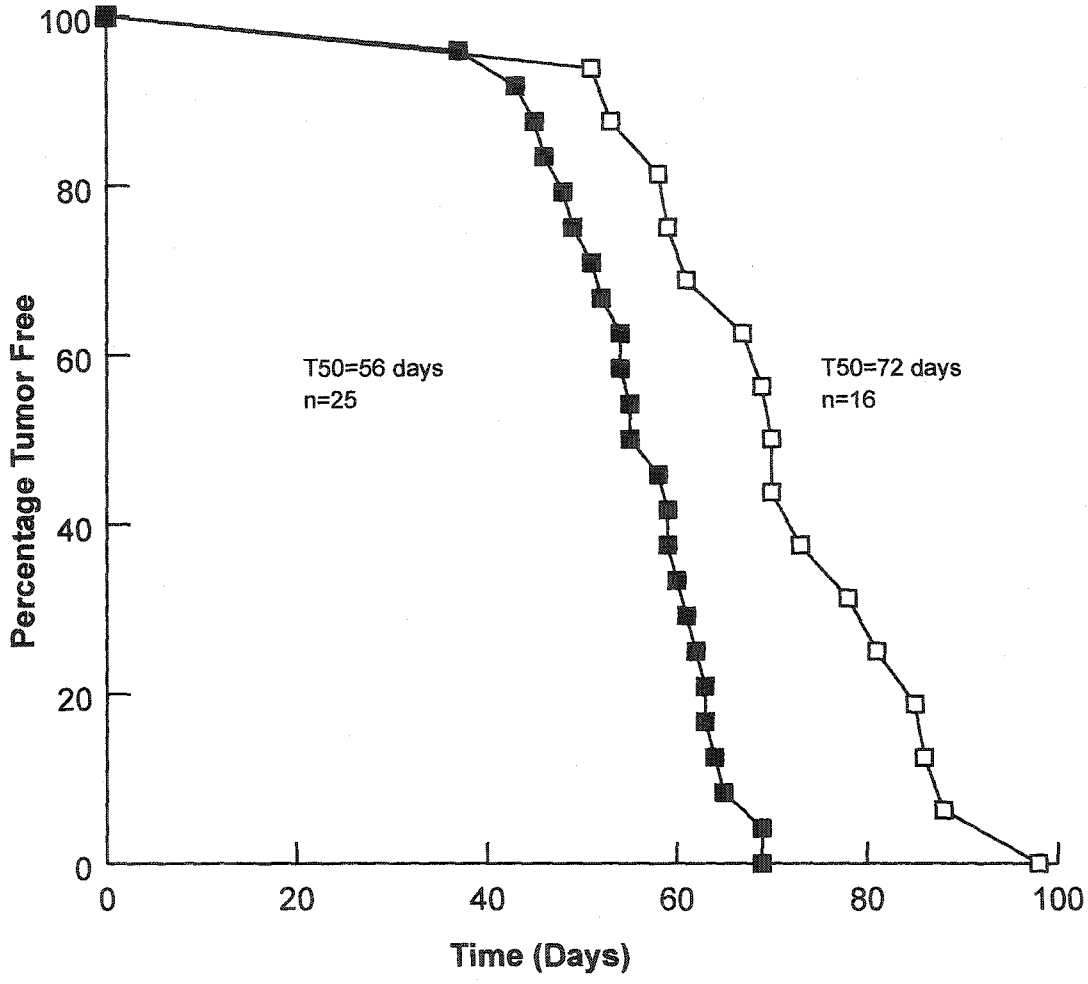

■ - MMTV-MT MMTV-Cre ErbB2$^{Flox/WT}$

□ - MMTV-MT MMTV-Cre ErbB2$^{Flox/Flox}$

tumorigenesis in 50% of female mice by 72 days. While there was a clear increase in tumor latency, the eventual tumor load borne by the mice was not noticeably different. Indeed, females from both lines developed multifocal mammary tumors in all of the mammary glands by the endpoint. The MT mediated tumors that developed in the mammary glands with and without the targeted ablation of ErbB2 contained no discernable histological differences (data not shown). Future investigations will be directed toward examining these tumors with various immunohistochemical markers to determine whether these tumors are distinct on the molecular level.

In addition to developing mammary carcinomas, the MMTV-MT mice have been established as an excellent model in which to examine pulmonary metastasis (Guy *et al.*, 1992). To determine whether the mammary specific ablation of *erbB2* would result in an inhibition of pulmonary metastasis, MMTV-MT tumor bearing mice with and without the ablation of *erbB2* were examined. A single lobe of the lung was assayed through standard hematoxylin and eosin staining in thin sections. The results of this assay are shown in Figure 4.7, Panels A-D. Mice with function ErbB2 were noted to have numerous small pulmonary metastases (Figure 4.7, Panel A). However, MMTV-MT mice with a conditional deletion of *erbB2* in the mammary gland were also seen to have numerous small metastases in the lung (Figure 4.7, Panel B). These metastases were examined at a higher magnification and were clearly seen to be established colonies within the lung and are not simply tumor emboli within vessels (Figure 4.7, Panels C and D). These results suggest that there are no differences in metastasis in the MMTV-MT mice with and without the targeted deletion of *erbB2*.

Figure 4.7 – Lack of ErbB2 has no Effect on Lung Metastasis

MMTV-MT tumors have been previously illustrated to develop pulmonary metastasis with complete penetrence. To determine whether the loss of ErbB2 resulted in a difference in the metastatic potential, the lungs from MMTV-MT induced tumors, with and without ErbB2, were compared at the endpoint. In the low magnification image from the control (A) and the conditional ablation of *erbB2* (B), a large number of tumor nests are clearly seen. At higher magnification, these areas were examined to determine whether the tumors were emboli within the vessels or whether the tumor cells had extravasated into the lungs. In both the control (C) and the conditional null samples (D), the tumors are clearly seen to colonizing in the pulmonary space and are not simply emboli.

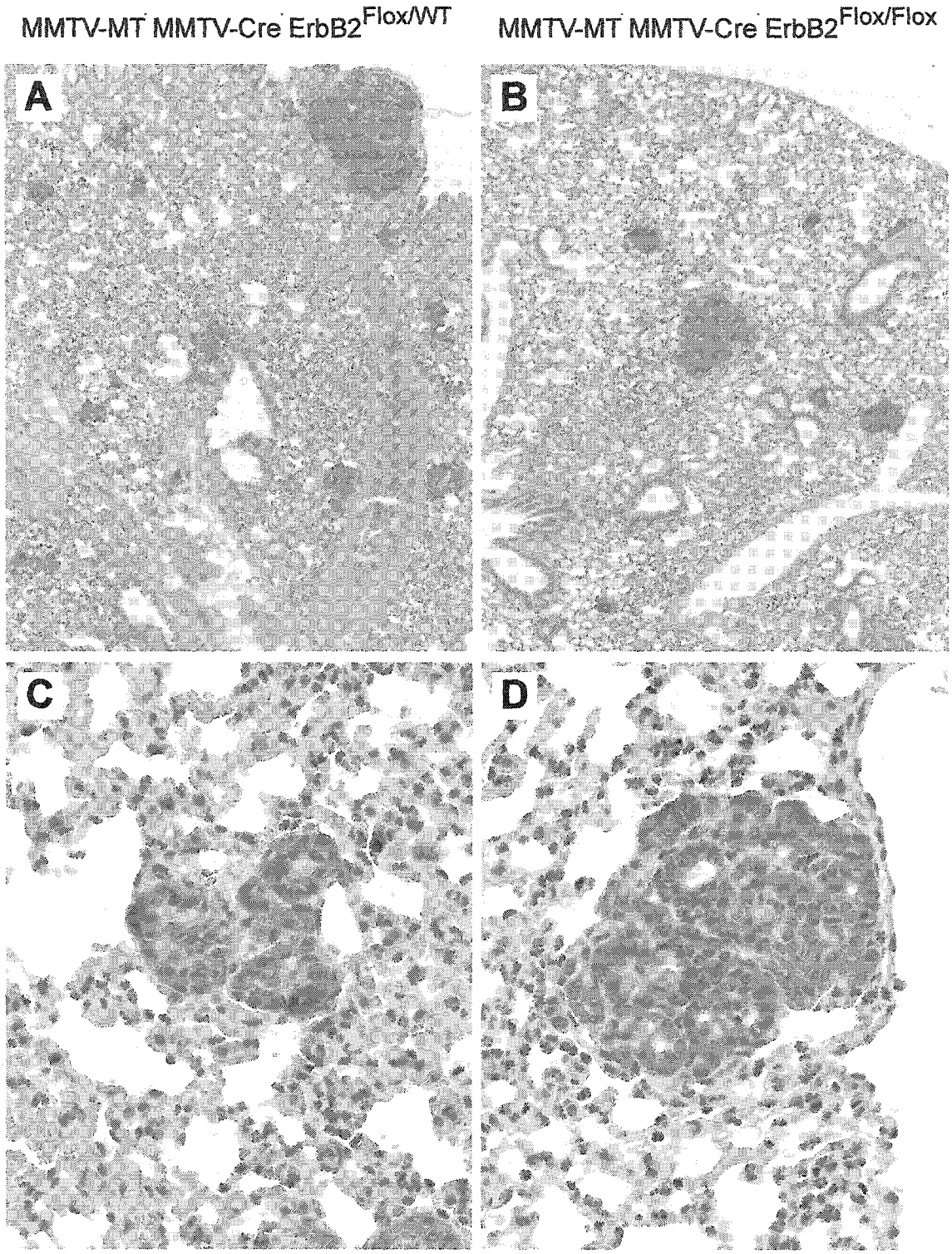
MMTV-MT MMTV-Cre ErbB2Flox/WT
MMTV-MT MMTV-Cre ErbB2Flox/Flox
A
B
C
D

While the latency of MT mediated tumor formation was increased with the conditional deletion of *erbB2*, to determine that the tumors that developed did indeed lack ErbB2 expression, a Western analysis was completed. Using controls for ErbB2 overexpression from conditionally activated ErbB2 mediated tumors and MMTV-MT driven tumors, ErbB2 overexpression was observed (Figure 4.8). Interestingly, in tumors from three ErbB2$^{Flox/Flox}$ MMTV-Cre MMTV-MT mice, ErbB2 was frequently expressed in the primary and secondary tumors at levels higher than the controls. After examination of 24 separate tumors expression of ErbB2 was noted in 70% of the samples at widely divergent levels. Taken together, these results indicate that the deletion of *erbB2* in the mammary gland is not complete, but does delay MT mediated tumorigenesis.

4.3 Discussion

Since ErbB2 is overexpressed and amplified in a large percentage of human mammary tumors, the role of ErbB2 in mammary gland development was examined in a mouse model. During this analysis, the first exon of the endogenous *erbB2* allele was replaced with a loxP flanked rat *neu* cDNA. Given the similarity of the sequence and the high homology of the proteins, it was not surprising that the knock-in was able to rescue the embryonic lethality associated with the germline ablation of *erbB2*. Indeed, the ErbB2$^{Flox/Flox}$ mice were indistinguishable from the wild type controls in all aspects of development. However, it was interesting that the levels of ErbB2 expression in the ErbB2$^{Flox/Flox}$ mice were only 10% of the level observed in the ErbB2$^{WT/WT}$ controls. This

Figure 4.8 – ErbB2 Overexpression in ErbB2$^{Flox/Flox}$ MMTV-Cre MMTV-MT Tumors

To determine whether the tumors that developed in the ErbB2$^{Flox/Flox}$ MMTV-Cre MMTV-MT mice had developed from a precursor population that lacked ErbB2, tumors were generated and examined. Four samples were collected from each mouse with tumors at the endpoint. The tumor samples are labelled 1-4 with sample 1 being the primary tumor while samples 2-3 were smaller tumors and sample 4 contained a hyperplastic mammary gland when possible. Protein from these various samples was collected and levels of ErbB2 were assayed by Western analysis. Controls for ErbB2 expression in both ErbB2 (TM15) and MT mediated tumors were included. Clearly there are several tumors that have high levels of ErbB2 overexpression in the the ErbB2$^{Flox/Flox}$ MMTV-Cre MMTV-MT mice.

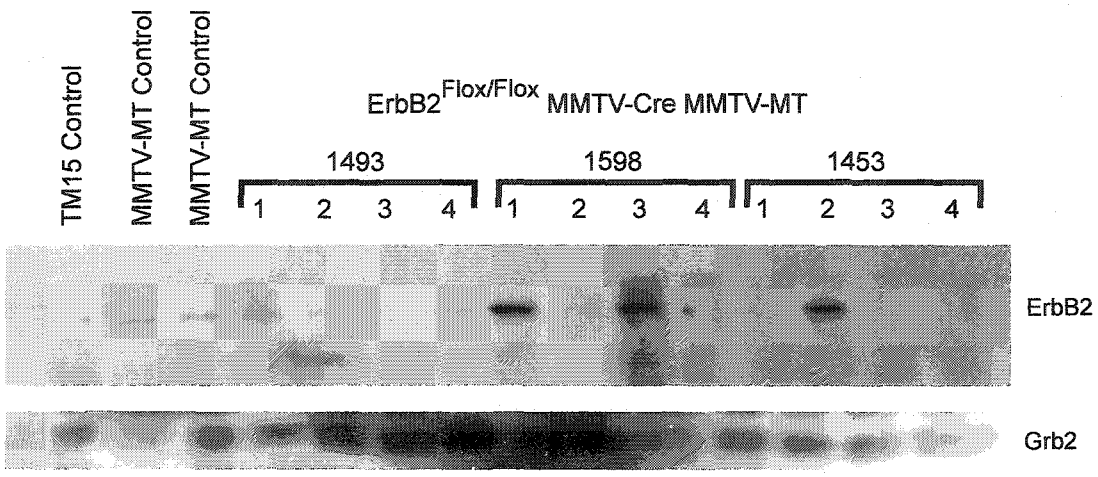
TM15 Control
MMTV-MT Control
MMTV-MT Control
ErbB2Flox/Flox MMTV-Cre MMTV-MT
1493
1598
1453
1 2 3 4 1 2 3 4 1 2 3 4
ErbB2
Grb2

was not unexpected given that other knock-in constructs using the same targeting sequence have previously been observed to have reduced levels of ErbB2 (Chan *et al.*, 2002). Indeed, it was observed that while the level of transcript was identical between wild type and knock-in samples, the level of ErbB2 was significantly reduced. This reduced level of protein can be explained by inefficient translocation of the mRNA since there were no splice donor or splice acceptor sites. However, it is important to note that while the level of ErbB2 was reduced, the mammary gland of these mice was indistinguishable from the wild type controls.

To determine the role of ErbB2 in mammary gland development, the $ErbB2^{Flox/Flox}$ mice were interbred with the MMTV-Cre transgenic mice. After subsequent matings the $ErbB2^{Flox/Flox}$ MMTV-Cre mice were obtained at the expected frequency, indicating that any inappropriate expression of the MMTV-Cre transgene in tissues such as the heart was not significant enough to induce the embryonic lethality observed in the germline ablation of ErbB2. Upon examination of the $ErbB2^{Flox/Flox}$ MMTV-Cre mammary gland for excision in a mixed background, excision was not detected. While the control illustrated that the loxP flanked allele was indeed functional and while previous results have shown the efficacy of the MMTV-Cre transgenic (See Chapter 3), I was unable to detect excision in numerous mammary glands from the $ErbB2^{Flox/Flox}$ MMTV-Cre mice. It has previously been shown that a single interbreeding into the Balb/c background can cause methylation of promoters driving transgene expression (Schweizer *et al.*, 1998) and the Balb/c background constituted 25% of the genetic background in the $ErbB2^{Flox/Flox}$ MMTV-Cre mice. Importantly, it has also been

shown that methylation of the MMTV promoter / enhancer silences the promoter activity (Zhou *et al.*, 2001). Therefore, it was not surprising that after interbreeding into a pure FVB background I was able to detect excision of the loxP flanked allele and the generation of a mammary specific *erbB2* null allele.

Upon examination of the ErbB2$^{Flox/Flox}$ MMTV-Cre mice, it was noted that the mammary specific ablation of *erbB2* resulted in a developmental delay in the outgrowth of the ductal network and in a reduction in lateral branching. While this is a striking result, it is consistent with previous data regarding the role of the EGFR family in ductal proliferation. For instance, the ductal network in ovariectimized mice implanted with EGF or TGFα pellets is re-induced to proliferate and forms TEBs (Coleman *et al.*, 1988; Snedeker *et al.*, 1991). However, given the ability of the EGFR family to heterodimerize and the lack of a defined ligand for ErbB2, the work presented in this chapter illustrates that the other EGFR family members cannot compensate for the loss of ErbB2 in maintaining normal ductal morphogenesis. Interestingly, this phenotype is manifested primarily during the course of hormone induced proliferation. Given the role of estrogen in elevating levels of EGF and TGFα, these results suggest that ErbB2 is an integral heterodimerization partner in the response to hormonally induced ductal extension and branching. While a developmental delay in the formation of the TEBs was noted, the TEBs eventually did appear suggesting that ablation of ErbB2 was not sufficient to inhibit TEB formation. Further, these results suggest that the other EGFR family members can compensate for ErbB2 loss, albeit with reduced effectiveness. It will be

interesting in the future to dissect which signaling pathways downstream of ErbB2 heterodimers are specifically required for the ductal outgrowth.

The examination of the conditional deletion of ErbB2 in comparison to the various controls revealed an effect only in the ErbB2$^{Flox/Flox}$ MMTV-Cre mice. Interestingly, this defect in mammary gland growth and branching was not seen even in the ErbB2$^{Flox/Flox}$ mice which were shown to have only 10% of the wild type ErbB2 levels. The further reduction in the level of ErbB2 in the mammary epithelial cells expressing Cre recombinase resulted in the phenotypic alterations. These results strongly suggest that there is a threshold level for ErbB2 expression required for normal mammary development. While the excision was not complete in the mammary gland, the phenotypic alterations seen in the ErbB2$^{Flox/Flox}$ MMTV-Cre mice have been mirrored in recent results from another laboratory where mammary buds from ErbB2 null mice were used to derive mammary glands that completely lack ErbB2 in recipient mice (A. Jackson-Fisher and D.F. Stern, Personal Communication). The complete ablation of ErbB2 in this manner did not appear to have any more profound effect on mammary gland development. The theory of a required threshold level for ErbB2 was also seen in additional experiments in other tissues from the ErbB2$^{Flox/Flox}$ mice (See Chapter 5) and clearly illustrates the importance of this gene in normal development and is discussed further in Chapter 6.

While there was a striking effect on ductal morphogenesis in the first 12 weeks of development, the ErbB2$^{Flox/Flox}$ MMTV-Cre mammary gland eventually was indistinguishable from the wild type controls. Indeed, even during pregnancy, lactation

and regression there were no striking differences observed between the wild type control and the conditional deletion of *erbB2*. Interestingly, this data conflicts with the transgenic dominant negative ErbB2 results, where mild defects were noted in lactation (Jones and Stern, 1999). Clearly the dominant negative ErbB2 is acting not only on the wild type ErbB2 but also on all other members of the EGFR family. When considered with the expression patterns of the EGFR family members, it is likely that the dominant negative is inhibiting ErbB4 since it is expressed at maximal levels in the late stages of pregnancy and the earliest stages of lactation. The results I have presented show that ErbB2 is not required for normal lactation or involution.

The previous results have aided in defining the role of ErbB2 in mammary gland development, however ErbB2 is also involved in mediating tumor progression. While amplification and overexpression of this gene plays a causal role in the etiology of breast cancer, ErbB2 has also implicated as part of the multistep pathway activated in other tumors. Mouse mammary tumors mediated by expression of Polyomavirus Middle T antigen under the control of the MMTV promoter were initially considered to be a model where very few additional steps were required to induce tumorigenesis (Guy *et al.*, 1992). However, although the MT mediated tumors develop with a remarkably short latency, it has become clear that several additional events are required for the rapid development of tumors. Indeed, I have shown here that ErbB2 is overexpressed in the MT mediated tumors but not in the hyperplasia. Consistent with this, others have shown in detail that ErbB2 is overexpressed during the transition from hyperplasia to tumor (Personal Communication with J. Pollard). However, in addition to documenting the

overexpression of ErbB2 in these tumors, I have also shown that *erbB2* is not amplified. These results suggest that there should then be a corresponding upregulation in transcription factors that are able to activate ErbB2 expression. One transcription factor that has been shown to regulate the level of *erbB2* is PEA3 (Xing *et al.*, 2000) and when inhibited through a dominant negative approach PEA3 extends the latency of MMTV-Neu mediated tumors (Shepherd *et al.*, 2001). Interestingly, PEA3 RNA levels have been shown to be dramatically elevated in MT mediated tumors but not in the adjacent tissue (Trimble *et al.*, 1993). In the future, it will be interesting to examine other transcription factors that are known to regulate ErbB2 levels to determine both how they are activated and whether they are involved in ErbB2 mediated tumorigenesis.

When the latency of MMTV-MT driven tumorigenesis was examined in mice that should be lacking ErbB2 expression in the mammary gland, it was noted that the latency had increased by over two weeks. However, multifocal mammary tumors did develop and the histological examination of the tumors failed to reveal any differences. Further, the rate of metastasis to the lung was unchanged and the resulting pulmonary metastases were indistinguishable. However, ErbB2 expression was detected in 70% of these MMTV-MT tumors that should lack ErbB2 expression. Since excision was clearly not complete in the ErbB2$^{Flox/Flox}$ MMTV-Cre mice, it is not surprising that an epithelial population retaining ErbB2 expression still exists in the mammary gland. Conversely, since MT and Cre recombinase expression is controlled by identical MMTV promoters, it stands to reason that all cells expressing MT should also be expressing Cre recombinase and should therefore contain a null *erbB2* allele. While these two promoters have two

separate sites of integration, Cre recombinase was shown to be expressed at high levels (See Chapter 3) and once excision occurs, the recombinant null allele will be passed on to all daughter cells. That a tumor can differentially express transgenes using identical promoters presents a paradox that is worthy of future investigation.

The increased latency of MT mediated tumorigenesis in mammary glands with a conditional ablation of *erbB2* is significant. However, the reduced latency can be attributed to a number of factors. Since the ErbB2$^{Flox/Flox}$ MMTV-Cre mice have mammary glands that are developmentally delayed and have a markedly reduced volume of epithelium in a ductal network compared to the controls at the same time points, it is apparent that the reduction in epithelium simply offers fewer cells that are susceptible to transformation. However, by simply reducing the number of cells that could be transformed, there may not necessarily be a delay in tumorigenesis. Indeed, when the wholemounts are compared, it can be seen that by 4 weeks of development the ErbB2$^{Flox/Flox}$ MMTV-Cre mice have already far surpassed the extent of outgrowth observed in the wild type controls only one week previously. Based on these results, a delay in tumor latency of over two weeks should not be expected. However, if this theory is then extended to a reduced population of mammary epithelial cells with even fewer cells expressing ErbB2, the target population of cells susceptible to tumorigenesis may now be depleted sufficiently to cause an increase in latency. Indeed, if these cells must also express the MT transgene but not the Cre transgene, the population of suitable tumorigenic precursor cells is greatly reduced. Thus, the relatively small increase in latency is surprising given the apparently strong selective pressure for ErbB2 expression

and a loss of Cre expression in MT mediated tumorigenesis. Taken together, these results suggest an integral role for ErbB2 in MT mediated tumorigenesis. In the future, it would be interesting to generate ErbB2$^{Flox/Flox}$ MMTV-MT cell lines, infect them with an adenovirus containing Cre recombinase and then implant these cells subcutaneously and in a cleared fat pad to determine whether the complete lack of ErbB2 would inhibit tumorigenesis or metastasis.

CHAPTER 5

THE ROLE OF ERBB2 IN SKELETAL MUSCLE DEVELOPMENT AND MAINTENANCE

5.1 Introduction

The importance of the various EGFR family members in the regulation of embryonic development has been well illustrated. For example, null mutations for *erbB2* or *erbB4* result in mice that suffer from cardiac and neural defects and succumb to embryonic lethality at day 10.5 of embryogenesis (Gassmann *et al.*, 1995; Lee *et al.*, 1995). While mice lacking *erbB3* also suffer from embryonic lethality, the cardiac defects are less severe than the defects in Schwann cell differentiation (Erickson *et al.*, 1997; Riethmacher *et al.*, 1997; Britsch *et al.*, 1998). Further, the knockout of the EGFR receptor results in perinatal lethality in a strain dependent manner (Threadgill *et al.*, 1995; Hansen *et al.*, 1997; Sibilia *et al.*, 1998). Clearly these receptor tyrosine kinases are an integral part of signaling during embryonic development.

The elucidation of role of the EGFR family in the maintenance and development of adult tissues has not been addressed due to the lethality observed in the various null mutant strains. To examine the importance of ErbB2 in various adult tissues, the Cre / LOXP1 recombinase system was previously employed. This method was used to generate peripheral a nerve specific deletion of *erbB2,* which resulted in extensive

neuronal demylination (Garratt *et al.*, 2000). However, in addition to expression in neural tissues, ErbB2 expression has been noted in skeletal muscle along with ErbB3 and ErbB4 (Altiok *et al.*, 1995; Moscoso *et al.*, 1995; Zhu *et al.*, 1995). Expression of an ErbB3 ligand, NRG, has also been noted in the skeletal muscle (Moscoso *et al.*, 1995). While the importance of these genes in muscle development and maintenance is not known, NRG mediated ErbB2/ErbB3 heterodimers can stimulate the phosphadityl inositol 3′ kinase (PI-3′K) cell survival pathway (Tansey *et al.*, 1996). Stimulation of this pathway has been implicated in the activation of a number of important cell survival elements including Akt serine kinase (Kita *et al.*, 1994; Soltoff *et al.*, 1994; Burgering and Coffer, 1995; Franke *et al.*, 1995). The results suggest an important role for the EGFR family, however, the precise roles of the individual family members in muscle physiology have not been previously elucidated.

To address the functional significance of ErbB2 in muscle development and maintenance, a muscle specific ablation of *erbB2* in adult skeletal muscle using mice expressing Cre Recombinase under the control of the muscle creatine kinase (Mck) (Bruning *et al.*, 1998; Zisman *et al.*, 2000) promoter enhancer allowed the role of *erbB2* to be examined. Strikingly, mice lacking ErbB2 in skeletal muscle had proprioception defects visible during rest and in their normal gait. Interestingly, mice with a conditional deletion of *erbB2* lacked muscle spindles. ErbB2 was also shown to be expressed in the region of the muscle spindle that was heavily innervated. While the wild type and conditional null muscle was histologically quite similar, the muscle specific ablation of *erbB2* correlated with an induction of apoptosis in myoblasts upon differentiation to

myofibers. These results correlate with the observation of a reduced regenerative capacity of muscle lacking ErbB2 *in vivo*. Conceivably, the increased apoptotic death that is noted in the ErbB2 null myoblasts following induction of differentiation could result from the inefficient activation of PI-3K Akt signaling cascade or MAPK activity. These results illustrate a dual role for ErbB2 in signaling and survival during myoblast differentiation and for maintenance of muscle spindles.

5.2 Results

5.2.1 Proprioception Defects Due to Loss of Muscle Spindles in Muscle Specific ErbB2 Null Mice

The generation of mice lacking ErbB2 expression in skeletal muscle was accomplished by interbreeding the ErbB2$^{Flox/Flox}$ mice (See Chapter 4) with mice expressing Cre Recombinase under the control of the Muscle Creatine Kinase (MCK-Cre) promoter (Bruning *et al.*, 1998; Zisman *et al.*, 2000). This interbreeding theoretically should cause the generation of a null allele for *erbB2* specifically in the skeletal muscle (Figure 5.1, Panel A). In a Southern analysis using a portion of the *neomycin* cDNA as a probe, there is a predicted shift in size from 10 kb for the ErbB2$^{Flox/Flox}$ allele to 6 kb for the targeted null allele. A Southern analysis from various tissues in an adult ErbB2$^{Flox/Flox}$ MCK-Cre mouse illustrated that excision is limited to the cardiac tissue and the skeletal muscle (Figure 5.1, Panel B). In these ErbB2$^{Flox/Flox}$ MCK-

Figure 5.1 – Muscle Specific Excision in ErbB2$^{Flox/Flox}$ MCK-Cre Mice

To determine the role of ErbB2 in muscle development and regeneration the ErbB2$^{Flox/Flox}$ mice were interbred with MCK-Cre transgenic mice. The schematic representation of the recombinant allele before and after MCK-Cre mediated excision is shown. Further, the size of bands detected in a Southern analysis after a HindIII digest using a portion of the neomycin allele as a probe are shown (A). In a survey of various tissues, the unexcised allele at 10 kb is readily observed (B). However, in both the heart and the muscle the presence of the null allele at 6 kb is also observed.

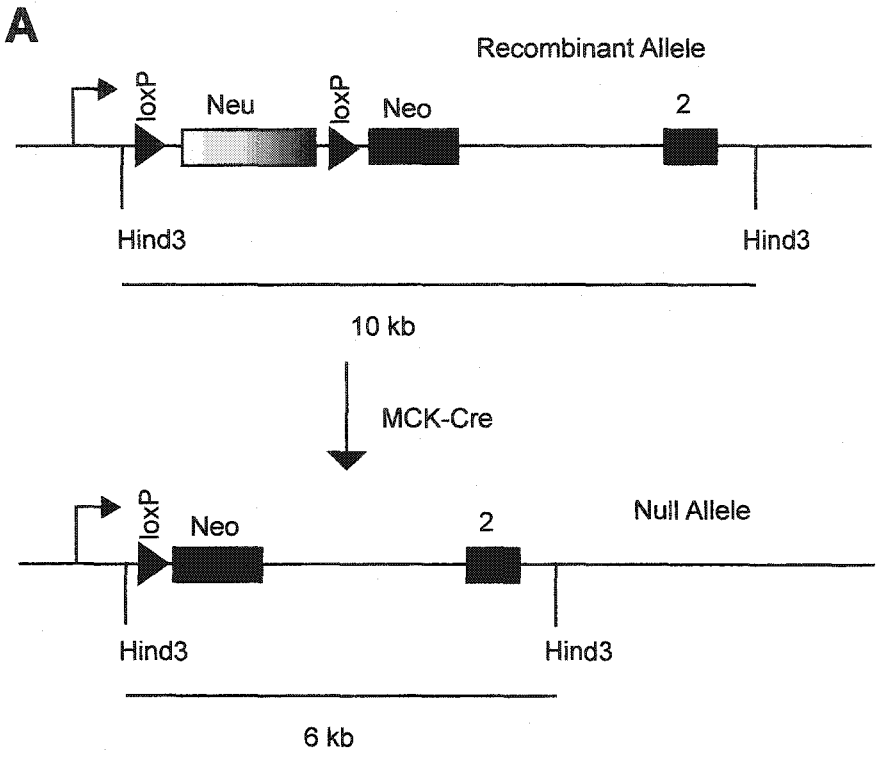
A
Recombinant Allele
loxP
Neu
loxP
Neo
2
Hind3
Hind3
10 kb
MCK-Cre
loxP
Neo
2
Null Allele
Hind3
Hind3
6 kb

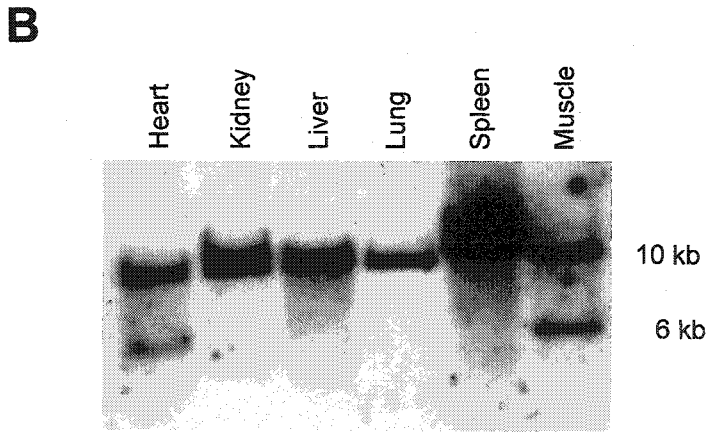
B
Heart
Kidney
Liver
Lung
Spleen
Muscle
10 kb
6 kb

Cre mice, the development and maintenance of the skeletal muscle will now occur in the absence of ErbB2. However, the excision that was detected was not complete as the 10 kb band for the ErbB2$^{Flox/Flox}$ allele is still readily visible (Figure 5.1, Panel B). Excision was then examined in numerous additional mice (Figure 5.2, Panel A). The Southern analysis was completed on pooled hind limb muscle and eight samples are shown. Additionally an ErbB2$^{Flox/Flox}$ control and a K-In / Flox K-Out sample are shown to illustrate no excision and excision that is 50% complete respectively. The K-In / Flox K-Out control has one recombinant Knock-In allele at 10 kb and has one Flox Knock-Out allele where excision is complete at 6 kb from an embryonic control (sample kindly provided by R. Chan). Lanes 3-10 clearly indicate that excision is not complete in any samples from pooled hindlimb muscle. Further, the degree of the phenotype in these mice is variable but it should also be noted that extent of excision did not correlate with severity of the phenotype (Lanes 3-6 vs. 7-10). Quantification by phosphoimager analysis revealed that the extent of excision ranged between 30 and 40% complete in these various samples. Since the skeletal muscle is not simply composed of differentiated muscle fibers, it is conceivable that a portion of the unexcised product originated in cells that were not part of the muscle lineage. To examine whether excision was complete in a pure culture of muscle cells, myoblasts were cultured from various ErbB2$^{Flox/Flox}$ MCK-Cre mice. The myoblast cell lines represent muscle cells that have not yet undergone differentiation and fusion and have not yet expressed MCK-Cre. According, excision was not expected to be observed in the undifferentiated cell lines. However, during the process of differentiating the myoblast cells to fused myofibers, the MCK promoter is

Figure 5.2 – Extent of Excision in ErbB2Flox/Flox MCK-Cre Muscle and Myotubes

To determine the whether the incomplete excision in the muscle observed previously (Figure 5.1), muscle from several mice was examined for the extent of excision (A). While the controls show an absence of excision (lane 1) and 50% excision (lane 2), the remainder of samples exhibiting a range of phenotypes have comparable excision that remains incomplete. By phosphoimager analysis, the extent of excision averages at approximately 30%. Given the presence of other cell types within muscle not expressing the MCK transgene, we determined the extent of excision in a pure culture of myoblasts derived from ErbB2Flox/Flox MCK-Cre mice (B). Myoblasts are precursors to multinucleated myotubes in vitro and do not express MCK until they are differentiated through a change in the culture conditions. At the 36 hour point of differentiation from myoblasts to myotubes, MCK begins to be expressed. The presence of the MCK-Cre transgene should then cause the excision of the loxP flanked erbB2 allele. Comparing Panel B Lanes 1 and 4 it is clear that by 48 hours in differentiation media, the MCK-Cre transgene has been expressed and is causing the excision of erbB2. However, by day 6 of differentiation, excision remains incomplete. D – Day of Differentiation, measured at day 0 (D0) to day 6 (D6).

A

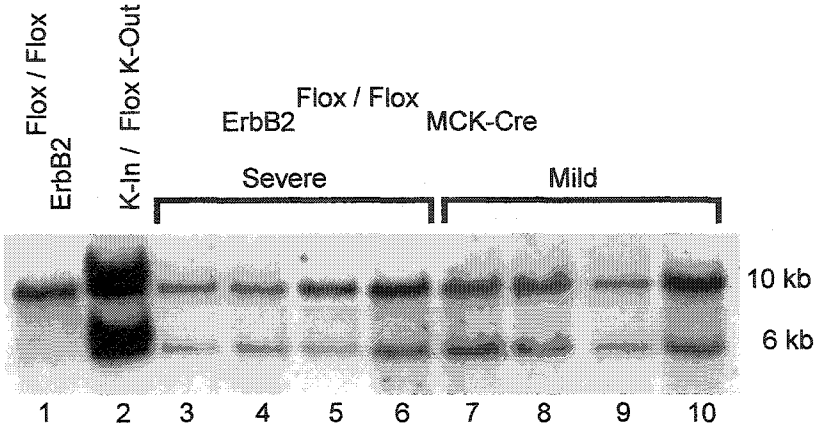
Flox / Flox
ErbB2
K-In / Flox K-Out
Flox / Flox
ErbB2
MCK-Cre
Severe
Mild
10 kb
6 kb
1 2 3 4 5 6 7 8 9 10

B

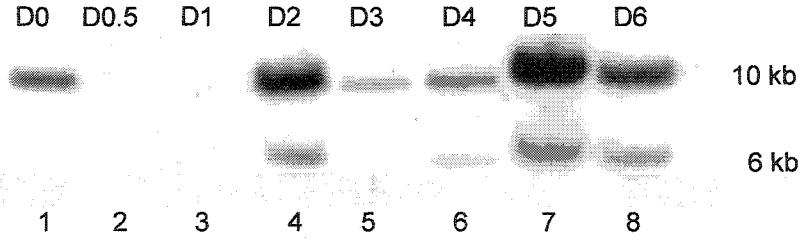
D0 D0.5 D1 D2 D3 D4 D5 D6
10 kb
6 kb
1 2 3 4 5 6 7 8

normally active between 36 and 48 hours (Chamberlain *et al.*, 1985; Jaynes *et al.*, 1986). Thus, excision should be complete 3 days following the initiation of differentiation. To examine this hypothesis, the myoblast cell lines from the ErbB2$^{Flox/Flox}$ MCK-Cre mice were allowed to differentiate and DNA was harvested at various days of differentiation (Figure 5.2 Panel B, D0 to D6). As expected, the Southern blot reveals that excision has not occurred without differentiation (Lane 1). Further, the expected induction of MCK expression does result in the observation of excision by 48 hours of differentiation (Lane 4). However, excision remains incomplete even after six days of differentiation when the cell lines have terminally differentiated. The terminal differentiation at this point was assessed by visual examination of the multinucleated myofibers. This analysis was conducted in three cell lines from three separate ErbB2$^{Flox/Flox}$ MCK-Cre mice. The extent of excision shown in Figure 5.2 Panel B was consistent for all three cell lines (data not shown).

Despite the moderate levels of excision observed in both myoblast cell lines and in the pooled hindlimb muscle from the ErbB2$^{Flox/Flox}$ MCK-Cre mice, approximately 50% of susceptible mice from the initial cross exhibited a significant loss of motor coordination by two to three months of age. These mice also displayed an altered gait and often maintained their limbs in an abnormal posture. Over time, the abnormal posture changed from a flexor to an extensor posture in these severely affected mice. The altered gait was examined in mice with a flexor posture by dipping the hind limbs into India Ink and allowing the mice to walk across a sheet of blotting paper to leave a record of their track. In contrast to the wild type control (Figure 5.3, Panel A), the ErbB2$^{Flox/Flox}$

Figure 5.3 – Phenotypic Effects of a Muscle Specific Ablation of ErbB2

A comparison of ErbB2$^{Flox/Flox}$ MCK-Cre and wild type controls revealed that there was an altered gait and posture in the conditional deletion of ErbB2. The hindlimbs of a wild type mouse (A) and an ErbB2$^{Flox/Flox}$ MCK-Cre mouse (B) were immersed in India Ink and the mouse was permitted to move down a corridor on a sheet of blotting paper. The mice were moving from left to right across the sample area in a normal gait. For the wild type mouse it is clear from the track that only the footpad was in contact with the surface that it moved across. The track from a ErbB2$^{Flox/Flox}$ MCK-Cre mouse as it moves across the blotting paper reveals several distinct differences. In addition to the footpad coming in contact with the surface the mouse was traversing, a large region of the leg also was in contact due to incomplete extension of the leg during movement (closed arrow). Additionally, due to abnormal weight bearing on the hocks, the toes are turned in during movement, resulting in the pigeon-toed track (open arrow). These alterations in the gait appear to be due to a lack of complete extension of the hindlimbs during movement. In addition to the altered gait, the Mck/Cre ErbB2$^{Flox/Flox}$ mice have an abnormal posture at rest. In comparison to wild type (C) and ErbB2$^{Flox/Flox}$ controls, the severely affected ErbB2$^{Flox/Flox}$ Mck/Cre mice (D) suffer from an extensor posture, extending their limbs and resting upon the abdomen.

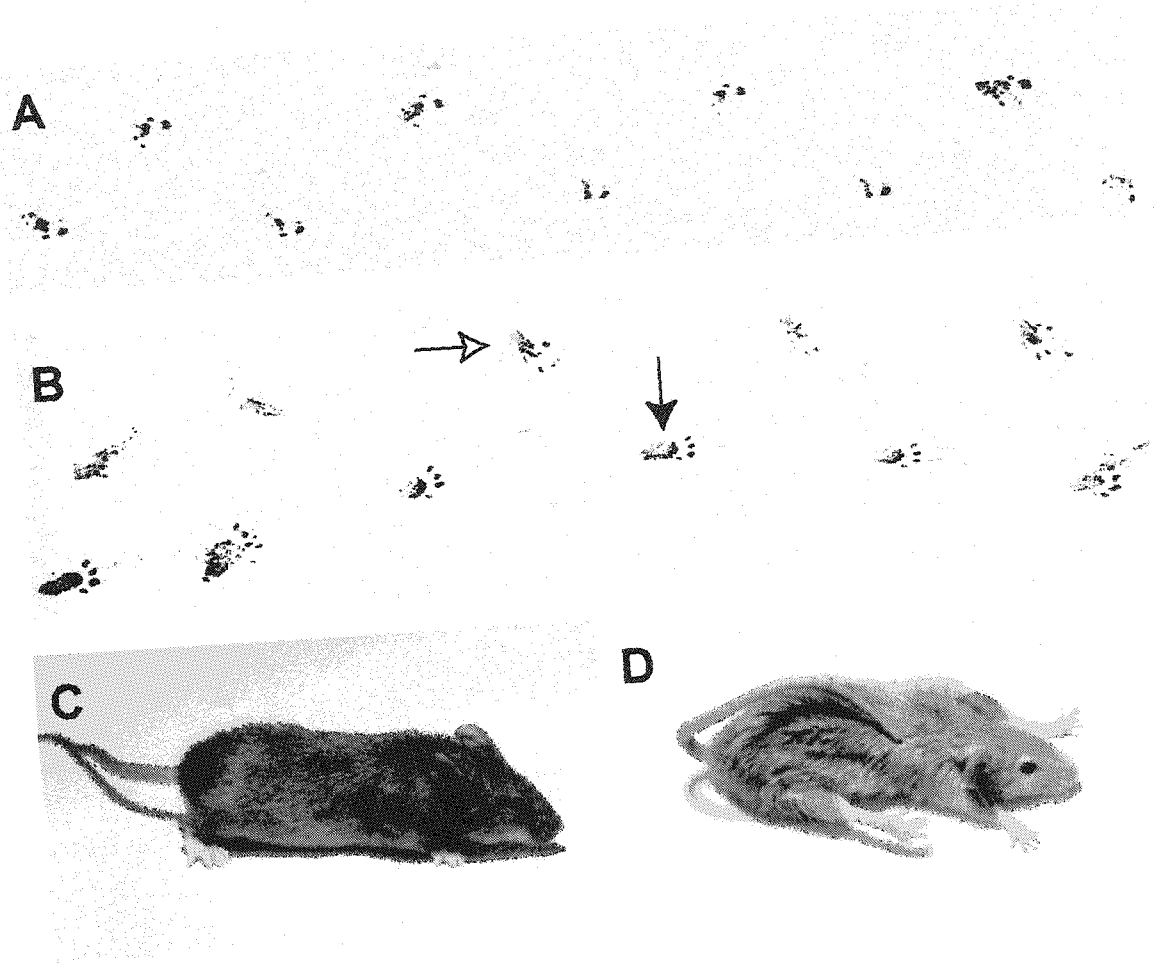
A
B
C
D

MCK-Cre mice (Figure 5.3, Panel B) exhibited several abnormalities in their gait. While both the wild type control and mutant footprints are both evenly spaced, the amount of leg coming in contact with the surface clearly differs. While controls only placed their footpad on the surface, the ErbB2$^{Flox/Flox}$ MCK-Cre track revealed that the portion of the hind limb from the knee to the footpad was coming into contact with the surface the mice were moving across (Figure 5.3, B, Solid Arrow). Further, since the hind limbs were being maintained in a flexor posture and a large portion of the weight was being borne on the hocks, the hindlimbs of the ErbB2$^{Flox/Flox}$ MCK-Cre mice were rotated medially resulting in what appears as a pigeon toed track (Figure 5.3, B, Open Arrow). As these affected mice aged, the phenotype progressed from maintaining the limbs in a flexor posture to an extensor posture. Age matched control and mice with a conditional deletion of ErbB2 in the skeletal muscle are shown (Figure 5.3, Panels C and D). In comparison to the wild type, the ErbB2$^{Flox/Flox}$ MCK-Cre mouse has clearly extended the limbs and is resting upon the abdomen. In addition to the motor control and posture abnormalities there are several other phenotypic effects that likely stem from these conditions. The ErbB2$^{Flox/Flox}$ MCK-Cre mice often suffer from malocclusions, poor body condition and wasting which sporadically results in early mortality. Aggressive care and frequent treatment for malocclusions reduced the poor body condition and early mortality.

As discussed above, the phenotype was only 50% penetrent in the initial crosses. However, since the initial interbreeding was conducted on a mixed background, the affected mice were interbred and an 80% penetrence of the phenotype was observed. The efforts to obtain full penetrence were likely hampered by an inability of the severely

affected mice to breed. Backcrossing the mice onto a pure FVB background also revealed a similar penetrence of the phenotype in the initial crosses. Thus, the variable penetrence of the phenotype is likely due to various genetic modifiers inherent in the background of these mice.

To explore the physiology behind the gait and posture abnormalities, the muscle was examined through histological methods. Given the similarity of the phenotype to previously reported phenotypes in mice lacking muscle spindles in various null backgrounds (Ernfors *et al.*, 1994; Klein *et al.*, 1994; Tourtellotte and Milbrandt, 1998), we examined the muscle spindles in the wild type, ErbB2$^{Flox/Flox}$, and ErbB2$^{Flox/Flox}$ MCK-Cre mice through urea silver nitrate staining. This nonselective silver stain is preferentially taken up by the annulospirial endings in the equatorial region of the muscle spindle and is an established method for detecting and examining muscle spindles. While muscle spindles were detected in the wild type controls (Figure 5.4, Panel A and B), they were not detected in the mice harboring a conditional deletion of ErbB2 in skeletal muscle. Although the muscle spindles were not detected in the ErbB2$^{Flox/Flox}$ MCK-Cre mice, the other expected neuronal structures were present in the muscle (Figure 5.4, Panel C) indicating that the staining procedure was functional. Interestingly, initial observations through standard hematoxylin and eosin staining revealed that the ErbB2$^{Flox/Flox}$ mice had far fewer muscle spindles than expected. Since the urea silver nitrate stain in serial sections in a rapid and accurate approach to quantify the number of muscle spindles in a given muscle (Butler and Payk, 1986), this was examined in greater detail. Thick serial sections were cut through the entire EDL muscle from ErbB2$^{WT/WT}$,

Figure 5.4 – Muscle Spindles are Dependent on ErbB2 expression.

Logitudinal thick sections of the EDL muscle were examined for the presence of muscle spindles through urea-silver nitrate staining. Muscle spindles were easily detected in wild type muscle (A) since the non-selective silver stain is preferentially taken up by the neurons. The smaller diameter muscle fibers are surrounded by neurons in a corkscrew nature at the equatorial region of the intrafusal muscle fibers as shown in panel A and B. Moving distal to the equatorial region, the neurons become aligned with the encapsulated muscle fibers. While the muscle spindles were readily observed in EDL from the wild type mice, no muscle spindles were detected in serial sections through the entire EDL muscle in $ErbB2^{Flox/Flox}$ Mck/Cre mice. However, the normal motor innervation was readily detected in this strain. Interestingly, it was also difficult to detect muscle spindles in the EDL from $ErbB2^{Flox/Flox}$ mice.

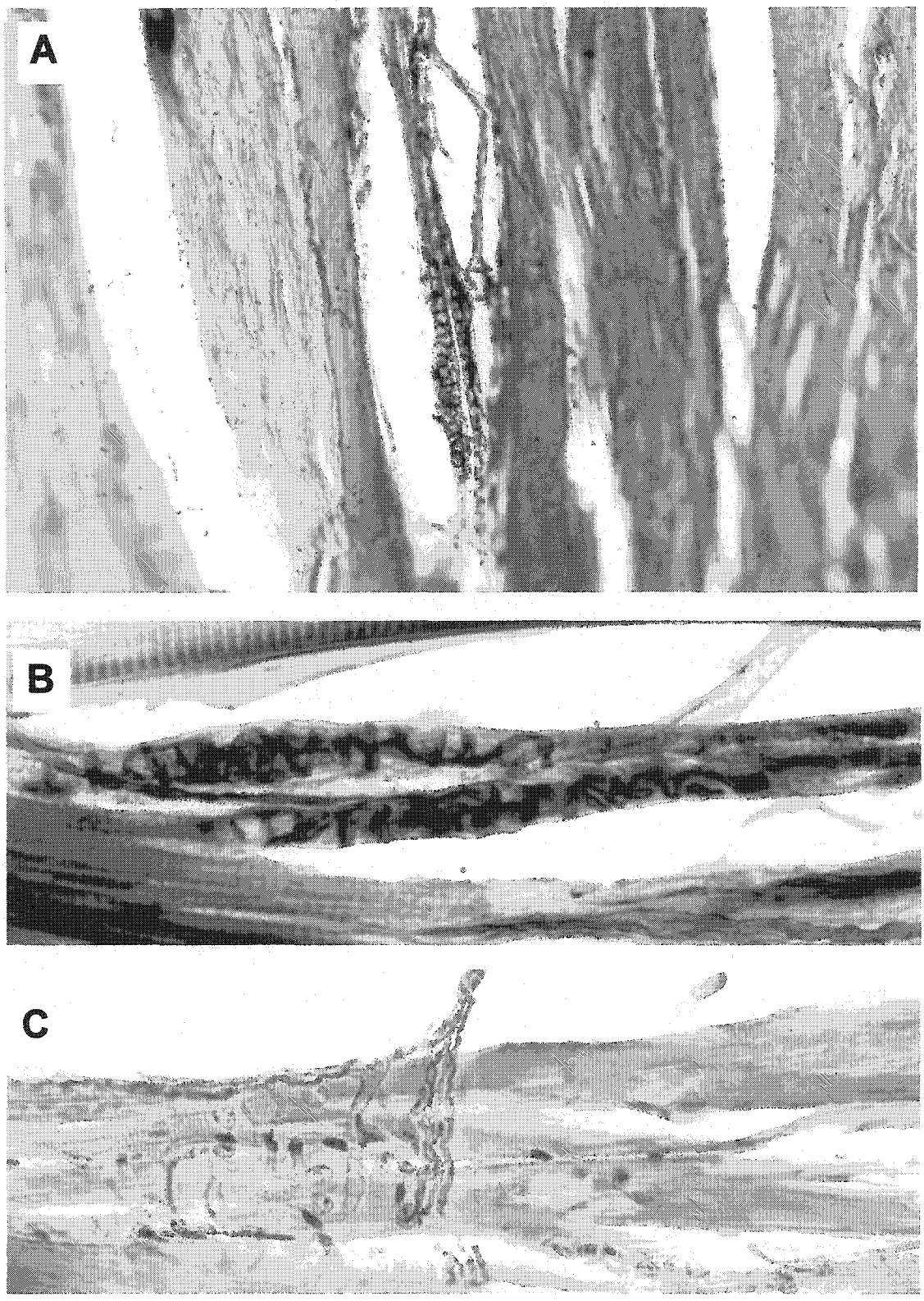
A
B
C

ErbB2$^{Flox/Flox}$, and ErbB2$^{Flox/Flox}$ MCK-Cre mice. After urea silver nitrate staining the serial sections were examined for the presence of muscle spindles and the number was recorded for each genotype (n=6 for each). On average there were approximately 11 spindles in the EDL muscle of a wild type mouse (Figure 5.5). This analysis also confirmed the observation that there were no muscle spindles in the EDL muscle of the ErbB2$^{Flox/Flox}$ MCK-Cre mice. Interestingly, the ErbB2$^{Flox/Flox}$ mice had a reduced number of muscle spindles with an average of 2.3 per EDL muscle. After close observation, although the ErbB2$^{Flox/Flox}$ mice have a reduced number of muscle spindles, they do not appear to suffer from any defects in gait or proprioception and are indistinguishable from the wild type controls.

The absence of muscle spindles in mice with a muscle specific excision of erbB2 raised the question of where ErbB2 was expressed in the muscle spindle. Previously published data examining the expression pattern of ErbB2 in skeletal muscle has not examined ErbB2 and muscle spindles. Accordingly, serial cross sections were cut across a wild type tibealis anterior (TA) muscle and the expression of ErbB2 was examined in the equatorial (Figure 5.6, Panels A-C) and the distal region (Figure 5.6, Panels D-F) of the muscle spindles. Standard hematoxylin and eosin staining reveals the structural differences between the equatorial and distal regions of the muscle spindle (Figure 5.6 Panel A vs. D). Immunohistochemistry in adjacent sections revealed ErbB2 expression in the equatorial region. Specifically, the muscle spindle in the equatorial region showed expression of ErbB2 in the intrafusal muscle fibers, the capsule surrounding these fibers and in the associated neural structures. Interestingly, when the distal region was

Figure 5.5 – Enumeration of Muscle Spindles in Wild Type and ErbB2 Null Muscle

The number of spindles in serial sections through EDL muscles from $ErbB2^{WT/WT}$, $ErbB2^{Flox/Flox}$ and $ErbB2^{Flox/Flox}$ MCK-Cre mice were counted. The result of the spindle enumeration is shown. Strikingly, the number of spindles observed in $ErbB2^{Flox/Flox}$ mice was significantly reduced when compared to wild type, although no phenotypic effects were visible in these mice. The further reduction in ErbB2 levels in $ErbB2^{Flox/Flox}$ MCK-Cre mice correlated with a complete loss of spindles and the associated proprioreception defects as previously described.

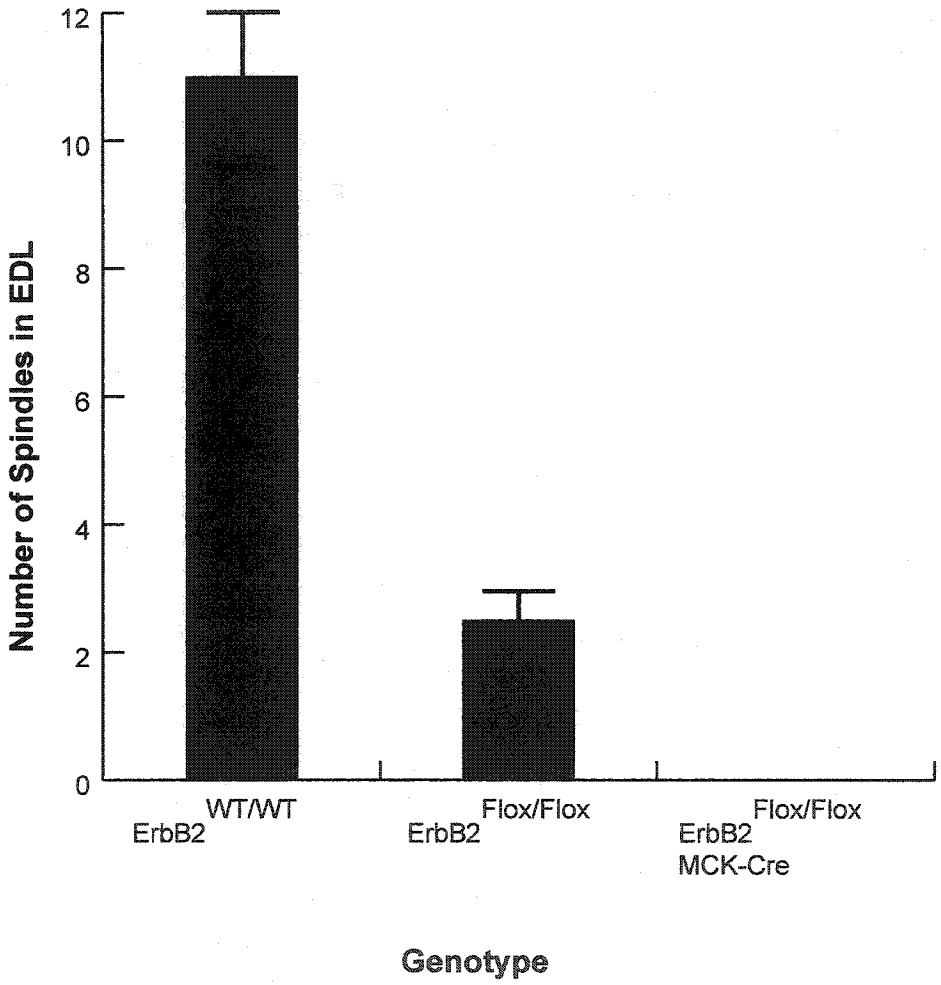
12
10
8
6
4
2
0
Number of Spindles in EDL
WT/WT
ErbB2
Flox/Flox
ErbB2
Flox/Flox
ErbB2
MCK-Cre
Genotype

Figure 5.6 – ErbB2 is expressed in the Intrafusal Muscle Fibers in the Equatorial Region of the Muscle Spindle

To determine whether ErbB2 was expressed in the muscle spindle, serial sections were cut containing a muscle spindle from a wild type control. Standard hematoxylin and eosin staining revealed the expected structural differences in the equatorial region (A) and the distal region (D) of the muscle spindle. Panel A illustrates the structure of the muscle spindle in cross section. The muscle spindle is composed of the neuron (Letter N), and a capsule (Letter C) surrounding several intrafusal muscle fibers (Letters IF) which are much smaller in diameter than the extrafusal muscle fibers (Letters EF) that constitute the major portion of the muscle. Immunohistochemistry for ErbB2 in adjacent sections both with (B, E) and without (C, F) the primary antibody revealed a distinct staining pattern. Strikingly, ErbB2 is localized to the intrafusal muscle fibers, the capsule surrounding the fibers and in the associated neural structures in the equatorial region (B). In the distal portion of the muscle spindle, the capsule and neural structures stain weakly. Clearly, ErbB2 is expressed at high levels in the muscle where there is extensive innervation.

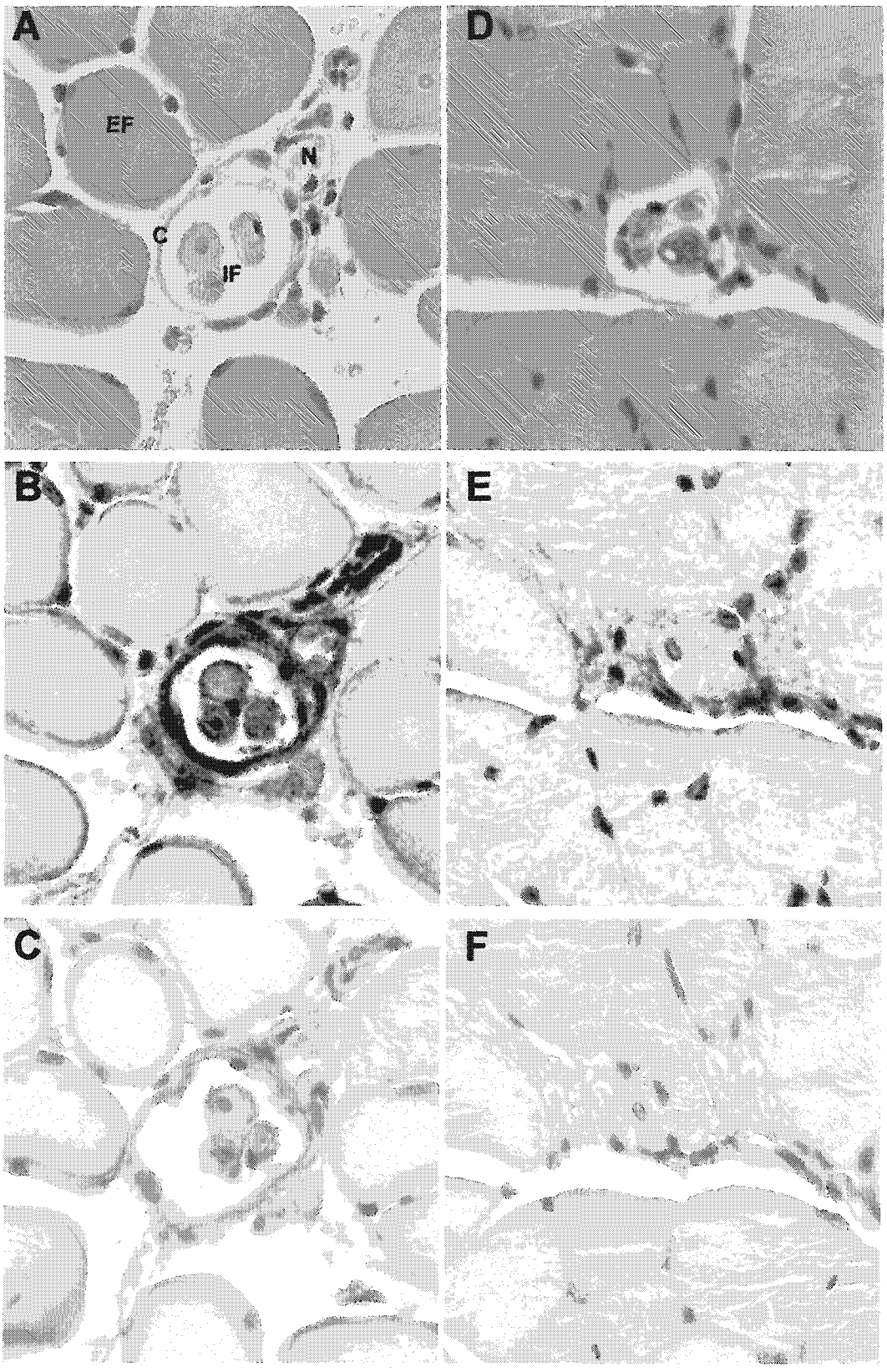
A
EF
N
C
IF
D
B
E
C
F

compared to this staining at the equatorial region, it was noted that the staining was far less intense and was not noted in the intrafusal muscle fibers. Clearly, ErbB2 is localized in the muscle spindles to the areas surrounded by the annulospirial neural endings and the elimination of ErbB2 in this region causes the loss of the entire structure.

5.2.2 Reduced Regenerative Capacity of Muscle Lacking ErbB2

The expression pattern of ErbB2 has previously indicated that there are low levels of ErbB2 expression throughout the extrafusal muscle fibers. To examine the skeletal muscle in detail for phenotypic effects, cross sections of the TA muscle were prepared. Other than the absence of muscle spindles as previously discussed, the wild type (Figure 5.7, Panel A) is essentially indistinguishable from the ErbB2$^{Flox/Flox}$ MCK-Cre TA muscle (Figure 5.7, Panel B). It should be noted that there are not a high number of centrally located nuclei in either sample and that the fibers appear to be similar in diameter. To further examine the role of ErbB2 in muscle development, myoblast cell lines were prepared from wild type and ErbB2$^{Flox/Flox}$ controls as well as the ErbB2$^{Flox/Flox}$ MCK-Cre mice. These myoblast cell lines exhibited similar morphology and growth kinetics. However, upon differentiation to myofibers it was noted that there was still reduced expression of ErbB2 in cell lines prepared from ErbB2$^{Flox/Flox}$ MCK-Cre mice (data not shown). To examine myoblast differentiation in the complete absence of ErbB2, wild type, ErbB2$^{Flox/Flox}$ and ErbB2$^{Flox/Flox}$ MCK-Cre (Aff2) cell lines were infected with a recombinant adenovirus expressing Cre recombinase. As a control for effects induced by the recombinant adenovirus infection, ErbB2$^{Flox/Flox}$ myoblast cell lines were subject to a

Figure 5.7 – Histological Similarity in ErbB2$^{WT/WT}$ and Mck/Cre ErbB2$^{Flox/Flox}$ Mice

A cross section of Tibealis Anterior muscle reveals the presence of numerous muscle spindle cells in the wild type controls (A, arrows). However, these muscle spindles were not observed in serial sections of Mck-Cre ErbB2$^{Flox/Flox}$ mice (B). Of note, in all other aspects there are no discernable differences between histology of wild type and condition null muscle (A vs. B). The diameter of the extrafusal muscle fibers is similar for the two samples and there are not a high number of centrally located nuclei in either sample.

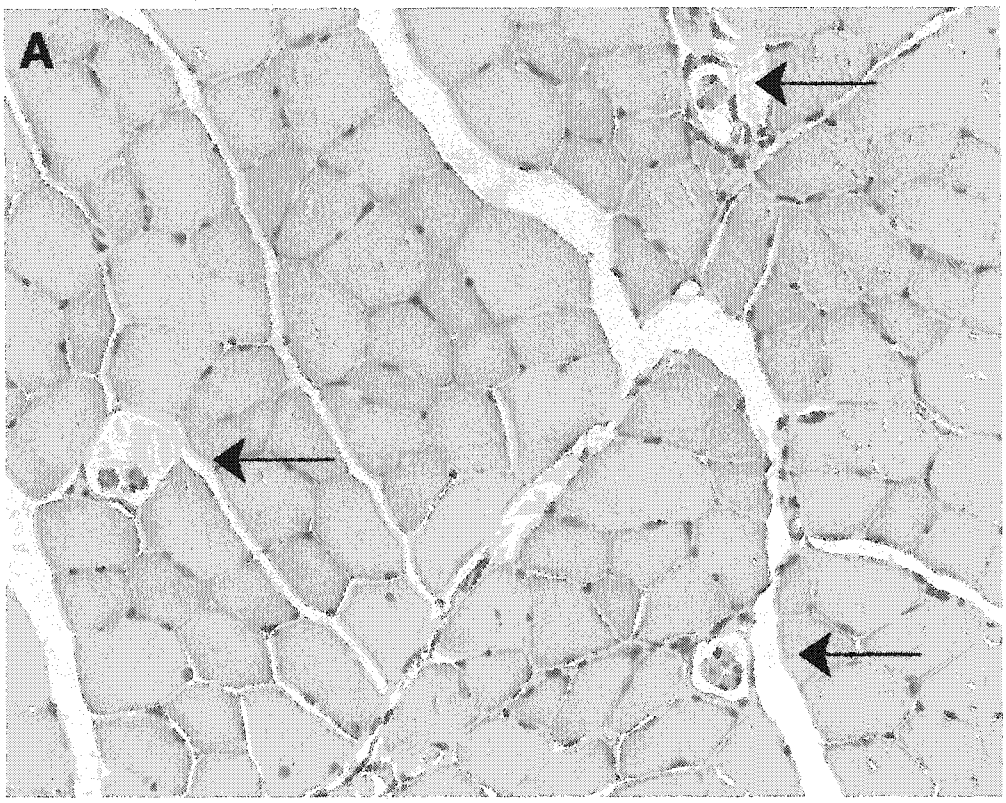
A

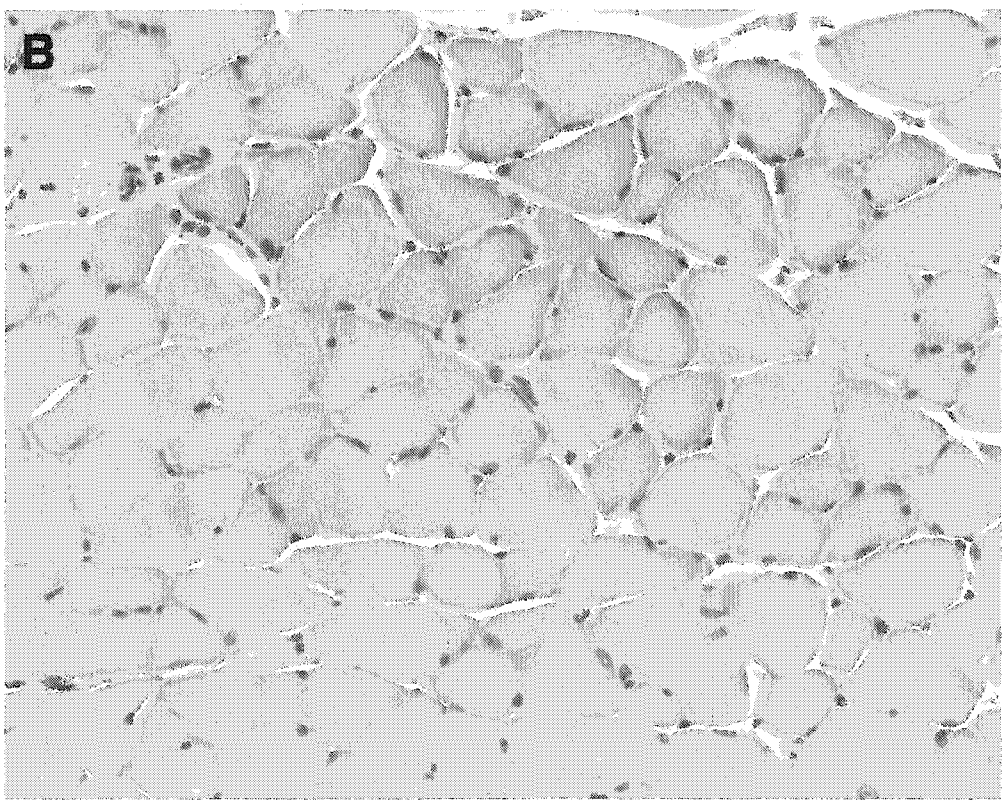
B

mock infection control and a recombinant adenovirus expressing β-galactosidase. Staining for β-galactosidase revealed that there was a greater than 95% infection rate (data not shown). The various myoblast cell lines were then differentiated into multinucleated myofibers and the levels of ErbB2 were assayed in a Western analysis. Consistent with the hypomorphic levels of ErbB2 seen in the $ErbB2^{Flox/Flox}$ mice (See Chapter Four), the level of ErbB2 seen in the $ErbB2^{Flox/Flox}$ controls was reduced in comparison to the wild type control (Figure 5.8, Panel A, Lanes 1 vs. 2-3). With the addition of the recombinant adenovirus expressing Cre recombinase, ErbB2 could no longer be detected in the myofibers (Lanes 4-5). Grb2 was included as a loading control. To determine whether the loss of ErbB2 would be compensated for by the other EGFR family members, EGFR, ErbB3 and ErbB4 levels were examined by Western analysis. ErbB3 levels in the cell lines with and without ErbB2 do not change (Figure 5.8, Panel B). The immunoblots for the remaining EGFR family members were identical to the ErbB3 immunoblot (data not shown) indicating that there is no compensation in the levels of the EGFR family members upon the elimination of ErbB2 expression. During the differentiation of the myoblast cell lines with and without ErbB2 from myoblasts to myofibers, it was noted that there were a large number of cells in suspension in cell lines lacking ErbB2. Trypan blue exclusion revealed that the vast majority of these cells were not viable (data not shown). To determine the number of cells in suspension during each day of myoblast differentiation, the media was harvested during each day of differentiation and the number of cells in suspension was determined and was compared to the number of cells remaining on the tissue culture plate. This quantification revealed

Figure 5.8 – Increased Apoptosis in ErbB2 null Myoblasts during Differentiation

Myoblast cells were prepared from adult FVB wild type controls, ErbB2$^{Flox/Flox}$ and ErbB2$^{Flox/Flox}$ MCK-Cre mice. Given the residual ErbB2 expression in ErbB2$^{Flox/Flox}$ MCK-Cre cell lines (not shown), we infected ErbB2$^{Flox/Flox}$ and ErbB2$^{Flox/Flox}$ MCK-Cre (designated Aff2) cell lines with an adenovirus containing Cre recombinase. A mock infection and adenovirus containing the gene for B-galactosidase were included as controls. At day five of differentiation, ErbB2 was detected in the wild type and ErbB2$^{Flox/Flox}$ controls (A, Lanes 1-3), but was not seen in the ErbB2$^{Flox/Flox}$ Ad-Cre or Aff2 Ad-Cre cells (A, Lanes 4-5). ErbB3 was found to be present at equal levels in all cells and Grb2 was included as an internal loading control (B). During differentiation, it was noted that a large number of cells were lifting off the plates in cell lines lacking ErbB2. Quantification of the percentage of cells in suspension at each differentiation time point revealed that in cells containing ErbB2 there were usually less than 5% of the cells in suspension (● - FVB, □ - MOCK, ▲ - B-gal). In contrast, by day three of differentiation there were on average 12 % and 25% of cells in suspension in the ErbB2$^{Flox/Flox}$ Ad-Cre (◆) and Aff2 Ad-Cre (■) cell lines respectively.

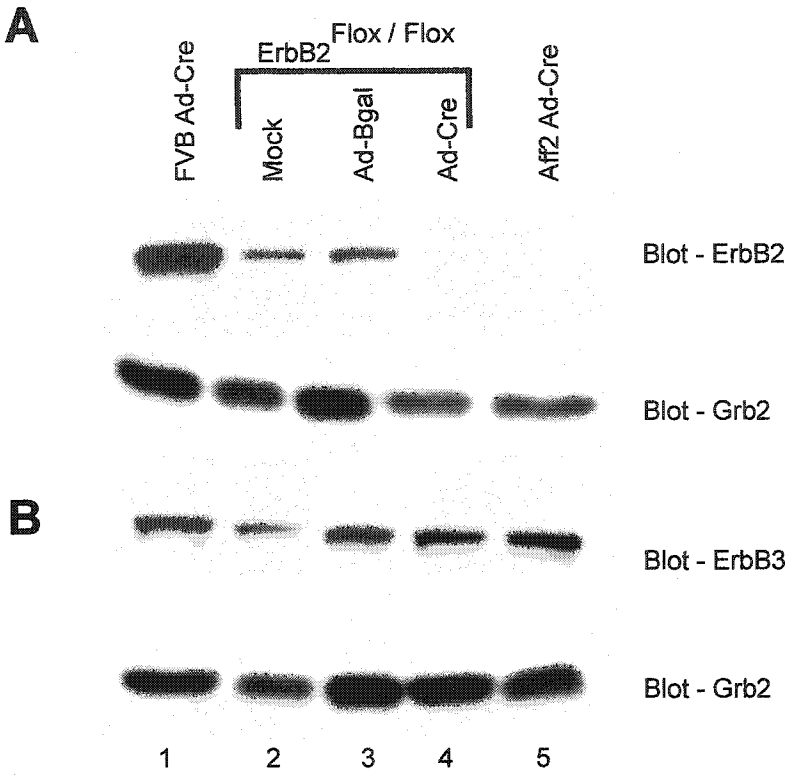
A
FVB Ad-Cre
ErbB2 Flox / Flox
Mock
Ad-Bgal
Ad-Cre
Aff2 Ad-Cre
Blot - ErbB2
Blot - Grb2
B
Blot - ErbB3
Blot - Grb2
1
2
3
4
5

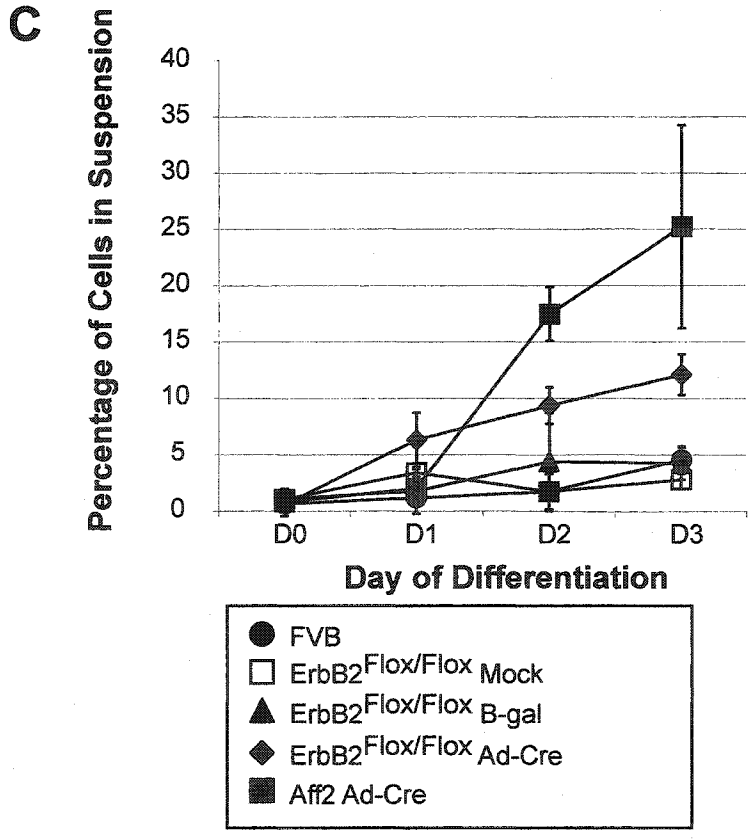
C
Percentage of Cells in Suspension
40
35
30
25
20
15
10
5
0
D0
D1
D2
D3
Day of Differentiation
FVB
ErbB2Flox/Flox Mock
ErbB2Flox/Flox B-gal
ErbB2Flox/Flox Ad-Cre
Aff2 Ad-Cre

that in the wild type cell lines there were normally up to 5% of the cells in suspension during the course of differentiation (Figure 5.8, Panel C). However, with the loss of ErbB2, by day three of differentiation there were up to 25% of cells in suspension in a cell line lacking ErbB2. The quantification was not extended past the third day of differentiation as multinucleated myofibers began to be detected in suspension. This analysis was completed in three separate cell lines for each data point shown. Clearly the loss of ErbB2 causes cell death during the differentiation of myoblasts to myofibers.

To examine whether the lack of ErbB2 in differentiating myoblasts was causing cell death through apoptosis or necrosis, Annexin / Propidium Iodide staining was completed after the second day of differentiation on cells that were still adhering to the collagen coated plates (Figure 5.9, Panels A-D). This analysis clearly illustrated that undifferentiated myoblasts lacking ErbB2 were apoptotic (Figure 5.9, Panel D) and the quantification of apoptotic cells to viable cells was consistent with the results observed previously in Figure 5.8. Panel C.

Although ErbB2 null myoblasts underwent apoptosis during differentiation to myofibers, it was noted that the remaining viable cells were still capable of terminal differentiation. Since it would be possible for a selective pressure to be applied to select for myoblasts still expressing ErbB2 after introduction of the adenovirus expressing Cre recombinase, it is important to note that the levels of ErbB2 that were examined in the various cell lines after differentiation into myofibers (Figure 5.8). To determine whether the myofibers with and without ErbB2 had reached terminal differentiation, immunostaining for a marker of terminal differentiation, myosin heavy chain (MF20),

Figure 5.9 – ErbB2 Null Myoblasts Undergo Apoptosis but Remaining Cells are Capable of Terminal Differentiation.

ErbB2 null myoblasts were previously noted to be in suspension during differentiation (Figure 5.8). To determine whether the cells were undergoing apoptosis or necrosis, Annexin / Propidium Iodide staining was used. By light microscopy at day two of differentiation, wild type myoblasts (A) and myoblasts lacking ErbB2 (C) were observed to adhere to the culture dish. Very few annexin or propidium iodide positive cells were observed for the wild type cell line in an overlay of both detection spectrums (B). However, when ErbB2 null myoblast cell lines were examined (D) it was clear that the cells were undergoing apoptosis. Although many cells lacking ErbB2 underwent apoptosis, the remaining myoblasts were still capable of terminal differentiation. $ErbB2^{Flox/Flox}$ myoblast cell lines with a mock Ad infection (E) and after infection by Ad-Cre (F) at day five of differentiation are shown after immunostaining for myosin heavy chain (MF20). No differences were noted in the ability of either cell line to reach terminal differentiation.

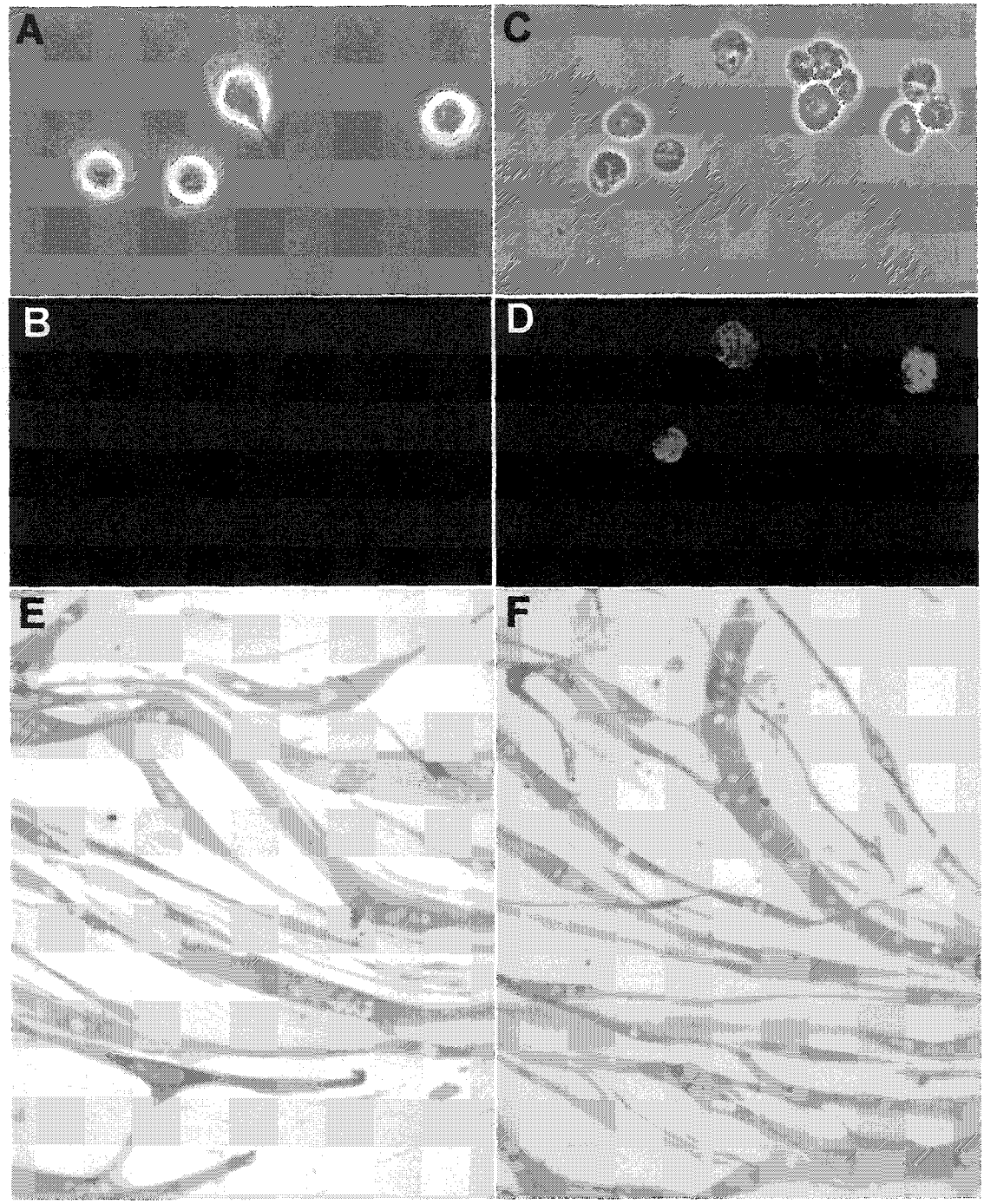
A
C
B
D
E
F

was completed. No apparent differences were noted in cell lines with (Figure 5.9, Panel E) or without ErbB2 (Figure 5.9, Panel F).

While the *in vitro* results appeared to illustrate defects in differentiation in myoblasts lacking ErbB2, the sections of the TA muscle did not illustrate a difference in the standard histological hallmarks of muscle regeneration (Figure 5.7). In order to investigate the regenerative properties of the TA muscle *in vivo*, a mechanical crush injury was applied to $ErbB2^{WT/WT}$, $ErbB2^{Flox/Flox}$ and $ErbB2^{Flox/Flox}$ MCK-Cre mice. Two weeks following the application of the injury the mice were examined. Prior to euthanization of the mice, it was observed that the conditional ErbB2 null mice were attempting to avoid the use of the limb with the applied injury while the controls were moving normally. Two weeks following the applied injury the muscle should have completely regenerated and the only evidence of an injury are the centrally located nuclei where the muscle fibers have regenerated. The normal regeneration was noted in the $ErbB2^{WT/WT}$ and $ErbB2^{Flox/Flox}$ controls (Figure 5.10, Panel A). The presence of centrally located nuclei demarcates the site of injury (arrow). Further, the muscle fibers surrounding the injury are continuous and are aligned with the surrounding extrafusal fibers. In contrast, the longitudinal section of the crushed TA muscle from mice with a muscle specific deletion of ErbB2 at the same time point shows a marked defect in regeneration (Figure 5.10, Panel B). There are areas with encapsulated cellular debris and the muscle fibers are not aligned nor are they continuous. Clearly with the ablation of ErbB2 there are defects in regeneration consistent with the *in vitro* defects previously described.

Figure 5.10 – Regeneration Defects in Muscle Lacking ErbB2

Given the apoptosis observed during the differentiation of myoblast cell lines lacking ErbB2, the regenerative capacity of muscle lacking ErbB2 was tested *in vivo*. Two weeks after a mechanical crush injury was applied to the TA muscle in wild type controls, regeneration is essentially complete as seen in a longitudinal section (A). Continuous fibers with normal caliber are aligned normally and the only evidence of the crush injury are the areas with increased numbers of centrally located nuclei (A – arrow). In contrast, the ErbB2$^{Flox/Flox}$ MCK-Cre muscle has not completely regenerated at the same time point. Numerous regions with encapsulated cellular debris are observed at the site of injury (B). Further, the fibers are no longer aligned normally and are clearly not continuous. Consistent with these results was the observation of the mice prior to examination, the wild type mice had a normal gait while the ErbB2$^{Flox/Flox}$ MCK-Cre mice showed reluctance to utilize the leg which had suffered the crush injury.

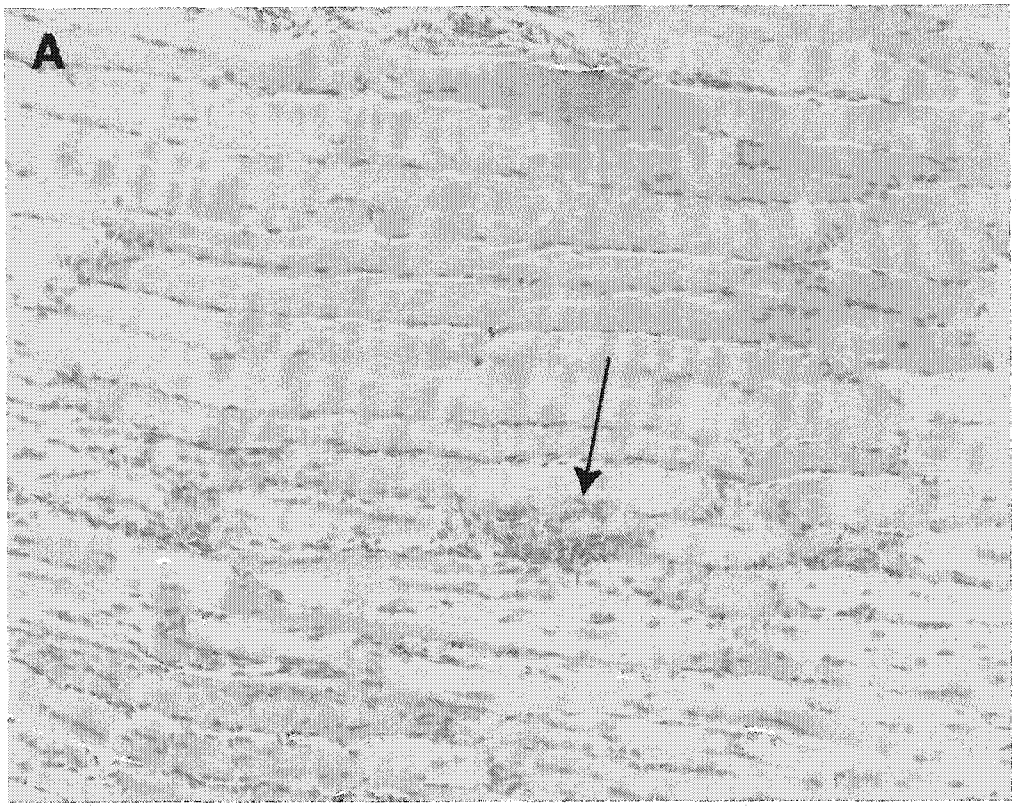
A

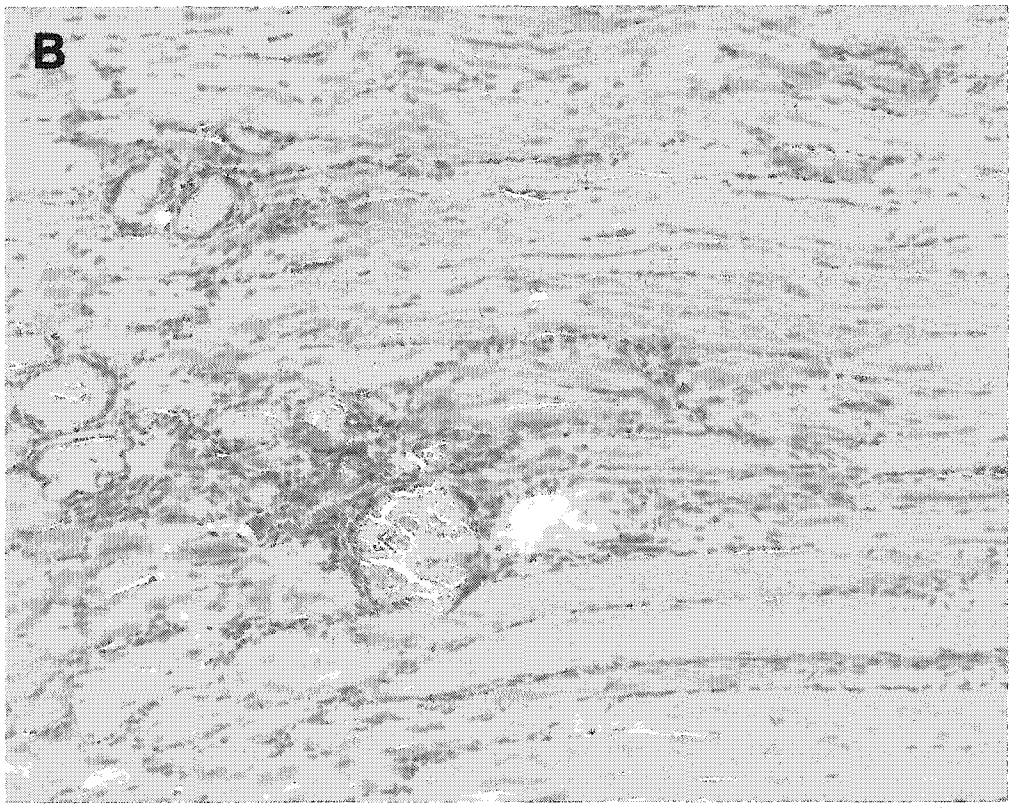
B

5.2.3 Impaired ErbB3 signaling in myotubes lacking ErbB2

One potential explanation for the enhanced apoptotic response during myoblast differentiation and the impaired regeneration is that ErbB2 provides a critical cell survival signal during the differentiation process. Indeed, it has previously been demonstrated that ErbB2 can stimulate the PI-3'/Akt kinase survival pathway through its heterodimerization with ErbB3 (Kita *et al.*, 1994; Soltoff *et al.*, 1994). To further explore this possibility, we treated the various myoblast cell lines with NRG, a ligand for ErbB3. Consistent with several previously published reports, NRG stimulation of primary myofibers containing ErbB2 resulted in the transphosphorylation of ErbB3 (Figure 5.11, Panel A, Lanes 1-3) (Altiok *et al.*, 1995; Si *et al.*, 1996). In contrast, NRG stimulation of ErbB2 deficient cells failed to show detectable ErbB3 phosphorylation (Lanes 4-5). The inability to detect ErbB3 transphosphorylation was not due to differences in ErbB3 protein since these cells expressed comparable levels of ErbB3 protein (Figure 5.11, Panel A). These results illustrate that in the absence of ErbB2, ErbB3 is unable to respond appropriately to NRG stimulation. Further, these results illustrate that the other EGFR family members are unable to compensate for the loss of ErbB2 in these cell lines.

Since stimulation of cells expressing ErbB2 and ErbB3 with NRG is also known to result in heterodimerization and the concomitant activation of the MAP and Akt serine kinases (Altiok *et al.*, 1995), we also measured the state of phosphorylation of Akt and MAPK serine kinases using phospho-specific antibodies. The results of these analyses revealed that NRG stimulated ErbB2 null muscle cells were severely impaired in their

Figure 5.11 – ErbB3 is not activated in cells lacking ErbB2 upon NRG Stimulation

To examine NRG mediated stimulation of the MAPK and PI3'K pathways *in vitro*, we stimulated differentiated myofibers with recombinant NRG and examined ErbB3 at 5 minutes post stimulation for phosphorylation. After immunoprecipitation of ErbB3 and immunoblotting for phosphorylated tyrosine, activation of ErbB3 in cells containing ErbB2 was clearly visible (A). However, the level of phosphorylated tyrosine residues in ErbB3 in cells lacking ErbB2 was greatly reduced and was difficult to detect (A). To ensure equal loading, the immunoprecipitation was also immunoblotted for ErbB3. Since the activation of ErbB3 was clearly impaired, we examined the activation of Erk1 and Erk2 with an antibody that detects phosphorylated MapK (P-MAPK) (B). Clearly the level of phosphorylation of Erk1 and Erk2 is reduced in the cell lines lacking ErbB2. To ensure equal protein loading, the immunoblot for P-MapK was stripped and reblotted for MapK. This revealed equal levels of Erk1 and Erk2 in all cell lines. Given the apoptosis observed during differentiation, we examined activation of AKT. Using an antibody that recognizes phosphorylated AKT (P-AKT), we show that the level of activated AKT in cell lines lacking ErbB2 is clearly reduced (C). To ensure equal loading, we stripped the blots and immunoblotted for AKT and Grb2. The immunoblot for Grb2 illustrates equal loading while the immunoblot for AKT shows a slight reduction in the level of AKT in the Aff2 cell line.

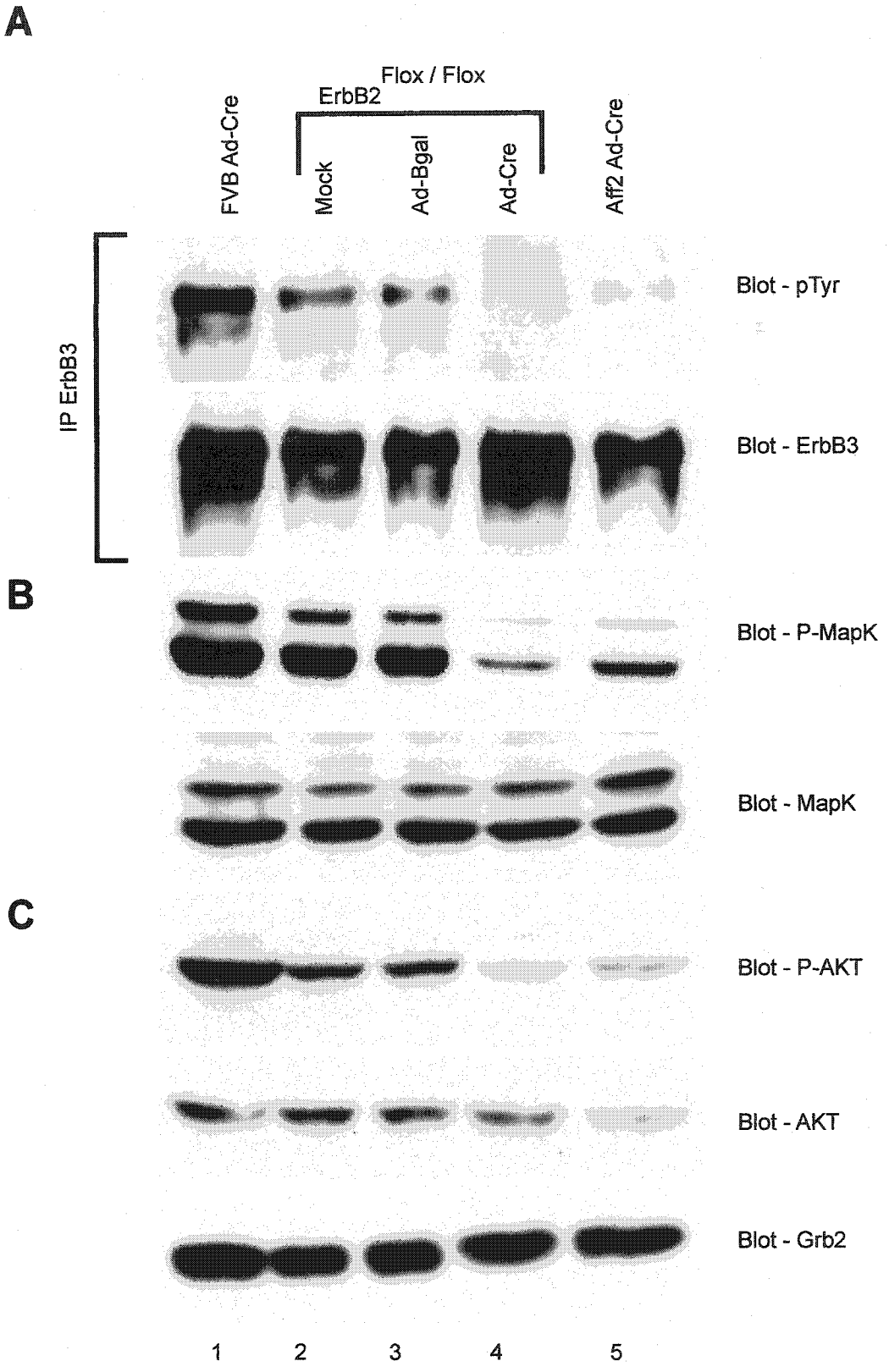
A
Flox / Flox
ErbB2
FVB Ad-Cre
Mock
Ad-Bgal
Ad-Cre
Aff2 Ad-Cre
IP ErbB3
Blot - pTyr
Blot - ErbB3
B
Blot - P-MapK
Blot - MapK
C
Blot - P-AKT
Blot - AKT
Blot - Grb2
1
2
3
4
5

capacity to activate either Akt or MAPK. (Figure 5.11, Panel B and C, Lanes 1-3 vs. 4-5). The reduction of Akt and MAPK stimulation was not due to the reduction in levels of these serine kinases, since these cell lines expressed comparable levels of MAPK and slightly reduced levels of AKT (Figure 5.11, Panel B and C, Lanes 1-5). Given the importance of Akt and MAPK in cell survival, these data argue that observed levels of apoptotic cell death during muscle differentiation and regeneration in muscle cells lacking ErbB2 function is due to inability to activate these critical cell survival pathways.

5.3 Discussion

To determine to importance of ErbB2 expression in skeletal muscle development and maintenance, transgenic mice expressing Cre recombinase under the control of the MCK promoter were interbred with the ErbB2$^{Flox/Flox}$ mice to create a muscle specific knockout. After generating ErbB2$^{Flox/Flox}$ MCK-Cre mice, excision of the loxP flanked allele was noted in the heart and skeletal muscle. Although the ErbB2 null mice suffered embryonic lethality due to defects in cardiac development (Lee *et al.*, 1995), the cardiac excision described for this tissue specific deletion of ErbB2 did not cause embryonic lethality. Interestingly, although prior reports suggested that excision in the muscle using the MCK-Cre transgene was greater than 95% effective (Bruning *et al.*, 1998; Zisman *et al.*, 2000), the data shown here indicated that excision was limited to 30-40% completion. Although inconsistent with previous reports, these data are consistent with the extent of excision in other reports describing a tissue specific deletion of ErbB2 (Crone *et al.*, 2002). Further characterization of the extent of excision through culture of myoblast cell

lines revealed that even in pure cultures of differentiated muscle there was still incomplete excision. Importantly, these cell lines were still capable of undergoing excision since the addition of a recombinant adenovirus expressing Cre recombinase completely abrogated ErbB2 expression. However, despite these moderate levels of excision of the loxP flanked allele, there was a striking phenotypic effect in the $ErbB2^{Flox/Flox}$ MCK-Cre mice.

The muscle specific deletion of ErbB2 was associated with a profound loss of proprioception. After a detailed examination of the histological sections of various hind limb muscles, it was noted that the $ErbB2^{Flox/Flox}$ MCK-Cre mice lacked muscle spindles. This analysis was conducted when the mice were exhibiting a phenotype at several months of age. These experiments did not address whether ErbB2 was necessary for the development or for the maintenance of the muscle spindles. However, when $ErbB2^{Flox/Flox}$ MCK-Cre mice were visually examined in the first weeks of development, few abnormalities in gait or posture were noted. These results suggest that the muscle spindles initially developed normally in the juvenile muscle but were lost during the transition to the adult form lacking ErbB2. Interestingly, while there is a loss of muscle spindles in these mice, motor innervation appeared to be normal in all other respects suggesting that the defects in gait and posture were solely due to the absence of muscle spindles.

While the conditional deletion of ErbB2 resulted in a complete lack of muscle spindles, the $ErbB2^{Flox/Flox}$ mice also exhibited a reduction in the number of muscle spindles. However, these mice did not exhibit any abnormalities in gait or posture, even

when examined at two years of development. Although the numbers of muscle spindles were reduced, there is no quantified loss in proprioception. Interestingly, the level of ErbB2 in the ErbB2$^{Flox/Flox}$ mice was previously illustrated to be 10% of wild type levels (Chapter Four). The correlation of a reduction of number of muscle spindles with a reduction in ErbB2 levels suggests that there is a critical ErbB2 threshold in muscle spindles for their proper development and maintenance. While other work describing a muscle specific deletion for ErbB2 have not described a muscle spindle defect (Crone *et al.*, 2002; Ozcelik *et al.*, 2002), the introduction of excision in 40% of cells by MCK-Cre in the already hypomorphic ErbB2$^{Flox/Flox}$ mice would result in a further reduction in the levels of ErbB2. Further support for the argument of a critical ErbB2 threshold was seen when ErbB2$^{Flox/KO}$ mice, which should have 5% of wild type ErbB2 levels, were observed to suffer from embryonic lethality (data not shown). Taken together, these results strongly suggest that if other published reports did not reduce the levels of ErbB2 in a great proportion of muscle fibers one would not expect to see defects in proprioception, reinforcing the theory of a threshold level of ErbB2.

While other reports of a muscle specific knockout of ErbB2 did not describe a loss of muscle spindles or proprioception, defects in cardiac development were noted. Indeed, the cardiac defects often seen in human breast cancer patients treated with Herceptin were mimicked in these mice (Crone *et al.*, 2002; Ozcelik *et al.*, 2002). During the analysis of the ErbB2$^{Flox/Flox}$ MCK-Cre mice it was noted that these mice suffered from enlarged hearts (data not shown) but these results were not pursued.

While there was a dramatic loss of muscle spindles in the ErbB2$^{Flox/Flox}$ MCK-Cre mice, the histological sections revealed otherwise normal muscle fibers and architecture of the muscle. Given the expression pattern of ErbB2, the role in differentiation was examined in detail *in vitro*. When myoblasts lacking ErbB2 were differentiated to fuse and form multinucleated myofibers, cell death through apoptosis was noted by day two of differentiation. However, the ErbB2 null myoblasts that escaped apoptosis were capable of terminal differentiation. These results suggested that ErbB2 plays a critical role during the differentiation process. To test this theory, regeneration was induced through a muscle crush in ErbB2$^{WT/WT}$, ErbB2$^{Flox/Flox}$ and ErbB2$^{Flox/Flox}$ MCK-Cre mice. Importantly, the *in vitro* results illustrating a block in differentiation in myoblasts lacking ErbB2 were mirrored in the *in vivo* results. Mice lacking ErbB2 in skeletal muscle were unable to appropriately repair damage to the muscle. Taken together, these results suggest that although differentiation can occur in the absence of ErbB2, it provides an important survival signal during the transition from myoblasts to myofibers.

An explanation for the impaired differentiation of myoblasts lacking ErbB2 lies in the reduced ability of the myoblasts to activate critical proliferative and cell survival pathways. A potential candidate for this cell survival signal is activation of PI-3K/Akt signaling pathway (Figure 1.2). Consistent with this hypothesis, ablation of ErbB2 results in a dramatic reduction in ErbB3 tyrosine phosphorylation in response to NRG stimulation in the primary myofibers. Because the kinase activity of ErbB3 is naturally impaired, this data argues that the ErbB2/ErbB3 heterodimer is absolutely essential for recruitment of the PI-3' / Akt kinase pathway. Conceivably, the increased apoptotic

death that is noted in the ErbB2 null myoblasts following induction of differentiation could result from inefficient activation of PI-3K Akt signaling cascade. Indeed, recruitment of the PI-3K/Akt signaling pathway has proven to be important cell survival pathway in a number of distinct cell lineages. Thus, functional ErbB2 is required during myoblast differentiation for transactivation of ErbB3 and subsequent engagement of the PI-3K signaling cascade. Additionally, the ability of the myofibers to stimulate the MAPK pathway was examined. These results clearly illustrated a reduced ability of ErbB2 null myofibers to activate the MAPK pathway upon NRG stimulation. Taken together, these data suggest that several critical cell signaling pathways have been disrupted in the ErbB2 null myofibers which may directly impact upon their survival during differentiation.

In addition to being expressed in the muscle spindle, ErbB2 expression has previously been noted at the neural muscular junction along with ErbB3 and ErbB4. Further, previous studies have also implicated ErbB2 in the induction of various acetylcholine receptor subunits at the NMJ (Altiok *et al.*, 1995; Jo *et al.*, 1995; Si *et al.*, 1996; Tansey *et al.*, 1996; Fischbach and Rosen, 1997; Won *et al.*, 1999). While clear defects in rate of cell survival during differentiation were noted in the ErbB2 deficient myoblast cell lines, we failed to note any effect on induction of acetylcholine receptor ε subunit in ErbB2 null myoblasts or myofibers (data not shown). Further, during urea silver nitrate staining, normal innervation of the neural muscular junction was noted in the $ErbB2^{Flox/Flox}$ MCK-Cre mice. These results argue that the presence of ErbB2 is dispensable for induction of acetylcholine receptor subunits and the switch from the

juvenile to adult AChR isoform. Given the presence of other members of EGFR family at the NMJ, including ErbB3 and ErbB4, this data also argues that the other EGFR family members may compensate for loss of ErbB2 in the induction of acetylcholine receptor subunits. Future studies with muscle cell specific ablations of other EGFR family members should allow this hypothesis to be tested.

During the analysis of the proprioception defects in the ErbB2$^{Flox/Flox}$ MCK-Cre mice, it was noted that there was a striking similarity to various other knockout mouse models. Indeed, the ablation of EGR3 in mice results in a loss of spindles and the associated proprioception defects (Tourtellotte and Milbrandt, 1998). Given the similarity of the two phenotypes, it is conceivable that ErbB2 and EGR3 funnel through a shared signaling pathway required for muscle spindle development or maintenance. Interestingly, data from a breast cancer cell line revealed that overexpression of ErbB2 resulted in overexpression of EGR3 (Sweeney *et al.*, 2001). While the signaling pathway downstream of ErbB2 that results in upregulation of EGR3 has not been clearly elucidated, it is possible that it funnels through the Shc adaptor molecule. Indeed, recent unpublished results indicate that mice lacking functional ShcA in the muscle do not maintain muscle spindles and suffer from proprioception defects (Personal communication, W.R. Hardy and T. Pawson)(Summarized Figure 5.12)

While EGR3 is integral for muscle spindle maintenance, another member of the EGR family, EGR2 (Krox20), and ErbB2 have both been shown to be required for Schwann cell development (Garratt *et al.*, 2000). Further, results shown in Chapter 3 illustrated that EGR2 is elevated in the conditionally activated NeuNT tumors.

Interestingly, recent work has illustrated that the EGR2 transcription factor is capable of binding the *erbB2* promoter and increases transcription by 3 fold (Brown, 2002). Taken together, these observations suggest that there is a strong interaction between ErbB2 and the EGR family during the development and maintenance of numerous cell lineages.

In addition to EGFR and EGR families, other receptor tyrosine kinases and their associated ligands have been implicated in the muscle / afferent relationship. For example, the neurotrophins and their receptors play an integral role in muscle spindle maintenance. Neurotrophin3 (NT-3) is expressed and released from the intrafusal muscle fiber and is critical for survival of the innervating afferent during development of the muscle spindle. Further, Tyrosine Kinase ReceptorC (TrkC) is the receptor for NT-3 and is found on the membrane of the afferent (Loeb and Fischbach, 1997). Consistent with their expression patterns, germline ablation of NT-3 or its receptor, TrkC, resulted in a loss of muscle spindles (Ernfors *et al.*, 1994; Klein *et al.*, 1994) (Figure 5.12). While these two strains of mice exhibited proprioception defects, they were far more severe than what was observed in the ErbB2 null mice and suffered from an early mortality as early as 3 weeks of age. Interestingly, one result of NT-3 stimulation of the TrkC receptor is the secretion of NRG from the neuron (Loeb and Fischbach, 1997). Given the importance of a functional ErbB2 / ErbB3 heterodimer in responding to NRG mediated activation of numerous signaling pathways in the muscle, these observations suggest that the NT-3 / TrkC signaling pathways may activate ErbB2 during development and maintenance of the muscle spindle. Indeed, the NT-3 / TrkC / NRG reciprocal signaling loop previously proposed for the maintenance of the intrafusal muscle fiber and their

Figure 5.12 –Proposed Reciprocal Signaling Loop in Muscle Spindle Maintenance

Various strains of knockout mice have been generated that have defects in proprioception due to a lack of muscle spindles. Upon closer examination of how these various genes are related, the reciprocal signaling loop originally proposed (Loeb and Fischbach, 1997) can be extended. Beginning with knockout strains that lack muscle spindles (designated with a *), it can be seen that these genes are expressed in both the afferent and the intrafusal muscle fiber. Beginning with the expression and secretion of NT-3 by the intrafusal muscle fiber, the signal moves to the afferent since it contains TrkC, the receptor for NT-3. Stimulation of TrkC by NT-3 has been shown to induce expression and release of NRG from afferents. The primary receptor for NRG on the muscle spindle is ErbB3 which preferentially heterodimerizes with ErbB2 to phosphorylate various tyrosine residues on the carboxy terminus of these two proteins. Shc is an adaptor molecule that binds to these phosphorylated tyrosine residues and can activate several signal transduction cascades. Overexpression of ErbB2 has also been shown to upregulate the levels of EGR2, a transcription factor that in turn can promote ErbB2 expression. Further, stimulation of ErbB2 has been illustrated to elevate the levels of EGR3. Finally, EGR3 null mice do not express NT-3, suggesting that EGR3 can modulate NT-3 expression. Taken together, this data illustrates a complete signaling loop that is necessary for the maintenance of the muscle spindle. Elevated levels are shown with double arrowheads, activation of signal transduction cascades is shown with single arrowheads.

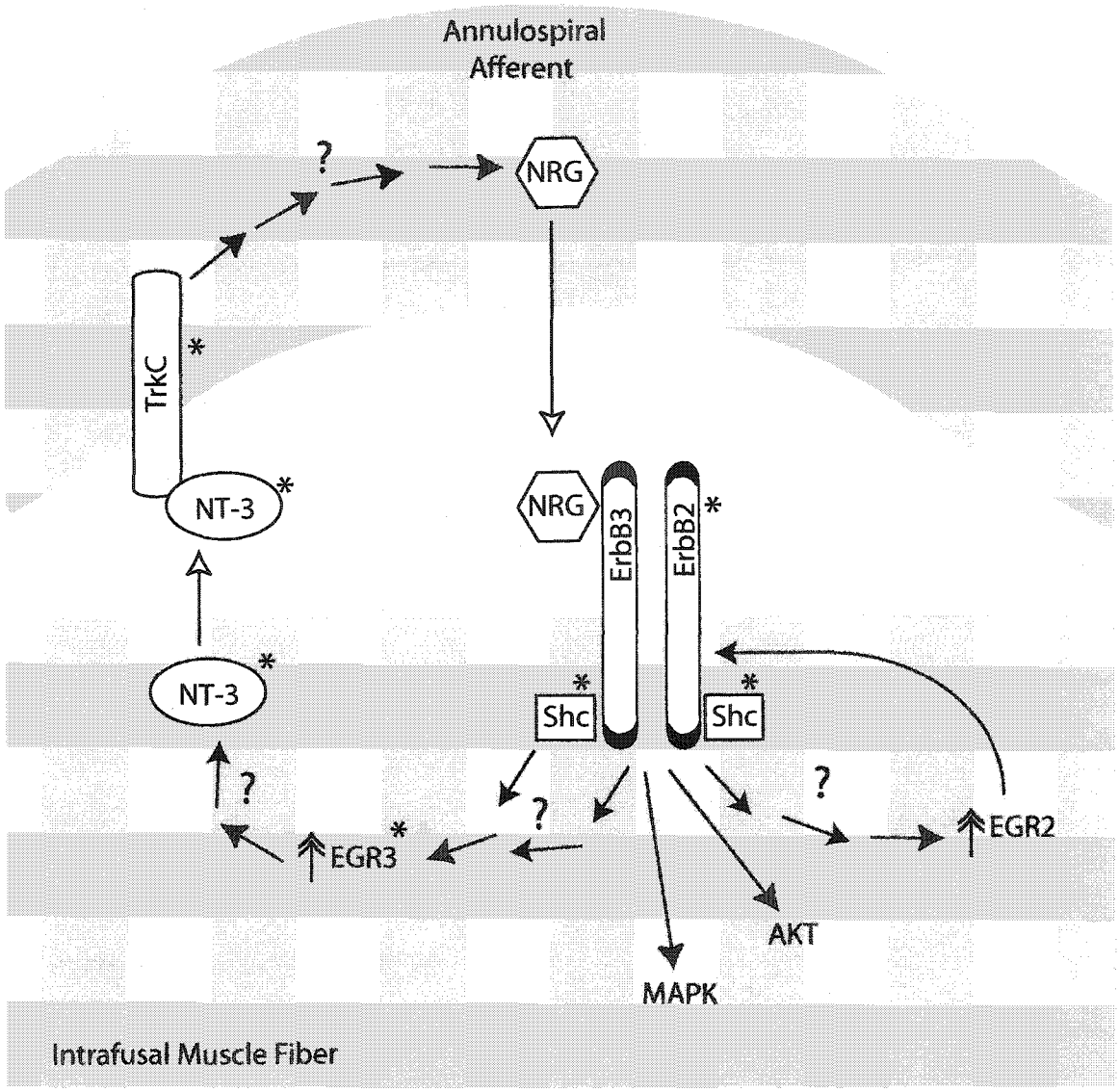
Annulospiral
Afferent
?
NRG
TrkC
*
NT-3
*
NRG
ErbB3
ErbB2
*
NT-3
*
*
Shc
*
Shc
?
?
?
EGR3
*
EGR2
AKT
MAPK
Intrafusal Muscle Fiber

afferents (Loeb and Fischbach, 1997) can now be extended to include ErbB2 (Figure 5.12). The previously discussed elevation of EGR3 in response to ErbB2 stimulation, albeit in a breast cancer cell line, also suggests that EGR3 is involved in this pathway. Further evidence for the involvement of EGR3 in the reciprocal signaling loop is derived from studies of the EGR3 null mice prior to degeneration of the muscle spindles. While wild type control intrafusal muscle fibers express NT-3, the EGR3 null mice do not (Chen *et al.*, 2002). Further, injections of NT-3 into the EGR3 null mice results in the restoration of the motor-sensory connections. These results indicate that EGR3 plays a role in regulating the level of NT-3 expressed in the muscle spindle. Taken together, a reciprocal signaling loop can be described that exists between the intrafusal muscle fiber and the afferent that composes the muscle spindle as shown in Figure 5.12. When any of the genes that are integral to this signaling loop are disrupted, the muscle spindles degenerate and the knockout mice suffer from proprioception defects. This theory also suggests that disruption of other members of this pathway should result in an identical phenotype. For example, a muscle specific ablation of ErbB3, the primary NRG receptor in the intrafusal muscle fiber, should result in mice lacking muscle spindles. Future work should allow this theory to be examined.

CHAPTER 6

CONCLUSIONS AND FUTURE DIRECTIONS

The prevalence of breast cancer in the human population has sparked an examination of the etiology of this disease. Consequently, it was observed that HER2 is amplified and overexpressed in 20-30% of all breast cancers and correlates with a poor prognosis (Slamon *et al.*, 1987; Slamon *et al.*, 1989; Andrulis *et al.*, 1998). Given the structure of the receptor and the expression pattern in both normal tissues and human breast cancer, disabling this pathway *in vivo* has become an attractive target for therapy. Although some success has been observed with this treatment, many aspects of HER2 mediated breast cancer are still poorly understood. To better understand the role of HER2 in this prevalent disease, numerous mouse models have been created.

Initial studies using the activated form of Neu under the control of the Mouse Mammary Tumor Virus (MMTV) promoter enhancer clearly revealed that expression of activated Neu in the mammary gland played a causal role in the etiology of the disease (Muller *et al.*, 1988). Additionally, several other MMTV mouse models with various Neu alleles have been created and have revealed insights into the requirement for activating mutations, expression of other family members and signal transduction pathways. However, while these studies have been extremely informative, they have all relied on a strong viral promoter with questionable relevance to the human disease.

Further, the MMTV promoter itself is regulated by hormonal influences such as estrogen and progesterone and given the importance of these hormones in the progression of breast cancer, these MMTV directed tumors are clearly not ideal models of the human condition. A portion of the experimental results presented within this thesis have described a new mouse model of Neu mediated tumorigenesis with remarkable similarity to the human condition.

The conditional expression of the activated *neuNT* allele under the control of the endogenous promoter in the mammary gland resulted in preneoplastic lesions that expressed markers associated with Neu and Ras mediated tumors (Morrison and Leder, 1994). However, these preneoplastic lesions required additional genetic events prior to the formation of mammary comedo-adenocarcinomas. Indeed, it was observed that the formation of tumors in this mouse model was associated with the amplification and overexpression of the recombinant *neuNT* allele (Chapter 3)(Andrechek *et al.*, 2000). In human breast cancer, amplification and overexpression of HER2 is associated with the amplification of genes that are chromosomally juxtaposed to the HER2 allele. The amplification of *grb7* and *cab1* is consistently observed in human tumors with an amplification of *HER2* (Kauraniemi *et al.*, 2001; Varis *et al.*, 2002). Interestingly, in the mouse model expressing *neuNT* under the control of the endogenous promoter, amplification of *grb7* and *cab1* was observed after the tumors were compared to an MMTV regulated model, illustrating the similarity to the human condition. In the same comparison of gene expression, it was noted that numerous transcription factors were elevated in tumors derived from mice conditionally expressing *neuNT* in the mammary

gland, many of which are also involved in the human disease. Recently it has been illustrated that a subset of these transcription factors are able to stimulate the Neu promoter and are also elevated in the human condition (Brown, 2002). An additional characterization of these mice through CGH and SKY analysis illustrated a loss in chromosome four (Montagna *et al.*, 2002), a region analogous to human chromosome 1p32-36, which has been previously demonstrated to be site of allelic loss in human cancers (Bieche *et al.*, 1993). While the comparison of gene expression between the conditional and MMTV regulated Neu tumors did not reveal a loss in expression for genes located on chromosome four, it is possible that this region is also lost in the MMTV regulated tumors. In the future, the relevant genes that are lost from chromosome four should be identified and their role and importance in the progression of Neu mediated tumorigenesis should be assessed.

In addition to mediating tumor formation, it was also observed that the mammary glands had increased branching with the conditional expression of *neuNT* under the control of the endogenous promoter in the mammary gland. During the development of the normal mammary gland, when developing ducts encounter other ducts or the periphery of the fat pad they either cease to extend or turn away from the negative stimulus. However, in the mammary gland that is conditionally expressing *neuNT*, the ductal network is not as sensitive to this regulation. Indeed, this reduction in sensitivity to negative regulatory stimuli was also observed in the ability of the ducts in these mammary glands to escape the confines of the normal fat pad. The increased branching due to activated *neu* expression is consistent with the idea that EGF promotes ductal

outgrowth and branching (Snedeker *et al.*, 1991) due to the ability of Neu to heterodimerize with the other EGFR family members. In order to examine the role of Neu in the development of the mammary gland, the conditional activation of *neuNT* can be compared to the conditional inactivation of *neu* (Figure 6.1). In contrast to the increased branching observed with the expression of an activated *neuNT* allele, the mammary specific inactivation of *neu* results in the developmental delay of mammary gland formation. Indeed, the *neu* null ductal network is seen to lag behind the wild type counterpart for the first 12 weeks of postnatal development. Taken together, the conditional activation and the conditional inactivation of *neu* in the mammary gland suggest that Neu is involved in the regulating of ductal branching in the mammary gland. Interestingly, Neu did not appear to have a major role in the lactation and involution of the mammary gland. These results were surprising in light of previous work indicating that Neu had a role in lactation (Jones and Stern, 1999). However, the previous results indicating a role for Neu in lactation were based on the expression of a dominant negative *neu* allele which would affect all members of the EGFR family. Indeed, when these data are considered in the light of the results presented in Chapter 4, it is clear that the EGFR family is involved in regulating lactation, but the loss of Neu expression was not sufficient to interfere with lactation. Moreover, given the expression patterns of the EGFR family members, it is likely that the dominant negative is inhibiting ErbB4 since it is expressed at maximal levels in the late stages of pregnancy and the earliest stages of lactation. These results suggest that while Neu may be a heterodimerization partner for ErbB4, the other family members are able to compensate for loss of *neu* expression in the

Figure 6.1 – The role of Neu in ductal extension and branching.

Mammary gland development proceeds through ductal extension after birth to generate a network of mammary epithelium that fills the fat pad. Shortly after birth, the wild type ducts begin to grow away from the nipple and follow the TEBs through the mammary gland (Panel taken from Figure 4.3). As these TEBs extravagate through the mammary gland, they form the ductal network observed in the adult murine mammary gland (Panel taken from Figure 3.12). To investigate the role of Neu in this process, the mammary specific activation and inactivation of Neu was examined. The mammary specific inactivation of Neu resulted in a delay of extension and reduced branching (Panel taken from Figure 4.3), although these mammary glands eventually were indistinguishable from the control glands. Conversely, the mammary specific expression of activated Neu resulted in increased branching and the formation of numerous lobuloalveolar side buds. These mammary glands also formed numerous preneoplastic lesions and were susceptible to tumorigenesis (Panel taken from Figure 3.12). These results illustrate two approaches to determine the role of Neu in the development of the mammary gland.

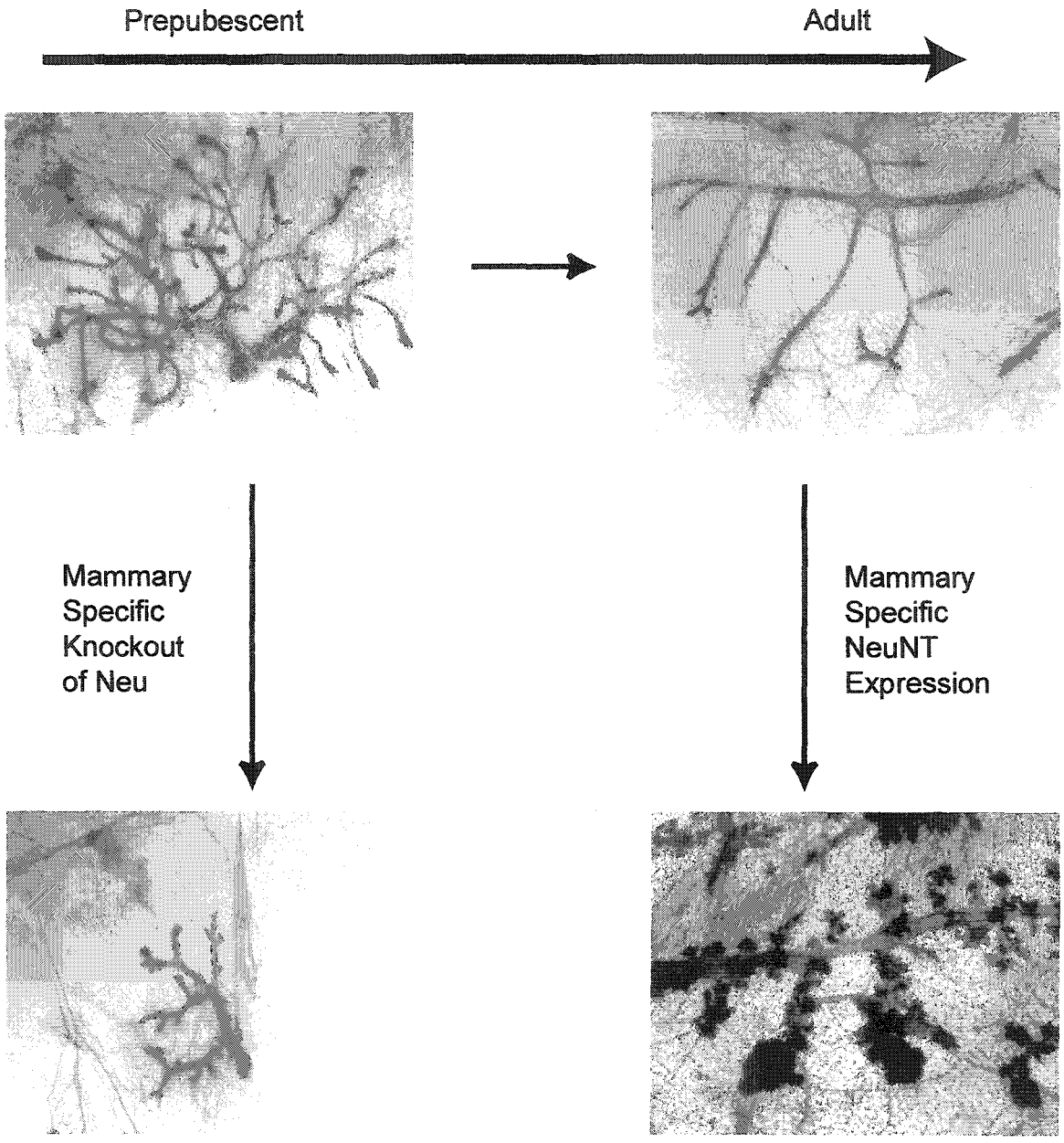
Prepubescent
Adult
Mammary
Specific
Knockout
of Neu
Mammary
Specific
NeuNT
Expression

lactating mammary gland. To test this principle, the ablation of the other family members, particularly ErbB4, should be examined both singly and in combination with a knockout of Neu.

The conditional activation and expression of a constitutively active *neuNT* allele under the control of the endogenous promoter resulted in the development of mammary adenocarcinomas with a remarkable similarity to the human disease. However, given the long latency of this tumor model, it is may not be an ideal choice for many studies into disease progression. In an attempt to decrease the latency of tumor formation in this model, I attempted to derive mice expressing two *neuNT* alleles under the control of the endogenous promoter in all tissues where the endogenous promoter is active. Not surprisingly, this resulted in mice that were not viable. The germline ablation of neu resulted in embryonic lethality due to a lack of cardiac trabeculation at 10.5 dpc (Lee *et al.*, 1995). Interestingly, mice expressing *neuNT* under the control of the endogenous promoter also had a defect in cardiac trabeculation, resulting in lethality two days after the germline ablation. Perhaps the most interesting results from this experiment were observed when the levels of Neu protein and mRNA were assessed. Based upon the wild type and heterozygous levels of *neu* mRNA, the observed level of *neu* mRNA in the homozygote was seen to be far lower than expected. This strongly suggested that there were molecular mechanisms in place to downregulate the levels or activity of *neu*, the promoter or the various signal transduction cascades when the activity of this receptor tyrosine kinase was no longer required. Indeed, one might expect that the expression of an activated *neuNT* allele would result in the activation of this feedback pathway at an

elevated level due to the potency of the oncogene. Additional work will be required to define and assess the regulation of this feedback loop both in the embryo and potentially in mammary gland development and tumorigenesis. The identification and exploitation of such a pathway could have beneficial effects on the development of therapies for HER2 mediated human breast cancer. Further, once this putative negative feedback loop is defined, it would also be interesting to examine the various components for loss of function mutations in HER2 induced tumors.

The theory of the ability of the molecular machinery within the cell to respond and regulate the level of *neuNT* expression can be extended when observations made in the comparison of the germline and conditional activation of *neuNT* expression are considered. The expression of *neuNT* in these two lines of mice was under the control of the endogenous promoter from the same original strain of mice. The only difference between the germline and conditional activation of *neuNT* was in the choice of promoter used to direct Cre recombinase expression. Importantly, the level of *neuNT* expression in the mammary glands of these two strains was shown to be identical. However, the germline *neuNT* mice did not develop tumors while the mammary specific conditional activation of *neuNT* resulted in the formation of mammary comedo-adenocarcinomas. These results share a remarkable similarity to results previously observed with RSV where the injections *in ovo* did not result in sarcomas, while injections in newly hatched chicks did result in the formation of sarcomas (Dolberg and Bissell, 1984; Howlett *et al.*, 1988). While it has been suggested that sarcoma formation in these chicks is due to inappropriate wound repair and complementation of host factors responsive to viral

expression (Dolberg *et al.*, 1985), wounding of the germline neuNT mice did not result in tumorigenesis. However, the regulation of additional factors or signalling pathways in response to expression of a potent oncogene from the earliest developmental stages is likely, analogous to the response of host factors in the RSV experiments. To determine whether the aberrant regulation of the various factors or signal transduction pathways has the ability in the germline *neuNT* mice to impede the formation of Neu mediated tumors, the germline *neuNT* mice could be interbred to a MMTV-Neu transgenic line. If there is a molecular compensation for expression of an activated *neu* allele, an increase in tumor latency should be observed. To assess the putative changes in signals to compensate for *neuNT* expressed under the endogenous promoter in the germline model, mammary epithelial cell lines could be generated from these mice and from wild type controls. Any changes in signaling activated through the addition of ligands for the EGFR family could then be assessed in these cell lines through immunoblots for downstream targets. The ability of the germline *neuNT* mice to adapt, preventing tumorigenesis due to the expression of a powerful oncogene should be the focus of future work in the hope that human therapies may be designed on the basis of these results.

When specific human therapies are designed, it should be a matter of procedure to examine the normal role of the target gene in the various tissues that may be affected by the treatment. For example, Herceptin, an antibody against the extracellular domain of HER2, has been approved and has shown clinical benefits in the treatment of human breast cancers that have overexpression of HER2 (Slamon *et al.*, 2001; Shawver *et al.*, 2002). However, given the embryonic lethality observed in the *erbB2* null mice due to a

lack of cardiac trabeculation, it is not surprising that Herceptin treatment in combination with other drugs resulted in cardiac dysfunction in up to 28% of patients receiving the treatment (Sparano, 2001). Interestingly, consistent with the human data, cardiomyopathy was observed in mice with a targeted deletion of *erbB2* in skeletal muscle (Crone *et al.*, 2002; Ozcelik *et al.*, 2002). While the results in Chapter 5 did not characterize dilated cardiomyopathy in the targeted deletion of *erbB2*, they did illustrate a role for ErbB2 in proprioception.

ErbB2 expression has previously been illustrated in skeletal muscle and to examine its role in muscle development and maintenance, ErbB2$^{Flox/Flox}$ MCK-Cre mice were generated. The muscle specific ablation of ErbB2 resulted in mice with proprioception defects due to the loss of muscle spindles. Interestingly, when various other mouse models with defects in muscle spindle maintenance were examined, a reciprocal signaling loop could be proposed. The proposed signaling loop suggests that the intrafusal muscle fiber and associated afferent require a constant molecular stimulation to maintain the muscle spindle. Through the inhibition of specific signal transduction pathways both *in vitro* and *in vivo*, future work will enable other molecules involved in this reciprocal loop to be elucidated. Further, based on predications from this pathway, predictions may be made and tested. For example, the role of ErbB3 in this signaling loop could be examined through a muscle specific deletion of ErbB3.

In addition to the proprioception defects observed in the muscle specific ErbB2 ablation, during *in vitro* differentiation of primary myoblast cells lacking ErbB2 a large number of these cells underwent apoptosis. These *in vitro* results were recapitulated *in*

vivo when mice lacking ErbB2 in muscle were subject to a crush experiment to examine regeneration. The enhanced apoptotic response in these cells may have been due to an inability to activate the AKT and MAPK pathways. Taken together, these results have illustrated the role of ErbB2 in both the reciprocal signaling loop that is required for maintenance of the muscle spindles and in the regeneration of the extrafusal muscle fibers. Clearly, ErbB2 has multiple roles in the maintenance, development and positioning of skeletal muscle. In the future it will be interesting to explore the role of other EGFR family members in both muscle spindle maintenance and in the development of the neuromuscular junctions.

Finally, a number of results presented herein have illustrated that there are strict requirements for various levels of ErbB2 for normal development. Using the $ErbB2^{Flox/Flox}$ mice, with a hypomorphic level of ErbB2 expression (see Chapter 4), it was noted that the mammary glands in these mice developed normally. With a further reduction in ErbB2 after Cre mediated excision, the mammary glands were developmentally delayed. In contrast to the normal mammary gland development in the $ErbB2^{Flox/Flox}$ mice, it was observed that they had a reduced number of muscle spindles (See Chapter 5). While the 5 fold reduction in the number of muscle spindles from the wild type did not result in phenotypic abnormalities, these results do indicate that there was a different threshold of Neu expression required for normal development. A further reduction in ErbB2 levels in the muscle of the $ErbB2^{Flox/Flox}$ mice through Cre expression resulted in the loss of muscle spindles. Taken together, these results suggest that there are various thresholds of ErbB2 expression required for development of various tissues.

It has been shown that the progression of human breast cancer involves the interaction of both genetic and hormonal factors. Mouse models of this complex disease have previously examined either one of these factors. The results presented herein have illustrated a new model of tumorigenesis where the endogenous promoter controls expression of an activated *neu* allele resulting in tumor formation with the normal response to hormonal stimuli. Additionally, this thesis has elucidated the role of Neu in the development of tissues where expression is normally found. Taken together, it is hoped that these results will provide a framework on which to base future investigations into strategies to treat breast cancers.

REFERENCES

Agus, D. B., R. W. Akita, W. D. Fox, G. D. Lewis, B. Higgins, P. I. Pisacane, J. A. Lofgren, C. Tindell, D. P. Evans, K. Maiese, H. I. Scher and M. X. Sliwkowski (2002). Targeting ligand-activated ErbB2 signaling inhibits breast and prostate tumor growth. Cancer Cell 2, 127-37.

Akiyama, T., S. Matsuda, Y. Namba, T. Saito, K. Toyoshima and T. Yamamoto (1991). The transforming potential of the c-erbB-2 protein is regulated by its autophosphorylation at the carboxyl-terminal domain. Mol Cell Biol 11, 833-42.

Alessi, D. R. and P. Cohen (1998). Mechanism of activation and function of protein kinase B. Curr Opin Genet Dev 8, 55-62.

Altiok, N., J. L. Bessereau and J. P. Changeux (1995). ErbB3 and ErbB2/neu mediate the effect of heregulin on acetylcholine receptor gene expression in muscle: differential expression at the endplate. Embo J 14, 4258-66.

Altucci, L. and H. Gronemeyer (2001). The promise of retinoids to fight against cancer. Nat Rev Cancer 1, 181-93.

Andrechek, E.R. (1997). Tissue Specific Activation and Inactivation of Neu / ErbB2. Fourth Year Undergraduate Thesis. McMaster University, Hamilton, Ontairo, Canada

Andrechek, E. R., W. R. Hardy, A. A. Girgis-Gabardo, R. L. Perry, R. Butler, F. L. Graham, R. C. Kahn, M. A. Rudnicki and W. J. Muller (2002). ErbB2 is required for muscle spindle and myoblast cell survival. Mol Cell Biol 22, 4714-22.

Andrechek, E. R., W. R. Hardy, P. M. Siegel, M. A. Rudnicki, R. D. Cardiff and W. J. Muller (2000). Amplification of the neu/erbB-2 oncogene in a mouse model of mammary tumorigenesis. Proc Natl Acad Sci U S A 97, 3444-9.

Andrulis, I. L., S. B. Bull, M. E. Blackstein, D. Sutherland, C. Mak, S. Sidlofsky, K. P. Pritzker, R. W. Hartwick, W. Hanna, L. Lickley, R. Wilkinson, A. Qizilbash, U. Ambus, M. Lipa, H. Weizel, A. Katz, M. Baida, S. Mariz, G. Stoik, P. Dacamara, D. Strongitharm, W. Geddie and D. McCready (1998). neu/erbB-2 amplification identifies a poor-prognosis group of women with node-negative breast cancer. Toronto Breast Cancer Study Group. J Clin Oncol 16, 1340-9.

Araki, K., M. Araki, J. Miyazaki and P. Vassalli (1995). Site-specific recombination of a transgene in fertilized eggs by transient expression of Cre recombinase. Proc Natl Acad Sci U S A 92, 160-4.

Arteaga, C. L. (2002). Overview of epidermal growth factor receptor biology and its role as a therapeutic target in human neoplasia. Semin Oncol 29, 3-9.

Bader, D., T. Masaki and D. A. Fischman (1982). Immunochemical analysis of myosin heavy chain during avian myogenesis in vivo and in vitro. J Cell Biol 95, 763-70.

Baert, J. L., D. Monte, E. A. Musgrove, O. Albagli, R. L. Sutherland and Y. de Launoit (1997). Expression of the PEA3 group of ETS-related transcription factors in human breast-cancer cells. Int J Cancer 70, 590-7.

Bargmann, C. I., M. C. Hung and R. A. Weinberg (1986). Multiple independent activations of the neu oncogene by a point mutation altering the transmembrane domain of p185. Cell 45, 649-57.

Bargmann, C. I., M. C. Hung and R. A. Weinberg (1986). The neu oncogene encodes an epidermal growth factor receptor-related protein. Nature 319, 226-30.

Bargmann, C. I. and R. A. Weinberg (1988). Increased tyrosine kinase activity associated with the protein encoded by the activated neu oncogene. Proc Natl Acad Sci U S A 85, 5394-8.

Bauknecht, T., M. Kohler, I. Janz and A. Pfleiderer (1989). The occurrence of epidermal growth factor receptors and the characterization of EGF-like factors in human ovarian, endometrial, cervical and breast cancer. EGF receptors and factors in gynecological carcinomas. J Cancer Res Clin Oncol 115, 193-9.

Bekri, S., J. Adelaide, S. Merscher, J. Grosgeorge, F. Caroli-Bosc, D. Perucca-Lostanlen, P. M. Kelley, M. J. Pebusque, C. Theillet, D. Birnbaum and P. Gaudray (1997). Detailed map of a region commonly amplified at 11q13-->q14 in human breast carcinoma. Cytogenet Cell Genet 79, 125-31.

Benz, C. C., R. C. O'Hagan, B. Richter, G. K. Scott, C. H. Chang, X. Xiong, K. Chew, B. M. Ljung, S. Edgerton, A. Thor and J. A. Hassell (1997). HER2/Neu and the Ets transcription activator PEA3 are coordinately upregulated in human breast cancer. Oncogene 15, 1513-25.

Bera, T. K., S. Lee, G. Salvatore, B. Lee and I. Pastan (2001). MRP8, a new member of ABC transporter superfamily, identified by EST database mining and gene prediction program, is highly expressed in breast cancer. Mol Med 7, 509-16.

Bieche, I., M. H. Champeme, F. Matifas, C. S. Cropp, R. Callahan and R. Lidereau (1993). Two distinct regions involved in 1p deletion in human primary breast cancer. Cancer Res 53, 1990-4.

Bieche, I. and R. Lidereau (1995). Genetic alterations in breast cancer. Genes Chromosomes Cancer 14, 227-51.

Blume-Jensen, P. and T. Hunter (2001). Oncogenic kinase signalling. Nature 411, 355-65.

Bodey, B., B. Bodey, Jr., A. M. Groger, J. V. Luck, S. E. Siegel, C. R. Taylor and H. E. Kaiser (1997). Clinical and prognostic significance of the expression of the c-erbB-2 and c-erbB-3 oncoproteins in primary and metastatic malignant melanomas and breast carcinomas. Anticancer Res 17, 1319-30.

Bouchard, L., L. Lamarre, P. J. Tremblay and P. Jolicoeur (1989). Stochastic appearance of mammary tumors in transgenic mice carrying the MMTV/c-neu oncogene. Cell 57, 931-6.

Brandt, R., R. Eisenbrandt, F. Leenders, W. Zschiesche, B. Binas, C. Juergensen and F. Theuring (2000). Mammary gland specific hEGF receptor transgene expression induces neoplasia and inhibits differentiation. Oncogene 19, 2129-37.

Breznik, T., V. Traina-Dorge, M. Gama-Sosa, C. W. Gehrke, M. Ehrlich, D. Medina, J. S. Butel and J. C. Cohen (1984). Mouse mammary tumor virus DNA methylation: tissue-specific variation. Virology 136, 69-77.

Britsch, S., L. Li, S. Kirchhoff, F. Theuring, V. Brinkmann, C. Birchmeier and D. Riethmacher (1998). The ErbB2 and ErbB3 receptors and their ligand, neuregulin-1, are essential for development of the sympathetic nervous system. Genes Dev 12, 1825-36.

Brown, S.T. (2002). Identification of Novel Transcription Factors for the Neu / ErbB2 Proto-Oncogene. Masters Thesis, McMaster University, Hamilton, Ontairo Canada.

Bruning, J. C., M. D. Michael, J. N. Winnay, T. Hayashi, D. Horsch, D. Accili, L. J. Goodyear and C. R. Kahn (1998). A muscle-specific insulin receptor knockout exhibits features of the metabolic syndrome of NIDDM without altering glucose tolerance. Mol Cell 2, 559-69.

Burgering, B. M. and P. J. Coffer (1995). Protein kinase B (c-Akt) in phosphatidylinositol-3-OH kinase signal transduction. Nature 376, 599-602.

Butler, R. and I. M. Payk (1986). Differential staining of different types of peripheral nerve and muscle. J Neurosci Methods 16, 265-76.

Canute, G. W., S. L. Longo, J. A. Longo, M. M. Shetler, T. E. Coyle, J. A. Winfield and P. J. Hahn (1998). The hydroxyurea-induced loss of double-minute chromosomes

containing amplified epidermal growth factor receptor genes reduces the tumorigenicity and growth of human glioblastoma multiforme. Neurosurgery 42, 609-16.

Canute, G. W., S. L. Longo, J. A. Longo, J. A. Winfield, B. H. Nevaldine and P. J. Hahn (1996). Hydroxyurea accelerates the loss of epidermal growth factor receptor genes amplified as double-minute chromosomes in human glioblastoma multiforme. Neurosurgery 39, 976-83.

Cardiff, R. D., M. R. Anver, B. A. Gusterson, L. Hennighausen, R. A. Jensen, M. J. Merino, S. Rehm, J. Russo, F. A. Tavassoli, L. M. Wakefield, J. M. Ward and J. E. Green (2000). The mammary pathology of genetically engineered mice: the consensus report and recommendations from the Annapolis meeting. Oncogene 19, 968-88.

Cardiff, R. D., E. Sinn, W. Muller and P. Leder (1991). Transgenic oncogene mice. Tumor phenotype predicts genotype. Am J Pathol 139, 495-501.

Cardiff, R. D. and S. R. Wellings (1999). The comparative pathology of human and mouse mammary glands. J Mammary Gland Biol Neoplasia 4, 105-22.

Carraway, K. L., 3rd, E. A. Rossi, M. Komatsu, S. A. Price-Schiavi, D. Huang, P. M. Guy, M. E. Carvajal, N. Fregien, C. A. Carraway and K. L. Carraway (1999). An intramembrane modulator of the ErbB2 receptor tyrosine kinase that potentiates neuregulin signaling. J Biol Chem 274, 5263-6.

Carraway, K. L., S. A. Price-Schiavi, M. Komatsu, N. Idris, A. Perez, P. Li, S. Jepson, X. Zhu, M. E. Carvajal and C. A. Carraway (2000). Multiple facets of sialomucin complex/MUC4, a membrane mucin and erbb2 ligand, in tumors and tissues (Y2K update). Front Biosci 5, D95-D107.

Carter, P., L. Presta, C. M. Gorman, J. B. Ridgway, D. Henner, W. L. Wong, A. M. Rowland, C. Kotts, M. E. Carver and H. M. Shepard (1992). Humanization of an anti-p185HER2 antibody for human cancer therapy. Proc Natl Acad Sci U S A 89, 4285-9.

Chaillet, J. R., D. S. Bader and P. Leder (1995). Regulation of genomic imprinting by gametic and embryonic processes. Genes Dev 9, 1177-87.

Chamberlain, J. S., J. B. Jaynes and S. D. Hauschka (1985). Regulation of creatine kinase induction in differentiating mouse myoblasts. Mol Cell Biol 5, 484-92.

Chan, R., W. R. Hardy, M. A. Laing, S. E. Hardy and W. J. Muller (2002). The catalytic activity of the ErbB-2 receptor tyrosine kinase is essential for embryonic development. Mol Cell Biol 22, 1073-8.

Chavrier, P., M. Zerial, P. Lemaire, J. Almendral, R. Bravo and P. Charnay (1988). A gene encoding a protein with zinc fingers is activated during G0/G1 transition in cultured cells. Embo J 7, 29-35.

Chen, H. H., W. G. Tourtellotte and E. Frank (2002). Muscle spindle-derived neurotrophin 3 regulates synaptic connectivity between muscle sensory and motor neurons. J Neurosci 22, 3512-9.

Chiang, S. Y., R. W. Burli, C. C. Benz, L. Gawron, G. K. Scott, P. B. Dervan and T. A. Beerman (2000). Targeting the ets binding site of the HER2/neu promoter with pyrrole-imidazole polyamides. J Biol Chem 275, 24246-54.

Chirgwin, J. M., A. E. Przybyla, R. J. MacDonald and W. J. Rutter (1979). Isolation of biologically active ribonucleic acid from sources enriched in ribonuclease. Biochemistry 18, 5294-9.

Choi, Y. W., D. Henrard, I. Lee and S. R. Ross (1987). The mouse mammary tumor virus long terminal repeat directs expression in epithelial and lymphoid cells of different tissues in transgenic mice. J Virol 61, 3013-9.

Chytil, F. and D. E. Ong (1976). Mediation of retinoic acid-induced growth and anti-tumour activity. Nature 260, 49-51.

Claus, E. B., J. M. Schildkraut, W. D. Thompson and N. J. Risch (1996). The genetic attributable risk of breast and ovarian cancer. Cancer 77, 2318-24.

Coleman, S., G. B. Silberstein and C. W. Daniel (1988). Ductal morphogenesis in the mouse mammary gland: evidence supporting a role for epidermal growth factor. Dev Biol 127, 304-15.

Coussens, L., T. L. Yang-Feng, Y. C. Liao, E. Chen, A. Gray, J. McGrath, P. H. Seeburg, T. A. Libermann, J. Schlessinger, U. Francke and et al. (1985). Tyrosine kinase receptor with extensive homology to EGF receptor shares chromosomal location with neu oncogene. Science 230, 1132-9.

Crone, S. A., Y. Y. Zhao, L. Fan, Y. Gu, S. Minamisawa, Y. Liu, K. L. Peterson, J. Chen, R. Kahn, G. Condorelli, J. Ross, Jr., K. R. Chien and K. F. Lee (2002). ErbB2 is essential in the prevention of dilated cardiomyopathy. Nat Med 8, 459-65.

Cunha, G. R. (1994). Role of mesenchymal-epithelial interactions in normal and abnormal development of the mammary gland and prostate. Cancer 74, 1030-44.

Cunha, G. R., P. Young, Y. K. Hom, P. S. Cooke, J. A. Taylor and D. B. Lubahn (1997). Elucidation of a role for stromal steroid hormone receptors in mammary gland

growth and development using tissue recombinants. J Mammary Gland Biol Neoplasia 2, 393-402.

Daniel, C. W., G. B. Silberstein, K. Van Horn, P. Strickland and S. Robinson (1989). TGF-beta 1-induced inhibition of mouse mammary ductal growth: developmental specificity and characterization. Dev Biol 135, 20-30.

Daniel, C. W., P. Strickland and Y. Friedmann (1995). Expression and functional role of E- and P-cadherins in mouse mammary ductal morphogenesis and growth. Dev Biol 169, 511-9.

Dankort, D. L. and W. J. Muller (1996). Transgenic models of breast cancer metastasis. Cancer Treat Res 83, 71-88.

D'Cruz, C. M., E. J. Gunther, R. B. Boxer, J. L. Hartman, L. Sintasath, S. E. Moody, J. D. Cox, S. I. Ha, G. K. Belka, A. Golant, R. D. Cardiff and L. A. Chodosh (2001). c-MYC induces mammary tumorigenesis by means of a preferred pathway involving spontaneous Kras2 mutations. Nat Med 7, 235-9.

D'Cruz, C. M., S. E. Moody, S. R. Master, J. L. Hartman, E. A. Keiper, M. B. Imielinski, J. D. Cox, J. Y. Wang, S. I. Ha, B. A. Keister and L. A. Chodosh (2002). Persistent parity-induced changes in growth factors, TGF-beta3, and differentiation in the rodent mammary gland. Mol Endocrinol 16, 2034-51.

Debnath, J., K. R. Mills, N. L. Collins, M. J. Reginato, S. K. Muthuswamy and J. S. Brugge (2002). The role of apoptosis in creating and maintaining luminal space within normal and oncogene-expressing mammary acini. Cell 111, 29-40.

Deckard-Janatpour, K., Muller, W.J., Chodosh, L.A., Gardner, H.P., Marquis, S.T., Coffey, R. and R.D. Cardiff (1997). Differential Expression of the *neu* transgene in murine mammary tissue. Int J Oncology 11, 235-241.

Desai, K. V., N. Xiao, W. Wang, L. Gangi, J. Greene, J. I. Powell, R. Dickson, P. Furth, K. Hunter, R. Kucherlapati, R. Simon, E. T. Liu and J. E. Green (2002). Initiating oncogenic event determines gene-expression patterns of human breast cancer models. Proc Natl Acad Sci U S A 99, 6967-72.

Di Fiore, P. P., J. H. Pierce, M. H. Kraus, O. Segatto, C. R. King and S. A. Aaronson (1987). erbB-2 is a potent oncogene when overexpressed in NIH/3T3 cells. Science 237, 178-82.

Dolberg, D. S. and M. J. Bissell (1984). Inability of Rous sarcoma virus to cause sarcomas in the avian embryo. Nature 309, 552-6.

Dolberg, D. S., R. Hollingsworth, M. Hertle and M. J. Bissell (1985). Wounding and its role in RSV-mediated tumor formation. Science 230, 676-8.

Donehower, L. A., M. Harvey, B. L. Slagle, M. J. McArthur, C. A. Montgomery, Jr., J. S. Butel and A. Bradley (1992). Mice deficient for p53 are developmentally normal but susceptible to spontaneous tumours. Nature 356, 215-21.

Dougall, W. C., X. Qian, N. C. Peterson, M. J. Miller, A. Samanta and M. I. Greene (1994). The neu-oncogene: signal transduction pathways, transformation mechanisms and evolving therapies. Oncogene 9, 2109-23.

Dulbecco, R., W. R. Allen, M. Bologna and M. Bowman (1986). Marker evolution during the development of the rat mammary gland: stem cells identified by markers and the role of myoepithelial cells. Cancer Res 46, 2449-56.

Dulbecco, R., M. Henahan and B. Armstrong (1982). Cell types and morphogenesis in the mammary gland. Proc Natl Acad Sci U S A 79, 7346-50.

Dulbecco, R., M. Unger, B. Armstrong, M. Bowman and P. Syka (1983). Epithelial cell types and their evolution in the rat mammary gland determined by immunological markers. Proc Natl Acad Sci U S A 80, 1033-7.

Earp, H. S., T. L. Dawson, X. Li and H. Yu (1995). Heterodimerization and functional interaction between EGF receptor family members: a new signaling paradigm with implications for breast cancer research. Breast Cancer Res Treat 35, 115-32.

Elledge, R. M. and D. C. Allred (1994). The p53 tumor suppressor gene in breast cancer. Breast Cancer Res Treat 32, 39-47.

Elledge, R. M. and D. C. Allred (1998). Prognostic and predictive value of p53 and p21 in breast cancer. Breast Cancer Res Treat 52, 79-98.

Erickson, S. L., K. S. O'Shea, N. Ghaboosi, L. Loverro, G. Frantz, M. Bauer, L. H. Lu and M. W. Moore (1997). ErbB3 is required for normal cerebellar and cardiac development: a comparison with ErbB2-and heregulin-deficient mice. Development 124, 4999-5011.

Ernfors, P., K. F. Lee, J. Kucera and R. Jaenisch (1994). Lack of neurotrophin-3 leads to deficiencies in the peripheral nervous system and loss of limb proprioceptive afferents. Cell 77, 503-12.

Feinberg, A. P. and B. Vogelstein (1983). A technique for radiolabeling DNA restriction endonuclease fragments to high specific activity. Anal Biochem 132, 6-13.

Fendrick, J. L., A. M. Raafat and S. Z. Haslam (1998). Mammary gland growth and development from the postnatal period to postmenopause: ovarian steroid receptor ontogeny and regulation in the mouse. J Mammary Gland Biol Neoplasia 3, 7-22.

Fischbach, G. D. and K. M. Rosen (1997). ARIA: a neuromuscular junction neuregulin. Annu Rev Neurosci 20, 429-58.

Ford, A. C. and J. R. Grandis (2003). Targeting epidermal growth factor receptor in head and neck cancer. Head Neck 25, 67-73.

Fowler, K. J., F. Walker, W. Alexander, M. L. Hibbs, E. C. Nice, R. M. Bohmer, G. B. Mann, C. Thumwood, R. Maglitto, J. A. Danks and et al. (1995). A mutation in the epidermal growth factor receptor in waved-2 mice has a profound effect on receptor biochemistry that results in impaired lactation. Proc Natl Acad Sci U S A 92, 1465-9.

Franke, T. F., S. I. Yang, T. O. Chan, K. Datta, A. Kazlauskas, D. K. Morrison, D. R. Kaplan and P. N. Tsichlis (1995). The protein kinase encoded by the Akt proto-oncogene is a target of the PDGF-activated phosphatidylinositol 3-kinase. Cell 81, 727-36.

Garcia, J. M., J. M. Silva, G. Dominguez, R. Gonzalez, A. Navarro, L. Carretero, M. Provencio, P. Espana and F. Bonilla (1999). Allelic loss of the PTEN region (10q23) in breast carcinomas of poor pathophenotype. Breast Cancer Res Treat 57, 237-43.

Garratt, A. N., O. Voiculescu, P. Topilko, P. Charnay and C. Birchmeier (2000). A dual role of erbB2 in myelination and in expansion of the schwann cell precursor pool. J Cell Biol 148, 1035-46.

Gassmann, M., F. Casagranda, D. Orioli, H. Simon, C. Lai, R. Klein and G. Lemke (1995). Aberrant neural and cardiac development in mice lacking the ErbB4 neuregulin receptor. Nature 378, 390-4.

Gilbertson, R., R. Hernan, T. Pietsch, L. Pinto, P. Scotting, R. Allibone, D. Ellison, R. Perry, A. Pearson and J. Lunec (2001). Novel ERBB4 juxtamembrane splice variants are frequently expressed in childhood medulloblastoma. Genes Chromosomes Cancer 31, 288-94.

Gilmour, L. M., K. G. Macleod, A. McCaig, W. J. Gullick, J. F. Smyth and S. P. Langdon (2001). Expression of erbB-4/HER-4 growth factor receptor isoforms in ovarian cancer. Cancer Res 61, 2169-76.

Greenberg, P. A., G. N. Hortobagyi, T. L. Smith, L. D. Ziegler, D. K. Frye and A. U. Buzdar (1996). Long-term follow-up of patients with complete remission following combination chemotherapy for metastatic breast cancer. J Clin Oncol 14, 2197-205.

Grosse, R., F. D. Bohmer, B. Binas, A. Kurtz, E. Spitzer, T. Muller and W. Zschiesche (1992). Mammary-derived growth inhibitor (MDGI). Cancer Treat Res 61, 69-96.

Grunt, W., E. Dittrich, M. Offterdinger, S. M. Schneider, C. Dittrich and H. Huber (1998). Effects of retinoic acid and fenretinide on the c-erbB-2 expression, growth and cisplatin sensitivity of breast cancer cells. Br J Cancer 78, 79-87.

Gu, H., J. D. Marth, P. C. Orban, H. Mossmann and K. Rajewsky (1994). Deletion of a DNA polymerase beta gene segment in T cells using cell type-specific gene targeting. Science 265, 103-6.

Guy, C. T., R. D. Cardiff and W. J. Muller (1992). Induction of mammary tumors by expression of polyomavirus middle T oncogene: a transgenic mouse model for metastatic disease. Mol Cell Biol 12, 954-61.

Guy, C. T., R. D. Cardiff and W. J. Muller (1996). Activated neu induces rapid tumor progression. J Biol Chem 271, 7673-8.

Guy, C. T., M. A. Webster, M. Schaller, T. J. Parsons, R. D. Cardiff and W. J. Muller (1992). Expression of the neu protooncogene in the mammary epithelium of transgenic mice induces metastatic disease. Proc Natl Acad Sci U S A 89, 10578-82.

Guy, P. M., J. V. Platko, L. C. Cantley, R. A. Cerione and K. L. Carraway, 3rd (1994). Insect cell-expressed p180erbB3 possesses an impaired tyrosine kinase activity. Proc Natl Acad Sci U S A 91, 8132-6.

Halter, S. A., P. Dempsey, Y. Matsui, M. K. Stokes, R. Graves-Deal, B. L. Hogan and R. J. Coffey (1992). Distinctive patterns of hyperplasia in transgenic mice with mouse mammary tumor virus transforming growth factor-alpha. Characterization of mammary gland and skin proliferations. Am J Pathol 140, 1131-46.

Han, D. C. and J. L. Guan (1999). Association of focal adhesion kinase with Grb7 and its role in cell migration. J Biol Chem 274, 24425-30.

Hansen, L. A., N. Alexander, M. E. Hogan, J. P. Sundberg, A. Dlugosz, D. W. Threadgill, T. Magnuson and S. H. Yuspa (1997). Genetically null mice reveal a central role for epidermal growth factor receptor in the differentiation of the hair follicle and normal hair development. Am J Pathol 150, 1959-75.

Harris, A. L., S. Nicholson, R. Sainsbury, C. Wright and J. Farndon (1992). Epidermal growth factor receptor and other oncogenes as prognostic markers. J Natl Cancer Inst Monogr 181-7.

Hazan, R., B. Margolis, M. Dombalagian, A. Ullrich, A. Zilberstein and J. Schlessinger (1990). Identification of autophosphorylation sites of HER2/neu. Cell Growth Differ 1, 3-7.

Heldin, C. H. (1995). Dimerization of cell surface receptors in signal transduction. Cell 80, 213-23.

Henderson, B. E., R. K. Ross and M. C. Pike (1991). Toward the primary prevention of cancer. Science 254, 1131-8.

Hennighausen, L. and G. W. Robinson (1998). Think globally, act locally: the making of a mouse mammary gland. Genes Dev 12, 449-55.

Hennighausen, L. G. and A. E. Sippel (1982). Mouse whey acidic protein is a novel member of the family of 'four-disulfide core' proteins. Nucleic Acids Res 10, 2677-84.

Henrard, D. and S. R. Ross (1988). Endogenous mouse mammary tumor virus is expressed in several organs in addition to the lactating mammary gland. J Virol 62, 3046-9.

Hogg, N. A., C. J. Harrison and C. Tickle (1983). Lumen formation in the developing mouse mammary gland. J Embryol Exp Morphol 73, 39-57.

Howlett, A. R., V. C. Carter, G. S. Martin and M. J. Bissell (1988). pp60v-src tyrosine kinase is expressed and active in sarcoma-free avian embryos microinjected with Rous sarcoma virus. Proc Natl Acad Sci U S A 85, 7587-91.

Humphreys, R. C., M. Krajewska, S. Krnacik, R. Jaeger, H. Weiher, S. Krajewski, J. C. Reed and J. M. Rosen (1996). Apoptosis in the terminal endbud of the murine mammary gland: a mechanism of ductal morphogenesis. Development 122, 4013-22.

Hynes, N. E. and D. F. Stern (1994). The biology of erbB-2/neu/HER-2 and its role in cancer. Biochim Biophys Acta 1198, 165-84.

Jaenisch, R. (1980). Retroviruses and embryogenesis: microinjection of Moloney leukemia virus into midgestation mouse embryos. Cell 19, 181-8.

Jaynes, J. B., J. S. Chamberlain, J. N. Buskin, J. E. Johnson and S. D. Hauschka (1986). Transcriptional regulation of the muscle creatine kinase gene and regulated expression in transfected mouse myoblasts. Mol Cell Biol 6, 2855-64.

Jepson, S., M. Komatsu, B. Haq, M. E. Arango, D. Huang, C. A. Carraway and K. L. Carraway (2002). Muc4/sialomucin complex, the intramembrane ErbB2 ligand,

induces specific phosphorylation of ErbB2 and enhances expression of p27(kip), but does not activate mitogen-activated kinase or protein kinaseB/Akt pathways. Oncogene 21, 7524-32.

Jerry, D. J., F. S. Kittrell, C. Kuperwasser, R. Laucirica, E. S. Dickinson, P. J. Bonilla, J. S. Butel and D. Medina (2000). A mammary-specific model demonstrates the role of the p53 tumor suppressor gene in tumor development. Oncogene 19, 1052-8.

Jhappan, C., C. Stahle, R. N. Harkins, N. Fausto, G. H. Smith and G. T. Merlino (1990). TGF alpha overexpression in transgenic mice induces liver neoplasia and abnormal development of the mammary gland and pancreas. Cell 61, 1137-46.

Jo, S. A., X. Zhu, M. A. Marchionni and S. J. Burden (1995). Neuregulins are concentrated at nerve-muscle synapses and activate ACh-receptor gene expression. Nature 373, 158-61.

Jones, F. E. and D. F. Stern (1999). Expression of dominant-negative ErbB2 in the mammary gland of transgenic mice reveals a role in lobuloalveolar development and lactation. Oncogene 18, 3481-90.

Jones, F. E., T. Welte, X. Y. Fu and D. F. Stern (1999). ErbB4 signaling in the mammary gland is required for lobuloalveolar development and Stat5 activation during lactation. J Cell Biol 147, 77-88.

Jungbluth, A. A., E. Stockert, H. J. Huang, V. P. Collins, K. Coplan, K. Iversen, D. Kolb, T. J. Johns, A. M. Scott, W. J. Gullick, G. Ritter, L. Cohen, M. J. Scanlan, W. K. Cavanee and L. J. Old (2003). A monoclonal antibody recognizing human cancers with amplification/overexpression of the human epidermal growth factor receptor. Proc Natl Acad Sci U S A

Kamalati, T., B. Niranjan, J. Yant and L. Buluwela (1999). HGF/SF in mammary epithelial growth and morphogenesis: in vitro and in vivo models. J Mammary Gland Biol Neoplasia 4, 69-77.

Kauraniemi, P., M. Barlund, O. Monni and A. Kallioniemi (2001). New amplified and highly expressed genes discovered in the ERBB2 amplicon in breast cancer by cDNA microarrays. Cancer Res 61, 8235-40.

Kavanaugh, W. M., C. W. Turck and L. T. Williams (1995). PTB domain binding to signaling proteins through a sequence motif containing phosphotyrosine. Science 268, 1177-9.

Keegan, K. and J. A. Cooper (1996). Use of the two hybrid system to detect the association of the protein-tyrosine-phosphatase, SHPTP2, with another SH2-containing protein, Grb7. Oncogene 12, 1537-44.

Kiguchi, K., D. Bol, S. Carbajal, L. Beltran, S. Moats, K. Chan, J. Jorcano and J. DiGiovanni (2000). Constitutive expression of erbB2 in epidermis of transgenic mice results in epidermal hyperproliferation and spontaneous skin tumor development. Oncogene 19, 4243-54.

Kita, Y. A., J. Barff, Y. Luo, D. Wen, D. Brankow, S. Hu, N. Liu, S. A. Prigent, W. J. Gullick and M. Nicolson (1994). NDF/heregulin stimulates the phosphorylation of Her3/erbB3. FEBS Lett 349, 139-43.

Kjellen, L., I. Pettersson, P. Lillhager, M. L. Steen, U. Pettersson, P. Lehtonen, T. Karlsson, E. Ruoslahti and L. Hellman (1989). Primary structure of a mouse mastocytoma proteoglycan core protein. Biochem J 263, 105-13.

Klein, R., I. Silos-Santiago, R. J. Smeyne, S. A. Lira, R. Brambilla, S. Bryant, L. Zhang, W. D. Snider and M. Barbacid (1994). Disruption of the neurotrophin-3 receptor gene trkC eliminates la muscle afferents and results in abnormal movements. Nature 368, 249-51.

Klijn, J. G., P. M. Berns, P. I. Schmitz and J. A. Foekens (1992). The clinical significance of epidermal growth factor receptor (EGF-R) in human breast cancer: a review on 5232 patients. Endocr Rev 13, 3-17.

Knighton, D. R., D. L. Cadena, J. Zheng, L. F. Ten Eyck, S. S. Taylor, J. M. Sowadski and G. N. Gill (1993). Structural features that specify tyrosine kinase activity deduced from homology modeling of the epidermal growth factor receptor. Proc Natl Acad Sci U S A 90, 5001-5.

Korach, K. S. (1994). Insights from the study of animals lacking functional estrogen receptor. Science 266, 1524-7.

Korach, K. S., J. F. Couse, S. W. Curtis, T. F. Washburn, J. Lindzey, K. S. Kimbro, E. M. Eddy, S. Migliaccio, S. M. Snedeker, D. B. Lubahn, D. W. Schomberg and E. P. Smith (1996). Estrogen receptor gene disruption: molecular characterization and experimental and clinical phenotypes. Recent Prog Horm Res 51, 159-86; discussion 186-8.

Krane, I. M. and P. Leder (1996). NDF/heregulin induces persistence of terminal end buds and adenocarcinomas in the mammary glands of transgenic mice. Oncogene 12, 1781-8.

Kraus, M. H., W. Issing, T. Miki, N. C. Popescu and S. A. Aaronson (1989). Isolation and characterization of ERBB3, a third member of the ERBB/epidermal growth factor receptor family: evidence for overexpression in a subset of human mammary tumors. Proc Natl Acad Sci U S A 86, 9193-7.

Lasky, L. A., M. S. Singer, D. Dowbenko, Y. Imai, W. J. Henzel, C. Grimley, C. Fennie, N. Gillett, S. R. Watson and S. D. Rosen (1992). An endothelial ligand for L-selectin is a novel mucin-like molecule. Cell 69, 927-38.

Leder, A., P. K. Pattengale, A. Kuo, T. A. Stewart and P. Leder (1986). Consequences of widespread deregulation of the c-myc gene in transgenic mice: multiple neoplasms and normal development. Cell 45, 485-95.

Lee, K. F., H. Simon, H. Chen, B. Bates, M. C. Hung and C. Hauser (1995). Requirement for neuregulin receptor erbB2 in neural and cardiac development. Nature 378, 394-8.

Lemoine, N. R., D. M. Barnes, D. P. Hollywood, C. M. Hughes, P. Smith, E. Dublin, S. A. Prigent, W. J. Gullick and H. C. Hurst (1992). Expression of the ERBB3 gene product in breast cancer. Br J Cancer 66, 1116-21.

Li, Y., J. Ren, W. Yu, Q. Li, H. Kuwahara, L. Yin, K. L. Carraway, 3rd and D. Kufe (2001). The epidermal growth factor receptor regulates interaction of the human DF3/MUC1 carcinoma antigen with c-Src and beta-catenin. J Biol Chem 276, 35239-42.

Liao, D. J. and R. B. Dickson (2000). c-Myc in breast cancer. Endocr Relat Cancer 7, 143-64.

Lin, W., H. B. Sanchez, T. Deerinck, J. K. Morris, M. Ellisman and K. F. Lee (2000). Aberrant development of motor axons and neuromuscular synapses in erbB2-deficient mice. Proc Natl Acad Sci U S A 97, 1299-304.

Loeb, J. A. and G. D. Fischbach (1997). Neurotrophic factors increase neuregulin expression in embryonic ventral spinal cord neurons. J Neurosci 17, 1416-24.

Luetteke, N. C., H. K. Phillips, T. H. Qiu, N. G. Copeland, H. S. Earp, N. A. Jenkins and D. C. Lee (1994). The mouse waved-2 phenotype results from a point mutation in the EGF receptor tyrosine kinase. Genes Dev 8, 399-413.

Mangues, R., S. Schwartz, I. Seidman and A. Pellicer (1995). Promoter demethylation in MMTV/N-rasN transgenic mice required for transgene expression and tumorigenesis. Mol Carcinog 14, 94-102.

Matsui, Y., S. A. Halter, J. T. Holt, B. L. Hogan and R. J. Coffey (1990). Development of mammary hyperplasia and neoplasia in MMTV-TGF alpha transgenic mice. Cell 61, 1147-55.

Megeney, L. A., B. Kablar, K. Garrett, J. E. Anderson and M. A. Rudnicki (1996). MyoD is required for myogenic stem cell function in adult skeletal muscle. Genes Dev 10, 1173-83.

Melton, D. A., P. A. Krieg, M. R. Rebagliati, T. Maniatis, K. Zinn and M. R. Green (1984). Efficient in vitro synthesis of biologically active RNA and RNA hybridization probes from plasmids containing a bacteriophage SP6 promoter. Nucleic Acids Res 12, 7035-56.

Miki, Y., J. Swensen, D. Shattuck-Eidens, P. A. Futreal, K. Harshman, S. Tavtigian, Q. Liu, C. Cochran, L. M. Bennett, W. Ding and et al. (1994). A strong candidate for the breast and ovarian cancer susceptibility gene BRCA1. Science 266, 66-71.

Missias, A. C., G. C. Chu, B. J. Klocke, J. R. Sanes and J. P. Merlie (1996). Maturation of the acetylcholine receptor in skeletal muscle: regulation of the AChR gamma-to-epsilon switch. Dev Biol 179, 223-38.

Missias, A. C., J. Mudd, J. M. Cunningham, J. H. Steinbach, J. P. Merlie and J. R. Sanes (1997). Deficient development and maintenance of postsynaptic specializations in mutant mice lacking an 'adult' acetylcholine receptor subunit. Development 124, 5075-86.

Mitchell, P. J. and R. Tjian (1989). Transcriptional regulation in mammalian cells by sequence-specific DNA binding proteins. Science 245, 371-8.

Montagna, C., E. R. Andrechek, H. Padilla-Nash, W. J. Muller and T. Ried (2002). Centrosome abnormalities, recurring deletions of chromosome 4, and genomic amplification of HER2/neu define mouse mammary gland adenocarcinomas induced by mutant HER2/neu. Oncogene 21, 890-8.

Morris, J. K., W. Lin, C. Hauser, Y. Marchuk, D. Getman and K. F. Lee (1999). Rescue of the cardiac defect in ErbB2 mutant mice reveals essential roles of ErbB2 in peripheral nervous system development. Neuron 23, 273-83.

Morrison, B. W. and P. Leder (1994). neu and ras initiate murine mammary tumors that share genetic markers generally absent in c-myc and int-2-initiated tumors. Oncogene 9, 3417-26.

Moscoso, L. M., G. C. Chu, M. Gautam, P. G. Noakes, J. P. Merlie and J. R. Sanes (1995). Synapse-associated expression of an acetylcholine receptor-inducing protein,

ARIA/heregulin, and its putative receptors, ErbB2 and ErbB3, in developing mammalian muscle. Dev Biol 172, 158-69.

Mukku, V. R. and G. M. Stancel (1985). Regulation of epidermal growth factor receptor by estrogen. J Biol Chem 260, 9820-4.

Muller, W. J., C. L. Arteaga, S. K. Muthuswamy, P. M. Siegel, M. A. Webster, R. D. Cardiff, K. S. Meise, F. Li, S. A. Halter and R. J. Coffey (1996). Synergistic interaction of the Neu proto-oncogene product and transforming growth factor alpha in the mammary epithelium of transgenic mice. Mol Cell Biol 16, 5726-36.

Muller, W. J., E. Sinn, P. K. Pattengale, R. Wallace and P. Leder (1988). Single-step induction of mammary adenocarcinoma in transgenic mice bearing the activated c-neu oncogene. Cell 54, 105-15.

Muthuswamy, S. K. and W. J. Muller (1994). Activation of the Src family of tyrosine kinases in mammary tumorigenesis. Adv Cancer Res 64, 111-23.

Muthuswamy, S. K. and W. J. Muller (1995). Direct and specific interaction of c-Src with Neu is involved in signaling by the epidermal growth factor receptor. Oncogene 11, 271-9.

NCIC (2002) Canadian Cancer Statistics 2002. National Cancer Institute of Canada Brochure found at http://www.cancer.ca 02/06/2003

Nesbit, C. E., J. M. Tersak and E. V. Prochownik (1999). MYC oncogenes and human neoplastic disease. Oncogene 18, 3004-16.

Nikitin, A. Y., J. J. Jin, J. Papewalis, S. N. Prokopenko, K. M. Pozharisski, E. Winterhager, A. Flesken-Nikitin and M. F. Rajewsky (1996). Wild type neu transgene counteracts mutant homologue in malignant transformation of rat Schwann cells. Oncogene 12, 1309-17.

Normanno, N., F. Ciardiello, R. Brandt and D. S. Salomon (1994). Epidermal growth factor-related peptides in the pathogenesis of human breast cancer. Breast Cancer Res Treat 29, 11-27.

Ozcelik, C., B. Erdmann, B. Pilz, N. Wettschureck, S. Britsch, N. Hubner, K. R. Chien, C. Birchmeier and A. N. Garratt (2002). Conditional mutation of the ErbB2 (HER2) receptor in cardiomyocytes leads to dilated cardiomyopathy. Proc Natl Acad Sci U S A 99, 8880-5.

Padhy, L. C., C. Shih, D. Cowing, R. Finkelstein and R. A. Weinberg (1982). Identification of a phosphoprotein specifically induced by the transforming DNA of rat neuroblastomas. Cell 28, 865-71.

Parks, W. P., E. M. Scolnick and E. H. Kozikowski (1974). Dexamethasone stimulation of murine mammary tumor virus expression: a tissue culture source of virus. Science 184, 158-60.

Pawson, T. (1995). Protein modules and signalling networks. Nature 373, 573-80.

Pegram, M. D., A. Lipton, D. F. Hayes, B. L. Weber, J. M. Baselga, D. Tripathy, D. Baly, S. A. Baughman, T. Twaddell, J. A. Glaspy and D. J. Slamon (1998). Phase II study of receptor-enhanced chemosensitivity using recombinant humanized anti-p185HER2/neu monoclonal antibody plus cisplatin in patients with HER2/neu-overexpressing metastatic breast cancer refractory to chemotherapy treatment. J Clin Oncol 16, 2659-71.

Peles, E., R. B. Levy, E. Or, A. Ullrich and Y. Yarden (1991). Oncogenic forms of the neu/HER2 tyrosine kinase are permanently coupled to phospholipase C gamma. Embo J 10, 2077-86.

Penington, D. J., I. Bryant and D. J. Riese, 2nd (2002). Constitutively active ErbB4 and ErbB2 mutants exhibit distinct biological activities. Cell Growth Differ 13, 247-56.

Perou, C. M., T. Sorlie, M. B. Eisen, M. van de Rijn, S. S. Jeffrey, C. A. Rees, J. R. Pollack, D. T. Ross, H. Johnsen, L. A. Akslen, O. Fluge, A. Pergamenschikov, C. Williams, S. X. Zhu, P. E. Lonning, A. L. Borresen-Dale, P. O. Brown and D. Botstein (2000). Molecular portraits of human breast tumours. Nature 406, 747-52.

Pertschuk, L. P., J. G. Feldman, D. S. Kim, K. Nayeri, K. B. Eisenberg, A. C. Carter, W. T. Thelmo, Z. T. Rhong, P. Benn and A. Grossman (1993). Steroid hormone receptor immunohistochemistry and amplification of c-myc protooncogene. Relationship to disease-free survival in breast cancer. Cancer 71, 162-71.

Pierce, D. F., Jr., M. D. Johnson, Y. Matsui, S. D. Robinson, L. I. Gold, A. F. Purchio, C. W. Daniel, B. L. Hogan and H. L. Moses (1993). Inhibition of mammary duct development but not alveolar outgrowth during pregnancy in transgenic mice expressing active TGF-beta 1. Genes Dev 7, 2308-17.

Plowman, G. D., J. M. Culouscou, G. S. Whitney, J. M. Green, G. W. Carlton, L. Foy, M. G. Neubauer and M. Shoyab (1993). Ligand-specific activation of HER4/p180erbB4, a fourth member of the epidermal growth factor receptor family. Proc Natl Acad Sci U S A 90, 1746-50.

Prigent, S. A. and W. J. Gullick (1994). Identification of c-erbB-3 binding sites for phosphatidylinositol 3'-kinase and SHC using an EGF receptor/c-erbB-3 chimera. Embo J 13, 2831-41.

Quinn, C. M., J. L. Ostrowski, S. A. Lane, D. P. Loney, J. Teasdale and F. A. Benson (1994). c-erbB-3 protein expression in human breast cancer: comparison with other tumour variables and survival. Histopathology 25, 247-52.

Rahman, N. and M. R. Stratton (1998). The genetics of breast cancer susceptibility. Annu Rev Genet 32, 95-121.

Rajkumar, T., G. W. Stamp, H. S. Pandha, J. Waxman and W. J. Gullick (1996). Expression of the type 1 tyrosine kinase growth factor receptors EGF receptor, c-erbB2 and c-erbB3 in bladder cancer. J Pathol 179, 381-5.

Rando, T. A. and H. M. Blau (1994). Primary mouse myoblast purification, characterization, and transplantation for cell-mediated gene therapy. J Cell Biol 125, 1275-87.

Reis, R. M., D. Konu-Lebleblicioglu, J. M. Lopes, P. Kleihues and H. Ohgaki (2000). Genetic profile of gliosarcomas. Am J Pathol 156, 425-32.

Riese, D. J., 2nd, T. Komurasaki, G. D. Plowman and D. F. Stern (1998). Activation of ErbB4 by the bifunctional epidermal growth factor family hormone epiregulin is regulated by ErbB2. J Biol Chem 273, 11288-94.

Riethmacher, D., E. Sonnenberg-Riethmacher, V. Brinkmann, T. Yamaai, G. R. Lewin and C. Birchmeier (1997). Severe neuropathies in mice with targeted mutations in the ErbB3 receptor. Nature 389, 725-30.

Rosner, A., K. Miyoshi, E. Landesman-Bollag, X. Xu, D. C. Seldin, A. R. Moser, C. L. MacLeod, G. Shyamala, A. E. Gillgrass and R. D. Cardiff (2002). Pathway pathology: histological differences between ErbB/Ras and Wnt pathway transgenic mammary tumors. Am J Pathol 161, 1087-97.

Russo, J., B. A. Gusterson, A. E. Rogers, I. H. Russo, S. R. Wellings and M. J. van Zwieten (1990). Comparative study of human and rat mammary tumorigenesis. Lab Invest 62, 244-78.

Sakakura, T., Y. Sakagami and Y. Nishizuka (1982). Dual origin of mesenchymal tissues participating in mouse mammary gland embryogenesis. Dev Biol 91, 202-7.

Samanta, A., C. M. LeVea, W. C. Dougall, X. Qian and M. I. Greene (1994). Ligand and p185c-neu density govern receptor interactions and tyrosine kinase activation. Proc Natl Acad Sci U S A 91, 1711-5.

Sandgren, E. P., N. C. Luetteke, R. D. Palmiter, R. L. Brinster and D. C. Lee (1990). Overexpression of TGF alpha in transgenic mice: induction of epithelial hyperplasia, pancreatic metaplasia, and carcinoma of the breast. Cell 61, 1121-35.

Sandgren, E. P., J. A. Schroeder, T. H. Qui, R. D. Palmiter, R. L. Brinster and D. C. Lee (1995). Inhibition of mammary gland involution is associated with transforming growth factor alpha but not c-myc-induced tumorigenesis in transgenic mice. Cancer Res 55, 3915-27.

Schechter, A. L., M. C. Hung, L. Vaidyanathan, R. A. Weinberg, T. L. Yang-Feng, U. Francke, A. Ullrich and L. Coussens (1985). The neu gene: an erbB-homologous gene distinct from and unlinked to the gene encoding the EGF receptor. Science 229, 976-8.

Schechter, A. L., D. F. Stern, L. Vaidyanathan, S. J. Decker, J. A. Drebin, M. I. Greene and R. A. Weinberg (1984). The neu oncogene: an erb-B-related gene encoding a 185,000-Mr tumour antigen. Nature 312, 513-6.

Schneider-Maunoury, S., P. Topilko, T. Seitandou, G. Levi, M. Cohen-Tannoudji, S. Pournin, C. Babinet and P. Charnay (1993). Disruption of Krox-20 results in alteration of rhombomeres 3 and 5 in the developing hindbrain. Cell 75, 1199-214.

Schroeder, J. A. and D. C. Lee (1998). Dynamic expression and activation of ERBB receptors in the developing mouse mammary gland. Cell Growth Differ 9, 451-64.

Schweizer, J., P. Valenza-Schaerly, F. Goret and C. Pourcel (1998). Control of expression and methylation of a hepatitis B virus transgene by strain-specific modifiers. DNA Cell Biol 17, 427-35.

Schwidetzky, U., W. D. Schleuning and B. Haendler (1997). Isolation and characterization of the androgen-dependent mouse cysteine-rich secretory protein-1 (CRISP-1) gene. Biochem J 321 (Pt 2), 325-32.

Sebastian, J., R. G. Richards, M. P. Walker, J. F. Wiesen, Z. Werb, R. Derynck, Y. K. Hom, G. R. Cunha and R. P. DiAugustine (1998). Activation and function of the epidermal growth factor receptor and erbB-2 during mammary gland morphogenesis. Cell Growth Differ 9, 777-85.

Shawver, L. K., D. Slamon and A. Ullrich (2002). Smart drugs: tyrosine kinase inhibitors in cancer therapy. Cancer Cell 1, 117-23.

Sheng, Z., K. Wu, K. L. Carraway and N. Fregien (1992). Molecular cloning of the transmembrane component of the 13762 mammary adenocarcinoma sialomucin complex. A new member of the epidermal growth factor superfamily. J Biol Chem 267, 16341-6.

Sheng, Z. Q., S. R. Hull and K. L. Carraway (1990). Biosynthesis of the cell surface sialomucin complex of ascites 13762 rat mammary adenocarcinoma cells from a high molecular weight precursor. J Biol Chem 265, 8505-10.

Shepherd, T. G., L. Kockeritz, M. R. Szrajber, W. J. Muller and J. A. Hassell (2001). The pea3 subfamily ets genes are required for HER2/Neu-mediated mammary oncogenesis. Curr Biol 11, 1739-48.

Shih, C., L. C. Padhy, M. Murray and R. A. Weinberg (1981). Transforming genes of carcinomas and neuroblastomas introduced into mouse fibroblasts. Nature 290, 261-4.

Si, J., Z. Luo and L. Mei (1996). Induction of acetylcholine receptor gene expression by ARIA requires activation of mitogen-activated protein kinase. J Biol Chem 271, 19752-9.

Sibilia, M., J. P. Steinbach, L. Stingl, A. Aguzzi and E. F. Wagner (1998). A strain-independent postnatal neurodegeneration in mice lacking the EGF receptor. Embo J 17, 719-31.

Siegel, P. M., D. L. Dankort, W. R. Hardy and W. J. Muller (1994). Novel activating mutations in the neu proto-oncogene involved in induction of mammary tumors. Mol Cell Biol 14, 7068-77.

Siegel, P. M. and W. J. Muller (1996). Mutations affecting conserved cysteine residues within the extracellular domain of Neu promote receptor dimerization and activation. Proc Natl Acad Sci U S A 93, 8878-83.

Siegel, P. M., E. D. Ryan, R. D. Cardiff and W. J. Muller (1999). Elevated expression of activated forms of Neu/ErbB-2 and ErbB-3 are involved in the induction of mammary tumors in transgenic mice: implications for human breast cancer. Embo J 18, 2149-64.

Silberstein, G. B. (2001). Tumour-stromal interactions. Role of the stroma in mammary development. Breast Cancer Res 3, 218-23.

Silberstein, G. B. and C. W. Daniel (1987). Reversible inhibition of mammary gland growth by transforming growth factor-beta. Science 237, 291-3.

Simon, R., A. Nocito, T. Hubscher, C. Bucher, J. Torhorst, P. Schraml, L. Bubendorf, M. M. Mihatsch, H. Moch, K. Wilber, A. Schotzau, J. Kononen and G.

Sauter (2001). Patterns of her-2/neu amplification and overexpression in primary and metastatic breast cancer. J Natl Cancer Inst 93, 1141-6.

Sinn, E., W. Muller, P. Pattengale, I. Tepler, R. Wallace and P. Leder (1987). Coexpression of MMTV/v-Ha-ras and MMTV/c-myc genes in transgenic mice: synergistic action of oncogenes in vivo. Cell 49, 465-75.

Slamon, D. J., G. M. Clark, S. G. Wong, W. J. Levin, A. Ullrich and W. L. McGuire (1987). Human breast cancer: correlation of relapse and survival with amplification of the HER-2/neu oncogene. Science 235, 177-82.

Slamon, D. J., W. Godolphin, L. A. Jones, J. A. Holt, S. G. Wong, D. E. Keith, W. J. Levin, S. G. Stuart, J. Udove, A. Ullrich and et al. (1989). Studies of the HER-2/neu proto-oncogene in human breast and ovarian cancer. Science 244, 707-12.

Slamon, D. J., B. Leyland-Jones, S. Shak, H. Fuchs, V. Paton, A. Bajamonde, T. Fleming, W. Eiermann, J. Wolter, M. Pegram, J. Baselga and L. Norton (2001). Use of chemotherapy plus a monoclonal antibody against HER2 for metastatic breast cancer that overexpresses HER2. N Engl J Med 344, 783-92.

Snapka, R. M. and A. Varshavsky (1983). Loss of unstably amplified dihydrofolate reductase genes from mouse cells is greatly accelerated by hydroxyurea. Proc Natl Acad Sci U S A 80, 7533-7.

Snedeker, S. M., C. F. Brown and R. P. DiAugustine (1991). Expression and functional properties of transforming growth factor alpha and epidermal growth factor during mouse mammary gland ductal morphogenesis. Proc Natl Acad Sci U S A 88, 276-80.

Soltoff, S. P., K. L. Carraway, 3rd, S. A. Prigent, W. G. Gullick and L. C. Cantley (1994). ErbB3 is involved in activation of phosphatidylinositol 3-kinase by epidermal growth factor. Mol Cell Biol 14, 3550-8.

Southern, E. M. (1975). Detection of specific sequences among DNA fragments separated by gel electrophoresis. J Mol Biol 98, 503-17.

Sparano, J. A. (2001). Cardiac toxicity of trastuzumab (Herceptin): implications for the design of adjuvant trials. Semin Oncol 28, 20-7.

Stein, D., J. Wu, S. A. Fuqua, C. Roonprapunt, V. Yajnik, P. D'Eustachio, J. J. Moskow, A. M. Buchberg, C. K. Osborne and B. Margolis (1994). The SH2 domain protein GRB-7 is co-amplified, overexpressed and in a tight complex with HER2 in breast cancer. Embo J 13, 1331-40.

Stern, D. F., M. P. Kamps and H. Cao (1988). Oncogenic activation of p185neu stimulates tyrosine phosphorylation in vivo. Mol Cell Biol 8, 3969-73.

Sternberg, N., D. Hamilton, S. Austin, M. Yarmolinsky and R. Hoess (1981). Site-specific recombination and its role in the life cycle of bacteriophage P1. Cold Spring Harb Symp Quant Biol 45 Pt 1, 297-309.

Stewart, T. A., P. K. Pattengale and P. Leder (1984). Spontaneous mammary adenocarcinomas in transgenic mice that carry and express MTV/myc fusion genes. Cell 38, 627-37.

Strange, R., F. Li, S. Saurer, A. Burkhardt and R. R. Friis (1992). Apoptotic cell death and tissue remodelling during mouse mammary gland involution. Development 115, 49-58.

Sweeney, C. and K. L. Carraway, 3rd (2000). Ligand discrimination by ErbB receptors: differential signaling through differential phosphorylation site usage. Oncogene 19, 5568-73.

Sweeney, C., D. Fambrough, C. Huard, A. J. Diamonti, E. S. Lander, L. C. Cantley and K. L. Carraway, 3rd (2001). Growth factor-specific signaling pathway stimulation and gene expression mediated by ErbB receptors. J Biol Chem 276, 22685-98.

Tanaka, S., M. Mori, T. Akiyoshi, Y. Tanaka, K. Mafune, J. R. Wands and K. Sugimachi (1998). A novel variant of human Grb7 is associated with invasive esophageal carcinoma. J Clin Invest 102, 821-7.

Tansey, M. G., G. C. Chu and J. P. Merlie (1996). ARIA/HRG regulates AChR epsilon subunit gene expression at the neuromuscular synapse via activation of phosphatidylinositol 3-kinase and Ras/MAPK pathway. J Cell Biol 134, 465-76.

Threadgill, D. W., A. A. Dlugosz, L. A. Hansen, T. Tennenbaum, U. Lichti, D. Yee, C. LaMantia, T. Mourton, K. Herrup, R. C. Harris and et al. (1995). Targeted disruption of mouse EGF receptor: effect of genetic background on mutant phenotype. Science 269, 230-4.

Tourtellotte, W. G. and J. Milbrandt (1998). Sensory ataxia and muscle spindle agenesis in mice lacking the transcription factor Egr3. Nat Genet 20, 87-91.

Trimble, M. S., J. H. Xin, C. T. Guy, W. J. Muller and J. A. Hassell (1993). PEA3 is overexpressed in mouse metastatic mammary adenocarcinomas. Oncogene 8, 3037-42.

Ullrich, A., L. Coussens, J. S. Hayflick, T. J. Dull, A. Gray, A. W. Tam, J. Lee, Y. Yarden, T. A. Libermann, J. Schlessinger and et al. (1984). Human epidermal growth

factor receptor cDNA sequence and aberrant expression of the amplified gene in A431 epidermoid carcinoma cells. Nature 309, 418-25.

van de Vijver, M. J., J. L. Peterse, W. J. Mooi, P. Wisman, J. Lomans, O. Dalesio and R. Nusse (1988). Neu-protein overexpression in breast cancer. Association with comedo-type ductal carcinoma in situ and limited prognostic value in stage II breast cancer. N Engl J Med 319, 1239-45.

Varis, A., M. Wolf, O. Monni, M. L. Vakkari, A. Kokkola, C. Moskaluk, H. Frierson, Jr., S. M. Powell, S. Knuutila, A. Kallioniemi and W. El-Rifai (2002). Targets of gene amplification and overexpression at 17q in gastric cancer. Cancer Res 62, 2625-9.

Venter, D. J., N. L. Tuzi, S. Kumar and W. J. Gullick (1987). Overexpression of the c-erbB-2 oncoprotein in human breast carcinomas: immunohistological assessment correlates with gene amplification. Lancet 2, 69-72.

Vogel, C. L., M. A. Cobleigh, D. Tripathy, J. C. Gutheil, L. N. Harris, L. Fehrenbacher, D. J. Slamon, M. Murphy, W. F. Novotny, M. Burchmore, S. Shak, S. J. Stewart and M. Press (2002). Efficacy and safety of trastuzumab as a single agent in first-line treatment of HER2-overexpressing metastatic breast cancer. J Clin Oncol 20, 719-26.

Vogel, W., R. Lammers, J. Huang and A. Ullrich (1993). Activation of a phosphotyrosine phosphatase by tyrosine phosphorylation. Science 259, 1611-4.

Voiculescu, O., E. Taillebourg, C. Pujades, C. Kress, S. Buart, P. Charnay and S. Schneider-Maunoury (2001). Hindbrain patterning: Krox20 couples segmentation and specification of regional identity. Development 128, 4967-78.

Wang, T. C., R. D. Cardiff, L. Zukerberg, E. Lees, A. Arnold and E. V. Schmidt (1994). Mammary hyperplasia and carcinoma in MMTV-cyclin D1 transgenic mice. Nature 369, 669-71.

Webster, M. A., J. N. Hutchinson, M. J. Rauh, S. K. Muthuswamy, M. Anton, C. G. Tortorice, R. D. Cardiff, F. L. Graham, J. A. Hassell and W. J. Muller (1998). Requirement for both Shc and phosphatidylinositol 3' kinase signaling pathways in polyomavirus middle T-mediated mammary tumorigenesis. Mol Cell Biol 18, 2344-59.

Weichman, K. and J. R. Chaillet (1997). Phenotypic variation in a genetically identical population of mice. Mol Cell Biol 17, 5269-74.

Weiner, D. B., J. Liu, J. A. Cohen, W. V. Williams and M. I. Greene (1989). A point mutation in the neu oncogene mimics ligand induction of receptor aggregation. Nature 339, 230-1.

Wilkinson, D. G. and M. A. Nieto (1993). Detection of messenger RNA by in situ hybridization to tissue sections and whole mounts. Methods Enzymol 225, 361-73.

Williams, J. M. and C. W. Daniel (1983). Mammary ductal elongation: differentiation of myoepithelium and basal lamina during branching morphogenesis. Dev Biol 97, 274-90.

Witzemann, V., H. Schwarz, M. Koenen, C. Berberich, A. Villarroel, A. Wernig, H. R. Brenner and B. Sakmann (1996). Acetylcholine receptor epsilon-subunit deletion causes muscle weakness and atrophy in juvenile and adult mice. Proc Natl Acad Sci U S A 93, 13286-91.

Woldeyesus, M. T., S. Britsch, D. Riethmacher, L. Xu, E. Sonnenberg-Riethmacher, F. Abou-Rebyeh, R. Harvey, P. Caroni and C. Birchmeier (1999). Peripheral nervous system defects in erbB2 mutants following genetic rescue of heart development. Genes Dev 13, 2538-48.

Won, S., J. Si, M. Colledge, K. S. Ravichandran, S. C. Froehner and L. Mei (1999). Neuregulin-increased expression of acetylcholine receptor epsilon-subunit gene requires ErbB interaction with Shc. J Neurochem 73, 2358-68.

Wooster, R., G. Bignell, J. Lancaster, S. Swift, S. Seal, J. Mangion, N. Collins, S. Gregory, C. Gumbs and G. Micklem (1995). Identification of the breast cancer susceptibility gene BRCA2. Nature 378, 789-92.

Xing, X., S. C. Wang, W. Xia, Y. Zou, R. Shao, K. Y. Kwong, Z. Yu, S. Zhang, S. Miller, L. Huang and M. C. Hung (2000). The ets protein PEA3 suppresses HER-2/neu overexpression and inhibits tumorigenesis. Nat Med 6, 189-95.

Xu, X., K. U. Wagner, D. Larson, Z. Weaver, C. Li, T. Ried, L. Hennighausen, A. Wynshaw-Boris and C. X. Deng (1999). Conditional mutation of Brca1 in mammary epithelial cells results in blunted ductal morphogenesis and tumour formation. Nat Genet 22, 37-43.

Yu, Q., Y. Geng and P. Sicinski (2001). Specific protection against breast cancers by cyclin D1 ablation. Nature 411, 1017-21.

Zeillinger, R., F. Kury, K. Czerwenka, E. Kubista, G. Sliutz, W. Knogler, J. Huber, C. Zielinski, G. Reiner, R. Jakesz and et al. (1989). HER-2 amplification, steroid

receptors and epidermal growth factor receptor in primary breast cancer. Oncogene 4, 109-14.

Zhou, H., W. D. Chen, X. Qin, K. Lee, L. Liu, S. D. Markowitz and S. L. Gerson (2001). MMTV promoter hypomethylation is linked to spontaneous and MNU associated c-neu expression and mammary carcinogenesis in MMTV c-neu transgenic mice. Oncogene 20, 6009-17.

Zhu, X., C. Lai, S. Thomas and S. J. Burden (1995). Neuregulin receptors, erbB3 and erbB4, are localized at neuromuscular synapses. Embo J 14, 5842-8.

Zisman, A., O. D. Peroni, E. D. Abel, M. D. Michael, F. Mauvais-Jarvis, B. B. Lowell, J. F. Wojtaszewski, M. F. Hirshman, A. Virkamaki, L. J. Goodyear, C. R. Kahn and B. B. Kahn (2000). Targeted disruption of the glucose transporter 4 selectively in muscle causes insulin resistance and glucose intolerance. Nat Med 6, 924-8.

Zrihan-Licht, S., J. Lim, I. Keydar, M. X. Sliwkowski, J. E. Groopman and H. Avraham (1997). Association of csk-homologous kinase (CHK) (formerly MATK) with HER-2/ErbB-2 in breast cancer cells. J Biol Chem 272, 1856-63.